

A N N U A L R E P O R T

1 9 6 7

U. S. WATER CONSERVATION LABORATORY
Southwest Branch
Soil and Water Conservation Research Division
Agricultural Research Service
United States Department of Agriculture
Phoenix, Arizona

FOR OFFICIAL USE ONLY

This report contains unpublished and confidential information concerning work in progress. The contents of this report may not be published or reproduced in any form without the prior consent of the research workers involved.

TABLE OF CONTENTS

	<u>Title</u>	<u>Page</u>
Introduction	Changes in personnel	1
SWC W4-gG-1	Methods for water quality improvement and its storage underground.	
WCL-51	Waste water renovation by spreading treated sewage for groundwater recharge.	51-1
SWC W7-gG-2	Evaluation and control of seepage from water storage and conveyance structures.	
WCL-14	Field application of falling head technique for seepage meters and of double-tube method for hydraulic conductivity measurement.	14-1
WCL-25	Measuring horizontal and vertical conductivity of soil with the double-tube method.	25-1
WCL-37	Clay dispersants for the reduction of seepage losses from reservoirs	37-1
WCL-38	Waterborne sealants to reduce seepage losses from unlined channels and reservoirs.	38-1
SWC W7-gG-3	Suppression of evaporation from water surfaces.	
WCL-9	Application of hexadecanol-octadecanol monofilms to small ponds.	9-1
WCL-50	Use of floating solid and granular materials to reduce evaporation from water surfaces.	50-1
SWC W7-gG-4	Principles, facilities, and systems for water harvest.	
WCL-7	Soil treatment to reduce infiltration and increase precipitation runoff.	7-1
WCL-42	Materials and methods for water harvesting and water storage in the State of Hawaii.	42-1

	<u>Title</u>	<u>Page</u>
SWC W7-gG-5	Soil water movement in relation to the conservation of water supplies.	
WCL-13	Measurement and calculation of unsaturated conductivity and soil water diffusivity.	13-1
WCL-40	Dispersion and flocculation of soil and clay materials as related to the Na and Ca status of the ambient solution.	40-1
WCL-46	Study of unsaturated two-dimensional soil water flow using an analog computer.	46-1
WCL-49	Physical and chemical characteristics of hydrophobic soils.	49-1
SWC W9-gG-6	Factors governing evapotranspiration of water from cropped fields.	
WCL-23	Consumptive use of water by crops in Arizona.	23-1
WCL-29	Plant response to changes in evaporative demand and soil water potential, as shown by measurements of leaf resistance, transpiration, leaf temperature, and leaf water content.	29-1
WCL-29A	Plant processes as functions of the total environment.	29A-1
WCL-29B	Relations of energy balance components over natural surfaces.	29B-1
WCL-29C	Infrared thermometry of soils and vegetation.	29C-1
SWC W10-gG-7	Irrigation systems for efficient water use.	
WCL-2	Dynamic similarity in elbow flow meters.	2-1
WCL-43	Integrating velocity profile meters.	43-1
WCL-45	Irrigation outlet structures to distribute water onto erosive soils.	45-1

	<u>Title</u>	<u>Page</u>
WCL-48	Flow measurement in open channels with critical depth flumes	48-1
Appendix I	List of publications.	AI-1
Appendix II	Summation of important findings.	AII-1

CHANGES IN PERSONNEL

The Laboratory staff has been strengthened during 1967 by the addition of six new members. They are as follows:

- R. Congrove, Laboratory Technician
- D. A. Forstie, Physical Science Aid
- S. B. Idso, Research Soil Scientist
- J. L. Krebs, Laboratory Technician
- R. MacIntyre, Physical Science Aid
- C. D. Pullins, Physical Science Aid

Dr. F. D. Whisler, Research Soil Scientist, of the Soil and Water Conservation Research Division, Agricultural Research Service, U. S. Department of Agriculture, Urbana, Illinois, joined our staff on a temporary duty assignment until August 1967.

During 1967, there were six resignations. They are as follows:

- K. J. Brust, Agricultural Engineer
- J. J. Gruden, Physical Science Aid
- G. D. Overman, Physical Science Aid
- J. J. Rodriguez, Laborer
- C. H. M. van Bavel, Research Physicist
- C. D. Wakefield, Physical Science Aid

LABORATORY STAFF

Professional:

- Dr. H. Bouwer, Research Hydraulic Engineer
- Mr. K. J. Brust, Agricultural Engineer
- Mr. K. R. Cooley, Research Meteorologist
- Dr. W. L. Ehrler, Research Plant Physiologist
- Mr. L. J. Erie, Research Agricultural Engineer
- Dr. D. H. Fink, Research Soil Scientist
- Mr. G. W. Frasier, Agricultural Engineer
- Dr. S. B. Idso, Research Soil Scientist
- Dr. R. D. Jackson, Research Physicist
- Mr. L. E. Myers, Research Hydraulic Engineer and Director
- Dr. F. S. Nakayama, Research Chemist
- Mr. R. J. Reginato, Research Soil Scientist
- Dr. J. A. Replogle, Research Hydraulic Engineer
- Mr. R. C. Rice, Agricultural Engineer
- Dr. C. H. M. van Bavel, Research Physicist
- Dr. F. D. Whisler, Research Soil Scientist

Technicians:

R. Congrove, Laboratory Technician
D. A. Forstie, Physical Science Aid
O. F. French, Hydraulic Engineering Technician
J. L. Gale, Physical Science Aid
L. P. Girdley, Engineering Draftsman
J. R. Griggs, Physical Science Technician
J. J. Gruden, Physical Science Aid
J. L. Krebs, Laboratory Technician
R. MacIntyre, Physical Science Aid
J. B. Miller, Physical Science Technician
S. T. Mitchell, Physical Science Technician
K. G. Mullins, Physical Science Technician
G. D. Overman, Physical Science Aid
J. M. Pritchard, Physical Science Technician
C. D. Pullins, Physical Science Aid
B. A. Rasnick, Physical Science Technician
C. D. Wakefield, Physical Science Aid

Administrative, Clerical and Maintenance:

O. J. Abeyta, Laborer
I. G. Barnett, Janitor
E. D. Bell, General Machinist
E. E. De La Rosa, Janitor
B. E. Fisher, Library Assistant
D. S. Fry, Clerk-Stenographer
C. G. Hiesel, General Machinist
R. C. Klapper, Refrigeration and Air Conditioning Mechanic
J. M. R. Martinez, Laborer
R. S. Miller, Administrative Assistant
A. H. Morse, Clerk-Dictating Machine Transcriber
L. J. Orneside, Clerk-Stenographer
J. J. Rodriguez, Laborer
M. A. Seiler, Clerk-Stenographer
C. H. Tanner, Secretary
M. F. Witcher, Clerk-Stenographer

TITLE: DYNAMIC SIMILARITY IN ELBOW FLOW METERS

LINE PROJECT: SWC W10 gG-7

CODE NO.: Ariz.-WCL-2

INTRODUCTION:

See Annual Report for 1966.

The project was nearly inactive except for the preparation of a paper replying to questions raised by discussers of the original paper and some continuation of the search for suitable integrating devices that will operate with the elbow meters and certain other differential-head meters. The paper replying to the discussers will appear in a future issue of the Journal of the Irrigation and Drainage Division, ASCE.

PROCEDURE:

Minor modifications were made to the piping system in the hydraulics laboratory to permit installation of the 10-inch pipe elbows so that the integrating devices could be checked for operational problems.

RESULTS AND DISCUSSION:

The turbine-type meter that was tested earlier as an integrating device (see Annual Report for 1966) failed to turn freely after it had remained installed but idle for several months. Since it was a so-called "wethead" meter, that is, water was permitted to circulate through the dial mechanism, this result was not surprising.

What appears to be a superior meter at approximately the same cost has recently become commercially available. This meter is a dryhead, turbine-type meter that transmits the turning torque to the dial mechanism magnetically so that no rotating fluid seals are required. This meter has been purchased and has been installed on a 10-inch elbow meter but has not yet been operated in sufficient testing situations for evaluation.

The low differential pressures produced by the larger elbows at the flow rates possible with the present laboratory facilities presented some problems. The shunt-metering loop into which the turbine meter was installed (Figure 1) would not self-purge of air except at the very highest flow rates, because the differential pressure was insufficient to start the flow over the height of the meter loop. This can be overcome by priming the shunt-metering loop manually, or by shortening the height of the meter loop to facilitate self priming.

Since the larger elbow sizes do not quite correspond to a square-root relation, the error in accumulating an integrated total flow will be larger than with the 3-inch size elbows, but should remain within an acceptable $\pm 5\%$ limit if the flow range does not fluctuate widely.

SUMMARY AND CONCLUSIONS:

Results of the study on pipe elbows as flowmeters have been published. The report summarizes the findings from the investigations of a number of commercially available 90°-flanged elbows of several sizes, ranging from 3 inches to 12 inches in diameter which were calibrated as flow meters. The accuracy to which a calibration equation was predicted using only the nominal elbow size and the average calibration results of several similar elbows was determined to be $\pm 5\%$. This accuracy was improved to $\pm 3\%$ when precise measurements of the elbow diameter and radius of bend were obtained and incorporated into the calibration equation. A relatively simple and inexpensive method for accurately determining the radius of bend with casting plaster was described.

Efforts are continuing toward incorporating a low-cost, integrating device with the elbow flowmeter to convert it from a rate device to a total-quantity meter. A household-type water meter of the newer turbine design was operated as a shunt meter for several weeks then remained idle for several more weeks. Because of

the "wethead" feature of the meter, the gearing mechanism was exposed to the water flow and the meter failed to restart. Turbine meters of the dryhead type that use magnetic linkage and no rotating liquid seals are being tested. Results appear promising but have not been fully evaluated.

PERSONNEL: J. A. Replogle

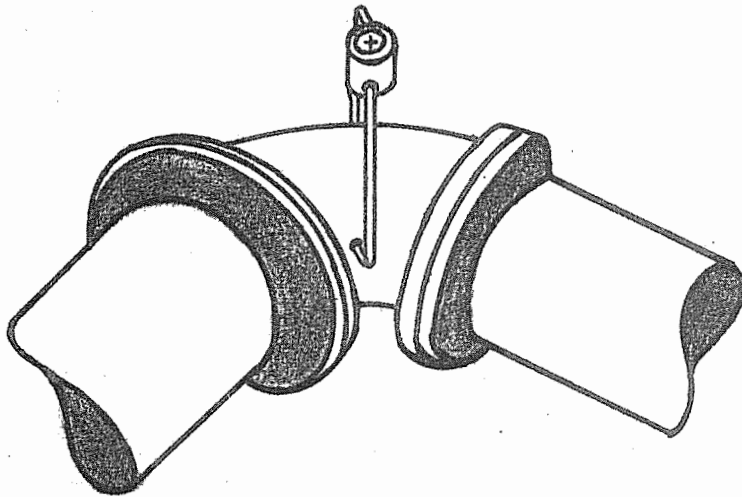


Figure 1. Typical shunt meter installation across an elbow flowmeter.

TITLE: SOIL TREATMENT TO REDUCE INFILTRATION AND INCREASE
PRECIPITATION RUNOFF.

LINE PROJECT: SWC W7-gG4

CODE NO.: Ariz.-WCL-7

INTRODUCTION:

Observations and measurements were continued at the Granite Reef testing site in the evaluation of different surface treatments for increasing precipitation runoff. No work was performed on the existing operational water harvesting installations with the exception of the Blue Mountain catchment which was retreated. The other catchments were inspected to observe the weathering performance of the treatments.

New field installations consisted of: two dual-purpose catchment and storage units installed near Flagstaff, Arizona, in cooperation with the Forest Service; a one-half acre catchment near Seneca, Arizona; and establishment of a 50 acre test site near Bylas, Arizona, in cooperation with the Bureau of Indian Affairs and the San Carlos Apache Indian Reservation. Laboratory studies were concerned with evaluating the relative resistance of low-cost soil stabilizers to erosion by simulated raindrops.

PART I. SOIL STABILIZATION.

Preliminary results reported in the 1966 Annual Report indicated that a soil stabilizer combined with a water repellent can increase runoff and at the same time reduce the erosion hazard. Although a satisfactory low-cost stabilizer for this purpose has not previously been available, there are resin emulsions and solutions that may be suitable. For reasons of economy, only materials dispersed or dissolved in water were considered.

Procedure:

Granite Reef soil, sieved through a 2.0 mm sieve to remove coarse sand and gravel, was packed into 15 x 90 mm glass petri dishes. Two 65 g increments of soil at 8% water content were packed in each dish. Each increment received 10 blows of a 580 g weight falling 30 cm on a 15 mm diameter tamping foot, resulting in a bulk density of 1.4.

The soil was dried at 49°C for 24 hours before treatment with the resin solutions or emulsions. A pipette was used to apply quantities of 20 g or more fluid per dish. Treatments of 10 g or less were applied by spraying and the soil sample was weighed before and after the application to verify the application rate. Treated soil samples were dried at 49°C for 24 hours before making erosion measurements.

Erosion resistance of treated and untreated soil was measured by subjecting them to drops of water 5.9 mm diameter falling a distance of 2.0 meters at a rate of 8 drops per minute. The water drops fell through a 10 cm I.D. plexiglass tube and all drops impacted on the soil within a 1.0 cm diameter area. Soil samples were placed in a large glass beaker under the dripper with the soil surface at about a 10% slope. Eroded soil particles were violently impacted onto the walls of the beaker and were readily detected visually even when the amount of erosion was too small to be detected by weighing the dried soil samples before and after the dripper test. Initial measurements involved the amount of erosion caused by various numbers of drops. It was subsequently decided that a satisfactory material should prevent any erosion. Accordingly, all soil samples were subjected to 600 drops over a period of 75 minutes and any sign of erosion was considered to be a failure.

Results:

Untreated soil samples eroded rapidly. Approximately 50 drops eroded a crater completely through the soil to the bottom of the petri dish. It is considered that the use of this soil under the imposed conditions constituted a severe test of the stabilizing materials as described in the following paragraphs.

Material 1 was a water soluble ethylene maleic anhydride copolymer that had reportedly been used in Canada for roadbed stabilization. All application rates, up to 20 g of 15% solids solution, eroded severely.

Material 2 was a petroleum resin emulsion sold commercially for preventing wind erosion of sandy soils. Maximum application recommended by the manufacturer equals about 40 g of 15% solids emulsion per petri dish. All applications, including 30 g of 30% emulsion, eroded severely.

Material 3 was a urea-formaldehyde formulation of 30% formaldehyde, 37.5% urea and 32.5% water by weight. This material reacts to form a hard compound with low water solubility. It is potentially attractive because of its low cost. Unfortunately, the reaction can be delayed or reduced by elements naturally present in soil. Soil treated with 13.5 g of 67.5% U-F eroded severely even after four weeks curing in a 120 F oven.

Material 4 was an emulsion of an unknown plastic resin sold commercially for controlling wind and rain erosion of fine materials. Erosion was stopped by an application of 5 g of 20% emulsion. All treated soil samples, including 20 g of 20% emulsion, crumbled easily upon drying.

Material 5 was the butyl latex emulsion described in the 1966 Annual Report. Erosion was stopped by 5 g of 20% solids emulsion. Field tests have shown that this material deteriorates rapidly upon exposure to sunlight.

Material 6 was a cationic polyethylene emulsion. The surfactant used as an emulsifier is water repellent and treated samples were hydrophobic to various degrees. Applications of 20 g of 20% solids emulsion stopped erosion but the dry treated soil crumbled easily.

Material 7 was a cationic emulsion of softer polyethylene than that used in material 6. Twenty grams of 20% solids stopped erosion. Despite the use of softer resin the dry treated soil was easily crumbled.

Material 8 was a polyvinyl acetate emulsion. Five grams of 20% solids stopped erosion. The wet soil was soft but dry treated soil,

particularly at higher rates of application, was bonded into a tough pavement.

Material 9 was a vinyl acrylic terpolymer emulsion. Five grams of 10% solids stopped erosion. The wet soil was firm. Soil treated at higher application rates was bonded into a tough pavement but showed signs of fine hairline cracking when dried.

Material 10 was a vinyl acetate copolymer emulsion. Ten grams of 5% solids stopped erosion. As with material 9, the wet soil was firm but higher application rates showed signs of hairline cracking when the treated soil was dried.

Material 11 was a low molecular weight polyvinyl alcohol that is soluble in cold water. All treated soil samples eroded severely.

Material 12 was a high molecular weight polyvinyl alcohol that is soluble in hot water but insoluble in cold water. Only 5 g of 2.5% solids solution stopped erosion. This is an application of 14 g resin per m².

The above tests indicate that materials 1 through 7 and 11 are not satisfactory soil stabilizers for our purpose. Materials 8, 9, 10 and 12 have promise and will be evaluated for relative resistance to mechanical damage and resistance to weathering damage.

Soil treated with 30 g of 3% R-20 (sodium methyl silanolate), the water repellent used in previously reported studies, was subjected to various numbers of drops. Erosion was reduced considerably below that occurring with untreated soil. From 100 to 200 drops, erosion was reduced more than 95%. From 400 to 600 drops, erosion was reduced more than 80%. A direct comparison with field data is not possible but these data qualitatively agree with findings from Granite Reef field plots.

Preliminary observations were made on soil samples treated with soil stabilizers plus R-20 water repellent. All of the promising stabilizers were compatible with R-20 so they could be combined and

applied as a single mixture. The amount of stabilizer required to stop erosion is not reduced by adding R-20. However, infiltration, which is not greatly reduced by low rates of stabilizer alone, can be reduced to zero by including R-20.

PART II. OPERATIONAL FIELD CATCHMENTS.

Nelson Road Catchment. The two-phase asphalt treatment installed on this catchment during the summer of 1964 was in excellent condition when inspected 3 August 1967 and 9 November 1967. The asphalt-fiberglas lined reservoir appears to be watertight. BIA personnel reported heavy use of water from the catchment by livestock and consider it a successful installation.

Blue Mountain Catchment. This catchment, treated during the summer of 1964 with a two-phase asphalt treatment, had deteriorated severely on the lower half during the winter of 1966-67. The upper half which had a top spray of flaked aluminum was in fair condition when inspected 4 April 1967. It was quite evident the aluminum spray coating had materially increased the life of the treatment. On 3 August 1967 the lower half of the catchment was treated with MC-250 cutback asphalt at a rate of $1.3 \text{ kg asphalt m}^{-2}$. On 9 November 1967 the lower $3/4$ portion of the catchment received a seal coat of RSK asphalt emulsion. The lower $1/4$ of the catchment was treated at a rate of $2.5 \text{ kg actual asphalt m}^{-2}$ and the remainder of the sprayed area treated at a rate of $1.5 \text{ kg actual asphalt m}^{-2}$. Approximately $1/4$ of the area which had been originally treated with the aluminum spray coating and still remained in good condition was not retreated. The entire catchment will be given a new top spray of aluminum early in 1968.

Flagstaff Cinders Catchment. This catchment, a two-phase asphalt treatment, was initially installed during the summer of 1964. Two years later in June 1966 maintenance was performed to repair shrinkage cracks in the pavement. The catchment was in excellent condition when inspected 4 April 1967.

Metate Catchment. The treatment of the Metate catchment, installed during the summer of 1965, consisted of 2 mil black polyethylene bonded to asphalt stabilized soil. This treatment was in poor condition when inspected 31 January 1967. There were numerous holes in the sheeting, several approximately 1 ft. in diameter. Three Yucca plants were growing through the pavement. It was also evident that asphalt was migrating through the polyethylene sheeting. The asphalt-fiberglas lining for the reservoir appeared watertight but the reservoir was leaking. On 13 July 1967 the leak was found to be through the reservoir outlet. Recommendations were made to BIA personnel for repair of the outlet. After the outlet is repaired the catchment will be recovered with fiberglas and asphalt.

San Vicente Catchment. This catchment, covered with a 20 mil chlorinated polyethylene sheeting, was installed during the summer of 1965. The sheeting was in good condition when inspected 2 May 1967. There were two small holes caused by coyotes and two locations where previous patches had failed, probably because the repair was made when the weather was too cold. The sheeting appears to resist weathering damage and is easy to repair if mechanically damaged. The reservoir, which is lined with the same material, was in fair condition at time of inspection. Two seams needed minor repair and there was one small hole next to the outlet.

Mescal Catchment. The Mescal catchment, covered with 20 mil chlorinated polyethylene, was in good condition when inspected on 31 January 1967. There were approximately 25 small holes caused by varmints. It appears the sheeting attracts small animals that tear small holes in the material for unknown reasons. BIA personnel report it is necessary to perform maintenance at about 3 month intervals. Even with the maintenance required, they believe this to be a very successful catchment.

Dual-Purpose Catchments. Two dual-purpose catchment and storage units were installed in cooperation with the U. S. Forest Service

near Flagstaff, Arizona. These units, installed 5 April 1967, were designed to provide water for wildlife and for fighting forest fires by providing emergency water supplies at strategic locations in the forest. Each unit consists of a 6.1×6.1 m catchment and a 5600 liter storage bag. The catchment and bag were both constructed from 20 mil nylon reinforced butyl. Fire fighters can obtain water from the bag through a T-valve installed in the pipe between the bag and watering trough. These units were successfully used for wildlife watering during the summer of 1967. To date, it has not been necessary to use the water for firefighting.

Seneca Catchment. This catchment is a new installation on the San Carlos Indian Reservation near Seneca, Arizona, installed in cooperation with the Bureau of Indian Affairs and the Anchor Seven Cattlemen's Association. The installation consists of a 1935 m^2 catchment area and a 500,000 liter storage reservoir. The catchment is on an 8-10% slope with a good covering of grass. We plan to burn the grass and treat the undisturbed soil with a water repellent-soil stabilizer treatment in 1968.

On 26 June 1967 the reservoir was lined with 20 mil nylon reinforced butyl sheeting. A precalibrated V-notch, critical depth flume with a capacity range of 0.01 to 10 cfs was installed to measure runoff from the plot into the reservoir. The flume is equipped with a strip-chart water stage recorder capable of operating 90 days unattended. The recorder is modified to record rainfall amounts as sensed by a tipping bucket raingage. For the period of 7 July 1967 through 12 December 1967, a total of 244.4 mm of rain was recorded, with 116.2 during July and 38.0 mm on 27 July 1967. The runoff data have not been analyzed.

Original plans called for treating the catchment in the fall of 1967. The treatment will require approximately 10,000 liters of water and we planned to use the reservoir lining as a rainfall catchment to obtain the necessary quantity of water. An inspection trip

on 18 September showed that well over 10,000 liters of water had been collected. Unfortunately, a bear had climbed into the reservoir for a bath and tore the lining while climbing back out. Most of the water was lost. The damaged lining was repaired by BIA personnel and it is hoped sufficient water will be collected by the spring of 1968 to permit treating the catchment.

PART III. MONUMENT TANK TESTING SITE.

The Monument Tank testing site is a new installation on the San Carlos Indian Reservation approximately 40 miles east of Globe, Arizona, in an estimated 400 mm rainfall zone. The installation will be used for large scale field evaluation of low cost water harvesting treatments. The site is a cooperative installation between the San Carlos Apache Indian Tribe, Ash Creek Cattlemen's Association, the Bureau of Indian Affairs and the U. S. Water Conservation Laboratory. The site consists of approximately 30 hectares (80 acres), with 20 hectares (50 acres) fenced, above an existing earth reservoir which has a storage capacity of 16,000 - 18,500 m³ (13-15 acre feet). Within the fenced area, three separate watersheds ranging in size from 2 hectares to 4 hectares (5 acres to 9 acres) have been selected for study. A fourth watershed of 8 hectares (20 acres) extends outside the fenced area.

Procedure.

On two of the watersheds, No. 1 and No. 4, the runoff water flows down the natural channel to the measuring point. On watersheds No. 2 and No. 3 the runoff water is intercepted in lined collection ditches before reaching the natural channels. These ditches, each approximately 300 m long, were constructed with a bulldozer and roadgrader. After construction the ditches were sprayed with water to settle the dust and partially compact the soil. The ditches were then sprayed on 15 May 1967 with RC-70 cutback asphalt at a rate of 2.1 m kg actual asphalt m⁻². An inspection trip two weeks later showed

the asphalt had penetrated approximately 6 to 18 mm with very little asphalt left on the soil surface. On 5 June 1967, MC-250 cutback asphalt was sprayed on the ditches at a rate of 1.9 kg asphalt m². This asphalt remained essentially on the soil surface.

Each of the four watersheds has a V-notch, critical depth flume with a capacity range of 0.003 to 2.3 m³ sec⁻¹ (0.1 to 80 cfs). These flumes were constructed at the Laboratory and assembled at the site. Each flume is equipped with a strip-chart water stage recorder capable of running for 90 days unattended. Other instrumentation at the site consists of 10 storage type raingages, one vector pluviometer and one mechanical weather station which records wind speed, wind direction, air temperature and rainfall as sensed by a tipping bucket raingage. The mechanical weather station is able to run unattended for 30 days.

Runoff will be measured from the untreated watersheds for a period of 1 to 3 years to determine the runoff from untreated soil. Channel losses for watersheds 1 and 4 will be determined by comparison with 2 and 3 where there will be no channel losses. Subsequent treatments will be determined after studying untreated watershed performance and evaluating other field and laboratory data.

Results:

The flumes were installed on 9 October 1967. The limited runoff data collected to date have not been analyzed. A storage raingage installed at the site has collected a total of 364 mm of rain from 21 March 1967 through 10 January 1968.

PART IV. GRANITE REEF TESTING SITE.

During the summer of 1967, the ridge and furrow plots R-5 through R-8 were reshaped to a 5% longitudinal slope and zero slide slope, and four 6 m × 30 m plots were installed. These are labelled "A" plots. Fifteen new plots, 1.25 m × 8 m each, were constructed to replace the old 9.3 m² plots. Steel borders were placed around all the new plots and the old L-Plots to better define the catchment area and improve the accuracy of the runoff measurements.

Data from the raingage network have not been completely analyzed. Preliminary analyses indicate up to a 10% variation in rainfall per storm within the test area, but there is no consistent pattern to the variation. Pending complete rainfall pattern analysis, runoff from the plots is compared to the standard 20.32 cm storage raingage. For the year a total rainfall of 272.1 mm was measured in 23 separate storms. Following are the results of the runoff measured from the different plots.

Esso Plots. The four-plot test unit constructed in cooperation with Esso Research Corporation of Linden, New Jersey, in December 1964, with a one-phase treatment of Eastern asphalt, has lasted considerably longer than was expected. For the year, Plot E-1 treated with 1.95 kg asphalt m^{-2} averaged 72% runoff; plot E-2 treated with 1.85 kg asphalt m^{-2} averaged 62% runoff; and plot E-4 treated with 2.2 kg asphalt m^{-2} averaged 75% runoff. Runoff from the plots is approximately 10% lower than the runoff in 1966. The asphalt is now cracking and breaking up and runoff is expected to decrease more rapidly.

Paved Plots. Treatments applied to the paved plots are listed in Table 1 and the runoff results are presented in Table 2.

The bonded, 1.5 mil black polyethylene on Plot L-1a failed in its original purpose. It had been hoped that the film would eliminate the discoloration of runoff water from asphalt pavements caused by the deterioration of asphalt. The thin polyethylene, which is easily bonded to the soil with asphalt, should prevent the underlying asphalt from oxidizing. It was found, however, that the bonding asphalt migrated through the film, oxidized on the film surface, and discolored the runoff water. By July 1967 the 29 month old film was becoming brittle and showing signs of deterioration. Runoff from the plot from 1 January 1967 through 16 July 1967 averaged 85%. The deteriorated film was removed in July 1967 and the plot retreated.

The new treatment on the plot listed in Table 1 as Plot L-1b consisted of MC-250 at 1.5 kg asphalt m^{-2} for a basecoat with a supposedly improved polyethylene as a top sheeting. The lower 20 ft of the plot was covered with 20 mil sheeting and the remainder covered with 12 mil sheeting. The new sheeting underwent significant shrinkage upon exposure and did not reduce the problem of asphalt migration. From 2 September 1967 through the remainder of the year, the treatment averaged 95% runoff. The sheeting has subsequently been removed.

Runoff from Plot L-4, the butyl sheeting standard, averaged 97% for the year. The plot has some retention pockets which significantly reduce runoff from small rainstorms. Over 45% of the storms in 1967 were less than 5 mm.

Runoff from the two-phase asphalt treatment Plots L-5 and L-6 did not compare as favorably as in previous years. Plot L-5 averaged 99.9% runoff and Plot L-6 averaged 90.5% runoff. Preliminary analysis of the data indicate two possible explanations: (1) the lower edge of Plot L-6 may have some retention due to reduction of lateral slope when the new steel borders were installed; and (2) Plot L-6 slopes to the east and Plot L-5 slopes to the north. Vector pluviometer data presented in Table 3 show that 63% of the rainstorms during 1967 came from the north and west. Further analysis of the data is necessary to prove the exact effect of plot exposure on rainfall runoff. The two asphalt plots are in good condition with only minor cracking of the pavements.

Plot L-7 was reshaped during the year and on 3 August 1967 a basecoat of MC-250 cutback asphalt was applied at a rate of 1.5 kg asphalt m^{-2} . On 22 August 1967 a cover of 1 mil aluminum foil was bonded to the stabilized soil with RSK asphalt emulsion at a rate of 0.7 kg asphalt m^{-2} . The lap joints of the foil were sealed with a butyl cement. The runoff from the aluminum foil since treatment

averaged 87% for the remainder of 1967. The runoff reduction below 100% apparently results from retention of water in small wrinkles in the foil. This plot also has an easterly exposure which could have been a factor as explained with Plot L-6.

Plot A-1 is one of the new 6 m × 30 m plots. A basecoat of MC-250 at 1.5 kg asphalt m⁻² was applied 3 August 1967. On 22 August 1967 a top sheeting of 230 g m⁻² (3/4 oz ft²) chopped fiberglass matting was bonded to the soil and sealed with RSK asphalt emulsion applied at a rate of 1.4 kg asphalt m⁻². A protective top spray will be applied in 1968. From 22 August 1967 through the remainder of 1967 this plot averaged 99.3% runoff.

Plot A-2, also one of the new plots, was given a basecoat of MC-250 at a rate of 1.5 kg asphalt m⁻² on 3 August 1967. On 12 September 1967 a standard roof covering was installed by a commercial roofing company. This treatment consists of spot mopping cold adhesive over the asphalt stabilized soil, applying a covering of rag felt, saturating with cold adhesive, and covering with 6 to 9 mm diameter natural river run pea gravel at an approximate rate of 620 g m⁻². This treatment averaged 91.1 percent runoff for the remainder of 1967. The gravel covering has considerable retention and percent runoff for a full year, including warm weather months, is expected to be lower. Durability may be good. This covering is guaranteed for 10 years when applied to roofs.

Bare Soil Plots. The bare soil plots include all treatments where the soil is not completely paved. A description of these treatments at the Granite Reef site is presented in Table 4 with runoff data listed in Table 5.

Runoff from plots L-2 and E-3 averaged 29.0 and 29.5%, respectively, for the year. Plot A-3 averaged 34% runoff from 10 August through 31 December 1967. L-2 and E-3 both averaged 29% for this same period. The increased runoff from A-3 is thought to result from soil compaction during plot construction.

Ridge and furrow plot R-2, with 10% side slope, averaged 27.9% runoff. Plot R-1, with 20% side slope, averaged 27.6% runoff, indicating that increasing slope above 10% did not increase runoff. Both R-plots produced less runoff than plots L-2 and E-3 with 5% slope, which is the opposite of results for the previous two years. Reduced runoff is probably caused by increased erosion and increased infiltration in the furrow channel. The channels will be sealed in 1968 to evaluate this loss.

Watershed 3, hand cleared of brush in 1963, gave 24.2% runoff compared to 16.1% for W-2, which has a natural cover of scattered brush. In the four years since early 1964, when measurements began, brush clearing has increased runoff by more than 100 mm. Although some regrowth is developing from airborne seeds, reclearing of W-3 should not be necessary for at least two more years.

Plot L-3, treated with a water repellent in August 1965, yielded 63.5% runoff. This compares to 76% in 1966 and 94% for the latter part of 1965. The treatment is deteriorating for reasons outlined in the 1966 report. Deterioration may not be as great as these figures indicate, however. In 1966, L-3 produced 42% more runoff of the total rainfall than untreated plot L-2. In 1967, L-3 still produced 40% more runoff than L-2.

Ridge and furrow plot R-4, treated with sodium carbonate in May 1966, gave 38.2% runoff for the year. This is an increase of 10% over runoff from a similar untreated plot R-2. For the seven months after treatment in 1966, R-4 produced 22.5% more runoff than R-2. These figures indicate that the salt treatment has deteriorated significantly during the year following application.

SUMMARY AND CONCLUSIONS:

Laboratory studies have shown that several resin emulsions and solutions can be used at low application rates to stop or greatly reduce raindrop erosion. One resin was effective at a rate of

14 g m⁻². These materials are compatible with the R-20 water repellent, permitting application as a single mixture. Infiltration, which is not greatly reduced by low rates of stabilizer alone, can be reduced to zero by including water repellent.

Observations of the experimental operational catchments were continued. The protective coating of flaked aluminum on the upper half of the Blue Mountain catchment definitely increased the life of the asphalt treatment. The lower portion of the catchment without the protective coating deteriorated during the winter of 1966-67. The two-phase asphalt treatment on the Nelson Road catchment is still in good condition. The asphalt-fiberglas lined reservoir at Nelson Road appears completely sealed and BIA personnel consider this a successful installation. The two-phase asphalt treatment on the Flagstaff Cinders catchment was still good. The bonded 1.5 mil black polyethylene on the Metate catchment was in poor condition when inspected in January 1967. The asphalt-fiberglas reservoir lining is in good condition but is leaking at the outlet. After the outlet is repaired the catchment will be retreated. The 20 mil chlorinated polyethylene on the Mescal and San Vicente catchments is weathering satisfactorily. This material is easy to repair and a good catchment can apparently be maintained with a small amount of maintenance.

Two dual-purpose catchment and storage units designed to provide water for wildlife and provide emergency water supplies for fighting forest fires were installed in cooperation with the U. S. Forest Service near Flagstaff, Arizona. These units were successfully used for wildlife water during the summer of 1967, but it was not necessary to use the water for firefighting.

A new water harvesting catchment was established on the San Carlos Indian Reservation near Seneca, Arizona. This catchment will evaluate a low-cost water repellent-soil stabilizer treatment for increasing runoff. Runoff from the plot is measured with a

V-notch, critical depth flume and will be compared to the rainfall as measured by a tipping bucket raingage. This catchment will be treated in 1968.

Instrumentation of a new site for large scale evaluation of low-cost water harvesting treatments was started in 1967. This site is on the San Carlos Indian Reservation. Four small watersheds, of 5 to 20 acres each, were isolated and four 80 cfs, V-notch, critical depth flumes for measuring runoff were installed. Rainfall in the area is measured by a network of 11 raingages. Runoff from the untreated watersheds will be measured for a period of one to three years before any treatments are applied.

At the Granite Reef testing site four new 180 m² plots and 15 new 10 m² plots were constructed. These new plots plus the seven L-Plots had steel borders installed to better define the catchment area and improve the accuracy of the runoff measurements.

Runoff from the three plots treated in December 1964 with a one-phase treatment of Eastern asphalt declined to 60-75% during 1967, but the treatments have lasted considerably longer than was originally expected. Two plots with the two-phase asphalt treatment continue to look good with runoff 90% from one and 99% from the other. The reason for the difference in runoff is not apparent and will be investigated. Rainfall for 1967 came in 23 storms totalling 272 mm. Eleven of the storms were less than 5 mm and accounted for 12% of the total rainfall.

Runoff water from the asphalt bonded 1.5 mil black polyethylene continued to be discolored by asphalt deterioration by-products. The asphalt migrated through the film and deteriorated on the plot surface. The standard butyl plot averaged 97% runoff for the year. There is some retention on the plot which becomes significant in small rainstorms. A new plot of bonded 1 mil aluminum foil was installed. Runoff was 87%, lower than expected, probably because water is retained in wrinkles in the foil. A new plot of asphalt-

fiberglas was installed during August 1967. This treatment is relatively low-cost and is expected to be quite durable. Runoff from this treatment averaged 99%. A second plot was treated with a standard roofing treatment of asphalt, roofing felt, and gravel. This treatment has significant retention but is low in cost and is expected to have reasonably long life. Similar treatments on roofs are guaranteed for 10 years.

Runoff data from bare soil catchments at Granite Reef show that these treatments deserve serious consideration. An untreated watershed, with no channel losses, produced 16% runoff. Clearing the scattered brush increased runoff to 24% four years after clearing. Smoothing the soil resulted in 29% runoff six years after smoothing. Application of sodium carbonate produced 38% runoff during the record year after treatment. Application of a relatively low-cost water repellent produced 64% runoff during the third year after treatment. Current investigations indicate that reasonably durable, low-cost, bare soil treatments can be developed to produce more than 90% runoff.

PERSONNEL: Lloyd E. Myers, Gary W. Frasier.

Table 1. Waterproof treatments on large plots at Granite Reef Testing Site.

Plot	Treatment Date	Treatment
L-1a	10 Oct 1963	<u>Basecoat.</u> RC-Special at 2.0 kg asphalt m ⁻²
	1 Feb 1965	<u>Top Sheeting.</u> Black polyethylene, 1.5 mil bonded with a mixture of MC-70 and MC-250 at 1.2 kg asphalt m ⁻²
L-1b	8 Aug 1967	<u>Basecoat.</u> MC-250 at 1.5 kg asphalt m ⁻² <u>Top Sheeting.</u> Lower 20 ft - 20 mil black polyethylene, upper 25 ft - 12 mil black polyethylene bonded with RSK asphalt emulsion at 0.7 kg asphalt m ⁻²
L-4	30 Nov 1961	<u>Butyl Rubber Sheeting.</u> 15 mil
L-5	18 Sept 1962	<u>Basecoat.</u> S-1 at 1.04 kg asphalt m ⁻²
	16 Mar 1966	<u>Topcoat.</u> RSK asphalt emulsion at 0.6 kg asphalt m ⁻²
L-6	19 Apr 1963	<u>Basecoat.</u> RC-special at 1.5 kg asphalt m ⁻²
	8 May 1963	<u>Topcoat South Half.</u> SS-2 special asphalt emulsion at 0.65 kg asphalt m ⁻² with 3% butyl latex
	9 Jul 1963	<u>Topcoat North Half.</u> S-1 at 0.5 kg asphalt m ⁻² with 3% butyl latex
	17 Feb 1966	<u>Top Spray.</u> Aluminum coating TS-A-1 at 0.16 kg material m ⁻²
L-7	3 Aug 1967	<u>Basecoat.</u> MC-250 at 1.5 kg asphalt m ⁻²
	22 Aug 1967	<u>Top Sheeting.</u> 1 mil aluminum foil bonded with RSK asphalt emulsion at 0.7 kg asphalt m ⁻²
A-1	3 Aug 1967	<u>Basecoat.</u> MC-250 at 1.5 kg asphalt m ⁻²
	22 Aug 1967	<u>Top Sheeting.</u> 3/4 oz chopped fiberglass matting bonded with RSK asphalt emulsion at 1.4 kg asphalt m ⁻²

Table 1. Waterproof treatments on large plots at Granite Reef
Testing Site - continued.

Plot	Treatment Date	Treatment
A-2	3 Aug 1967	<u>Basecoat.</u> MC-250 at 1.5 kg asphalt m ⁻² <u>Top Sheeting.</u>
	12 Sept 1967	<u>Top Sheeting.</u> Standard rag felt-rock roofing treatment.

Table 2. Runoff results from rainfall on waterproof treatments at Granite Reef Testing Site.

Date	Total Rainfall		L-1a Runoff		L-1b Runoff		L-4 Runoff		L-5 Runoff		L-6 Runoff		L-7 Runoff		A-1 Runoff		A-2 Runoff	
	(mm)	(%)	(mm)	(%)	(mm)	(%)	(mm)	(%)	(mm)	(%)	(mm)	(%)	(mm)	(%)	(mm)	(%)	(mm)	(%)
1967	(mm)	(%)	(mm)	(%)	(mm)	(%)	(mm)	(%)	(mm)	(%)	(mm)	(%)	(mm)	(%)	(mm)	(%)	(mm)	(%)
23 Jan	4.1		4.2	102.0			4.4	107.3	4.4	107.3	4.3	105.1						
10 Mar	1.6		1.6	100.0			2.0	125.0	1.8	112.5	1.9	118.8						
29 Mar	14.8		13.2	89.2			14.3	96.6	14.7	99.3	15.3	103.6						
4 Apr	4.3		3.6	83.7			4.1	95.3	4.0	93.0	4.2	97.7						
11 Apr	3.1		2.6	83.9			3.0	96.8	3.0	96.8	3.0	96.8						
12 Apr	2.3		2.2	95.7			2.7	117.4	2.5	108.7	2.4	104.3						
29 May	3.2		2.5	78.1			2.8	87.5	2.6	81.3	2.8	87.5						
4 Jun	2.5		1.9	76.0			2.5	100.0	2.4	96.0	2.5	100.0						
18 Jun	4.8		3.2	66.7			4.3	89.0	4.1	85.4	4.0	83.3						
11 Jul	26.2		21.7	82.8			25.5	97.3	26.2	100.0 ^a	26.2	100.0 ^a						
16 Jul	24.3		20.9	86.0			24.3	100.0 ^a	24.3	100.0 ^a	24.3	100.0 ^a						
10 Aug	12.0						11.5	95.8	10.9	90.8	9.7	81.0						
2-3 Sept	10.2				9.5	93.1	9.3	91.2	8.2	80.4	7.0	68.6	10.4	101.6	6.8	66.6	10.0	98.0
22 Sept	1.6				0.8	50.0	0.7	43.8	0.4	25.0	0.4	25.0	0.7	43.8	0.9	56.0	0	0
3 Oct	4.0				3.8	95.0	3.8	95.0	3.6	90.0	2.8	69.7	3.3	82.5	3.9	97.5	3.1	77.5
21-22 Nov	5.3				4.9	92.5	5.0	94.3	5.1	96.2	4.0	75.5	4.0	75.5	5.6	105.7	5.2	98.1
26 Nov	18.2				17.4	95.6	17.1	94.0	18.9	103.8	16.9	92.9	14.8	81.3	18.8	103.3	18.5	101.6

^aPlot undergoing repair, runoff estimated at 100%.

Table 2. Runoff results from rainfall on waterproof treatments at Granite Reef Testing Site - continued.

Date	Total Rainfall	L-1a Runoff		L-1b Runoff		L-4 Runoff		L-5 Runoff		L-6 Runoff		L-7 Runoff		A-1 Runoff		A-2 Runoff	
	(mm)	(mm)	(%)	(mm)	(%)	(mm)	(%)	(mm)	(%)	(mm)	(%)	(mm)	(%)	(mm)	(%)	(mm)	(%)
1967																	
28-29 Nov	16.6			15.1	91.0	15.5	93.4	17.2	103.6	15.3	92.2	13.0	78.3	16.9	101.8	16.7	100.6
13 Dec	2.2			2.1	95.5	2.2	100.0	2.2	100.0	2.1	95.5	2.0	90.9	2.5	113.6	1.6	72.7
14 Dec	17.8			15.9	89.3	15.8	88.8	16.9	94.9	16.8	94.4	13.5	75.9	17.5	98.3	17.2	96.6
14-15 Dec	45.2			48.9	108.2	45.7	101.1	47.3	104.6	34.5	76.3	38.3	84.7	45.2	100.0 ^b	32.6	72.1
18-19 Dec	29.2			32.8	112.3	30.0	102.7	31.8	109.0	27.4	93.8	29.4	100.6	30.7	105.0	30.2	103.4
19 Dec	18.6			12.9	69.6	17.7	95.0	19.2	103.1	18.5	98.4	18.0	96.9	19.0	102.2	18.8	101.2
Total	272.1	77.6	85.1	164.1	97.2	264.2	97.1	271.7	99.9	264.3	90.5	147.4	87.3	167.8	99.3	153.9	91.1

^bWater ran into storage from outside, runoff estimated at 100%.

Table 3. Directional rainfall measurements by Vector pluviometer at Granite Reef Testing Site.

Date	Total Rainfall Collected	<u>Collection by Orifice Facing Direction Listed</u>							
		North		East		South		West	
1967	(ml)	(ml)	(%)	(ml)	(%)	(ml)	(%)	(ml)	(%)
23 Jan	58	7	12.1	0	0	13	22.4	38	65.5
10 Mar	0	Trace		0	0	0	0	0	0
29 Mar	184	41	22.2	60	32.6	27	14.7	56	30.5
4 Apr	88	31	35.2	42	47.7	0	0	15	17.1
11 Apr	73	10	13.7	3	4.1	10	13.7	50	68.5
12 Apr	54	23	42.6	1	1.9	3	5.5	27	50.0
29 May	17	5	29.4	12	70.6	0	0	0	0
4 Jun	33	Trace		33	100.0	0	0	0	0
18 Jun	29	5	17.2	23	79.4	0	0	1	3.4
11 Jul	872	248	28.5	15	1.7	425	48.7	184	21.1
16 Jul	546	362	66.3	21	3.8	38	7.0	125	22.9
10 Aug	350	170	48.6	37	10.6	23	6.6	120	34.2
2-3 Sept	41	23	56.1	0	0	10	24.4	8	19.5
22 Sept	0	0	0	0	0	0	0	0	0
3 Oct	23	4	17.4	2	8.7	17	73.9	0	0
21-22 Nov	45	19	42.2	7	15.6	7	15.6	12	26.6
26 Nov	354	121	34.2	10	2.8	81	22.9	142	40.1
28-29 Nov	315	70	22.2	5	1.6	60	19.0	180	57.2
13 Dec	11	0	0	6	54.5	3	27.3	2	18.2
14 Dec	235	111	47.2	2	0.9	50	21.3	72	30.6
14-15 Dec	1070	500	46.7	5	0.5	365	34.1	200	18.7
18-19 Dec	973	205	21.1	184	18.9	334	34.3	250	25.7
19 Dec	509	100	19.6	95	18.7	152	29.9	162	31.8
Total	5880	2055	34.9	563	9.6	1618	27.5	644	28.0

Table 4. Smooth soil treatments on large plots at Granite Reef Testing Site.

Plot	Treatment Date	Treatment
L-2	30 Nov 1961	Smoothed soil, 14.14 m × 14.14 m plot
L-3	4 Aug 1965	Smoothed soil, 14.14 m × 14.14 m plot treated with R-9 at 0.057 kg m ²
A-3	1 Aug 1967	Smoothed soil, 6 m × 30 m plot
E-3	10 Dec 1964	Smoothed soil, 7.6 m × 15.2 m plot
W-2	1 Dec 1963	Uncleared watershed
W-3	1 Dec 1963	Cleared watershed
R-2	1 Mar 1965	Ridge and Furrow - 10% side slope
R-4	13 May 1966	Ridge and Furrow - 10% side slope treated with 44.9 g m ⁻² sodium carbonate

Table 5. Runoff results from rainfall on smooth soil plots at Granite Reef Testing Site.

Date	Total Rainfall	L-2 Runoff		L-3 Runoff		A-3 Runoff		E-3 Runoff		W-2 Runoff		W-3 Runoff		R-2 Runoff		R-4 Runoff	
1967	(mm)	(mm)	(%)	(mm)	(%)	(mm)	(%)	(mm)	(%)	(mm)	(%)	(mm)	(%)	(mm)	(%)	(mm)	(%)
23 Jan	4.1	0.2	4.9	1.7	41.5			0.9	22.0	0.1	2.4	0.2	4.9	1.1	26.8	1.0	2.4
10 Mar	1.6	0	0	0.5	31.3			0	0	0	0	0	0	0	0	0	0
29 Mar	14.8	0.4	2.7	10.6	71.7			2.3	15.8	0	0	0.6	4.0	2.0	13.5	5.4	36.7
4 Apr	4.3	0.1	2.3	1.9	44.2			0.6	14.0	0	0	0.3	7.1	0	0	0.7	16.1
11 Apr	3.1	0.1	3.2	0.5	16.1			0.6	19.4	0.1	3.2	0.5	16.1	0	0	0	0
12 Apr	2.3	0.2	8.7	0.8	34.9			0.7	30.4	0	0	0	0	0.4	17.4	0	0
29 May	3.2	0	0	0.9	28.1			0.5	15.6	0.1	3.1	0	0	0	0	0	0
4 Jun	2.5	0	0	0.7	28.1			0.6	24.0	0.2	8.0	0.2	8.0	0	0	0	0
18 Jun	4.8	0	0	0.3	6.3			0.5	10.4	0	0	0	0	0	0	0	0
11 Jul	26.2	13.1	50.0 ^a	15.7	60.0 ^b			8.8	33.6	3.6	13.7	6.6	25.2	7.5	28.6	10.3	39.3
16 Jul	24.3	12.1	50.0 ^a	14.6	60.0 ^b			12.6	51.9	7.2	29.6	5.0	20.6	12.6	51.8	16.1	66.1
10 Aug	12.0	4.9	40.8	7.2	60.0 ^c	4.1	34.2	5.4	45.0	3.7	30.8	5.5	45.8	6.7	55.8	7.6	63.6
2-3 Sept	10.2	0	0	0.6	5.9	0	0	0	0	0	0	0	0	0	0	0	0
22 Sept	1.6	0	0	0	0	0	0	0	0	0	0	0	0	0	0	0	0
3 Oct	4.0	0	0	0	0	0	0	0	0	0	0	0	0	0	0	0	0
21-22 Nov	5.3	0	0	2.2	41.5	4.5	84.9	0	0	0	0	0.3	5.7	0	0	0	0

^aPlot undergoing repair, runoff estimated at 50% from similar storms 1966.

^bPlot undergoing repair, runoff estimated at 60% from similar storms 1966.

^cMeter plugged, runoff estimated at 60% from similar storms 1966.

Table 5. Runoff results from rainfall on smooth soil plots at Granite Reef Testing Site.

Date	Total Rainfall	L-2 Runoff		L-3 Runoff		A-3 Runoff		E-3 Runoff		W-2 Runoff		W-3 Runoff		R-2 Runoff		R-4 Runoff	
1967	(mm)	(mm)	(%)	(mm)	(%)	(mm)	(%)										
26 Nov	18.2	3.1	17.0	12.5	68.9	4.8	26.4	4.2	23.1	1.2	6.6	3.3	18.1	3.2	17.6	4.3	23.6
28-29 Nov	16.6	7.3	44.0	14.0	84.3	10.2	61.4	7.0	42.2	3.6	21.7	8.3	50.0 ^d	7.1	42.8	9.8	59.0
13 Dec	2.2	0	0	0	0	0	0	0	0	0	0	0	0	0	0	0	0
14 Dec	17.8	2.1	11.8	10.9	61.2	5.0	28.1	3.0	16.9	0	0	0	0	2.5	14.0	4.0	22.5
14-15 Dec	45.2	20.2	44.7	42.4	93.8	17.8	39.4	18.4	40.7	14.8	32.7	21.3	47.1	19.5	43.1	26.3	58.2
18-19 Dec	29.2	3.9	13.4	18.2	62.3	4.4	15.1	4.4	15.1	1.8	6.2	3.4	11.6	3.2	11.0	5.5	18.8
19 Dec	18.6	11.3	61.0	16.6	88.1	10.7	57.3	9.8	52.7	7.3	39.1	10.4	56.2	10.1	54.4	13.0	68.8
Total	272.1	79.0	29.0	172.8	63.5	61.5	34.0	80.3	29.5	43.7	16.1	65.9	24.2	75.9	27.9	104.0	38.2

^dRunoff into storage from outside, runoff estimated at 50% from similar storm 19 December 1967.

TITLE: APPLICATION OF HEXADECANOL - OCTADECANOL MONOFILMS
TO SMALL PONDS

LINE PROJECT: SWC W7 gG-3

CODE NO.: ARIZ.-WCL-9

INTRODUCTION:

Studies with long-chain alkanol dispersions for reducing evaporation were concluded this year with two studies in February and March 1967 simultaneously comparing the effectiveness of the dispersion and powdered alkanol.

PROCEDURE:

The dispersion used in the studies was a 1% alkanol dispersion diluted from a 10% concentration prepared as described in previous annual reports. The effectiveness of the treatments for reducing evaporation was determined on the 2.74 m diameter tanks as described in previous annual reports. The powdered alkanol and dispersion were both applied daily at the required application rate.

RESULTS AND DISCUSSION:

The first study was conducted for 7 days starting 27 February 1967. The dispersion and powdered alkanol were both applied at a rate of 1.1 grams of actual alkanol $m^{-2} month^{-1}$ [10 lbs acre $^{-1} month^{-1}$]. During this period, with an average untreated evaporation rate of 4.6 mm day $^{-1}$, there was no measurable reduction with the powdered alkanol. The dispersion reduced evaporation 28%. In the second study, conducted for 10 days starting 10 March 1967, the dispersion application rate was unchanged but the powdered alkanol application rate was increased to 5.5 grams of alkanol $m^{-2} month^{-1}$. For this study the average untreated evaporation rate was 3.3 mm day $^{-1}$. The dispersion reduced evaporation by 27% while the powdered alkanol reduced evaporation by 15%. During these studies there was a heavy layer of dust on the water surface. It was observed the dispersion compressed the dust into small patches while the powdered alkanol did not.

SUMMARY AND CONCLUSIONS:

Evaporation studies were conducted comparing the effectiveness of long-chain alkanol dispersions with that of powdered alkanol for reducing evaporation. The dispersion, a 1% dispersion diluted from a 10% concentration, and the powdered alkanol were both applied at a rate of 1.1 grams alkanol m^{-2} month $^{-1}$. Evaporation was reduced 28% with the dispersion, but there was no measurable reduction from the powdered alkanol. In a second study the same rate of dispersion was applied and the powdered alkanol rate increased to 5.5 grams alkanol m^{-2} month $^{-1}$. The dispersion reduced evaporation by 27% while the powdered alkanol reduced evaporation by 15%.

These studies indicate the dispersions are more effective in reducing evaporation with lower application rates than can be achieved with powdered alkanols.

PERSONNEL: L. E. Myers and G. W. Frasier

TITLE: MEASUREMENT AND CALCULATION OF UNSATURATED CONDUCTIVITY
AND SOIL WATER DIFFUSIVITY

LINE PROJECT: SWC W7 gG-5 CODE NO.: Ariz.-WCL-13

INTRODUCTION:

The objectives and need for study for this project were given in the 1961 Annual Report of the U. S. Water Conservation Laboratory. Annual Reports for 1962, 1963, and 1965 reported work concerning conductivity and soil water diffusivity measurements at several porosities and temperatures. The 1966 report concerned deviations from Darcy's law for flow of water through fine pores. This report contains data on the flow of various polar and nonpolar liquids through two ceramic plates in an attempt to elucidate the effect of structuring of polar molecules and electrokinetic effects on flow through very fine pores.

When a polar fluid such as water flows through a porous material, an interaction between the polar molecules and the charged pore surface occurs, which results in a retardation of flow. The degree of interaction and the amount of flow retardation are functions of pore size and the degree of polarization of the molecule. A review of Henniker (1) shows data indicating that water has an apparent increase in viscosity due to this interaction. This viscosity increase has been reported to extend a distance of 1500 \AA from the wall. If true, such interactions would greatly retard flow through fine pores and thin water films in unsaturated soils.

When ions are present in the fluid a "double layer" is set up near the wall due to the interaction between the ions and the pore wall. When water flows through the pore, some ions are swept along creating a streaming potential that retards flow. This electrokinetic flow retardation has been treated as an apparent increase in viscosity. Rice and Whitehead (3) presented a theory for electrokinetic flow in fine pores that predicted a maximum retardation occurred at a pore radius of 5.1×10^{-5} cm for pure water.

Most reported experimental studies with polar fluids and electrokinetic flow were for pores of $> 5 \times 10^{-5}$ cm radius, and for a polar and nonpolar fluid. The results presented here are from experiments using ceramics with pore radius of 1.5×10^{-5} and 5×10^{-6} cm and for several polar fluids having differing degrees of polarization.

MATERIALS AND METHODS:

Two ceramic plates of nominal pore radius of 1.5×10^{-5} and 5×10^{-6} cm were used in the experiments. The ceramic plates were epoxied between two glass funnels which in turn were epoxied to an all glass falling head permeameter similar to Figure 3 page 13-12 of the 1966 Annual Report. Solutions of 0.1, 0.01, and 0.001 N KCl, LiCl, and NaCl were separately used as the permeating fluid for experiments concerning electrokinetic flow retardation. Benzene, nitrobenzene, acetone, and chloroform were used in the experiments concerning flow retardation due to interaction between polar molecules and pore walls. Physical properties of the organic fluids obtained from various handbooks are given in Table 1.

RESULTS AND DISCUSSION:

Permeability data for various salt solutions and organic fluids are given in Tables 2, 3, and 4. Tables 2 and 3 show that the permeability increases with increasing salt concentration as electrokinetic flow theory would predict. However, when the theory of Rice and Whitehead is applied to the data, the results are inconsistent. The theory predicts a lower value of permeability for the 0.001 M KCl solution than was actually measured. This discrepancy is greater for the 5×10^{-6} cm pore radius ceramic than for the 1.5×10^{-5} cm ceramic. A probable explanation of this is that solutes dissolved from the ceramic cause the solution within the pores to be more concentrated than the original solution. Experiments are now underway to ascertain the equilibrium concentration within the pores.

Tables 2 and 3 show that different monovalent salts yield very nearly the same permeabilities. For the salts, the permeabilities are $KCl > NaCl > LiCl$ in the same order the cations are classified as "water structure makers" or "water structure breakers." Horne (2) presents data showing K as a "structure breaker" and Li as a "structure maker," with Na intermediate. Our data show that the "water structure" effect due to dissolved ions has a measurable effect on water flow through fine pores, but that the effect is small.

The four organic fluids were chosen to give a range of dipole moments. Dipole moments were taken to be a measure of the polarizability of the molecule and thus an indication of the degree of structuring due to the interaction between the pore wall and polar molecules. Figure 1 shows for the 1.5×10^{-5} cm pore radius ceramic, that the permeabilities decrease with increasing dipole moment. Data for the 5×10^{-6} cm pore radius ceramic, given in Table 4, show a similar decrease. Data for nitrobenzene are not yet available so comparisons between pore sizes will be made later. Preliminary calculations indicate that there is no simple relation between pore size and flow retardation due to interaction between pore walls and polar molecules. Future experimental data may clarify this point.

Figure 1 shows that the permeabilities for 0.1 M KCl and benzene are nearly the same. The 0.1 M KCl is of sufficient concentration to compress the double layer and minimize electrokinetic effects and is a "water structure breaker." Benzene is nonpolar and therefore structuring due to the charged pore wall should not be present. For the finer pored ceramic, the 0.1 KCl and benzene are also nearly the same (Tables 3 and 4).

The main conclusion from these data is that water permeability for flow through fine pores is not very different than for other polar fluids. Earlier literature (4) reported that water permeabilities were 6- to 10-fold less than for other polar fluids. These data were for sandstones containing a small amount of clay. We conclude that

clay migration may have caused the reduction but not water structure, electrokinetic effects, and interaction between the pore wall and the polar fluids.

SUMMARY AND CONCLUSIONS:

Flow of polar and nonpolar fluids and salt solutions through ceramic plates having nominal pore radii of 1.5×10^{-5} and 5×10^{-6} cm was measured. The objective was to determine the effect of interaction between pore walls and polar and nonpolar fluids on flow through fine pores, and to determine the effect of salts on the flow of water through pores of these sizes. For the 1.5×10^{-5} cm pores, flow rates decreased with an increase in dipole moment of the permeating fluid. Flow rates were in the order benzene > chloroform > acetone > nitrobenzene. A 0.1 N KCl solution yielded identical permeability as benzene. Permeabilities decreased with decreasing concentration of salt with a 5% difference between 10^{-1} and 10^{-3} N, and only 15% difference between 10^{-1} N KCl and water containing only dissolved substances from the plate. Permeabilities were on the order of 2×10^{-12} cm².

Permeabilities for the ceramic with 5×10^{-6} cm pore radii for different salt solutions show similar trends to the other ceramic. Permeabilities were on the order of 5×10^{-14} cm². Polar and non-polar fluids also show similar trend to the other ceramic.

The main conclusion from this study is that structuring of fluids due to interaction of polar molecules with pore walls reduce flow, but only to a small degree, generally less than 10%. Electrokinetic flow reduction occurs, but is also small.

REFERENCES:

1. Henniker, J. C. The depth of the surface zone of a liquid. Rev. of Mod. Phys. 21:322-341. 1949.
2. Horne, R. A. Cation exclusion from gels. Commun. to the Editor. Jour. Phys. Chem. 70:1335-1336. 1966.

3. Rice, C. L., and Whitehead, R. Electrokinetic flow in a narrow cylindrical capillary. Jour. Phys. Chem. 69:4017-4024. 1965.
4. Von Engelhardt, Wolf, and Tunn, W. L. M. The flow of fluids through sandstones. Heidelberger Beitr. zur Min. un Petrographic. 2:12-25. 1954.

PERSONNEL: R. D. Jackson and F. S. Nakayama

Table 1. Physical properties of fluids used.

Fluid	Density g cm ⁻³	Viscosity cgs	Dipole Moment
Benzene	0.879	0.00602	0
Chloroform	1.498	0.00535	1.15×10^{-18}
Acetone	0.792	0.00307	2.8×10^{-18}
Nitrobenzene	1.119	0.0184	4.23×10^{-18}
Water	0.998	0.00895	1.84×10^{-18}

Table 2. Permeabilities of the 1.5×10^{-5} cm pore radius ceramic to various salt solutions.

Salt	Permeability ($\text{cm}^2 \times 10^{12}$)			
	Salt concentration (moles liter ⁻¹)			
	a	0.001	0.01	0.1
KCl		2.23	2.28	2.30
LiCl		2.19	2.26	2.27
NaCl		2.22	2.27	2.27
Water-solutes	2.01			
from ceramic	2.08			
	2.13			
	2.17			

^a An unknown concentration of solutes resulted from dissolution of the ceramic plate. This concentration increased with time.

Table 3. Permeabilities of the 5×10^{-6} cm pore radius ceramic to various salt solutions.

Permeability ($\text{cm}^2 \times 10^{14}$)				
Salt	Salt concentration (moles liter ⁻¹)			
	a	0.001	0.01	0.1
KCl		5.08	5.21	5.31
LiCl		4.99	5.14	5.21
Water-solutes from ceramic	5.07			

^a An unknown concentration of solutes resulted from dissolution of the ceramic plate. This concentration increased with time.

Table 4. Permeability of ceramic plates to several organic fluids.

Fluid	Permeabilities	
	Ceramic plate	
	1.5×10^{-5} cm radius	5×10^{-6} cm radius
Benzene	2.29×10^{-12}	5.41×10^{-14}
Chloroform	2.16×10^{-12}	5.14×10^{-14}
Acetone	2.10×10^{-12}	4.77×10^{-14}
Nitrobenzene	2.07×10^{-12}	--

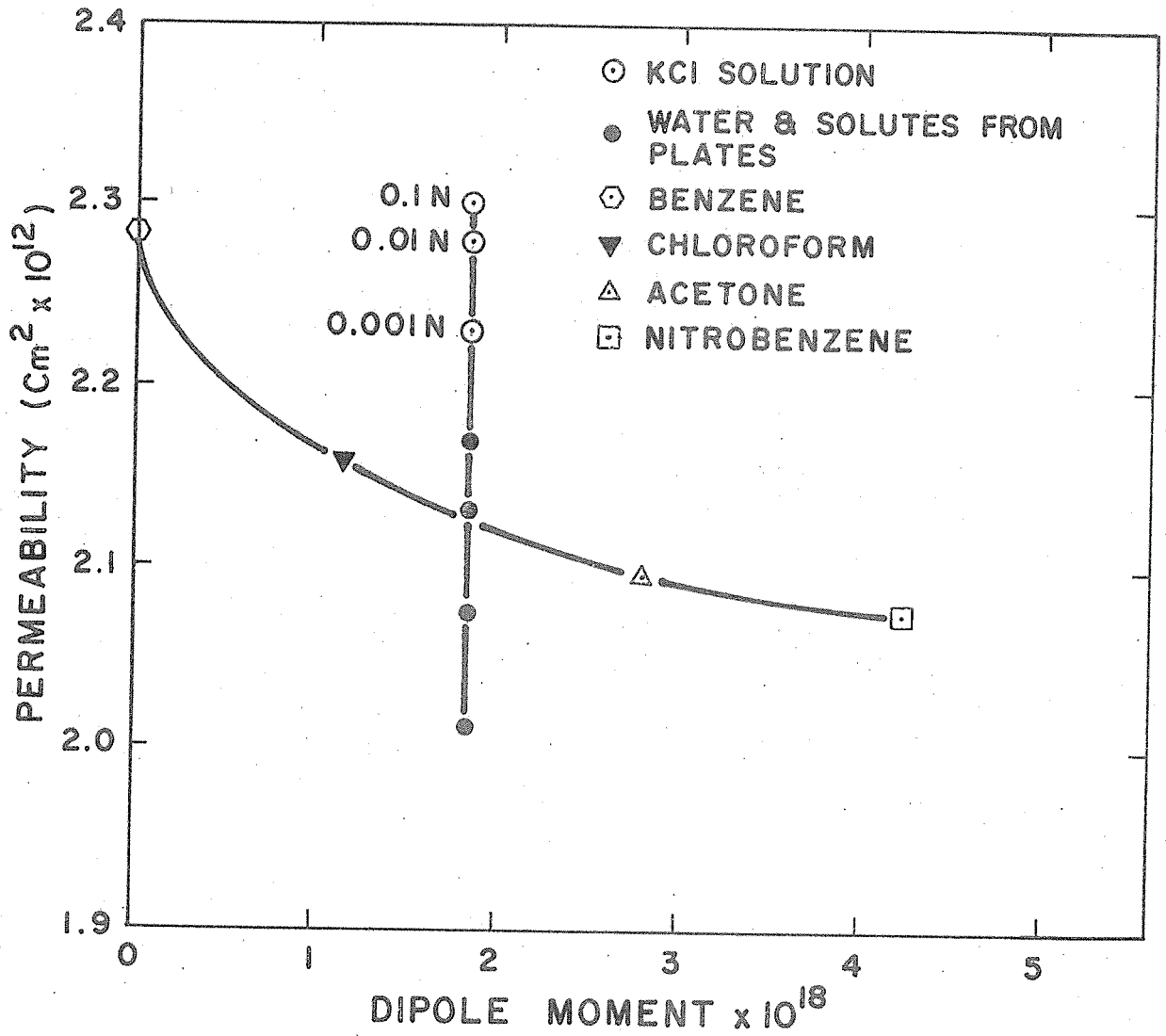


Figure 1.

TITLE: FIELD APPLICATION OF FALLING HEAD TECHNIQUE FOR SEEPAGE METERS AND OF DOUBLE-TUBE METHOD FOR HYDRAULIC CONDUCTIVITY MEASUREMENT

LINE PROJECT: SWC W7 gG-2

CODE NO.: Ariz.-WCL-14

INTRODUCTION:

Field studies with the salt penetration technique for seepage measurement were continued to develop a workable field procedure, particularly where the velocity of the water in the channel makes it difficult to obtain sufficient coverage and contact time of the salt on the bottom.

PROCEDURE:

Two field tests were conducted in canals of the Salt River Project. The first measurement was obtained in a canal south of Tempe, Arizona. The canal had a velocity of about 0.3 m/sec and relatively turbid water. The bottom consisted of very loose, fine material in a layer of 0.4 m thick. Core samples were obtained to determine the porosity of the loose material. Aluminum sulphate was applied to cover two strips approximately 1 m wide across the channel. The depth of the electrical-conductivity peak (point P, see Annual Report 1966) was measured at about 10 points in this strip at 2, 4, and 21 hours after the salt was applied. The conductivity probe and method of determining the depth of point P were described in Annual Report 1966.

The second test was in a canal north of Mesa, Arizona. Because of relatively high velocity in the canal and a water depth of 3 ft, the salt crystals would not remain in place long enough to permit sufficient amounts of salt to enter the soil. Thus, an alternate method of application had to be employed. Aluminum sulphate crystals were placed in a burlap sack to obtain a confined "body" of salt of sufficient flexibility to conform to the bottom of the channel. The sack was maneuvered into place with four guide ropes (one on each corner) and allowed to stay at one place from 10 to 20 minutes, after which it was moved to the next location, etc. Two men, one on each side of

the canal, were required to maneuver the sack. The depth of the conductivity peak was measured from 1 to 6 hours after the salt had been applied.

RESULTS AND DISCUSSION:

The advance of the conductivity peak after salt application is shown in Figure 1 for the two locations of the first test. Each dot represents an average of about 10 points. The graph shows that the peak advances at a constant rate. Assuming that the seepage was constant during this period, this illustrates the piston-flow movement of the peak. The lines do not pierce the origin, indicating an immediate advance of point P at the time of salt application. This was probably due to the very loose and soft bottom material, which the salt crystals could very easily have penetrated for 1/2 to 1 cm upon application. The porosity of the loose bottom material was 0.66. Porosity values obtained in previous tests for relatively dense bottom materials ranged from 0.4 to 0.5. In many cases, an estimate of the bottom porosity in the range 0.4-0.6 will yield sufficiently accurate values for the seepage rate. This eliminates the need for obtaining core samples for porosity determination in the laboratory, and thus enhances the utility of the salt penetration technique for routine seepage measurements.

Results from the second test indicated that the technique of applying salt with the burlap sack technique worked satisfactorily and enabled sufficient salt penetration under conditions of high velocity in the channel. The burlap sack must be kept in place for 20 minutes per location to yield a well-defined conductivity peak in the bottom material. The seepage rate for these tests was about 8 cm/day.

SUMMARY AND CONCLUSIONS:

Field tests using the salt penetration method for measuring seepage losses from canals were conducted to develop field techniques and to demonstrate the usefulness of the procedure. A field test

confirmed previous laboratory tests that the advance of the salt concentration peak is essentially a process of piston flow for a depth up to 15 cm. For deep or fast-flowing channels, a special application technique using burlap sacks filled with the salt was developed to keep the salt in place and to maintain sufficient contact time to obtain a well-defined conductivity peak. The burlap sacks should be kept in place for a period of 20 minutes, after which it can be moved to another part of the channel bottom.

PERSONNEL: Herman Bouwer and R. C. Rice.

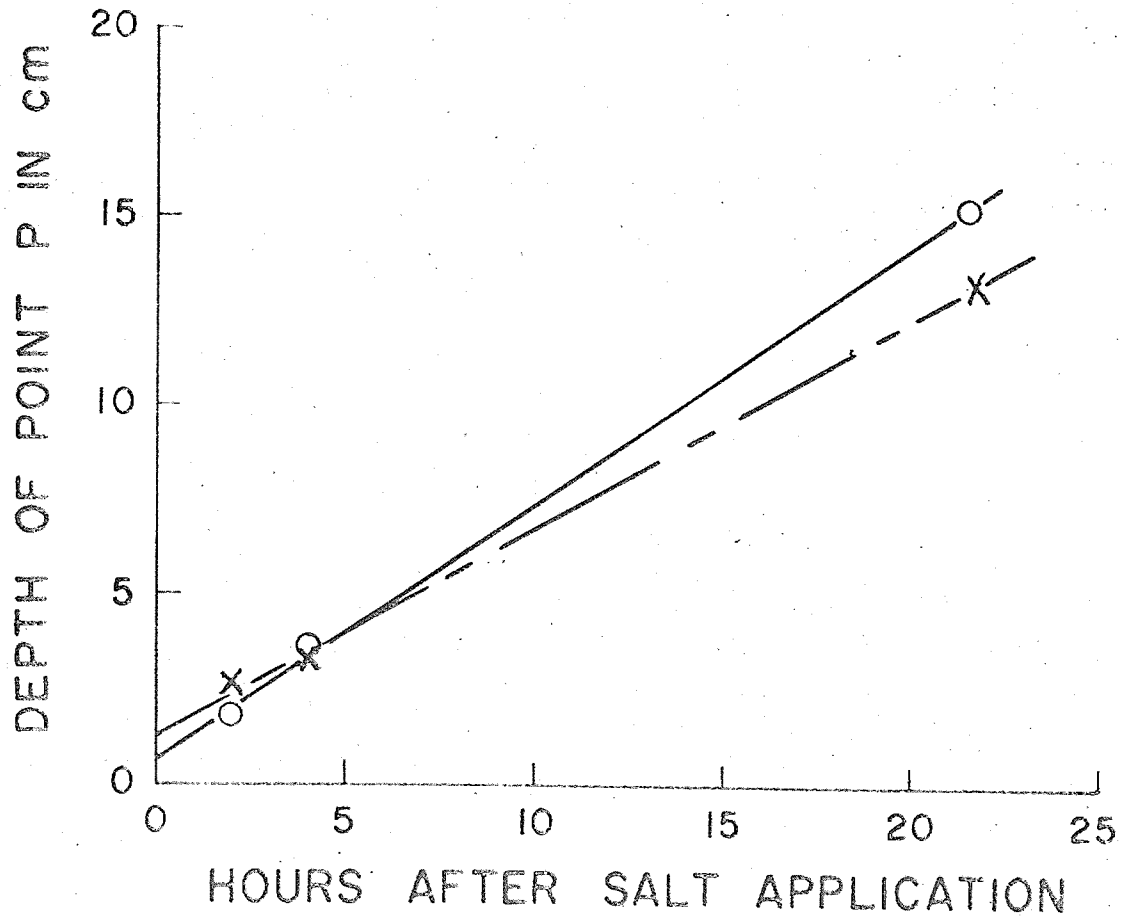


Figure 1. Depth of point P versus time after salt application in irrigation channel.

TITLE: CONSUMPTIVE USE OF WATER BY CROPS IN ARIZONA
LINE PROJECT: SWC W9 gG-6 CODE NO.: Ariz.-WCL-23
PART I: RELATIONSHIP OF METEOROLOGICAL MEASUREMENTS WITH
CONSUMPTIVE USE FOR OPTIMUM COTTON PRODUCTION.

INTRODUCTION:

For need of study, see Annual Reports for 1957, 1958 and 1966.

OBJECTIVES:

1. To correlate certain meteorological measurements with water management on cotton.
2. To determine the comparative production of present-day cotton varieties with older varieties, under a previously determined irrigation schedule.
3. To determine the comparative consumptive use for several varieties of cotton.

PROCEDURE:

The experiment is located on Field C-1 at the University of Arizona Cotton Research Center, Phoenix, Arizona. The field was planted to cotton in 1966 and to alfalfa during the previous two years. 100 lbs of nitrogen were applied on 16 Dec. 1966. The field was plowed, furrowed out, and a pre-planting irrigation given on 7 Mar. On 24 Mar., Deltapine Smoothleaf seed was planted on the East half of the field. The West half was planted in 4-row plots to five varieties: Deltapine Smoothleaf, Stoneville 213, Acala 44-10, Hopicala, and Pima S-4, in a randomized block design replicated four times.

Irrigations were given when visual plant symptoms and soil moisture determinations indicated the plants needed water. In so doing, an attempt was made to duplicate the 65% concept recommended by this office. All varieties in the treatment plots were irrigated on the same day, regardless of differences in soil moisture tensions.

Piche atmographs, net radiometers and anemometers were installed

in the East half of the field about 8 June. On 17 July, a hygro-thermograph was installed within the plant canopy.

Yield measurements were made on 244 ft of the two inside rows of the 4-row plots. Two pickings were made by machine. Samples were selected and processed to determine lint percentage.

Soil moisture measurements were made at three locations in the meteorological data area, and in three replications of each variety.

RESULTS AND DISCUSSION:

A good stand was attained, but cool temperatures in the early growing season (mean April temperature, 5° below normal) caused slow growth, thus plants were smaller than usual by mid-June. First blossoms did not open until about 25 June.

Excess shedding was noted early, and was believed to be due to lygus injury. Corn-ear worms also did considerable damage throughout the season. An extensive pink boll worm control program was carried out during the season beginning 12 July, with 14 spray applications being used.

Irrigations were given on 23 May, 29 June, 24 July, 15 Aug., and 12 Sept. The July and August irrigations were given later than visual plant symptoms indicated, to facilitate a supporting study on leaf temperature. Soil moisture depletion at these irrigation dates was somewhat greater than the 65% normally used to indicate need for irrigation. However, no extreme plant stress conditions were noted. It was felt that yield was affected more by corn-ear worm damage than by excessive soil-moisture stress on the short-staple varieties, but long-staple yield may have been lowered by the excessive soil-moisture stress.

SUMMARY AND CONCLUSIONS:

In spite of the generally unfavorable early growing season and the high worm and insect infestation, all cotton varieties used about the same amount of water (Table 1 and Figure 1). In 1966, Pima S-4 used considerably less water than the short-staple varieties. In

1967 it did not, but again the fact that corn-ear worm affected the long-staple considerably less than the short-staple varieties may have been a factor. Seasonal consumptive use was down about 7 in. from a long-term mean.

PART II: UP-DATING CONSUMPTIVE USE ESTIMATES FOR SORGHUM.

INTRODUCTION:

For need of study, see Annual Reports for 1956, 1957 and 1960.

OBJECTIVES:

1. To determine the consumptive use of, and make evaporimeter measurements on, one of the originally-used varieties (DD-38) and one of the present-day, popular hybrid varieties of sorghum.
2. To check for possible correlation of evaporation as indicated by Piche evaporimeter with consumptive use.

PROCEDURE:

The experimental plot is located on Field H, Borders 20, 21, 22 and 23 at the University of Arizona Mesa Experiment Farm, Mesa, Ariz. Minimum tillage was used prior to preparation of 40-in. beds. 75 lbs of nitrogen were applied and a pre-planting irrigation was given on 12 June. Borders 20 and 23 were planted to Hegari sorghum in an attempt to minimize bird damage to the main plots near time of harvest. Borders 21 and 22 were divided into four plots each. Two plots on each border were planted to DD-38 and two to NK-310, making a total of four replications for each variety.

Irrigations were given when visual plant symptoms and soil moisture determinations indicated the plants needed water. All varieties were irrigated on the same day regardless of differences in soil moisture tensions.

A Piche atmograph was installed over DD-38 in Border 22 on 4 Aug. Yield measurements were made on areas 90 ft x 13.3 ft in each plot. Soil moisture measurements were made at two locations in each of the three varieties.

RESULTS AND DISCUSSION:

Sorghum was planted on 22 June and an excellent stand obtained. An irrigation was given on 30 June for corn-borer control. Regular irrigations were given 1 Aug., 16 Aug., 1 Sept., and 27 Sept. DD-38 initially grew more rapidly than the other two varieties. It also headed sooner and matured faster than either the NK-310 or the Hegari.

The last irrigation was given when the DD-38 was already in the late dough stage. Soil moisture samples in the DD-38 plots indicated that enough available moisture remained to fully mature this variety. The NK-310 and the Hegari were still in the blossom-to-milk stage when the final irrigation was given. Consumptive use figures for the double-dwarf variety may be somewhat high because of this final irrigation.

Yield measurements were made only on DD-38 and NK-310. Yields were 5269 and 6156 lbs per acre, respectively, for the DD-38 and NK-310. This amounted to a 17% increase in favor of NK-310.

SUMMARY AND CONCLUSIONS:

DD-38 matured about two weeks earlier than NK-310 or Hegari. Since all varieties were within the same borders, irrigation of one necessitated the irrigation of the other. The fourth irrigation, though light, was necessary for the NK-310 and the Hegari, but not for the DD-38. Although the consumptive use for the DD-38 was measured at 30.7 in., it is estimated it would have been nearer 26 in. without the late, unnecessary irrigation (Figures 2, 3, and 4).

Studies in the late 1950's utilizing Hegari, RS-610, and DD-38 showed the need for correlating the last irrigation with the maturity date. These studies showed, as do this year's, that the number of irrigations are associated with the seasonal consumptive use, especially the last irrigation, which encourages second growth. In this year's study, if each of the first three irrigations could have been delayed three days, a fourth irrigation would probably not have been required for the Hegari or the NK-310. Early studies showed that the first

irrigation was necessary on DD-38 earlier than on Hegari. The response of NK-310 showed it to be similar to Hegari, and thus we can assume the water management for the hybrid NK-310 to be similar.

PERSONNEL: Leonard J. Erie and Orrin F. French

Table 1. Yield and consumptive use of water by cotton, 1967.

Varieties	Seed lb/plot	Lint %	Lint		Consumptive use
			lb/plot	bales/A	
Acala 44-10	397	39.8	158.0	2.1	34.5
Deltapine S.L. ^a	357	39.0	139.4	2.5	33.2
Pima S-4	397	37.0	146.9	2.0	34.3
Hopicala ^a	294	40.3	118.5	2.1	33.7
Stoneville 213	486	40.5	196.8	2.6	34.4

^a Only three replications used in yield measurements.

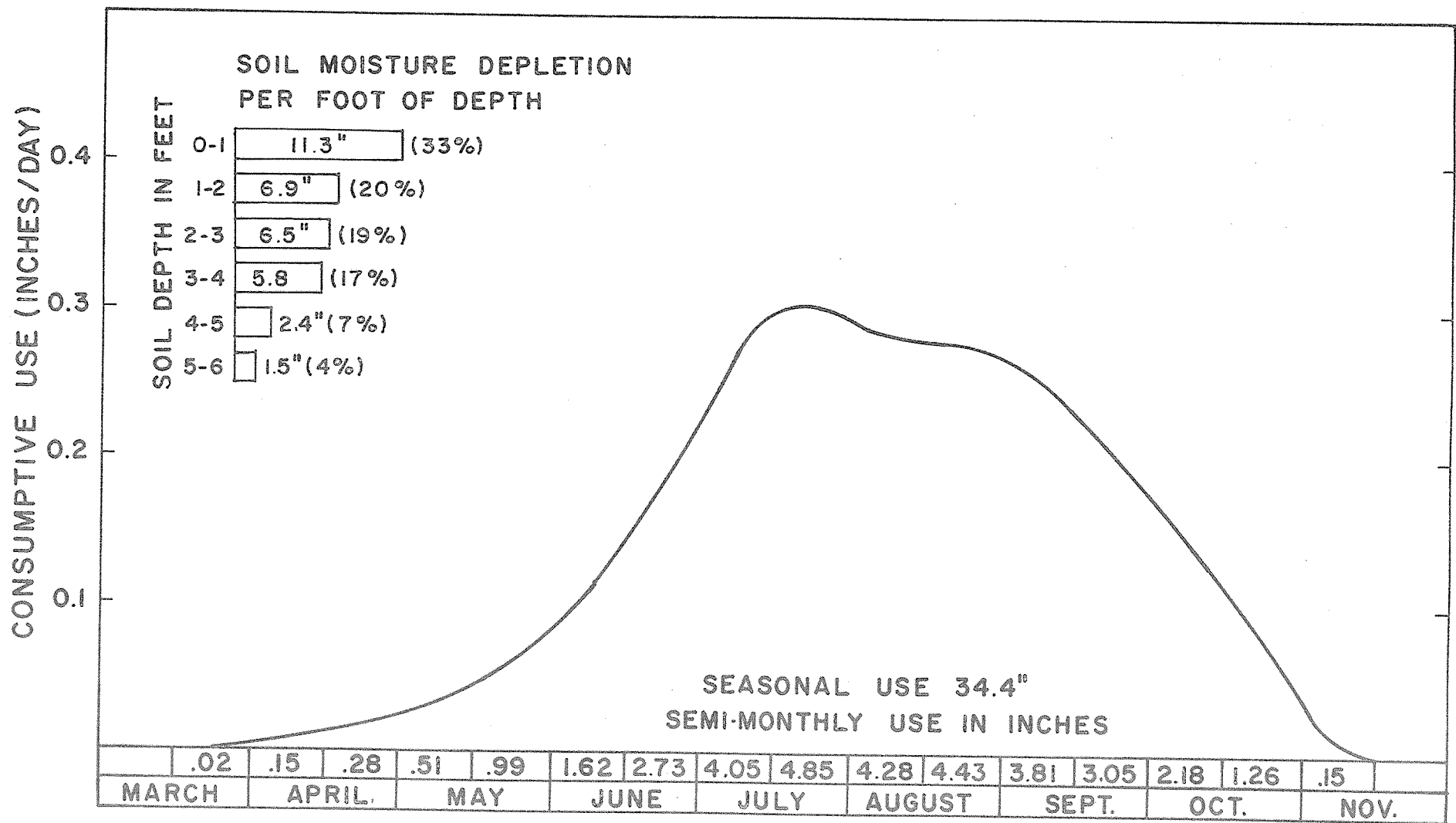


Figure 1. Consumptive use for cotton, at Cotton Research Center, Phoenix, Arizona 1967.

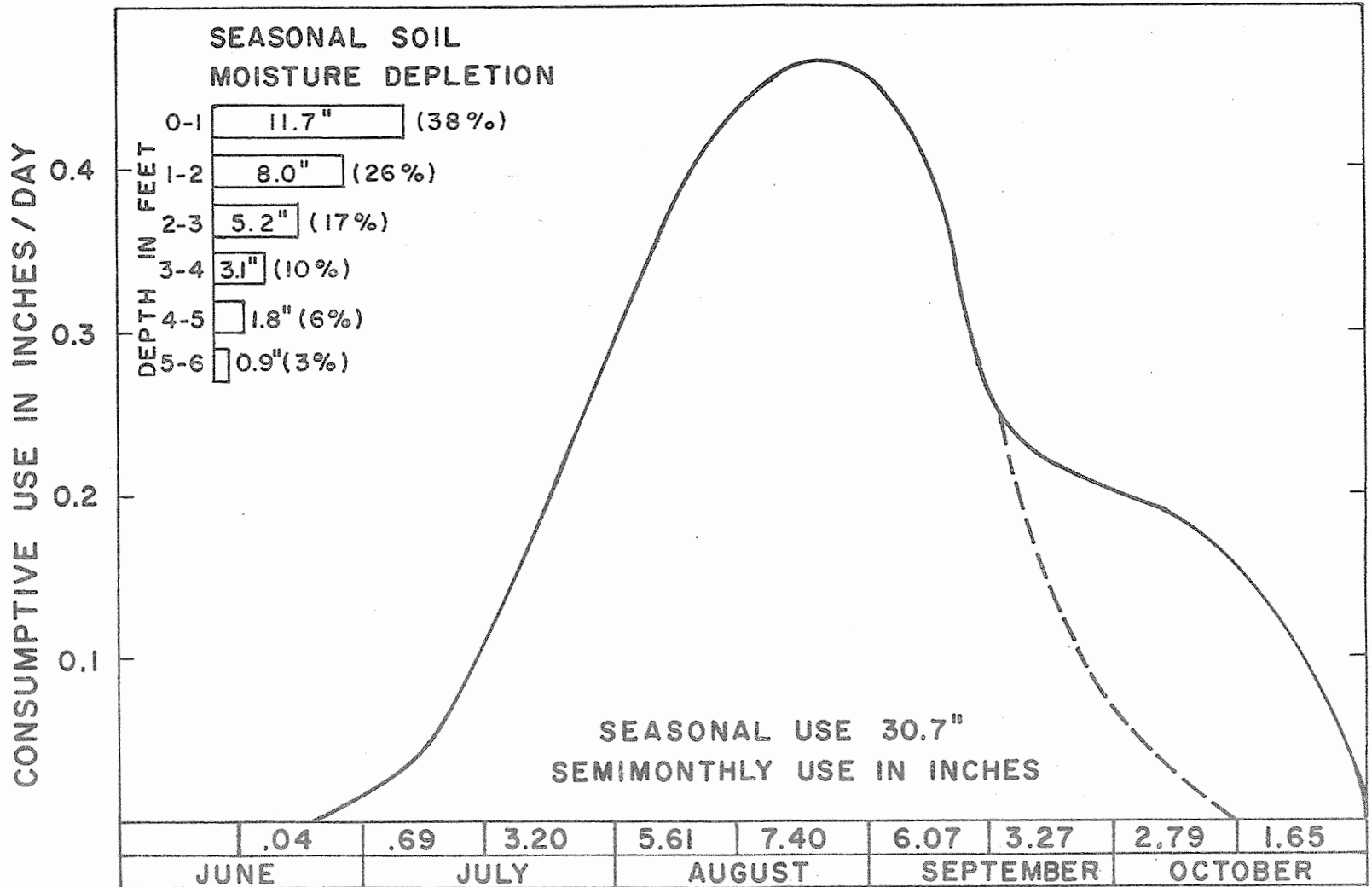


Figure 2. Consumptive use for sorghum (DD-38) at Mesa, Arizona 1967.

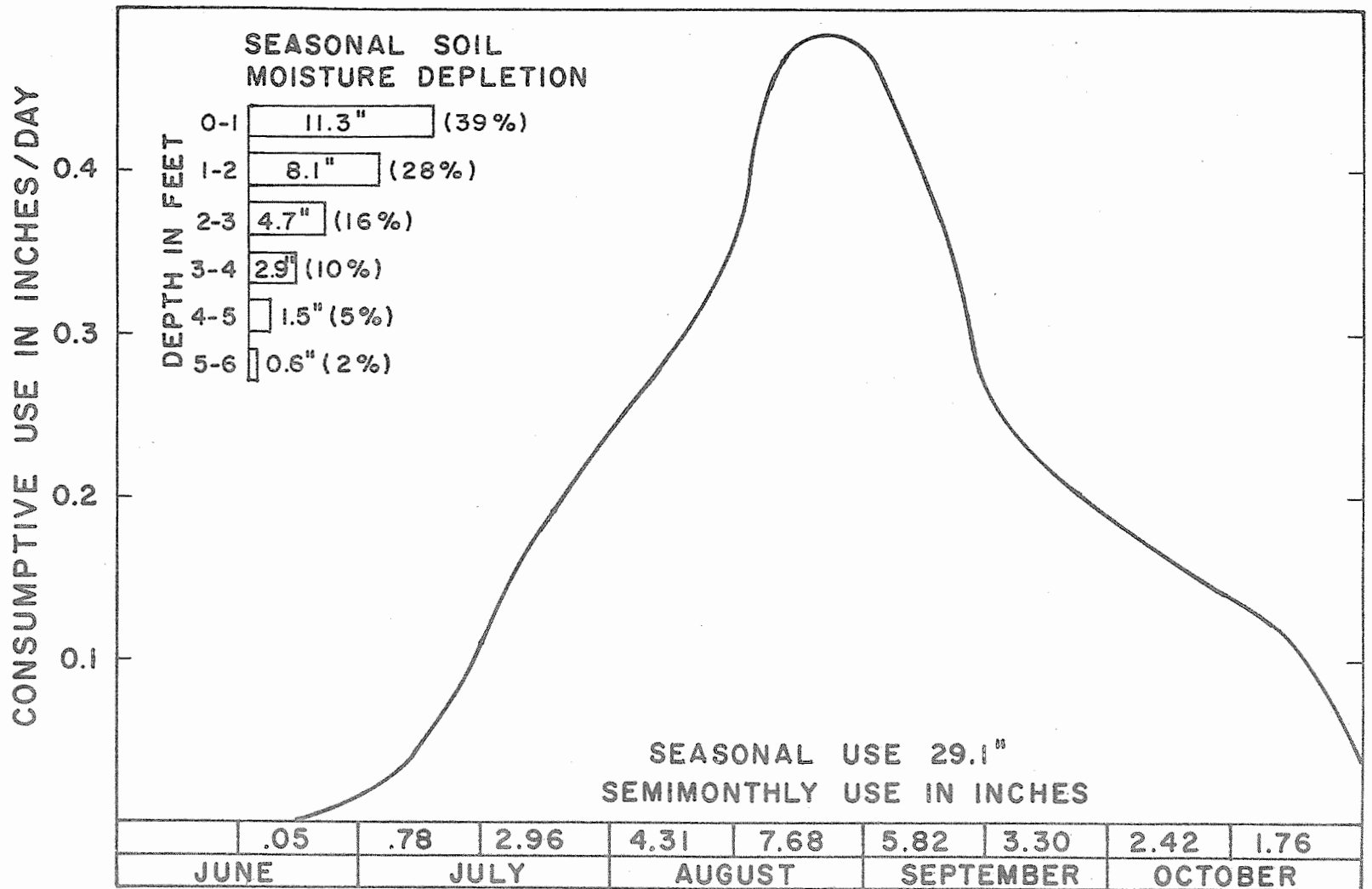


Figure 3. Consumptive use for sorghum (Hegari) at Mesa, Arizona 1967.

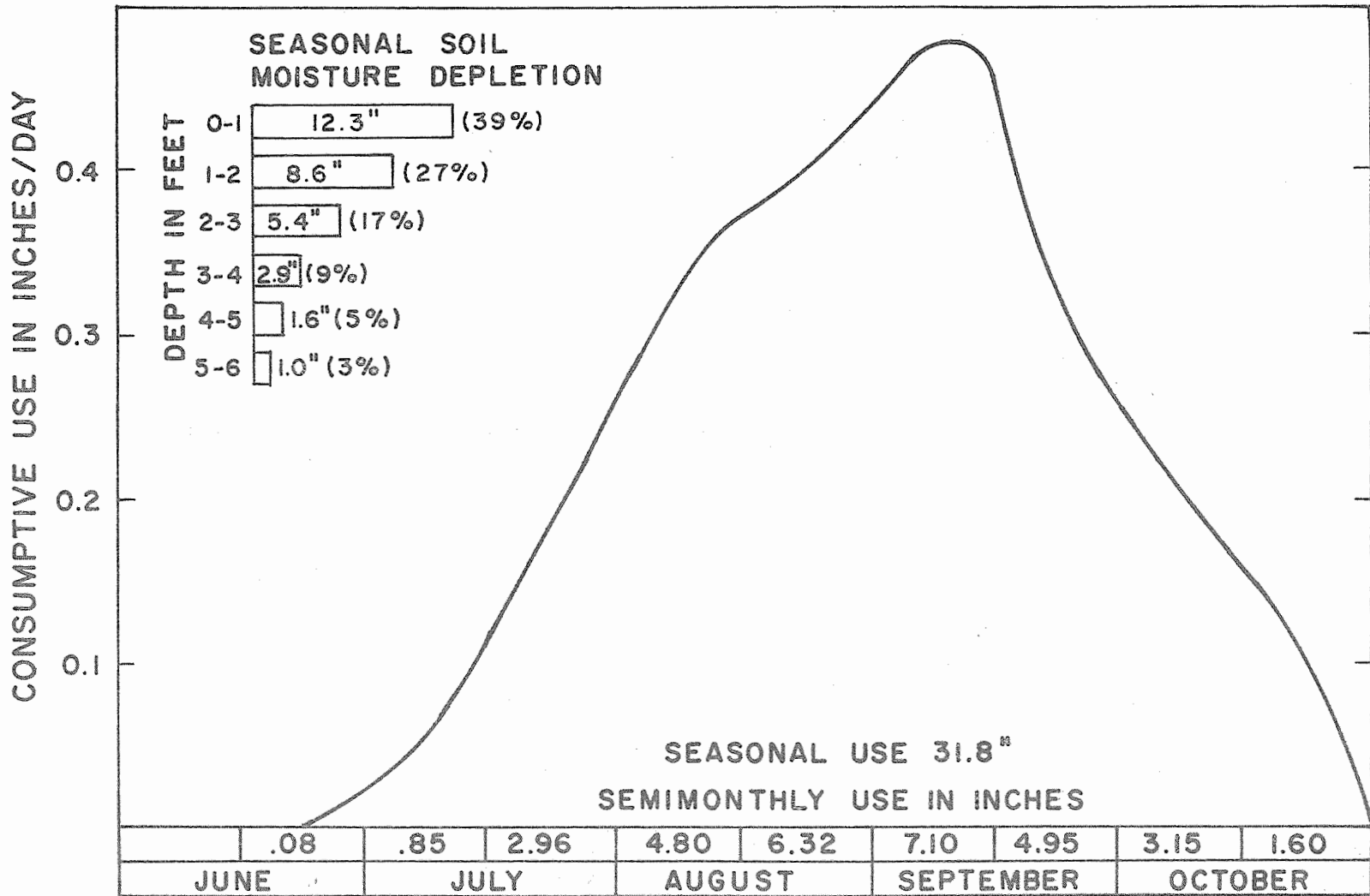


Figure 4. Consumptive use for sorghum (NK-310) at Mesa, Arizona 1967.

TITLE: MEASURING HORIZONTAL AND VERTICAL CONDUCTIVITY OF SOIL
WITH THE DOUBLE-TUBE METHOD

LINE PROJECT: SWC W7 gG-1

CODE NO.: Ariz.-WCL-25

INTRODUCTION:

Work was continued on the fast-response field tensiometer system as outlined in Annual Report 1966. The tensiometer system should be able to provide adequate and accurate pressure-head data for hydraulic conductivity and evapotranspiration measurements.

PROCEDURE:

The tensiometer system (see Annual Report 1966 for details) was installed at a new location in the bermudagrass lawn. The test plot was 150 cm square with a sheet metal border surrounding the plot. The area outside the test plot acted as a buffer zone. A neutron access tube was installed in the center of the plot for water content measurements. Location and depth of the tensiometers are shown in Figure 1.

The plot area was inundated to "saturate" the profile. The plot area was then covered with a plastic sheet to prevent evaporation, so that changes in water content were due to drainage alone. After drainage was essentially complete, the plot was uncovered and evaporation was allowed. Numerous wetting and drying cycles were conducted throughout the year.

When the pressure head at a certain depth became less than -800 cm, the tensiometers at that depth were disconnected to reduce the chance of air entering the rest of the tensiometer system. This was necessary only for the tensiometers at shallow depths.

RESULTS AND DISCUSSION:

The tensiometer system performed satisfactorily for a 10-month period.

Water content-pressure head curves were obtained for soil depths from 25 to 130 cm from the numerous wetting and drying cycles. These curves are shown in Figures 2 and 3. The unsaturated hydraulic

conductivity (K)-pressure head (P) relationship was obtained from the drainage of the plot when evaporation was excluded. This was done using the procedure of Van Bavel (see Annual Report 1966). The K-P curves are shown in Figures 4 and 5 for depths 40 to 130 cm.

Brooks and Cory (1) have shown that the relation between K and P should plot as two straight lines on log log paper and can be expressed by

$$K = K_0 \text{ for } P \geq P_a$$

and

$$K = K_0 \left(\frac{P_a}{P} \right)^\eta \text{ for } P < P_a$$

where

K_0 = K at $P = 0$,

P_a = air-entry pressure of the soil,

η = pore size distribution index.

Values of K_0 , P_a , and η are given below for the different depths.

Depth cm	K_0 cm/hr	P_a cm	η —
40	0.017	-35	1.76
55	0.029	-34	1.89
70	0.068	-21	1.60
85	0.087	-31	2.20
100	0.070	-29	2.33
130	0.077	-28	2.05

Brooks and Cory indicated that η can theoretically not be less than 2. The value of η may approach 2 when the medium has a very wide range of pore sizes. However, the work of Brooks and Cory was done on laboratory columns with soil that had no structure. Their theory

also states that K_0 is obtained at or near 100% saturation and at a pressure head between zero and P_a . Saturation of 100% is seldom attained in the field. Pressure heads between zero and P_a in this experiment occurred at 70 to 80% saturation. Since the lower limit of η is based on the relative saturation versus pressure relationship, this lower limit may have to be revised to compensate for the fact that 100% saturation is not achieved when P is between zero and P_a .

During evapotranspiration from the bermudagrass, a diurnal trend in the pressure head was observed, particularly at the shallower depths. An example of this behavior for the 5-cm depth is shown in Figure 6. A very rapid change in pressure occurred during the daylight hours and essentially no change occurred during the night. Data for depth from 10 to 70 cm also showed a higher rate of pressure change during the day than at night even though drainage was occurring at times. The high rate of pressure change during the day is indicative of water uptake by roots. From the unsaturated hydraulic conductivity characteristics and accurate hourly hydraulic gradient values, it may be possible to calculate root uptake in the profile and separate this from drainage on an hourly basis. Future work will be aimed toward this.

SUMMARY AND CONCLUSIONS:

The multiple tensiometer system consisting of a small volume displacement transducer connected to a number of tensiometers through a hydraulic scanning valve performed satisfactorily for 10 months under field conditions. Well-defined soil water characteristics were obtained for soil depths from 25 to 130 cm by using the tensiometer data in connection with water content measured with the neutron scattering method. The unsaturated hydraulic conductivity characteristic was obtained from a drainage cycle with evaporation excluded using the method of instantaneous profiles. The resulting curves showed that the theoretical relationships developed by Brooks and Cory do not hold for field soil. A diurnal behavior of the pressure head, probably due to higher rates of water uptake by the roots during

the day than during the night, was observed. The fast response of the tensiometer system may enable the evaluation of water uptake by roots on an hourly basis.

REFERENCES:

1. Brooks, R. H., and A. T. Cory. Hydraulic properties of porous media. Hydrology Paper No. 3, Colorado State University, Fort Collins, Colorado. March 1964.

PERSONNEL: Herman Bouwer and R. C. Rice.

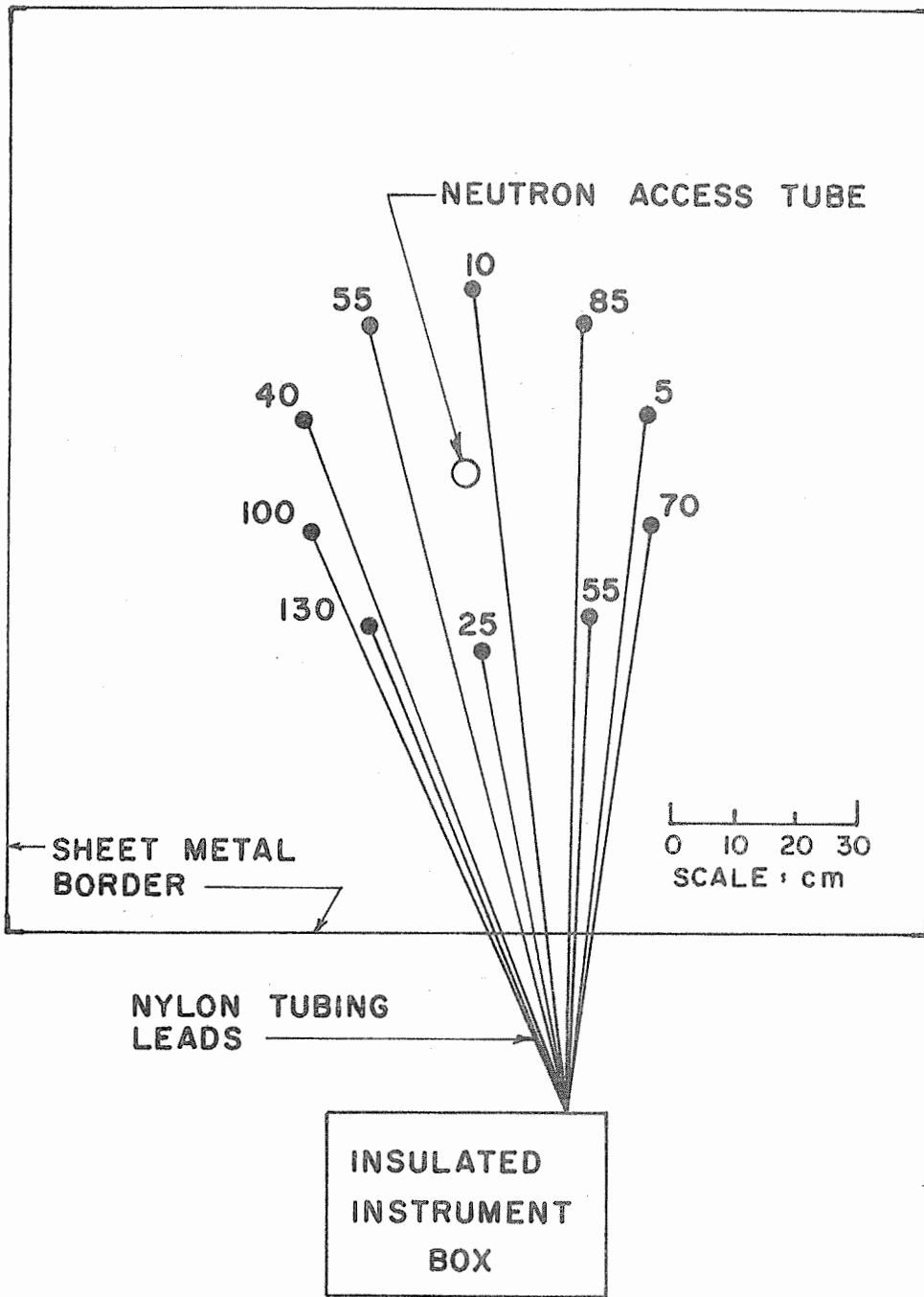


Figure 1. Location and depth in cm of tensiometers in field plot.

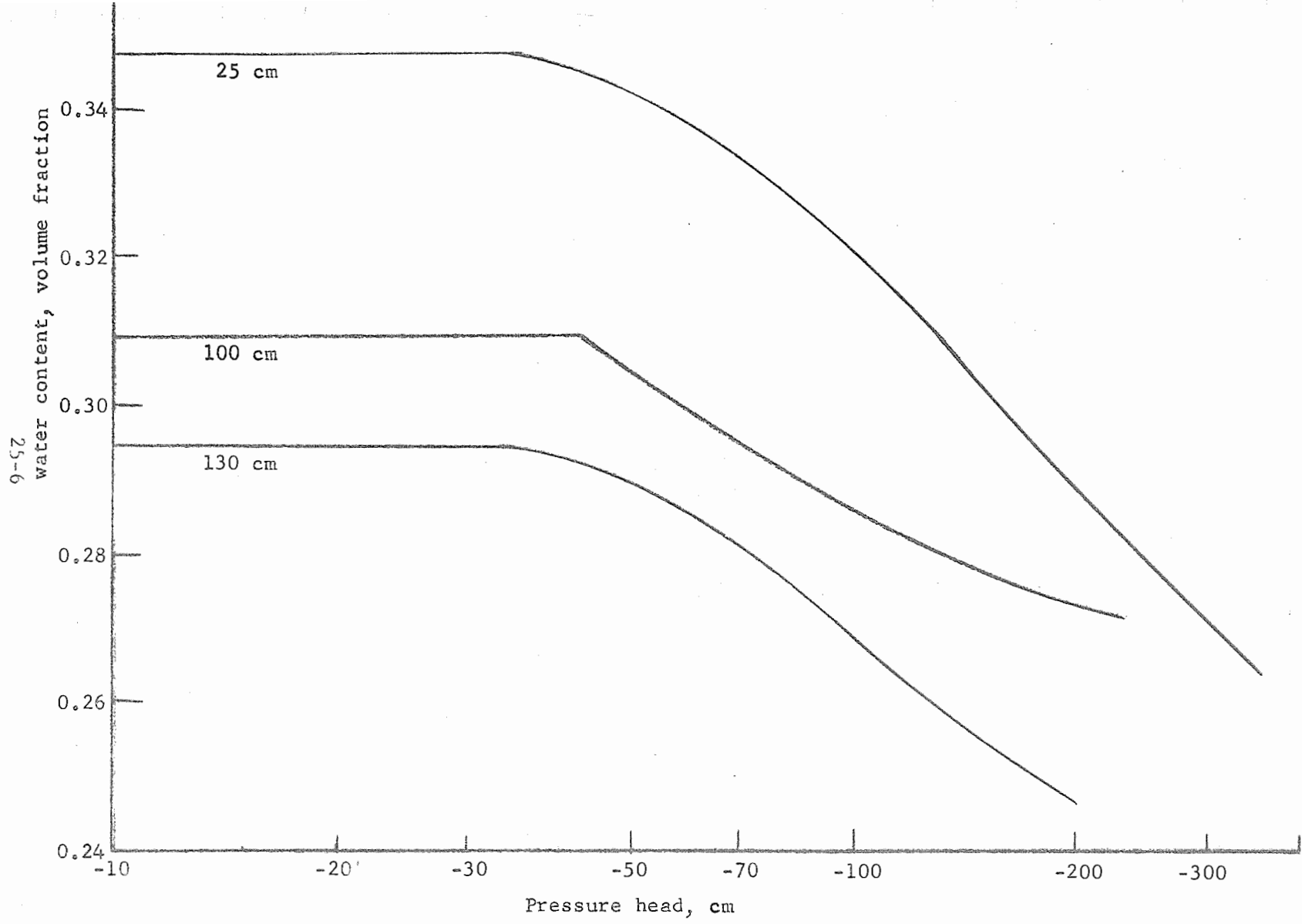


Figure 2. Water content-pressure curves for 25-, 100-, and 130-cm depths.

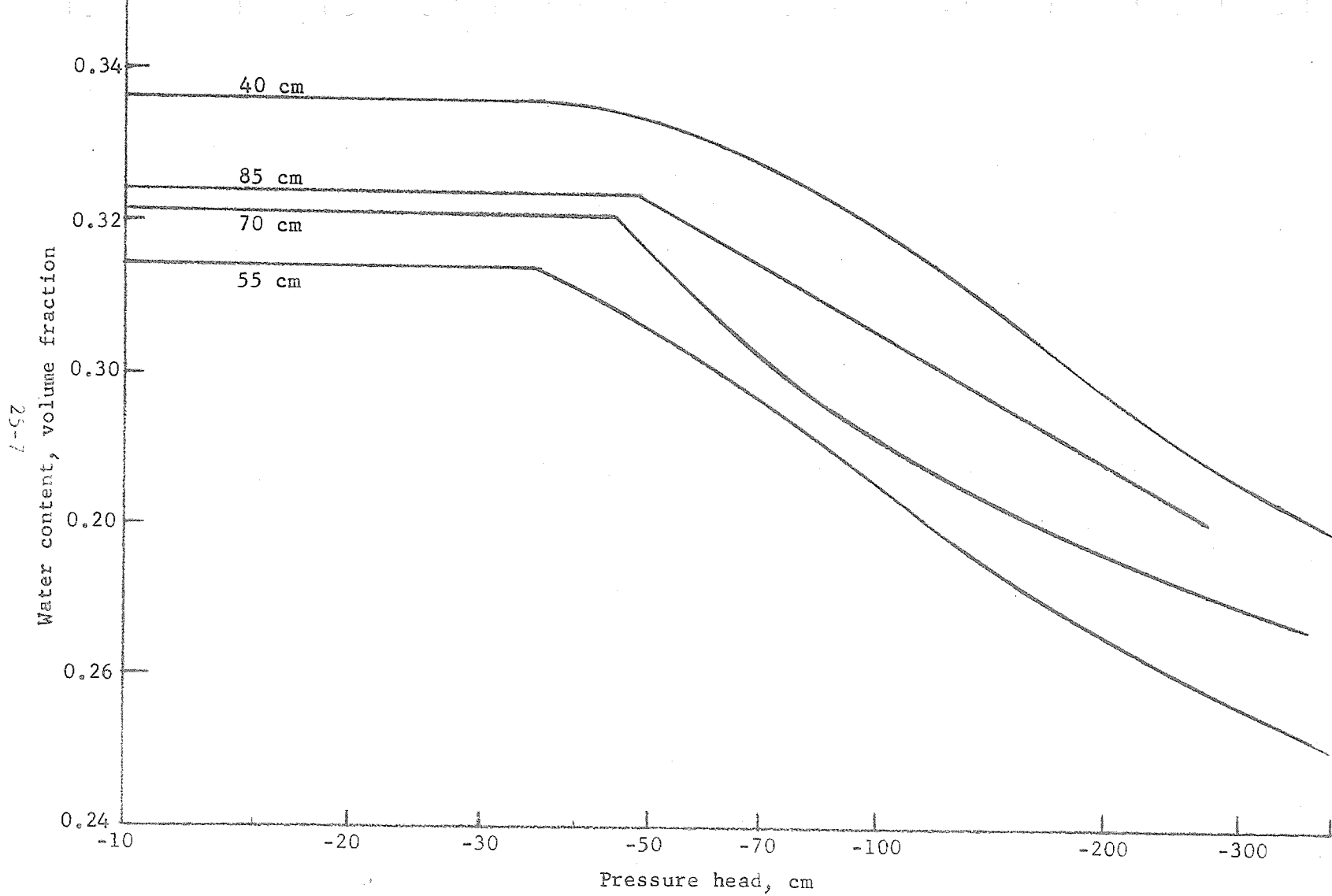


Figure 3. Water content-pressure curve for 40-, 55-, 70-, and 85-cm depths.

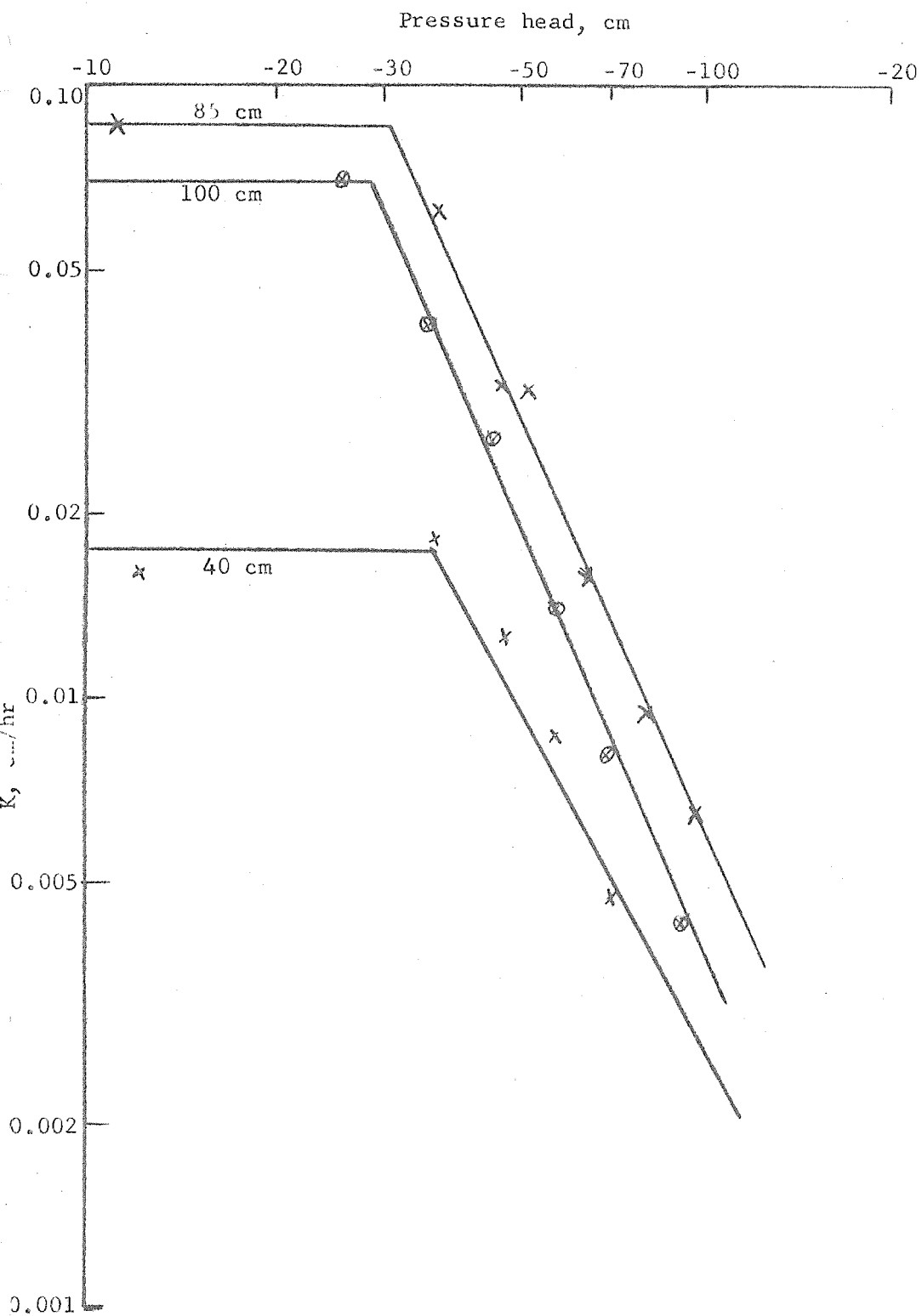


Figure 4. Hydraulic conductivity - pressure curve for 40-, 85-, and 100-cm depths.

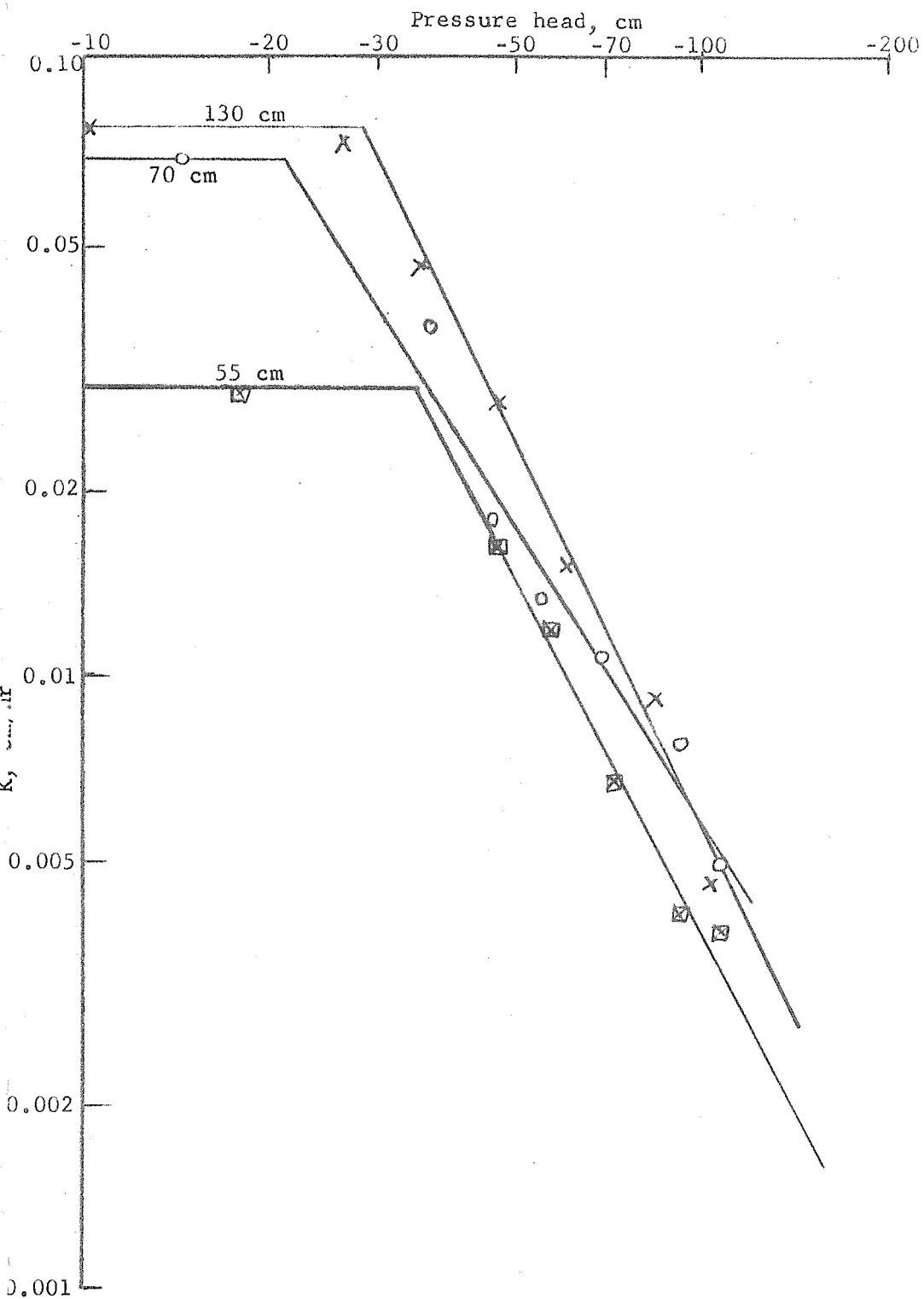


Figure 5. Hydraulic conductivity-pressure curve for 55-, 70-, and 130-cm depths.

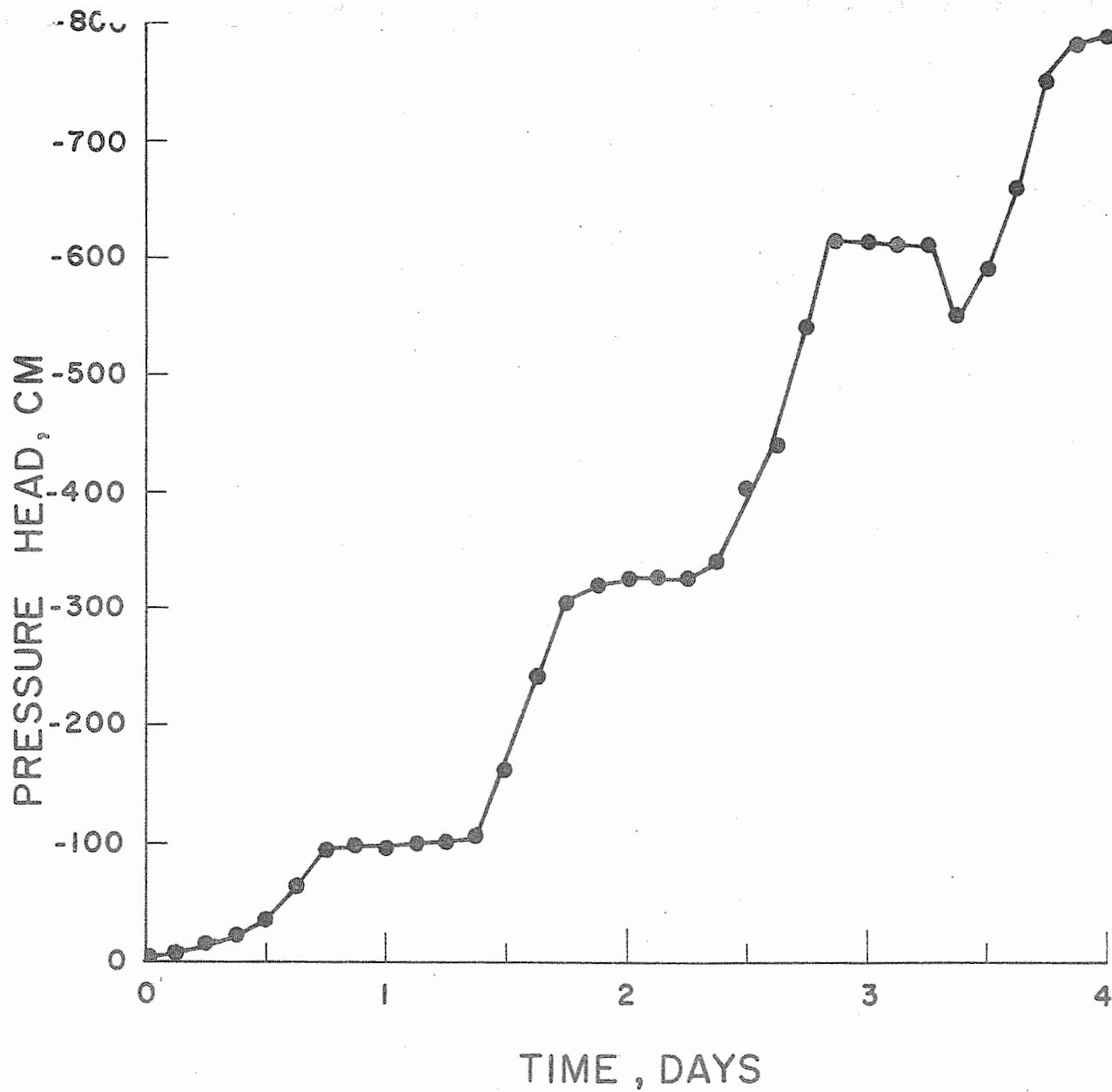


Figure 6. Pressure head record at 5-cm depth in Annual Report of the U.S. Water Conservation Laboratory cover. Day starts at midnight.

TITLE: PLANT RESPONSE TO CHANGES IN EVAPORATIVE DEMAND AND SOIL WATER POTENTIAL, AS SHOWN BY MEASUREMENTS OF LEAF RESISTANCE, TRANSPIRATION, LEAF TEMPERATURE, AND LEAF WATER CONTENT.

LINE PROJECT: SWC W9 gG-6 CODE NO.: Ariz.-WCL-29

PART I. LEAF TEMPERATURE OF TWO SPECIES OF COTTON PLANTS IN THE FIELD AS RELATED TO SOIL WATER DEPLETION.

INTRODUCTION:

The objective was to confirm with the cotton plant what had been demonstrated earlier with sorghum in the field, viz., that a decrease in soil water availability eventually caused a progressive increase in leaf temperature (T_L) due to stomatal closure. If such a plant response could be shown to occur generally, a sensitive measurement of T_L referenced to air temperature (T_A) might be used as a guide to timely irrigation. In the previous research with sorghum, substantial changes in T_L occurred, from at least 5 C below T_A in a recently irrigated soil to an equal amount above T_A when the soil was virtually depleted of available water in the 1.4 m soil profile. However, the extreme depletion of available soil water that was permitted for experimental purposes undoubtedly intensified T_L responses over what might be expected under conventional irrigation practices conducive to optimum yields.

Therefore, since the plan for cotton was to irrigate for maximum lint yield, at no time was it anticipated to permit such a severe soil water depletion as in the sorghum. Consequently, the adequacy of T_L as a guide to irrigation scheduling would be put to a more rigorous test than previously. Nevertheless, it was reasonable to expect a measurable rise in leaf temperature because of the plan for delaying irrigation until 65% of the available water in the upper m of soil was depleted. This schedule usually induces visual symptoms of moderate wilting, due to the prevailing high evaporative demand during midseason and later.

The loss of leaf turgidity is strikingly evident in long staple cotton, but much less so in short staple varieties. This pronounced difference provided a reason for comparing Pima and Deltapine in adjacent plots. The hypothesis was that T_L of both species would rise in response to soil water depletion, with possibly a greater effect in Pima than in Deltapine, due to the visibly greater desiccation in the former when the plants show an internal water deficit.

PROCEDURE:

The experiment was carried out in field C-1 of the University of Arizona Cotton Research Center, about one-half mile south of the Laboratory. The nine-acre field was split into approximately two halves, one a large, homogeneous stand of short staple cotton (Gossypium hirsutum var. Deltapine SL), the other a test comparing four varieties of short staple cotton with a long staple variety (Gossypium barbadense var. Pima S-4). Plant rows were 1 m apart, with a spacing of about 20 cm between plants. Irrigation scheduling of this field was in accordance with a backlog of experimental data gained by Leonard Erie during previous years. See Ariz.-WCL-23 for further details.

Mature leaves near the top of the plant were threaded with 0.1-mm diameter thermocouples, inserted in the midvein. One replication constituted four leaves distributed along 1 m of row length, wired in parallel. The first replication was far enough from the road to be relatively unaffected by dust. Two additional replications were in the same row, spaced 10 m apart. The plants with thermocouples were in the third row of the four-row unit planted to a given variety (Pima S-4). The adjacent four rows to the east were at the edge of a large block of Deltapine SL cotton. Thermocouples were placed in plants of the second row of the four-row unit. Again there were three replications, the sites being along the row, opposite to those of Pima, three rows away.

This arrangement provided a buffer row of each of the two

species; yet the two species being measured were only three rows apart, and therefore most likely were subjected to the same microclimate. Separate, insulated lead wires of copper and constantan led over the ground to a cold junction for temperature reference and to a shelter box housing a 12-point recorder. Hourly readings were printed out of the six sets of T_L and of T_A and vapor pressure, the latter two environmental measurements being taken 1 m above the crop in a ventilated, radiation-shielded housing. Printout of 12 channels took three minutes. As the crop grew, the thermocouples were moved to higher sites so as to be measuring well exposed, mature leaves. The data were obtained hourly over three irrigation cycles occurring in July, August, and September 1967. Four channels were reserved for measurement of boll temperatures later in the season. However, boll abscission at irregular intervals virtually eliminated conclusive data.

Leaf resistance (R_L) readings were taken several times per day on the day preceding irrigation and shortly thereafter, for correlation with T_L data.

Other information of probable value to interpretation of the data collected here, but taken by Leonard Erie and Fred French (See WCL-23) were net radiation 1 m above the crop, daily wind travel at 30 cm and 1 m above the crop, gravimetric soil water content changes with time, continuous Piche evaporimetric losses, and lint yields of the five cotton varieties.

RESULTS:

Figure 1 gives typical T_L results obtained at the time of maximum contrast, i.e., a three-day period including the days before, during, and after irrigation. Despite the visual wilt symptoms of much greater severity in Pima than in Deltapine on 12 September, T_L values were quite similar. At times, however, Deltapine rather than Pima was the warmer, by at least one degree. Leaf resistance readings, having a dependence on stomatal aperture similar to that of T_L ,

could be expected to respond in a manner consistent with T_L responses. However, this was true only part of the time. It is possible that another factor was of considerable importance in this regard; the difference in leaf angle between species.

The definite tendency of Deltapine leaves to assume a leaf angle nearly perpendicular to solar radiation may be more important in explaining differences in T_L between species than R_L data. The leaves of Pima, not having such a strong heliotropic response as those of Deltapine, may thereby avoid such a great radiant energy interception, and thus make a given stomatal aperture relatively more effective in evaporative cooling.

Although R_L data did not help explain differences in T_L between species, they were consistent with the overall change in T_L in response to soil water depletion. For example, the day before irrigation, 12 September, was cloudless, with illumination of 110 kilolux at 1400, when R_L measurements were taken; this illumination was much in excess of the value at which well watered plants show maximum stomatal opening (minimal R_L). Deltapine leaves had R_L values of 4.2 sec cm^{-1} , and Pima 2.6 sec cm^{-1} , as an average of both epidermes. Nine days later, in fully irrigated soil, R_L had dropped to 0.1 to 0.2 sec cm^{-1} in both species, the measurements again being taken at 1400 and in saturation illumination. These data indicate that soil water deficiency was inducing partial stomatal closure on 12 September.

Although the R_L data just cited for plants in dry soil can be described as only moderately high, they definitely indicated partial stomatal closure at the same time that T_L values were a few degrees above air temperature. Later, after a heavy irrigation, T_L dropped to a few degrees below air temperature in response to the decrease in R_L to minimal values.

Similar T_L changes were observed for the two other irrigation cycles. Occasional days showed somewhat greater differences between T_L and T_A than those of Figure 1.

SUMMARY AND CONCLUSIONS:

Field measurements confirmed the main hypothesis, viz., that leaf temperatures of cotton plants in the field respond to changes in soil water content. Negative evidence was obtained for the secondary hypothesis, viz., that long staple cotton (Pima S-4), which shows a much more severe visual wilt than short staple varieties, would show a greater rise in leaf temperature than Deltapine SL, in response to a soil water deficiency imposed by a drying cycle.

Extending over three irrigation cycles, hourly measurements were made of leaf temperatures of exposed leaves near the top of the plant (by use of thermocouples in the leaf midribs) in addition to air temperature and vapor pressure at 1 m above the crop. These measurements were supplemented by periodic leaf resistance readings at critical times. Supplementary data taken by personnel involved in another experiment with the same crop included changes in soil water content, net radiation, Piche evaporation, daily wind travel at two heights, and lint yields from five varieties of cotton.

The leaf temperature of both cotton species was quite similar, but tended to be higher in Deltapine than in Pima. This may have been due to leaf orientation in respect to sun angle, such that Deltapine absorbed more radiant energy than Pima. Leaf temperature changed from 2-3 degrees below air temperature in soil with freely available water to a like amount above air temperature in soil dry enough to cause wilting in early afternoon. Leaf resistance values changed accordingly, being moderately high ($3-4 \text{ sec cm}^{-1}$) in dry soil and negligible (0.1 sec cm^{-1}) in wet soil. In conclusion, with careful technique, it seems feasible to use leaf temperature of cotton as a guide to the irrigation scheduling conducive to favorable lint yields.

PART II. LEAF TEMPERATURE AND TRANSPIRATION OF THE AGAVE

INTRODUCTION:

A greenhouse experiment had shown that transpiration by agave at night over a 12-hour period was twice the daytime value. However, these higher rates at night still were quite low, only $30 \text{ g m}^{-2} \text{ hr}^{-1}$, or $1 - 2 \text{ g hr}^{-1}$ per plant. Due to weighing limitations, this low rate prevented study of a possible periodicity of water loss at night. The problem in essence was one of a low evaporative demand at night, due to the following factors: (1) a lower air temperature (T_A) at night than during the day (21 C vs. 35 C), (2) leaf temperature (T_L) near T_A , (3) vapor pressure maintained near 20 mb, and (4) negligible air movement. An additional factor was the use of a small plant with a consequent low leaf area.

A solution to the problem was sought by conducting an experiment in the controlled environment room. This transfer of experimental sites permitted a higher T_A and consequently T_L , lower vapor pressure (15 mb), and a somewhat greater air movement. In addition, purchase of a larger balance, with a capacity of 13 kg and a sensitivity of one gram, permitted use of a much larger plant than before, with a corresponding gain in leaf area. These measures contributed to an increase in nocturnal transpiration rate, losses of up to 20 g hr^{-1} being obtained. This rate was sufficient to detect significant changes in transpiration during a long period of darkness.

PROCEDURE:

An agave with a fresh weight of 4320 g was transplanted to a 5-1 pot of standard soil, the surface of which had a watertight seal. Greenhouse measurements established a transpiration norm of 20 g during 10-12 hours of daylight as compared to 200-300 g for the rest of the 24 hours.

On the day before the experiment, the plant was taken to the controlled environment room at 1500, where the illuminance of 52 kilolux was similar to that in the greenhouse just before transfer.

Air temperature was 30.0 ± 0.5 C, vapor pressure 15.1 ± 0.2 mb, and CO_2 350 ± 10 ppm. Weight loss measurements began at 1900 on 6 September, and were continued on an hourly schedule. At 2000 the lights were turned off. On 7 September the illumination was increased gradually to 52 kilolux (0.5 ly min^{-1}) from 0800 to 1000. From 0930 to 0940 the plant was irrigated to pot capacity. At 2000 all lights were turned off again. The weighings continued in the dark until 1400 on 8 September, with no further illumination. Therefore, the plant remained in darkness during the time it normally would have been exposed to a sunrise.

RESULTS:

Figure 2 clearly demonstrates the changing transpiration rate in a constant environment. The rate in light was low, and therefore consistent with previous results. Of primary importance is the rate change in darkness (after 2000). Although the data from only the second day are shown, essentially the same pattern occurred on both days. Starting from a low point at 2130, transpiration rose steadily to the peak rate at 0430, and then declined, reaching the low point of essentially no loss shortly after noon. The only notable difference in the responses on the two days was that the sharp peak at 0430 shown in Figure 2 was absent on the previous day. Exclusive of the peak at 0430, the average maximum rate in the dark on both days was 20 g hr^{-1} per plant ($30 \text{ g m}^{-2} \text{ hr}^{-1}$).

The T_L data agree with previous measurements. In the light T_L exceeded T_A 13 C due to radiant energy absorption at the time of a low transpiration rate, and hence of ineffective evaporative cooling. In the dark T_L began to decrease slowly as soon as the lights were turned off, but did not reach ambient temperature for two hours, because of the massive nature of the tissues (the thermocouple being in the center of a leaf 0.5 cm thick). Later, as the transpiration rate steadily increased, T_L gradually decreased, going below T_A . By 0430 T_L was lower than T_A by 2.3, 0.9, and 0.5 degrees, respectively,

for leaves located in descending order from the top.

SUMMARY AND CONCLUSIONS:

Progressive changes in the transpiration rate of agave occurred in the dark in an environment held at 30.0 ± 0.5 C, 15.1 ± 0.2 mb vapor pressure, 350 ± 10 ppm CO₂ content of the air, and with the soil at pot capacity. Leaf temperature data were consistent with transpiration measurements in indicating progressive stomatal opening in the dark. That the peak depression of T_L below T_A coincided with the maximum transpiration rate, illustrates the effectiveness of stomatal opening and its associated evaporative cooling, especially in view of the thickness of the leaves.

The peak transpiration rate occurred between 0400 and 0600 on both days, with the minimum shortly after noon, regardless of whether there was light or not. These results emphasize the importance of the time of day, rather than the presence or absence of light in the regulation of stomatal aperture. The data therefore are preliminary evidence for a circadian rhythm in stomatal opening in agave.

PART III. PLANT RESPONSE TO SOIL AND WATER DEPLETION UNDER A CONSTANT
EVAPORATIVE DEMAND.

INTRODUCTION:

Typical of other research findings is the observation at this Laboratory that evapotranspiration of sorghum in the field did not decrease for 25 days after irrigation, but then declined to 40% of the potential rate in three days. The rate of decrease in transpiration depends on the evaporative demand, the capillary conductivity of soil water, and on certain plant characteristics, such as the osmotic potential (O.P.), which affect the guard cell turgor pressure. Changes in turgor pressure ultimately regulate stomatal aperture. It is reasonable to expect some species differences in ability to regulate water loss by stomatal closure. Subjection of different plant species to an environment that induces wilting in a controlled manner may lead to a better understanding of the mechanism by which a plant regulates its water balance.

Previous work at this Laboratory focussed on induction of wilting by sudden increases in evaporative demand. The wilting was short-lived, however, and not as severe as is found in the field. This undoubtedly was due to the optimum conditions for water absorption afforded by the nutrient solution substrate. Therefore, it was decided to expose plants to a constant evaporative demand, and to induce wilting by limiting water absorption. Three alternatives were considered for depressing water uptake by roots: (1) lowering root temperature, (2) increasing the osmotic potential of the substrate, and (3) depleting available soil water by continued transpiration. Method No. 3 was chosen; this technique can duplicate in one day a drying cycle lasting for three or four weeks in the field.

Plant response to a water deficit can be characterized conveniently in terms of transpiration, leaf resistance, leaf temperature, and leaf water content. The study has been initiated with bean, will progress to other crops such as sorghum and citrus, and will conclude

with highly adapted desert plants such as palo verde (Cercidium floridum) and brittle bush (Encelia farinosa). Such a species comparison also will permit reexamination of the generally held view that mesophytes and xerophytes do not differ significantly in their capacity to deplete the soil of water.

MATERIALS AND METHODS:

Substrate. The requisites were that the substrate (1) provide adequate aeration to the roots, (2) be sufficiently homogeneous to be packed to a uniform bulk density, (3) release water over a range of energy of retention values to permit detection of decreased transpiration by weight loss, (4) be fertile enough to grow normal crops yet not be saline, and (5) have a high infiltration rate, so as to permit almost instantaneous irrigation at the end of a drying cycle.

These requirements were met by thoroughly mixing sphagnum peat moss, sand, and Adelanto loam in the ratio 2:2:1 by volume. Lucite pots 11.5 cm in diameter by 19.5 cm high were packed with six 2.5-cm increments of the standard mixture to a bulk density of 1.10 ± 0.05 .

Determination of Pot Capacity. During packing of the soil an aquarium aerator with a bubbling pressure of 2 mb was placed on the bottom of the pot. This permitted subsequent removal of excess water by vacuum filtration. Then the soil was saturated with a standard nutrient solution. Saturation was ensured by an overnight soaking and further small additions of solution, as judged by the absence of air in the profile and the presence of a surface film of moisture. Vacuum filtration at 333 mb for 15 minutes removed the excess water to a very uniform level, most of the excess being extracted in three minutes. A weight of the pot and contents before and after filtration established the pot capacity, i.e., the amount of water held by the soil after the large pores drained.

By use of an oxygen analyzer and a tensiometer, an air entry value of 19 mb was measured, occurring after eight minutes of vacuum filtration. At the end of the 15-minute filtration, the soil water

tension (SWT) was 25 mb. Therefore, the vacuum filtration succeeded in draining the large pores, and the SWT achieved by the standardized procedure was indeed that corresponding to pot capacity. The soil water content at this state was 0.33 by volume, having been reduced from the saturated value of 0.44.

Measurement of Bulk Density. The bulk density is needed to convert soil water content by weight to a volume basis. Bulk density was determined in the following manner: (1) by calibrating each pot for volume by weighing the pot filled to a reference line inscribed near the top edge, (2) packing the pot with six increments of air-dry soil and calculating the oven-dry equivalent, and (3) correcting the volume for the swelling of wetted soil by measuring the height rise above the reference mark. This procedure gave values for the standard soil of 1.12 to 1.20 for different pots, but with 1.14 as the mode.

Soil Water Characteristic Curves. Since earlier measurements had shown a difference between disturbed and core samples, all later determinations of the soil water content at a given SWT were made from core samples taken from a pot of soil packed by the standard method. The pressure cooker and pressure plate were used to equilibrate rings of soil at the following values of SWT, in bars: 0.050, 0.333, 0.500, 1.000, 5.000, 10.000, and 15.000. From 3 to 24 replications were run. By use of the bulk density values obtained from the whole pot, the gravimetric water content values of the core samples were converted to volumetric water contents. These data plotted on semi-logarithmic paper served as a master curve for conversion of water content to SWT, needed when the SWT exceeded the tensiometer range of 0.8 bar.

The filtrate obtained from saturated soil was analyzed for electrical conductivity. This value was considered as a measurement of the saturation extract, provided that care had been taken to add just the amount of nutrient solution to fill the soil pores

completely during saturation of the soil. If the saturation extract was saline, successive filtrations were carried out until the filtrate emerged with the same electrical conductivity as that of the nutrient solution, 1.2 mmho/cm. This low value was desired in order to avoid plant growth depression. By use of handbook data the conductivity value was converted to the equivalent O.P. value. Expressed in mb, the O.P. was added to the SWT value, also in mb, to give an estimate of the total soil water stress (TSWS). This value, recently being called total soil water potential in the literature, is a measure of the energy lowering of soil water, and is what plant roots must overcome to absorb water.

On the assumption that the O.P. increases in direct proportion to soil water depletion, the O.P. of the saturation extract was adjusted upward by calculation as the SWT increased. These adjustments permitted each point on the soil water characteristic curve to be expressed as a TSWS curve, which took account of both SWT and increasing solute concentration. This second curve was utilized as a master curve for relating plant response to TSWS.

Procedure for the Experiment with Bean. Soil was prepared in the standard manner. Bean seeds were sown directly in the soil on 7 April, and on 17 April thinned to one plant per pot. Four pots were used, the plants being grown in the greenhouse. Tensiometers in each pot permitted watering at a low SWT, except for three drying cycles that were instituted to adapt the plants to the stressful environment to be used later in the soil water depletion experiment. The tensiometer cups were located 2.5 cm up from the bottom of the pot. The soil water tension was indicated on a mercury manometer attached to each pot. Soil temperatures were taken with a mercury-in-glass thermometer during the growth in the greenhouse.

When the plants had formed the fifth trifoliate leaf, and the sixth was emerging, these leaves were excised, leaving four trifoliates with adequate leaf area for an accurate weight loss

measurement of transpiration. The primary leaves had abscised. The one plant judged most uniform was taken to the laboratory in the afternoon, subjected to the technique of nutrient solution infiltration to pot capacity, and wired with 0.1-mm diameter thermocouples, one for each of the 12 leaflets.

It was placed in the laboratory on a balance permitting weight loss to 0.1 g. Lead wires were soldered to the thermocouples and supported by a crossbar in such a manner as to add the minimum drag to the balance. Since the difference in weight was desired, rather than the absolute weight, the problem was to maintain a constant drag. This method avoided the use of special connectors for the total of 15 pairs of lead wires.

In addition to the 12 wires from the leaflets, there were leads from a thermocouple for air temperature located in the thermohm housing, as well as two thermocouples for soil temperature in the pot, at 3 cm and 13 cm below the surface.

All 15 thermocouples were referenced against a cold junction, and the output read on a multipoint recorder once per hour in the early part of the experiment, and every eight minutes from then on. In addition, a duplicate record of leaf temperature from one of the leaflets of leaf No. 4 was recorded continuously on a separate recorder, to serve as a visual guide to the plant's response.

"Standard" conditions were employed: air temperature 30 ± 0.2 C in the dark and ± 0.5 C in the high irradiance, vapor pressure 15.1 ± 0.2 mb, carbon dioxide 350 ± 10 ppm, and illuminance 55 ± 1.0 kilolux (irradiance 0.55 ± 0.01 ly min⁻¹, 1.5 m from the bank of 48 mercury vapor lamps). Light of 20 kilolux was used on the afternoon of preconditioning, lasting until 2000. After an overnight period of darkness, 10 lamps were turned on automatically at 0600. From 0930 on, additional lamps were turned on manually, a pair every five minutes, with a few gaps, until 1120. Weighings were begun at 1200. Saran sheeting and aluminum foil covers over the soil prevented

evaporation and partially reflected radiation. The plant was large enough to allow meaningful weight losses every half hour; these were continued until 2000 that day, along with tensiometer readings to the nearest mb.

At 0900 on the experimental day two beta ray gauges were placed on the plant. One was put on leaf No. 4, the uppermost, the other gauge on the lowest leaf. Each gauge was located about 5 cm back from the tip of a side leaflet, straddling the midrib. Alternate gauges were counted every three minutes for part of every hour, and more often at critical times.

Leaf resistance readings were started at 1200, and were made every half hour through 2000. All leaflets were measured except those with a beta gauge.

When the transpiration rate had decreased 50% due to soil water depletion, the total transpirational loss was restored in a five-minute period by addition of warm, distilled water. Tensiometer readings were taken every five minutes for a half hour. Weight loss readings were continued for one hour. At this time the lights were turned off for an overnight record that would terminate the experiment.

RESULTS:

Transpiration. The linear weight loss with time (Figure 3) indicates that transpiration proceeded at the potential rate for many hours, despite a gradual increase in SWT, illustrated by the lower curve. Not until 1630 did the actual transpiration rate deviate from the potential rate, as indicated by the dashed line. Although the potential rate was quite high, $450 \text{ g m}^{-2} \text{ hr}^{-1}$, the 2-1 pot of soil contained over 200 g of available water between the limits of pot capacity (SWT 45 mb) and the point at which the decline started (SWT 180 mb; TSWS 1.0 bar). Therefore, the depletion took considerable time. By the time of irrigation, transpiration had been depressed more than 50%, and SWT was 260 mb (TSWS 1.1 bars). After the

exact amount of water transpired was replaced, at 2010, SWT fell back gradually to the value characteristic of pot capacity. Since the soil mixture was quite permeable, infiltration of water to the bottom of the pot occurred within a minute. However, the tensiometer response was delayed, not reflecting irrigation for about 20 minutes.

Leaf Diffusion Resistance. In Figure 4 leaf diffusion resistance (R_L) is plotted separately for the upper and lower epidermes, the data being the harmonic mean of 12 leaflets; and for the whole leaf, as the harmonic mean of both epidermes. The three curves show essentially the same pattern, in regard to change with time; for several hours R_L remained fairly steady, but began to rise near 1600, after which time it rose more steeply. There is some evidence that R_L for the upper epidermis began to increase even before 1600, but a reference level is difficult to establish. The greater R_L of the upper epidermis undoubtedly was due to a lesser stomatal frequency, a typical finding with bean leaves.

It is significant that R_L did not return to previous low values following an irrigation which almost instantaneously replenished the soil water to the pot capacity level. The mean R_L associated with a 50% decrease in transpiration was 7 sec cm^{-1} , having risen from the initial value in wet soil of 2.4 sec cm^{-1} .

Leaf Temperature. Figure 5 demonstrates the progressive rise in leaf temperature, an average value for 12 leaflets, as compared to the steady mean air temperature. No definite inflection point exists, with the possible exception of that at 1630, which coincides with the time at which transpiration began to decline. Soil water depletion brought about a 4.5-degree rise in the mean leaf temperature. Although water was added almost instantaneously at irrigation, leaf temperature did not decline rapidly from the high value it had attained. On the other hand, turning off the lights brought an immediate decrease in leaf temperature from 36.5 C to the air temperature value of 30 C, due primarily to the removal of the incident

radiant energy.

Leaf Areal Density. The record obtained from a beta ray gauge (Figure 6) extends over a long time span. The areal density represents the leaf thickness per unit area, expressed in equivalent aluminum values. Decreases in leaf areal density presumably reflect decreases in leaf water content. The graph is for one leaflet of the lowermost of the four leaves on the plant. Leaf water content diminished from the very beginning of the measurements, even though soil water then was near pot capacity. This loss probably was a response to radiant energy, since the lights were turned on in sequence between 0930 and 1120. Therefore, the radiant environment was becoming more intense up to 1130, after which time it held steady at 0.55 ly min^{-1} . In comparison, leaf water content of the uppermost leaf decreased only slightly in the same period.

In contrast to the results with leaf temperature and leaf resistance, irrigation produced an effect on the leaf within five minutes. Leaf water content increased significantly, but did not achieve the value of the beginning of the experiment until the lights were turned off. With the lights off, however, full rehydration occurred in 10 minutes.

SUMMARY AND CONCLUSIONS:

Previous research at this Laboratory had shown that rapid increases in evaporative demand could wilt plants even in water cultures, where water absorption rates are highly favorable. However, the wilting was only moderate and short-lived. To induce a leaf water deficit comparable to that in the field, emphasis was shifted from short-term increases in evaporative demand to a restricting of water absorption by a plant exposed to a constant evaporative demand. The objective was to study the mechanism of transpiration control in plant species, with special emphasis on measurements of changes in leaf resistance, leaf temperature, and leaf water content as transpiration became limited by a progressively higher soil water

tension.

A standard technique was developed for producing a uniform substrate to be used in all subsequent experiments. The substrate was a mixture of soil, peat moss, and sand, packed to a uniform bulk density in 2-l pots, and equilibrated with a standard nutrient solution to give a predetermined low salt concentration in the saturation extract. The method involved removal of the excess solution by vacuum filtration for a prescribed interval. The soil then was at pot capacity, a very reproducible value, and then could be planted with seeds. Reirrigation was either by addition of the depleted water back to the known pot weight corresponding with pot capacity, or by a repetition of the technique described above, whenever it was desirable to add fertility in the form of nutrient solution. The soil water characteristic curve was determined by use of the pressure membrane and pressure plate. Knowledge of the salinity level of the saturation extract permitted corrections to be made, such that the total soil water stress could be calculated.

The first experiment was with the bean plant. Brought from the greenhouse and then preconditioned in the controlled environment room, the plant was subjected to a gradual increase in light for two hours. After that the environment was held constant at 30 C, 15.1 mb vapor pressure, 350 ppm CO₂, constant air movement, and a final irradiance of 0.55 ly min⁻¹. The soil had been watered to pot capacity the previous evening. Gradual soil water depletion by transpiration then was allowed to continue until the transpiration rate reached a value only one-half the initial rate. Then the plant was irrigated. About an hour later the lights were turned off.

Transpiration continued at the potential rate for many hours, not beginning to decrease until 1630, at which time the soil water tension (SWT) was 180 mb (total soil water stress, TSWS, 1.0 bar). It is significant that the leaf diffusion resistance (R_L), which had been holding steady, first began to rise at 1600, before the

transpiration decline. A steady rise in R_L beyond 1600 coincided with the progressive decline in transpiration. When the transpiration was depressed 50% below the potential rate, SWT was 260 mb (TSWS 1.1 bars). At this time the mean R_L was up to 7 sec cm^{-1} , having risen from the initial value of 2 sec cm^{-1} .

Leaf temperature (T_L) steadily rose from the initial value of 2 degrees C above air temperature to the 4.5 degree excess at irrigation. Therefore, T_L anticipated R_L as an indicator of imminent restriction in the rate of transpiration. That leaf water content steadily diminished is an indication of an excess transpiration over water absorption by the lower leaf (Figure 6), a condition that ultimately would bring about stomatal closure (higher R_L) and the rise in T_L already discussed. However, the upper leaf did not react so drastically as the lower. This result points to a need for measurement of leaf water potential rather than leaf water content in order to interpret these data.

In conclusion, the data obtained up to the present support the hypothesis that transpiration falls below the potential rate only when significant stomatal closure occurs (when R_L increases). An intriguing, but unanswered question, is whether the slight, but steady increase in T_L that occurred before the decline in transpiration is the result of a slight stomatal closure undetectable either by weighing or measurements of R_L , or the result of changes in leaf emissivity.

PERSONNEL: William L. Ehrler

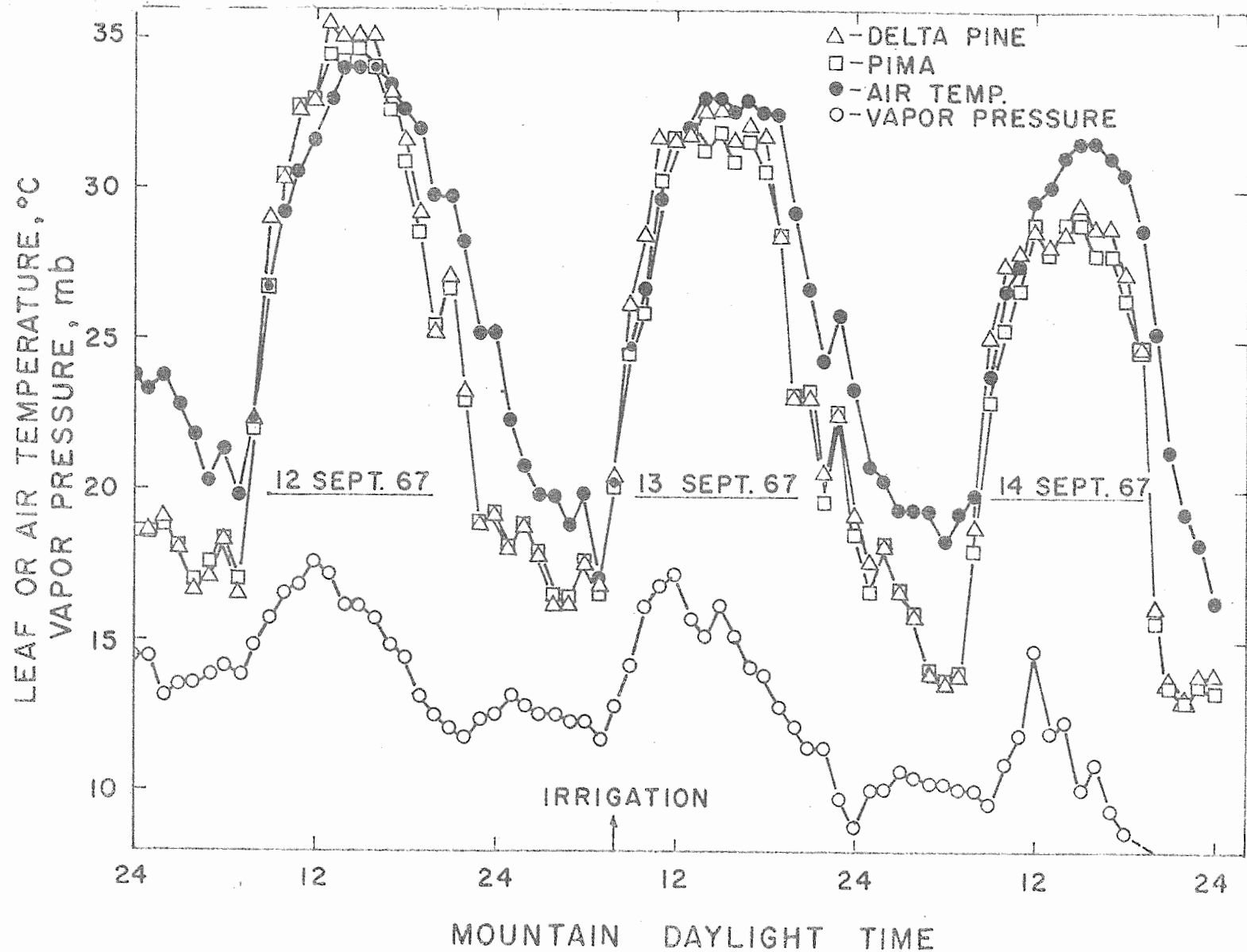


Figure 1. Air temperature and vapor pressure at 1 m above the crop, and leaf temperatures of cotton (Pima and Deltapine) in the field shortly before and after irrigation.

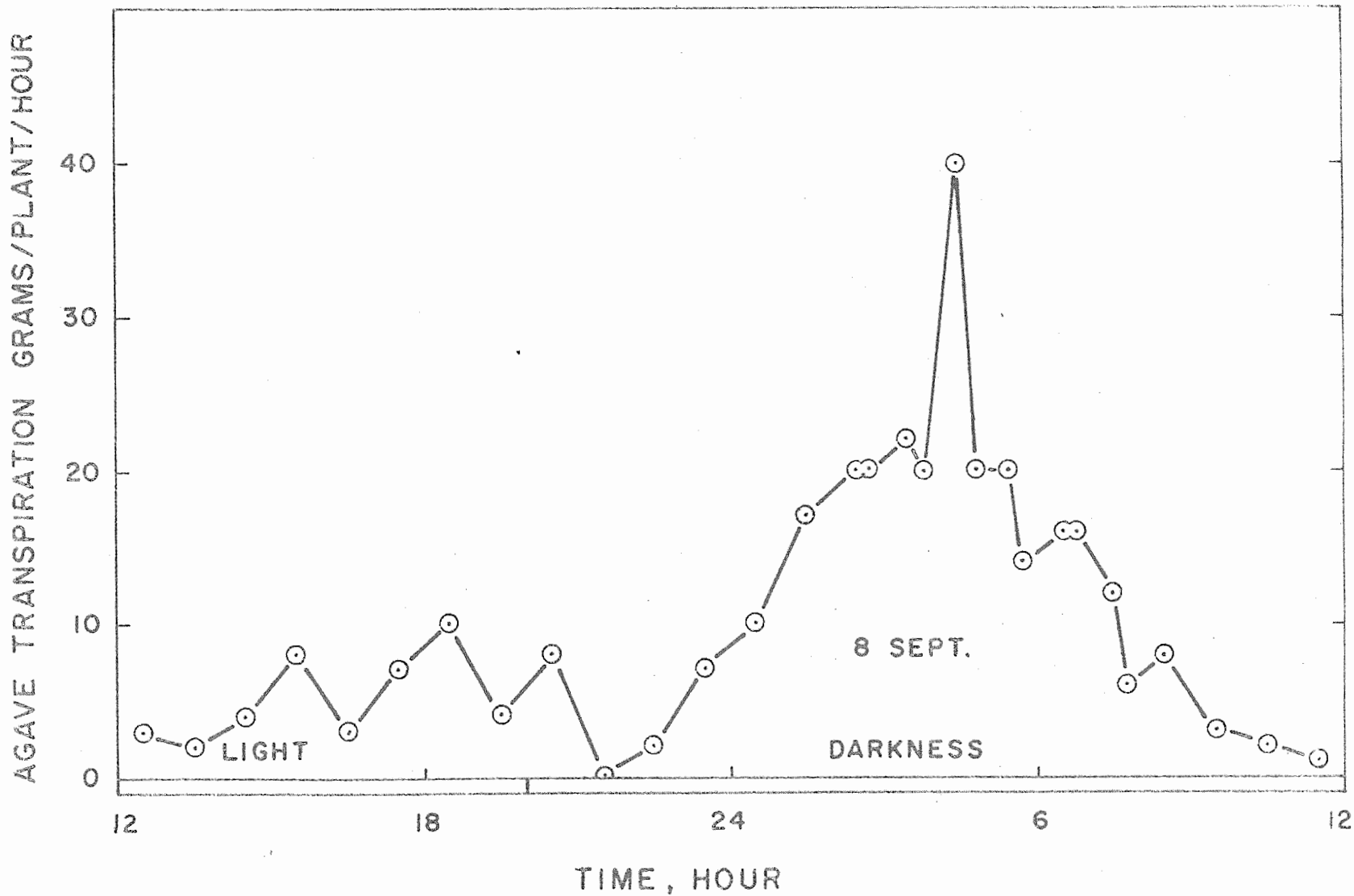


Figure 2. The transpiration rate of a large agave plant in a controlled environment.

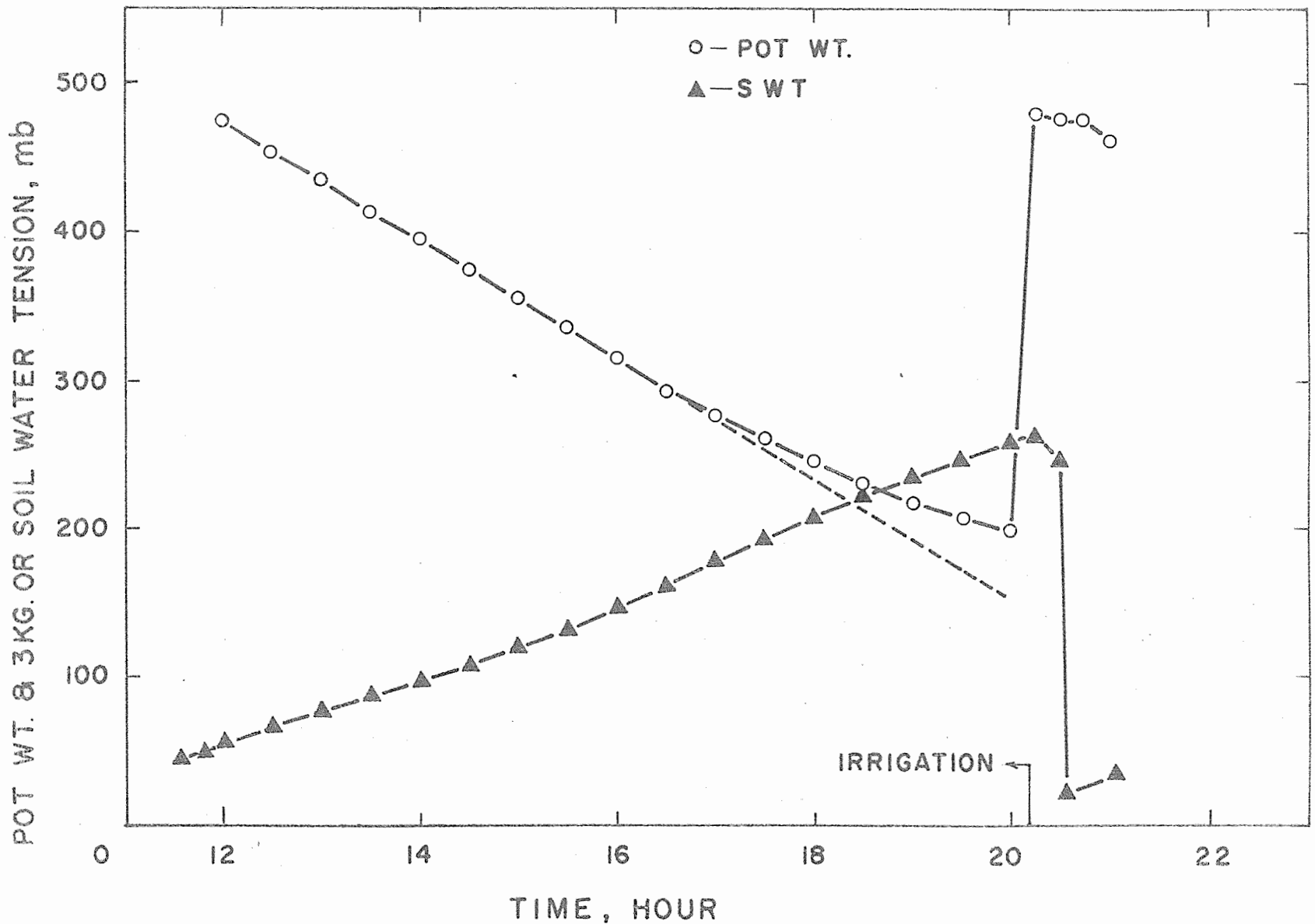


Figure 3. Transpiration (weight loss) of Bountiful bean and soil water tension in response to soil water depletion and replenishment.

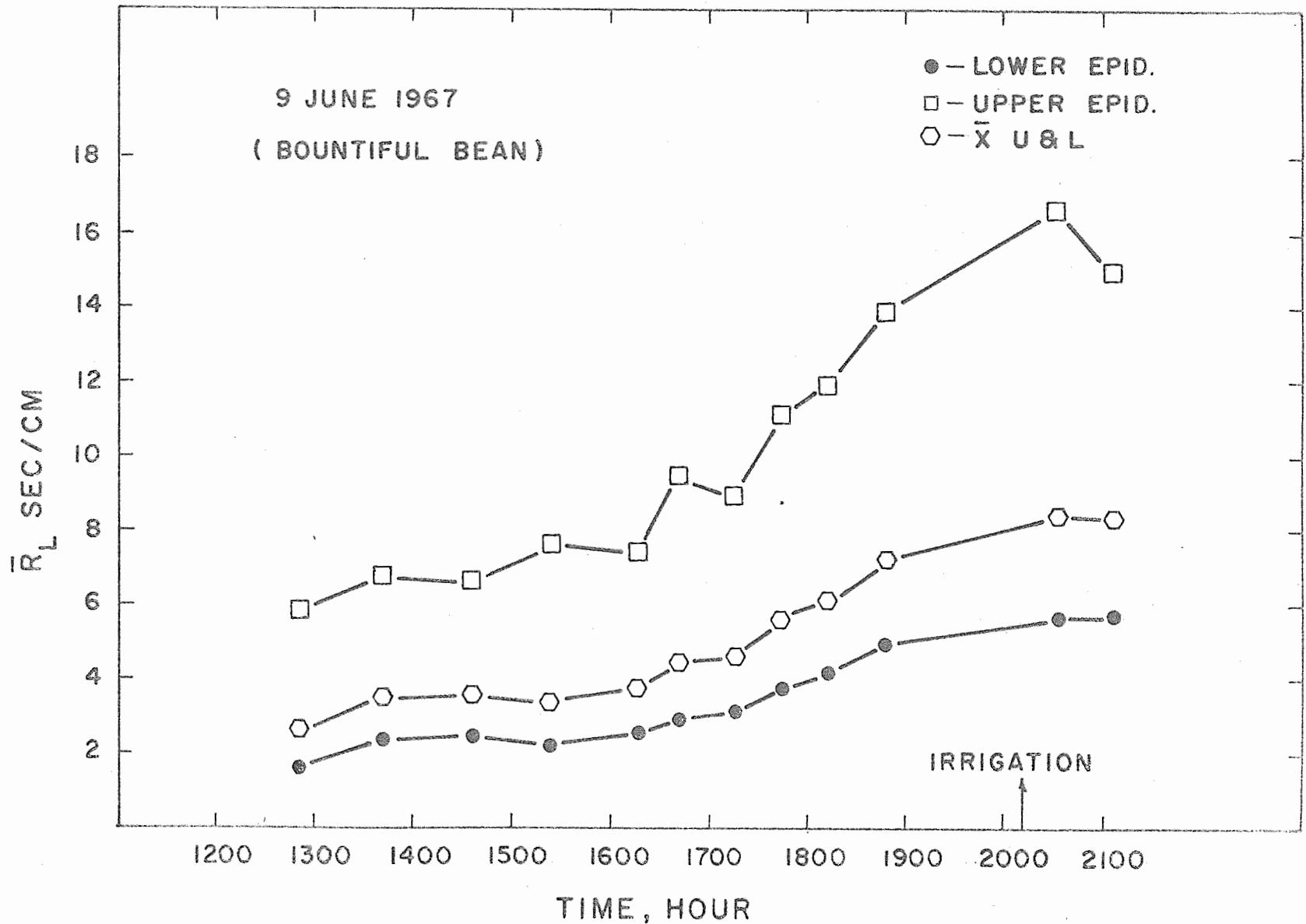


Figure 4. Leaf resistance (harmonic mean of 12 bean leaflets) in response to soil water depletion and replenishment. Annual Report of the U.S. Water Conservation Laboratory

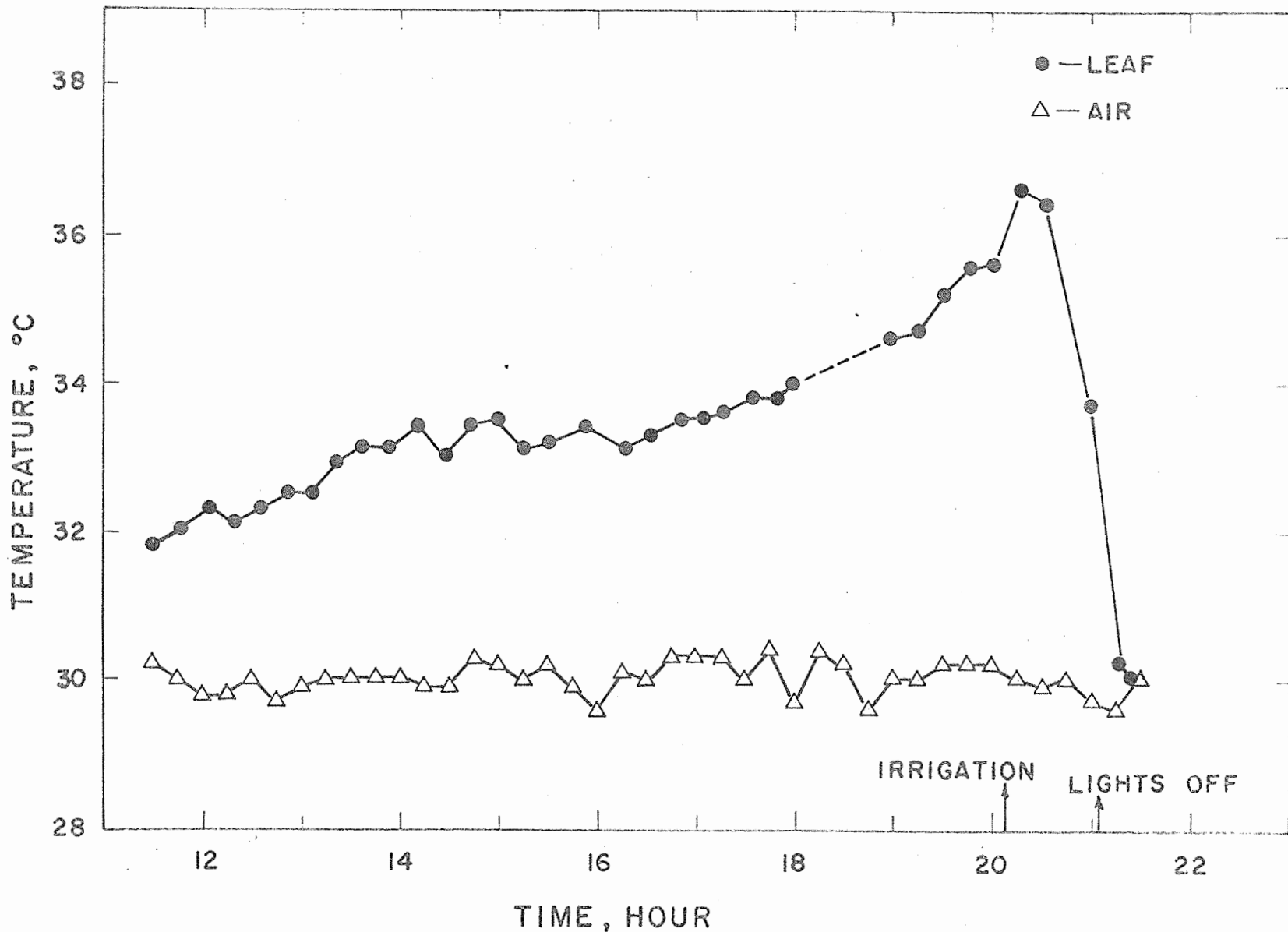


Figure 5. Air temperature in a controlled environment and leaf temperature (mean of 12 bean leaflets) while soil water was being depleted and suddenly replenished.

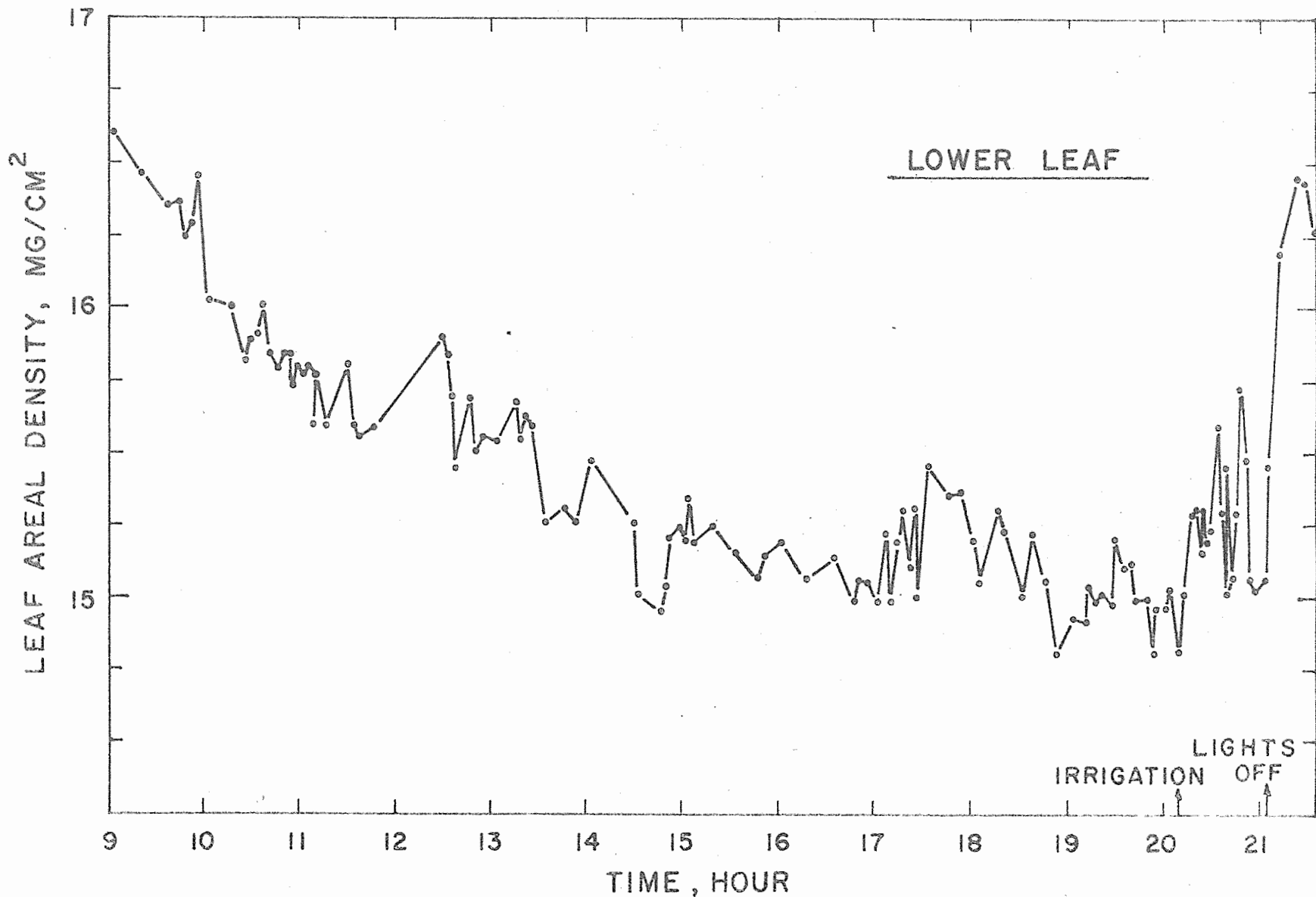


Figure 6. Areal density of the lowest of four trifoliolate bean leaves, in response to increased radiation (from 0930-1130), a progressive depletion of soil water, irrigation, and darkness.

TITLE: PLANT PROCESSES AS FUNCTIONS OF THE TOTAL ENVIRONMENT

LINE PROJECT: SWC W9 gG-6

CODE NO.: Ariz.-WCL-29A

INTRODUCTION:

A plant is not an isolated entity, but a responsive part of the dynamic plant-environment system. As such, plant processes are the integrated expressions of many interacting environmental parameters. Research conducted at the laboratory this year has emphasized this fact with the development of a method for calculating net crop photosynthesis, transpiration, and sensible heat exchange as functions of the combined effects of all of the major microclimatic variables. In this method the individual leaf is the focal point of attention; and results obtained for all of the differently oriented and distributed leaves of a canopy are integrated by means of a computer to give results for entire crops.

PROCEDURE:

Since net photosynthesis is in essence a photochemical reaction whereby carbon dioxide and water, in the presence of visible radiation and in association with chlorophyll in green plants, are combined to form organic compounds, this plant process must be directly governed by the supply of reactants (CO_2 and water), the amount and type of incident short-wave radiation, and the temperature of the reaction site. All other climatic parameters must exert their effects upon this process by influencing one or more of these four basic factors.

This concept is graphically portrayed by the hierarchy of environmental parameters presented in Figure 1. In the center of this figure are represented the photosynthetic and respiratory processes of the plant; and pointing to these processes are arrows from the four basic factors. As is indicated by the arrows, the effects of these four factors upon net photosynthesis must be obtained experimentally; and they are thus known in the form of correlations and not mathematical expressions. The one arrow leaving the photosynthetic and respiratory processes and returning to the basic factor,

CO₂ concentration, represents an effect of the plant upon this factor. In particular, it is the lowering of the carbon dioxide concentration of the canopy level air as the plant utilizes CO₂ in photosynthesis.

Besides the basic factors, there are also three other general types of parameters evident in Figure 1. First of all, there is the component primary factor. This is a factor, such as incoming direct short-wave radiation, which is actually a part or fraction of one of the four basic factors, in this instance, light intensity. Other factors of this type represented in Figure 1 are the remainder of the short-wave radiant energy fluxes and the three components of the leaf water availability factor. Secondly, there is the secondary factor. This factor is not a component of one of the basic factors, but instead plays a direct role in determining the value of one or more of them. The basic factor most involved in this relationship is leaf temperature, to which five arrows from secondary factors are seen to converge. Lastly, there is the tertiary factor, which operates upon the secondary factors in an analogous manner to their operation upon the four basic factors. The letters A, B, C, and D of Figure 1 represent some of this group. In particular,

- A = latitude, slope and aspect of ground, cloud cover, dust and atmospheric pollutants, reflectance of ground and near-by objects;
- B = cloud cover, temperature of ground and near-by objects, water vapor, and low level atmospheric ozone;
- C = precipitation, height of water table, soil moisture content, and thus soil physical properties such as structure, texture, etc.;
- D = soil chemical properties: clay minerals, base exchange properties, pH, anions, organic compounds, etc.

Besides bringing some order to the relationships among the various environmental parameters and the ways by which they influence net photosynthesis, Figure 1 performs two other utilitarian functions

too. It indicates by word the actual physical processes by which some of these relationships are sustained, and it notes by number the places in the plant-environment system where properties of the plant act as coupling devices between the environment and the plant. The identification of these properties is given below:

- 1 = absorptance, reflectance, and transmittance of plant leaves to direct and diffuse solar radiation, leaf distribution (of inclinations) function, leaf area index, canopy density, plant height, and percent cover of ground;
- 2 = same as 1;
- 3 = same as 1, but plant spectral properties here have reference to long-wave radiation;
- 4 = leaf convection coefficient: thus, leaf size, leaf shape, leaf hairs, etc.; also, crop density (affects wind speed);
- 5 = same as 4;
- 6 = total leaf diffusion resistance to transpiration: thus, diffusion resistances of cuticle, stomata, substomatal cavity, and cell wall;
- 7 = same as 6;
- 8 = resistances of various plant parts (surfaces of root hairs, cortex, endodermis, vessels and tracheids in xylem, leaf veins) to water flow;
- 9 = permeability of different plant cell membranes;
- 10 = plant height;
- 11 = correlations between the four basic factors and the photosynthetic and respiratory processes.

Within the framework established by Figure 1, the objective of the method is to specify a sufficient number of environmental parameters at one of the intermediate hierarchial levels to allow the calculation of simultaneous values of all four of the basic factors for all of the differently oriented and distributed leaves of a plant canopy. Knowledge of the values assumed by these factors then

determines the net photosynthetic rates of the individual leaves or leaf sections and thus that of the canopy as a whole.

The methods of calculation and the characteristics of the input data required are all described in great detail in reference (1). Also included in that reference are all of the computer programs utilized in the method, complete with format statements for some specific situations. In short, it contains all of the information needed for anyone to duplicate the calculations for any situation he may be interested in.

RESULTS AND DISCUSSION:

Tests of the method have been conducted at various levels of verification. In reference (1), for instance, the calculations are carried through to their completion for a corn crop growing at Ithaca, New York, as described by Dr. E. R. Lemon and his coworkers in several of their publications. The results of these calculations are shown in Figure 2 for five different values of soil moisture tension in the root zone. Superimposed upon them is the aerodynamically derived value obtained by Wright and Lemon (7), reduced by a factor of 3. Although there is a significant difference between the absolute magnitudes of the results of the two methods, both give similar relative variations. Theoretical considerations mentioned in (1) indicate that the aerodynamic technique may have a large absolute magnitude error associated with it and may overemphasize the degree of relative variations. The method here described is further thought to be the more accurate, due to the fact that the values of CO_2 concentration at the effective canopy exchange surface calculated as a by-product of the method for the case of 0.7 atm total soil moisture tension (TSMT) agree so well with the values of CO_2 concentration measured at this height by Wright and Lemon (7).

Due to the difficulties involved in making non-environmental disrupting measurements of net photosynthesis in situ, most tests of the method have been carried out on the level of the four basic

factors. In particular, leaf temperature calculations are the most complicated (next to the CO₂ concentration calculations), and thus the establishment of their validity is viewed as insuring the validity of the net photosynthesis calculations. Several of these temperature calculations have been carried out, and they are reported on in references (4, 5, 6). In all instances the results must be considered very favorable.

SUMMARY AND CONCLUSIONS:

A method for calculating net crop photosynthesis, transpiration, and sensible heat exchange has been developed which takes into consideration the direct effects and interactions of all of the major climatic variables. In this method the individual leaf is the basic unit of concern, and results for all of the differently oriented and distributed leaves of a plant canopy are integrated by a computer to give results for entire crops. Initial tests of the method on several levels of verification have been very encouraging. More rigorous tests will be conducted in the near future, upon completion of the construction of suitable chambers for precise net photosynthesis measurements.

REFERENCES:

1. Idso, S. B. A holocoenotic analysis of environment-plant relationships, with special emphasis being given to the calculation of net photosynthesis, transpiration, and sensible heat exchange. Minnesota Agr. Expt. Sta. Tech. Bull. In Press. 1968.
2. Idso, S. B. Atmospheric and soil induced water stresses in plants and their effects upon transpiration and photosynthesis. Jour. of Theoret. Biol. (Submitted). 1968.
3. Idso, S. B. Comments on paper by Richard Lee "The hydrologic importance of transpiration control by stomata." Water Resources Res. 4: In Press. 1968.
4. Idso, S. B., and Baker, D. G. Method for calculating the photosynthetic response of a crop to light intensity and leaf temperature by an energy flow analysis of the meteorological parameters. Agron. Jour. 59:13-21. 1967.

5. Idso, S. B., and Baker, D. G. The relative importance of re-radiation, convection, and transpiration in heat transfer from plants. *Plant Physiol.* 42:631-640. 1967.
6. Idso, S. B., and Baker, D. G. The naturally varying energy environment and its effects upon net photosynthesis. *Ecology*. (Submitted). 1968.
7. Wright, J. L., and Lemon, E. R. Photosynthesis under field conditions. IX. Vertical distributions of photosynthesis within a corn crop computed from carbon dioxide profiles and turbulence data. *Agron. Jour.* 58:265-268. 1966.

PERSONNEL: Sherwood B. Idso

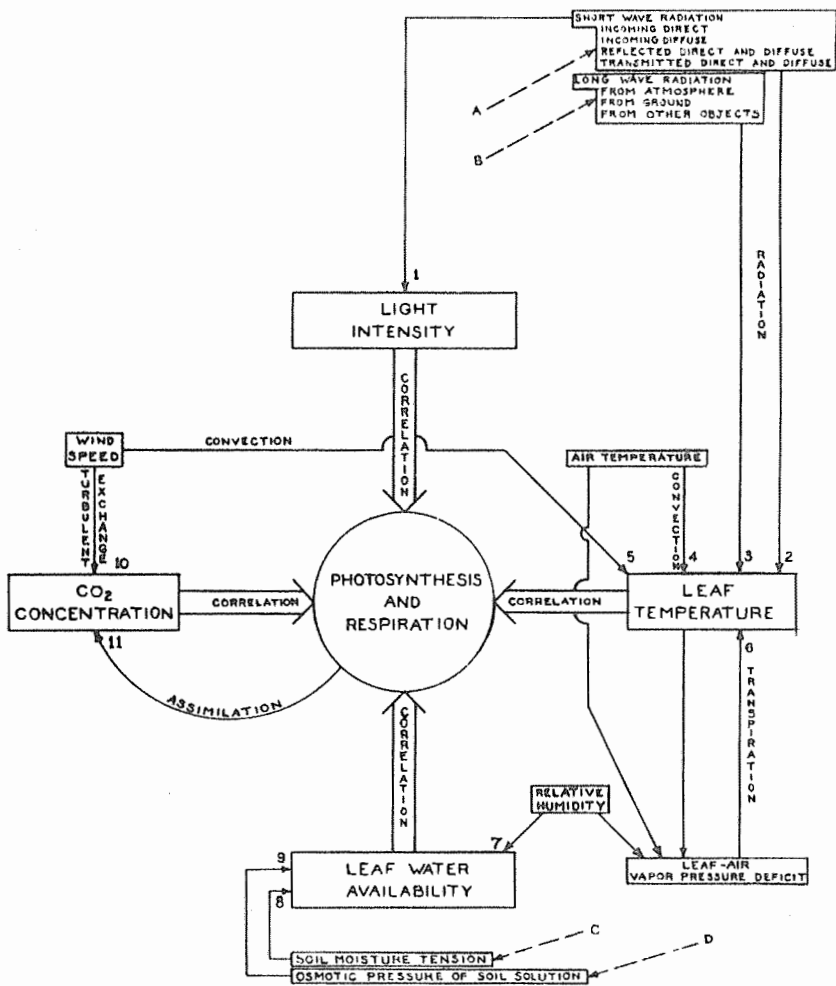


Figure 1. Diagrammatic representation of the interrelationships among various environmental parameters and the channeling of their effects into the net photosynthetic process through the four basic factors; light intensity, leaf temperature, leaf water availability, and carbon dioxide concentration.

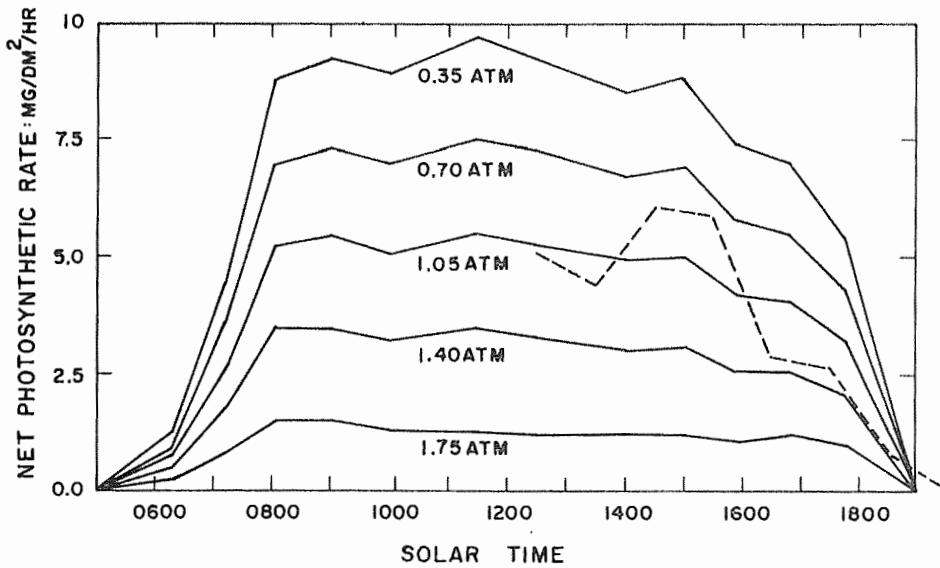


Figure 2. Calculated mean net photosynthetic rates of an entire corn canopy under various conditions of soil moisture stress. The dotted line is the aerodynamic result of Wright and Lemon (7) reduced by a factor of 3.

TITLE: RELATIONS OF ENERGY BALANCE COMPONENTS OVER NATURAL SURFACES

LINE PROJECT: SWC W9 gG-6

CODE NO.: Ariz.-WCL-29B

INTRODUCTION:

Two parameters descriptive of the energy balance of natural surfaces which have received special attention this year are the slope of the linear regression of solar on net radiation and the "heating coefficient" of Monteith and Szeicz (6), which relates the change in the net long-wave radiant heat loss of a surface to the net radiation income. Some controversies in the literature over the values of the first of these parameters in different areas have been settled by a theoretical analysis which renders the apparently contradictory experimental reports consistent. Analyses of the second parameter have shown it to be a good surface property only in areas where the diurnal variations of the major climatic variables are rather uniform from day to day.

PROCEDURE:

Regression Slopes. J. A. Davies (2) recently presented a plot of total daytime net radiation (R_N) against total solar radiation ($S + s$), received by personal communication from Dr. L. J. Fritschen (then a member of this laboratory staff), which he said was in agreement with the regression equation

$$R_N = 0.617 (S + s) - 24, \text{ cal cm}^{-2} \text{ day}^{-1} \quad (1)$$

to which he fitted data from 14 stations throughout the world with a correlation coefficient of $r = 0.99$. Shortly thereafter, however, Fritschen (3) refused to use this regression equation for calculations of total daily net radiation, since he felt the lack of data near the origin did not yield realistic intercepts. He instead determined the average rate of short-wave radiation reception for the day, used this value to determine an average net radiation rate from

pooled hourly regressions of net on solar radiation, and multiplied this average rate by the duration of daylight to get the total net radiation for the day.

The difference between these two approaches of obtaining R_N from $S + s$ is quite significant, for the slopes for the pooled hourly regressions are considerably greater than that obtained from the same data analyzed in the form of daily totals only. We can theoretically prove that the two slopes should be the same, however, and experimentally show that the method used by Fritschen is by far the superior of the two.

The average daily rate of short-wave radiation reception may be expressed by the equation

$$\bar{S} + \bar{s} = \frac{1}{T} \int_0^T [S(t) + s(t)] dt \quad (2)$$

where T = daylength, t = time, $S(t)$ = instantaneous rate of insolation, and $s(t)$ = instantaneous rate of diffuse skylight reception. From a regression of hourly totals of net on solar radiation, we then determine the average daily rate of net radiation reception to be

$$\bar{R}_N = a(\bar{S} + \bar{s}) + b \quad (3)$$

Since the total daily net radiation received must be

$$R_{N, T} = \bar{R}_N T \quad (4)$$

we thus have, substituting equation (3) into (4)

$$R_{N, T} = a(\bar{S} + \bar{s}) T + bT \quad (5)$$

However, further substitution of equation (2) into (5) gives the result

$$R_{N, T} = a \int_0^T [S(t) + s(t)] dt + bT \quad (6)$$

and we see that the slope of the regression line relating total net to total short-wave radiation reception should be the same as that relating hourly values of these two quantities. From a comparison of Fritschen's and Davies' results (Table 1 and equation (1), respectively), this is clearly not the case. Experimental data supplied by Dr. C. H. M. van Bavel (personal communication) allow us to determine which of the two are in error.

RESULTS AND DISCUSSION:

Regression Slopes. Figure 1 shows Van Bavel's plot of daily totals of net radiation vs. solar radiation as obtained in two widely separated areas, one of which includes some of the same data used by both Davies and Fritschen. Here Van Bavel has a good distribution of data points near the origin, however, satisfying the requirement that Fritschen felt was lacking in his data.

Van Bavel carried out three linear regressions on these data: one for Fritschen's data alone, one for his data alone, and one for their combined data. The resulting slopes were, respectively, 0.616, 0.805, and 0.803. Extremely striking is the very close agreement between the slope for Van Bavel's data alone and his and Fritschen's data combined, and the great discrepancy between them and the slope for Fritschen's data alone. Inclusion of Fritschen's data with those of Van Bavel, which appear separately to describe two significantly different relationships, has next to no effect upon the regression describing Van Bavel's data alone, for which there is a good distribution of data points about the origin. This clearly indicates that the data of Fritschen can be as easily fitted to a line of slope = 0.803 as they can to a line of slope = 0.616 if sufficient data points near the origin are considered.

It is easily seen why discrepancies in slopes arise between these two methods of regression analysis. In the early morning and late

afternoon, net radiation is usually slightly negative. The amount of negative net radiation thus accumulated is fairly constant and independent of daylength. Thus, for long days its effects are minimized, as it accounts for a relatively smaller proportion of the total net radiation. For short days, however, it becomes more significant and will cause the total net radiation for the day to be less than what would be predicted from the data of longer days. Thus, the inclusion of data points near the origin will tend to increase the slope of the regression of net on solar radiation. If the daily totals are such that they do not allow this, hourly plots are needed to present the true picture, as they will usually have a fairly uniform distribution of data points over the entire range of solar radiation intensities.

PROCEDURE:

Heating Coefficient. In 1961, Monteith and Szeicz (6) developed a new expression for the net radiation in terms of solar radiation:

$$R_N = \left(\frac{1 - \alpha}{1 + \beta} \right) (S + s) + L_o \quad (7)$$

where α = albedo, $L_o = R_A - R_G$ when $S + s = 0$, and where β was a new parameter, called by them the "heating coefficient" and defined as one minus the slope of the regression of net on net solar radiation divided by this slope. Their reason for calling this parameter the "heating coefficient" was that their derivation showed it to be related to the increase in net long-wave radiant heat loss of a surface ($R_G - R_A$) per unit increase in net radiation. For a constant atmospheric long-wave radiation emission, this reasoning is valid; if the atmospheric radiation is variable, however, little physical significance can be associated with the parameter. Thus, former experiments were checked and new experiments were carried out to determine the validity of the heating coefficient concept.

RESULTS AND DISCUSSION:

Heating Coefficient. In a cooperative study with the Minnesota

Agricultural Experiment Station carried out at St. Paul, Minnesota, Idso, Baker, and Blad (5) found the long-wave radiation from the sky to be highly variable and unpredictable, rendering the heating coefficient unstable and of almost no meaning whatever. Certain relations between the heating coefficient and the form of the daily cycle of net radiation traced as a function of net short-wave radiation were apparent, but these were more closely related to changes in atmospheric radiation (R_A) than they were to ground radiation (R_G).

Review of past experiments carried out at the laboratory in Phoenix, Arizona, however, showed quite opposite results. The diurnal variations in long-wave atmospheric radiation were rather uniform from day to day over long periods of time; and this allowed the heating coefficient to be rather well correlated with surface characteristic alterations. Figure 2, for instance shows the response of the heating coefficient of a field of sudangrass to irrigation at different stages of crop development, and part of Figure 3 shows the effects of differential heights of alfalfa on its heating coefficient. Irrigation caused the heating coefficient to decline greatly during the early period of crop development, but caused it to rise slightly for tall complete-cover crops later in the season. Also, the heating coefficient was usually smaller for the taller of two crops growing under the same prevailing weather conditions. All of these effects were easily explained in terms of the energy balances at the surfaces involved (4). In spite of the demonstration that the heating coefficient may indeed be a surface property under certain climatic conditions, however, the fact that the atmospheric radiation is not constant with time renders it of little physical significance. Only qualitative pronouncements at best can be made about any thermal characteristics of the ground surface.

SUMMARY AND CONCLUSIONS:

Experimental results have verified the theoretical prediction that regression slopes of net on solar radiation should be the same

for pooled hourly data and daily totals. This condition will only obtain in reality, however, if sufficient data points near the origin are available for the daily totals. The experimental results have shown the recent work of Davies (2) to be in error and that of Shaw (8), Scholte-Ubing (7), Chang (1), and Fritschen (3), which Davies calls inconsistent, to be the more correct.

The "heating coefficient" of Monteith and Szeicz (6) has been shown to be a good surface property only in climates where the diurnal variations of atmospheric long-wave radiation are fairly uniform from day to day. Even then, however, any implied relation between its value and the surfaces' thermal properties must be considered highly questionable.

REFERENCES:

1. Chang, Jen-hu. Microclimate of sugar cane. Hawaiian Planters' Record. 56:195-225. 1961.
2. Davies, J. A. A note on the relationship between net radiation and solar radiation. Quart. Jour. Roy. Meteorol. Soc. 93:109-115. 1967.
3. Fritschen, L. J. Net and solar radiation relations over irrigated field crops. Agr. Meteorol. 4:55-62. 1967.
4. Idso, S. B. A critical analysis of the heating coefficient concept of Monteith and Szeicz. Jour. Appl. Meteorol. (Submitted). 1968.
5. Idso, S. B., Baker, D. G., and Blad, B. L. Relations of energy balance components over natural surfaces. Quart. Jour. Roy. Meteorol. Soc. (Submitted). 1968.
6. Monteith, J. L., and Szeicz, G. The radiation balance of bare soil and vegetation. Quart. Jour. Roy. Meteorol. Soc. 87:159-170. 1961.
7. Scholte-Ubing, D. W. Over straling de warmtebalans en de verdamping van gras. Mededel. Landbouwhoogeschool, Wageningen.
8. Shaw, R. H. A comparison of solar radiation and net radiation. Bul. Amer. Meteorol. Soc. 37:205-206. 1956.

PERSONNEL: Sherwood B. Idso

Table 1. Slope of regression of net radiation on solar radiation for several different irrigated field crops at Phoenix, Arizona. Adapted from Fritschen (3).

Crop	Slope
Alfalfa	0.751
Barley	0.655
Wheat	0.808
Oats	0.750
Cotton	0.738
Sorghum	0.752
All Crops	0.734

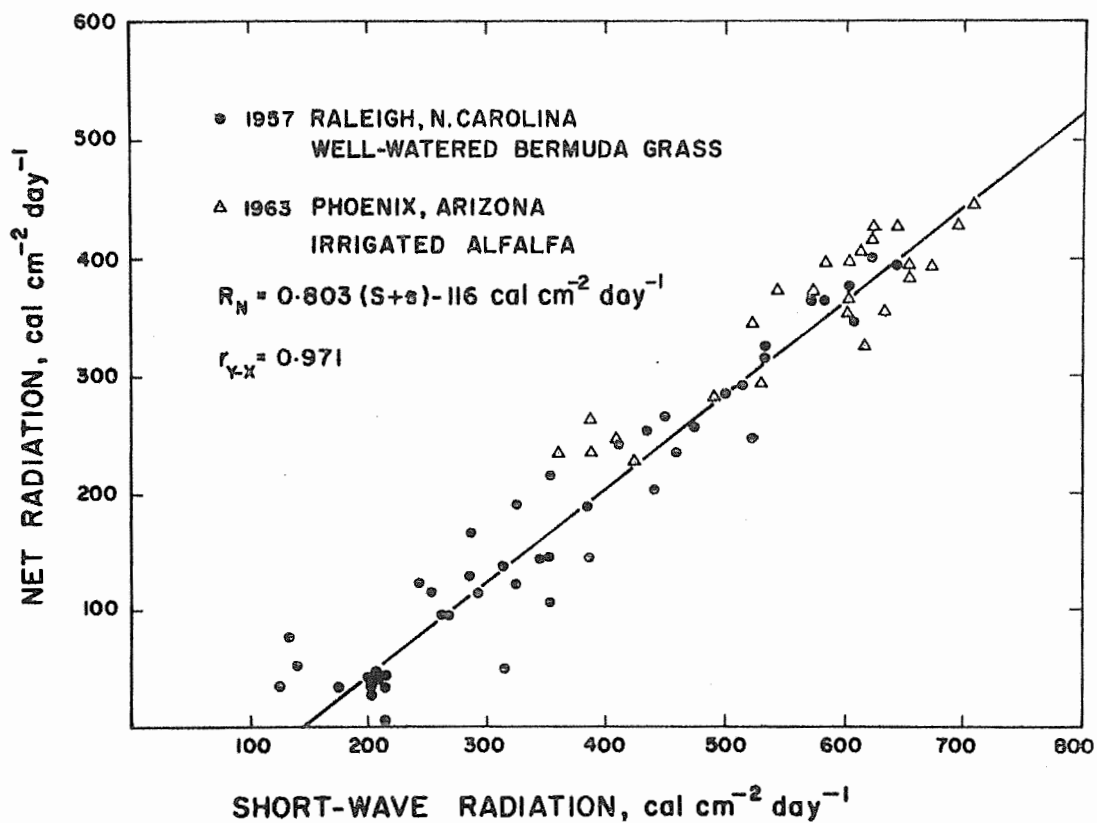


Figure 1. Combined regression of daily totals of net radiation on short-wave radiation for two different crops in two widely separated areas.

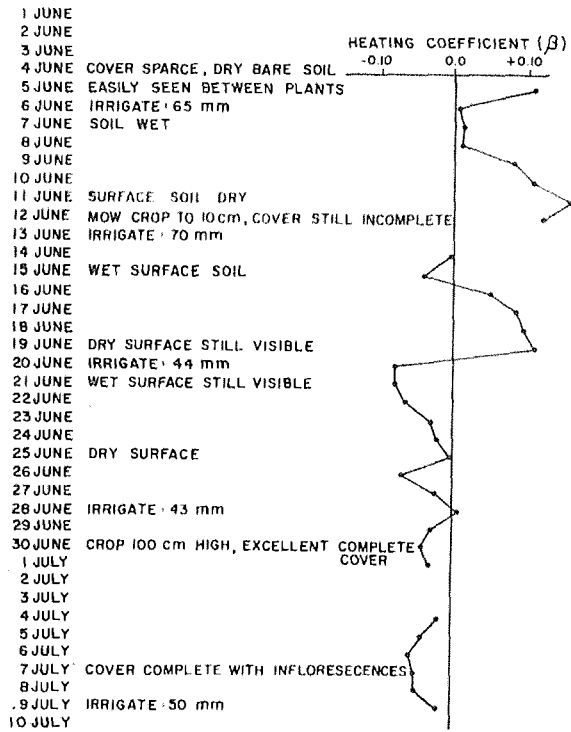


Figure 2. Variation of the heating coefficient of sudangrass during four consecutive irrigation cycles at Phoenix, Arizona.

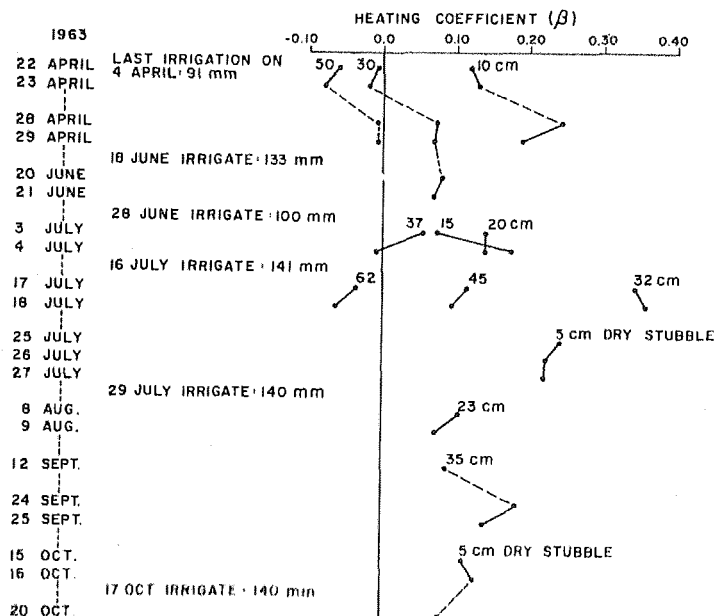


Figure 3. Variation of the heating coefficient of alfalfa of different heights over a period of several months at Phoenix, Arizona.

TITLE: INFRARED THERMOMETRY OF SOILS AND VEGETATION

LINE PROJECT: SWC W9 gG-6

CODE NO.: Ariz.-WCL-29C

INTRODUCTION:

In the measurement of surface temperatures of soils or vegetation, it is necessary to know the value of sky radiance incident upon the surface whose temperature is being monitored. If the sky radiance is relatively constant throughout the day, this imposes no real problem. If, however, it is variable with large deviations about a mean value, only the continuous monitoring of this parameter in the course of soil or vegetation temperature measurements will insure that the proper correction may be applied to account for the portion of this radiation which is reflected from the surface viewed by the infrared thermometer.

Recently, Conaway and Van Bavel (1, 2, 3, 4) reported large diurnal fluctuations in sky radiance of just this nature. Theoretical considerations of Idso and Jackson (6), however, indicated that the variations they observed were not physically possible. Thus it was decided to reexamine this phenomenon of sky radiance and determine the cause for the anomalous results of Conaway and Van Bavel. If sky radiance was relatively constant, contrary to their claims, this would greatly expedite the obtaining of surface temperatures of soil and vegetation by infrared thermometry.

PROCEDURE:

We constructed first an apparatus which every five minutes alternately exposed to the view of the infrared thermometer either a reflectance plate ($\epsilon = 0.467$) or a blackened aluminum plate ($\epsilon = 0.980$). The radiation environment of each plate was essentially unaltered in either position. Both plates had thermocouples imbedded just below their upper surfaces, and plate temperatures were thus acquired every five minutes.

Radiation and temperature data obtained from the reflectance plate were used to calculate sky radiance (W_T) from the formula

$$W_I = \frac{W_T - \epsilon W_S}{1 - \epsilon} \quad (1)$$

where W_T is the normal radiance of the surface as sensed by the infrared thermometer, W_S is the normal blackbody radiance as it would be sensed by the infrared thermometer, and ϵ is the effective surface emittance of the reflectance plate weighted by the filtering system of the infrared thermometer.

Radiation and temperature data obtained from the black plate were used to obtain a calibration curve for the infrared thermometer and thereafter act as a check upon the proper operation of the instrument.

We used the same IT-2 infrared thermometer that Conaway and Van Bavel used and a newer model IT-3. Prior to use we returned the IT-2 to the manufacturer for checking and servicing. Our initial measurements were thus made with the IT-3.

After obtaining six consecutive clear days' data, a calibration curve for the IT-3 was constructed from the black plate observations. As a first approximation it was assumed that the black plate had an emittance of 1.0, so that the energy sensed by the IT-3 could be obtained as the blackbody radiation emitted by the plate at the temperature sensed by the thermocouples just below its top surface. Using this calibration curve to obtain W_T for the reflectance plate in equation (1), W_I was calculated and found to be extremely constant over the entire six-day period. This allowed us to recalibrate the IT-3 in terms of the actual radiant energy emerging from the black plate surface:

$$W_T = 0.98 W_S + 0.02 W_I \quad (2)$$

The new calibration curve was only slightly different from the first one, especially in the range of radiation values for the reflectance plate. On a graph of the scale used by Conaway and Van Bavel (3), new values of W_I obtained with the second calibration could not be distinguished from the first values.

Upon return from the manufacturer, the IT-2 infrared thermometer was calibrated in a manner analogous to that used in calibrating the IT-3. During this time both instruments were operated simultaneously. As a check upon the reflectance plate method of obtaining sky radiance, both were at times pointed skyward to the zenith.

The final phase of our experimentation consisted of checking the effects of different ambient temperatures on the performance of the instruments. We first placed both sensing heads in a well-insulated box equipped with means for cooling and heating the air within. Holes in the side of the box allowed the sensing heads to monitor the radiance of a black plate in a fairly constant temperature laboratory room. After testing the sensing heads alone, the electronics consoles of both instruments were placed in the box with the heads and the test repeated. In both cases ambient temperatures from 15 to 50 C were traversed.

RESULTS AND DISCUSSION:

The results of some of our measurements of clear sky radiance (or radiant emittance) in the 600-to 1300- cm^{-1} waveband during the first phase of our experiment, when only the IT-3 infrared thermometer was in operation, are shown in Figure 1. Also shown there are the concurrent values of ozone concentration as recorded by the Air Pollution Branch of the Maricopa County Health Department. Although large variations in ozone concentration are evident, as they were in the experiments of Conaway and Van Bavel, the 200 to 400% daily increases in sky radiance which they characteristically observed and correlated with ozone are completely absent. Maximum daily deviations of sky radiance from each daily mean were $\pm 10\%$. For the

entire six-day period investigated at this time, they were generally not more than $\pm 15\%$.

Some of the results of the second phase of our experiment, when both the IT-2 and the IT-3 were in operation, are shown in Figure 2. Throughout this period the IT-3 was pointed skyward to the zenith. The IT-2 was similarly directed skyward on 15 November, but from then on was used to view the reflectance and black plates. Throughout 16 November and at one time on 17 November, and again on 19 and 20 November (not shown), broken intermediate height clouds were present. Both instruments responded well to the resulting increased thermal radiation at these times.

During the clear portion of this period, the IT-3 gave a relatively constant sky radiance. Between 1200 and 1800 on 15, 17, and 18 November, the IT-2 recorded increases of 40 to 70%, however. These increases always occurred during the hottest part of the day, suggesting a temperature effect on the instrument. The black plate data of 17 and 18 November indicated the IT-2 was malfunctioning at these times.

In the laboratory tests designed to check out possible temperature effects, we found the sensing head of the IT-3 stable, but that of the IT-2 subject to errors of from 20 to 30% between 45 and 50 C. These errors, however, were in the opposite direction from the one we had obtained outside. When the electronics consoles of the instruments were included in the test, we found that from 37 C and up the output of the IT-2 declined drastically, from 23 mv to 0 mv. Since the output of the infrared thermometers is inversely proportional to the energy sensed, this would be interpreted as an increase in incident energy, more than enough to account for the afternoon peaks we observed with the IT-2. The same effect can also explain the anomalous peaks observed by Conaway and Van Bavel (1, 2, 3, 4).

A similar effect was observed with the IT-3, but not until an ambient temperature of 47 C was achieved (see Figure 3). Since the

IT-3 always performed properly outside, this was interpreted as indicating that the instruments did not exceed 47 C. During the parts of the afternoons when air temperature rose above 25 C, however, the great intensity of solar radiation impinging on them must have raised their internal temperatures above 37 C, thus causing the IT-2 to malfunction while the IT-3 still worked properly.

The manufacturer's specifications indicate that the instruments operate normally for ambient temperature ranges of 1.7 to 40.5 C for the IT-2 and 4.4 to 49.0 C for the IT-3. We observed that both instruments began to deviate from their normal outputs about 2 or 3 C before their specified upper temperature limits were reached (see Figure 3). The rates of deviation with increased temperature were extremely rapid, much greater than we intuitively expected. Since the air temperature measured by Conaway and Van Bavel (3) on 6 May 1966 reached 35 C, it is conceivable that even the IT-3 would have malfunctioned in the intense solar radiation of the clear sky conditions that day. They had checked the output of the IT-2 over the range 4 to 30 C and found normal performance. Apparently they were unaware of the tremendous deviations the instrument would exhibit at temperatures above 37 C, temperatures easily attained with the electronics console when exposed to intense solar radiation.

Having substantiated the fact that clear sky radiance in the 600-to 1300-cm⁻¹ waveband is not subject to large fluctuations of the magnitude reported by Conaway and Van Bavel, we proceeded to determine whether the small fluctuations we did observe were large enough to necessitate the concurrent monitoring of this parameter in the course of soil or plant surface temperature measurements by means of infrared thermometry. Figure 4 summarizes the results of our calculations with respect to this question. Since the greatest accuracy claimed for the infrared technique of temperature measurement of soil and vegetation is 0.2 C (4, 5), it is evident that for almost all such applications only a few measurements or even a good estimate of

sky radiance should suffice.

SUMMARY AND CONCLUSIONS:

Theoretical reasons for doubting the existence of large fluctuations in clear sky radiance previously observed at this laboratory by Conaway and Van Bavel (1, 2, 3, 4), led us to reexamine this subject. We found the previous anomalous results to be due to an instrument malfunction. The fluctuations which did occur were so small as to elicit essentially no correction in the calculation of surface temperatures of soil or vegetation by means of infrared thermometry.

REFERENCES:

1. Conaway, J., and Van Bavel, C. H. M. Evaporation from the soil surface and soil moisture movement. Annual Report for 1966 of the U. S. Water Conservation Laboratory: 19-1 to 19-6. 1966.
2. Conaway, J., and Van Bavel, C. H. M. Remote measurement of surface temperature and its application to energy balance and evaporation studies of bare soil surfaces. Tech. Report ECOM 2-67P-1. 1966.
3. Conaway, J., and Van Bavel, C. H. M. Radiometric surface temperature measurements and fluctuations in sky radiant emittance in the 600 to 1300 cm^{-1} waveband. Agron. Jour. 59: 389-390. 1967.
4. Conaway, J., and Van Bavel, C. H. M. Evaporation from a wet soil surface calculated from radiometrically determined surface temperatures. Jour. Appl. Meteorol. 6:650-655. 1967.
5. Fuchs, M., and Tanner, C. B. Infrared thermometry of vegetation. Agron. Jour. 58:597-601. 1966.
6. Idso, S. B., and Jackson, R. D. The significance of fluctuations in sky radiant emittance for infrared thermometry. Agron. Jour. 60: In Press. 1968.

PERSONNEL: Sherwood B. Idso and Ray D. Jackson

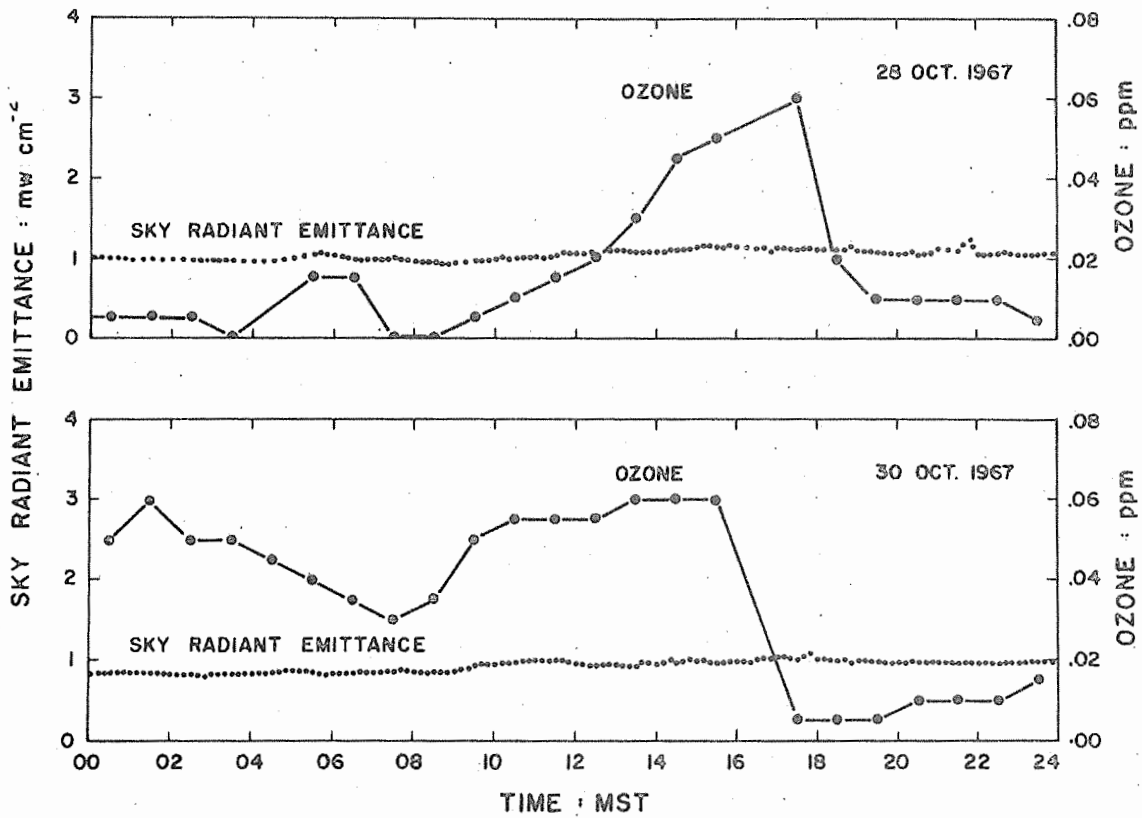


Figure 1. Clear sky radiance (or radiant emittance) and surface ozone concentration as measured on 28 and 30 October 1967 at Phoenix, Arizona.

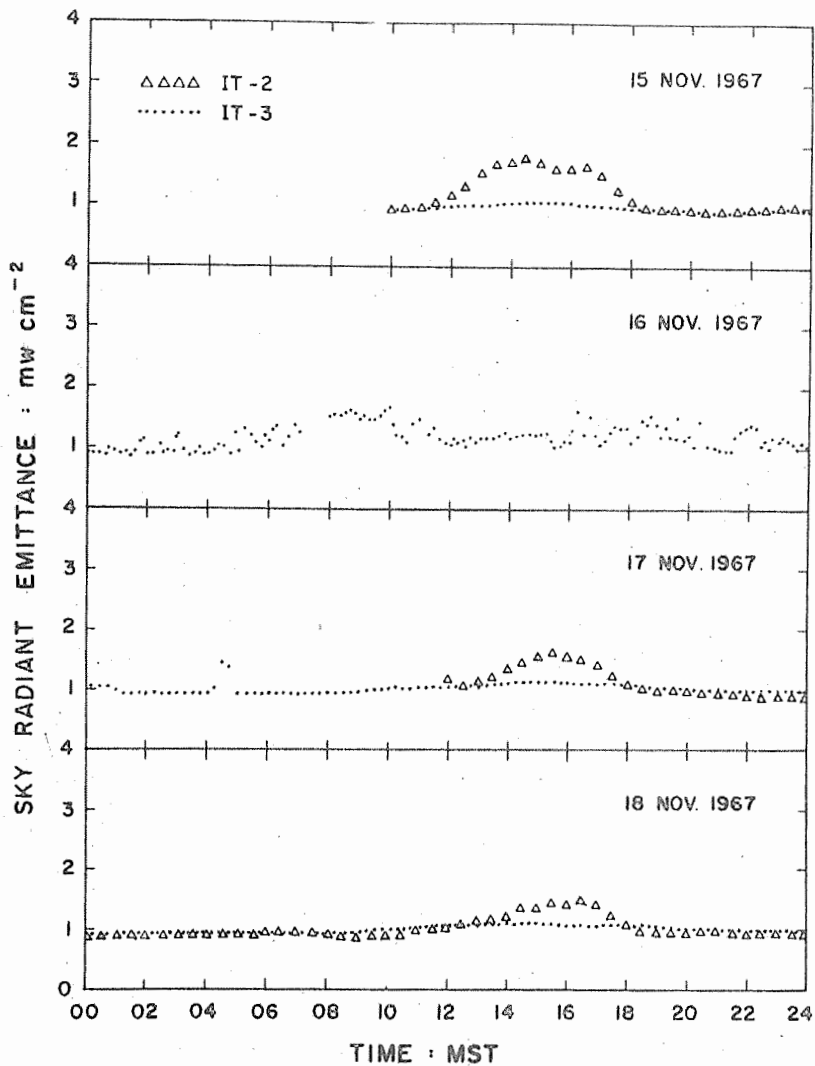


Figure 2. Sky radiance as measured over the period 15-18 October 1967 by Barnes IT-2 and IT-3 infrared thermometers at Phoenix, Arizona.

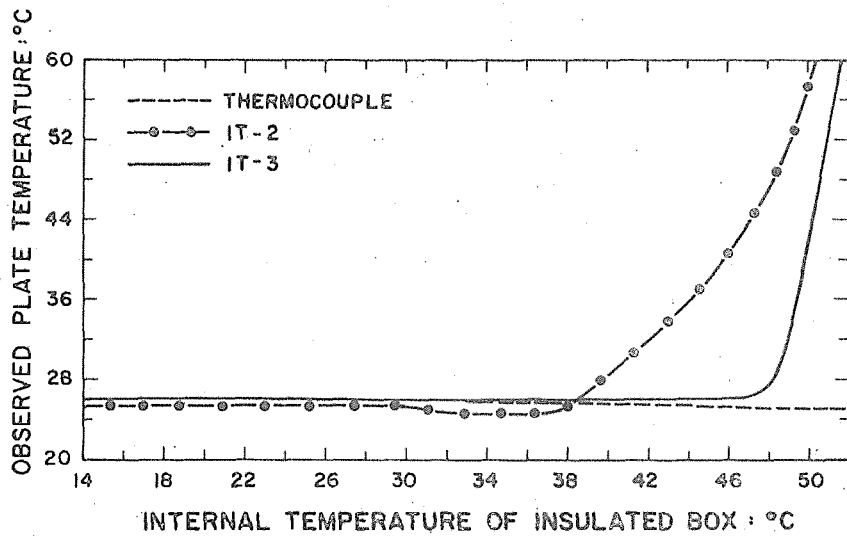


Figure 3. The temperature of a relatively constant temperature black plate as sensed by a thermocouple imbedded in the plate and IT-2 and IT-3 infrared thermometers located in an insulated box as a function of internal box temperature.

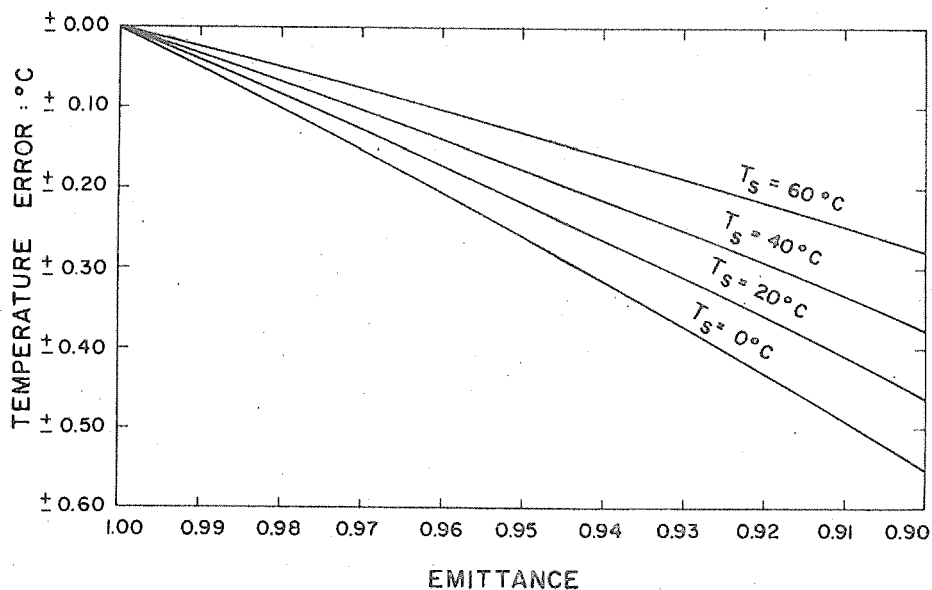


Figure 4. The error in radiometrically determined surface temperatures as a function of surface emittance for surface temperatures of 0, 20, 40, and 60 C, caused by assuming clear sky radiance constant at 1.00 mw cm^{-2} , when it actually varies by $\pm 15\%$.

TITLE: CLAY DISPERSANTS FOR THE REDUCTION OF SEEPAGE LOSSES
FROM RESERVOIRS

LINE PROJECT: SWC W7-gG-2

CODE NO.: Ariz.-WCL-37

INTRODUCTION:

Observations and soil and water analyses were made during 1967 on two stock tanks and one duck pond treated with sodium carbonate to reduce seepage. Dick Mason pond did not go dry and no soil samples were taken. House Mountain #1 pond did go dry in July and soil samples were taken. Swan Lake pond in Glendale, Arizona was treated with sodium carbonate in May 1967 and continuous water loss measurements have been made since treatment.

PROCEDURE:

Dick Mason Pond. Periodically during 1967 measurements were made on water depth, water level decline, and evaporation. The water level drop was measured periodically during one-week intervals with a F-1 waterstage recorder. Evaporation measurements were taken from a floating pan. The pan was made by cutting off the bottom 1/3 of a 55-gallon drum, placing an inflated bicycle inner tube around the outside top rim, and fastening four rulers 90 degrees apart on the inside of the pan. The pan was filled with water so that the water level inside the pan was equal to the pond water level. This left about a 2-inch freeboard. Water depth in the pan was noted at the beginning and at the end of the measurement period. It was assumed that floating pan evaporation is equal to pond evaporation. The seepage rate was calculated by subtracting the evaporation from the water level decline.

In addition to water loss measurements, chemical analyses were made on samples taken periodically from pond and runoff water and from soil solution extracts. Ceramic cups, installed in October 1965 at depths of 5, 10, and 20 cm were used to sample the soil solution.

House Mountain Pond #1. Water depth, water level decline, and evaporation were measured periodically during 1967 with the same

methods described for Dick Mason. Pond and runoff water and soil solution extracts were also taken during 1967.

In addition, soil samples were taken with a 6-inch bucket auger at one location in the pond bottom in July 1967. The pond went dry, not because of a high seepage loss, but because of low rainfall and runoff. From October 1965 through July 1967 we recorded only 97 mm rainfall at the pond.

Swan Lake. In April 1967 this 1520 m² pond was surveyed, and soil samples were taken with a 6-inch bucket auger from four locations in the pond bottom. From the soil analysis, it was decided that the pond could be sealed with sodium carbonate. In mid-May the pond was filled with water to obtain a pretreatment water loss record. On May 26 the pond was treated with salt. Eight areas of 190 m² each were staked out, and sodium carbonate at the rate of 0.24 kg m⁻² was broadcast on the soil surface. The treatment was designed to give an ESP (exchangeable sodium percentage) of 15 in the top 10 cm of soil. The salt was incorporated into the soil to a depth of 10 cm with a spike tooth harrow pulled behind a pickup truck. It took two men approximately 2 hrs to lay out the grid, broadcast the salt, and harrow the pond.

The pond was filled with water on 28 May. The pond went dry in about 10 days and was dry for 5 days. It was refilled on 12 June and has had water in it since that time.

Soil samples were taken from the pond bottom on 21 August and from the bank on 02 October 1967. These samples were taken from the pond with water in it by driving an 8-inch diameter cylinder 3 ft long 6 inches into the soil. The water was pumped out and a 4-inch bucket auger was used to obtain the soil samples.

Samples of the pond and filling water were taken periodically during the year. Water to fill the pond from the local irrigation district comes from a mixture of both surface and pumped water.

On 20 November additional sodium carbonate at the rate of 0.116 kg m⁻² was broadcast on the soil in a band around the edge

of the pond between the 52- and 73-cm level above the pond bottom. This partial retreatment was designed to bring the ESP up to 15 in the top 10 cm of soil.

RESULTS AND DISCUSSION:

Dick Mason Pond. During 1967 seepage in this pond averaged 1 to 2 mm day⁻¹ from water depths of 560 to 1080 mm. Sodium adsorption ratios of extracts and water samples taken during the year are shown in Figure 1. Evaporation during the year increased the sodium concentration in the pond water, although this was not reflected in the soil solution extracts. The reason for the sharp increase in SAR in the 5-cm depth and sharp decrease in the 10-cm depth in October is not known, but samples to be taken in 1968 may indicate the cause. In the range of SAR values shown on the graph, $SAR \approx ESP$, which means that if the soil solution is in equilibrium with the soil complex, low seepage rates can persist when the ESP is as low as 2 to 8.

House Mountain #1 Pond. Since the addition of sodium carbonate and sodium chloride to the pond water in November 1966 (see 1966 Annual Report for details), seepage prior to the July dryup ranged from 3 to 6 mm day⁻¹ with water depths of 770 to 1250 mm. After the pond had refilled, seepage rates were 2 to 3 mm day⁻¹ with water depths of 1200 to 1600 mm.

From water analyses taken during the year, SAR values have been calculated and are shown in Figure 2. The sodium in the pond water increases from January through May because of evaporation losses and then decreases as the pond is refilled by relatively pure runoff water.

It is felt that the lower seepage rates after the pond filled in August are due to the high SAR in the upper part of the soil. When the pond was dry in July, salts moved upward as water evaporated from the soil surface, and the sodium once again caused the soil to be dispersed. Notice also that the SAR in the soil solution at the

lower depths increase with time, indicating that sodium is moving down through the soil profile. Samples to be taken in 1968 should give an indication of how fast the sodium is moving and where it is going.

The soil analyses in Table 1 also show substantial increase since November 1966 in the exchangeable sodium remaining on the soil complex, and a high percentage of naturally dispersed clay in the 30- to 60-cm soil depth. It is quite likely that this is the predominant seepage controlling layer in the soil profile.

Swan Lake Pond. The pretreatment soil analysis on 25 April 1967 (Table 2) shows a relatively low ESP in the 0- to 30-cm depth. However, about 3 months after treatment the ESP ranged from 10 to 16 in the same depth. A plot of water loss rate (seepage + evaporation + transpiration by weeds on the bank) versus water depth is shown in Figure 3. The average water loss reduction for the water depth shown is 92%.

It can be seen that the loss rate was still high when the pond was full. This may be due to water flowing down past the roots of Johnsongrass growing in this area and/or a loss of sodium from the bank soil. Soil samples taken in the side of the pond on 02 October 1967 show an ESP of 5 to 7. We decided that additional sodium carbonate might reduce the high rate of loss, so more salt was added. Weather conditions have prevented us from taking further water loss measurements. The partial retreatment will be evaluated in 1968.

The average reduction in water loss as a function of time is shown in Figure 4. These values were calculated by taking the time (posttreatment) it took for the water level to drop a given distance as compared with the time (pretreatment) it took for the water level to drop the same distance. It is evident that it took about 2 months before the reduction reached 90%. This time dependency may be due to (1) sodium replacing calcium and magnesium on the soil (2) dispersed clay moving into the void space and (3) clay swelling in the voids. Also note that the temporary dryup in early June caused the reduction to be depressed slightly, but only for a short period of time.

SUMMARY:

Two and one-half years have passed since Dick Mason pond was treated with sodium carbonate to reduce seepage, and the seepage rate is still only 1 to 2 mm day⁻¹. This treatment has already lasted one year longer than when the pond was treated with tetrasodium polyphosphate. House Mountain #1 pond received an addition of sodium carbonate and sodium chloride to the pond water in November 1966, and the seepage rate has averaged 4 mm day⁻¹ since that time. The maintenance procedure for ponds initially treated with salt has been clearly demonstrated.

Swan Lake was treated with sodium carbonate in May 1967 and the water loss has been reduced 92% (on the average from 244 to 20 mm day⁻¹). It took about 2 months before the water loss reduction reached 90%. This time dependency may be due to (1) sodium replacing calcium and magnesium on the soil, (2) dispersed clay moving into the void space, and (3) clay swelling in the voids.

PERSONNEL: Robert J. Reginato, Lloyd E. Myers.

Table 1. Exchangeable sodium (ES) and naturally dispersed clay from House Mountain Pond No. 1.

Depth (cm)	Date	ES %	Dispersed clay < 2 μ %
0-15	11/66	2.3	2
	7/67	7.8	3
15-30	11/66	3.6	1
	7/67	6.5	5
30-45	11/66	2.3	2
	7/67	12.6	14
45-60	11/66	-	-
	7/67	9.7	14
60-75	11/66	-	-
	7/67	5.7	5

Table 2. Exchangeable sodium (ES) and dispersed clay from Swan Lake.

Date	Depth (cm)	Location	ES %	Naturally dispersed
				clay < 2 μ %
25 Apr 67	0-15	Pond bottom	2.0	3
	15-30	"	2.8	3
	30-45	"	3.3	2
	45-60	"	3.5	2
	60-75	"	3.9	1
	75-90	"	3.9	0
21 Aug 67	0-10	"	14.4	5
	10-20	"	16.1	7
	20-30	"	10.0	4
	30-40	"	7.2	4
	40-50	"	5.1	3
	50-60	"	4.7	3
02 Oct 67	0-10	Pond bank	6.3	-
	10-20	"	6.8	-
	20-30	"	5.2	-

37-8

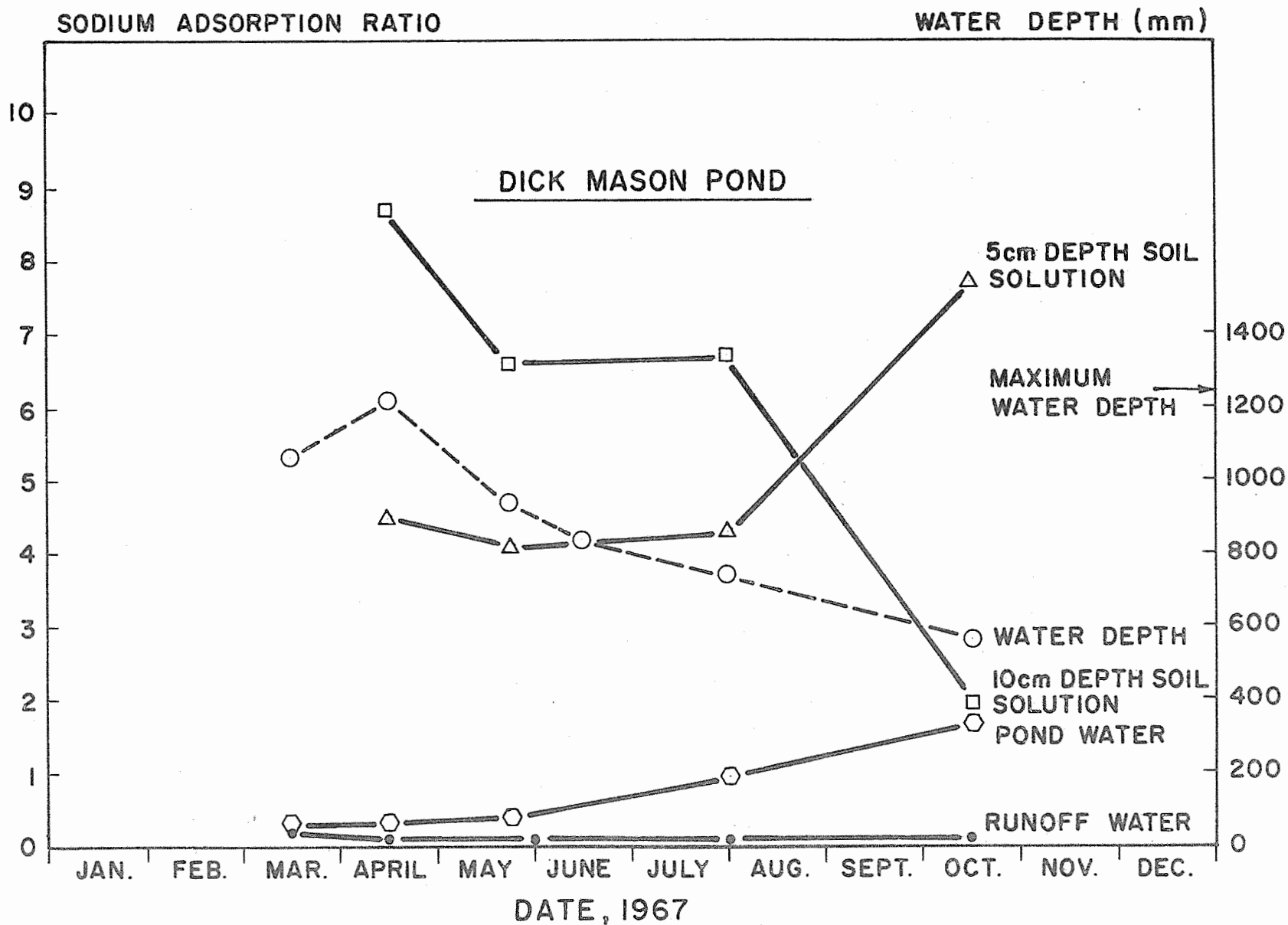


Figure 1. Sodium adsorption ratio (SAR) and water depth versus time for Dick Mason Pond. Annual Report of the U.S. Water Conservation Laboratory

37-9

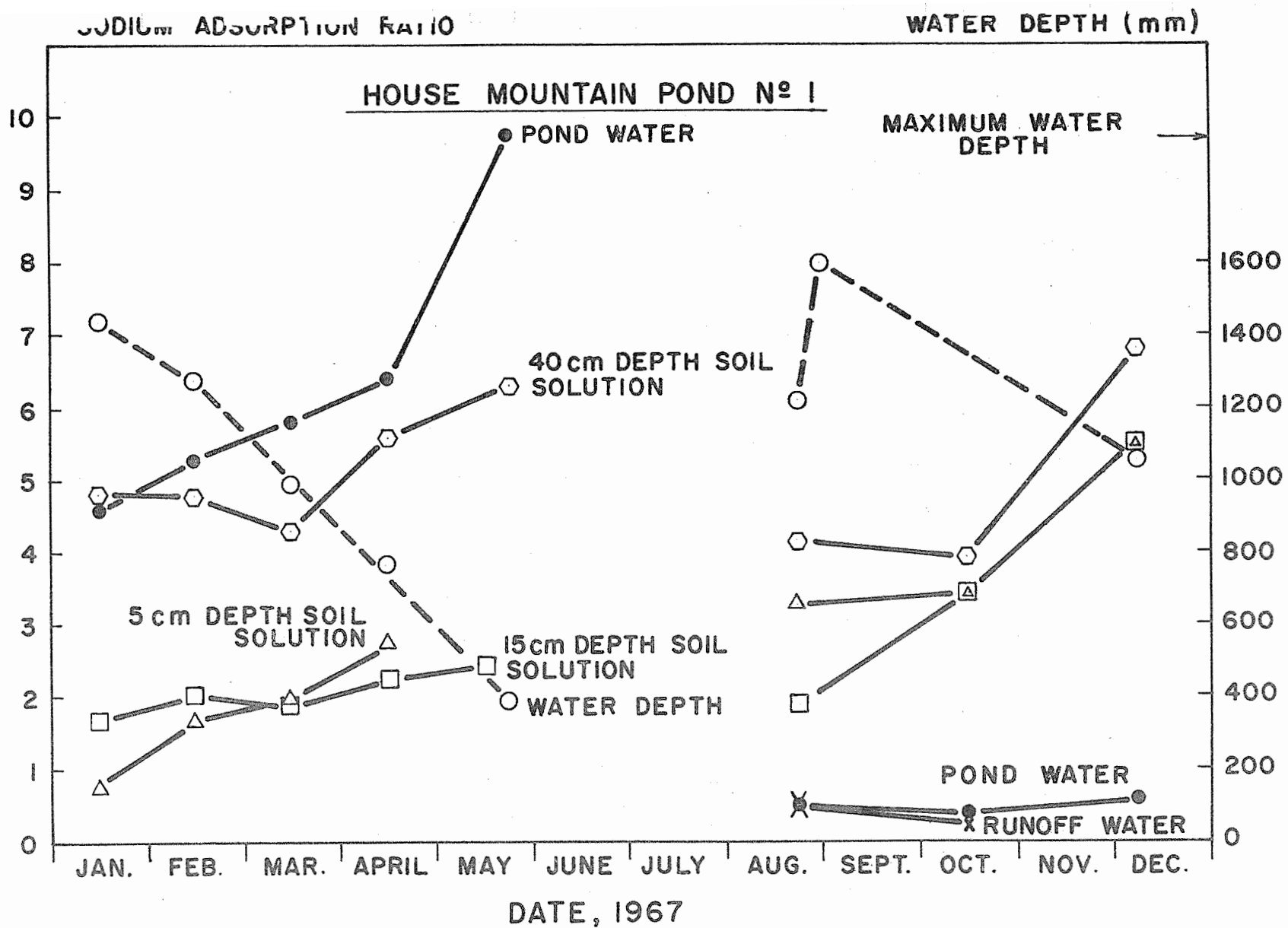


Figure 2. Sodium adsorption ratio (SAR) and water depth versus time for House Mountain Pond No. 1.

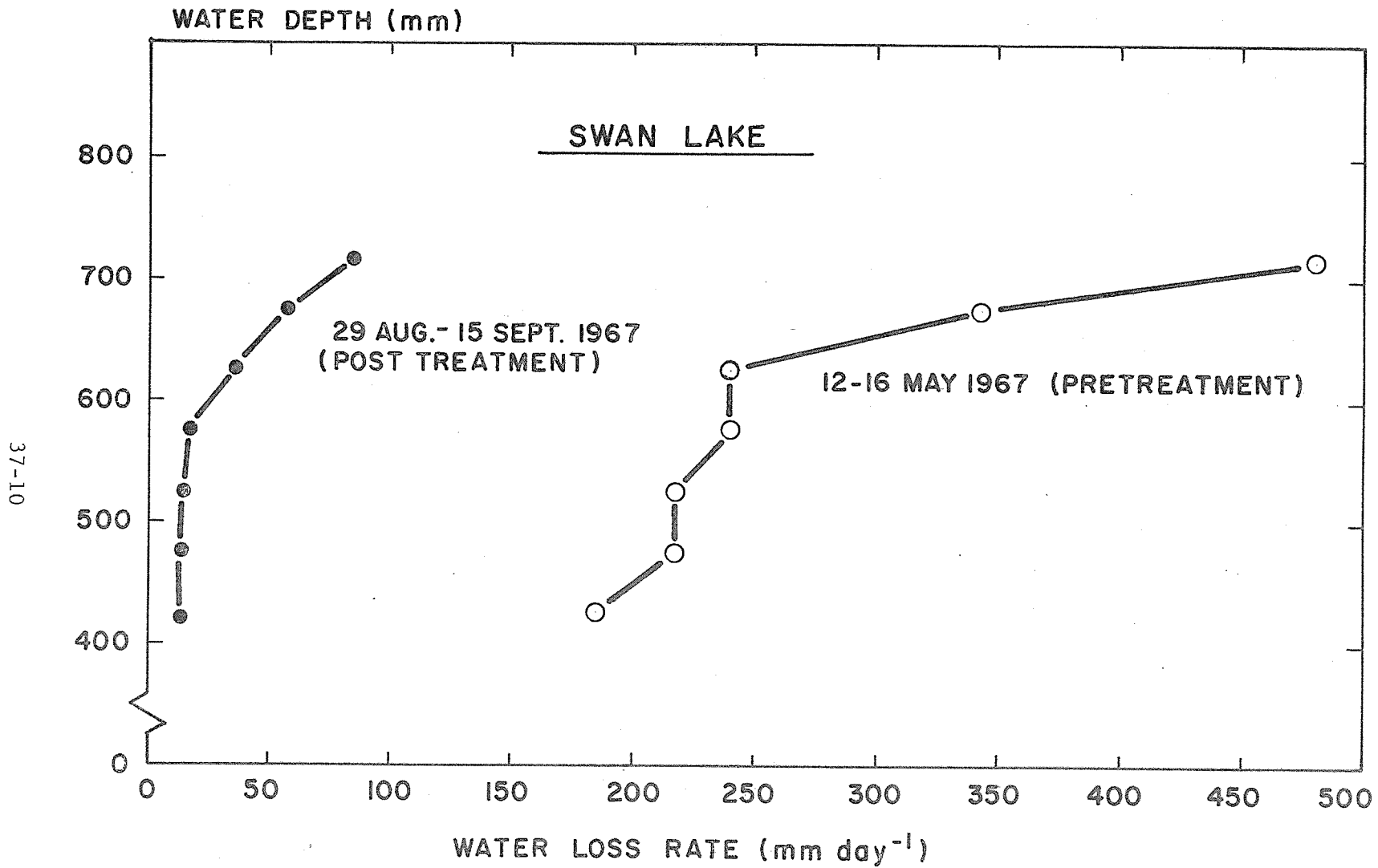


Figure 3. Rate of water loss versus water depth for Swan Lake.

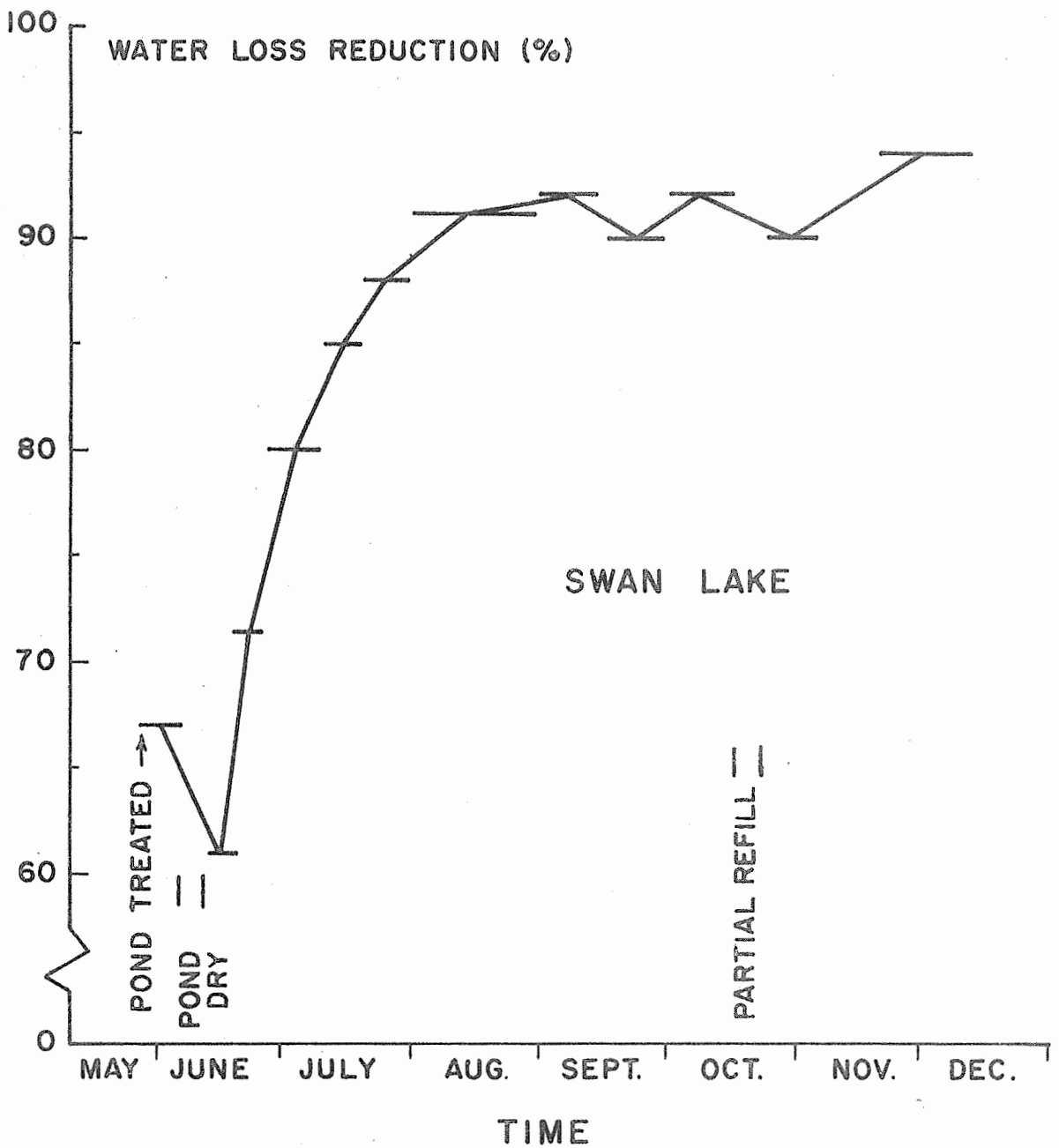


Figure 4. Average water loss reduction versus time for Swan Lake.

TITLE: WATERBORNE SEALANTS TO REDUCE SEEPAGE LOSSES FROM
UNLINED CHANNELS AND RESERVOIRS

LINE PROJECT: SWC W7 gG-2

CODE NO.: Ariz.-WCL-38

INTRODUCTION:

In May 1967 one reservoir was treated with a waterborne sealant to reduce seepage. Water loss measurements were made on this pond and on one treated with a different waterborne sealant in 1966.

PROCEDURE:

Salome No. 1. This reservoir had an initial water loss rate of 3.00 ft day⁻¹ at its operating level (4.7 ft deep). It was treated with sealant 10A (a rapid setting type asphalt emulsion) in October 1966 (see 1966 Annual Report for details). Water loss measurements, taken in May and September 1967, were made with an F-1 water stage recorder. The tests were started when the pond was full, and the water level decline was recorded for 3 to 5 days. This water loss is equal to seepage plus evaporation.

Salome No. 2. Located next to Salome No. 1 reservoir, No. 2 had a pretreatment seepage rate of 2.53 ft day⁻¹ at its operating level (5.5 ft deep).

Prior to treating the reservoir, eight 8-inch diameter x 18-inch long infiltration cylinders were placed 4 inches deep in the pond bottom and filled with water to a depth of 12 inches. Initial intake rates were measured by measuring the rate of fall of the water surface with a ruler and stopwatch. Duplicate cylinders were then treated as follows: (1) no emulsion added (2) 0.25 gal yd⁻² emulsion added (3) 0.50 gal yd⁻² emulsion added and (4) 0.75 gal yd⁻² emulsion added. Intake rates were again measured 18 hours after the emulsion was added.

In May 1967, 1100 gallons of sealant 13MR (a slow setting type asphalt emulsion) was added to the filling water in the reservoir resulting in an application rate of 0.75 gal yd⁻². Initially, we tried to pump the emulsion into the incoming water, but the intake

screen on the gear pump clogged. We then tipped the drums of asphalt emulsion on their sides and let the emulsion flow into the water from the pond bank. There was adequate mixing of emulsion with the water.

Emulsion 13MR was used instead of 10A because the former is much easier to manufacture than the latter. This may ultimately reduce the material costs to the buyer.

Two weeks after treatment, 360 additional gallons of 13MR (0.25 gal yd^{-2}) were added to the pond water (pouring emulsion from drums on pond bank) and the pond was refilled. Water loss measurements were taken in June, August, and September in the same manner as mentioned for Salome No. 1.

RESULTS AND DISCUSSION:

Salome No. 1. Water loss measurements taken in April showed a water loss rate of 0.19 ft day^{-1} at the operating level, or a water loss reduction of 94% (see Figure 1). In September, the loss had declined to 0.03 ft day^{-1} or a reduction of 99%. This additional reduction 11 months after treatment is not due to the asphalt per se, but to other factors. The asphalt decreased the water loss quite drastically initially. Subsequent reduction is thought to be due to silt blown into the pond or, more probably, by biological sealing. This latter effect may be due to fish and fish food put into the pond by the farmer. Catfish planted in the pond in April have not been affected by the asphalt seal.

Salome No. 2. The reduction in intake rates as determined by the cylinders was 83% at the 0.25 gal yd^{-2} treatment rate, 89% at the 0.50 gal yd^{-2} rate, and 94% at the 0.75 gal yd^{-2} rate. On the basis of these results the 0.75 gal yd^{-2} rate was used for the reservoir treatment.

The initial water loss of 2.53 ft day^{-1} declined to 1.78 ft day^{-1} during the week following the treatment (see Figure 1). Since this amounted to only a 30% reduction, it was decided to add more emulsion to the pond. Subsequently, 360 gal (0.25 gal yd^{-2})

of the sealant were added, and the water loss declined to 0.39 ft day⁻¹ (85% reduction) in early June. Apparently, our cylinder test was not representative of the conditions in the entire reservoir.

In August, the water loss had declined to 0.07 ft day⁻¹ (97% reduction) and in September to 0.03 ft day⁻¹ (99% reduction). This additional reduction, we feel, was due to factors mentioned under Salome No. 1.

Additional observations on both reservoirs during 1968 will be made to determine the longevity of the treatments.

SUMMARY:

Water loss measurements were made on Salome No. 1, a reservoir treated with a waterborne sealant (10A) in October 1966. The loss had declined from a pretreatment rate of 3.00 ft day⁻¹ to 0.03 ft day⁻¹, 11 months after treatment, or a reduction in water loss of 99%.

Salome No. 2 was treated with a waterborne sealant (13MR), which is easier to manufacture than 10A. Infiltration cylinder tests in the pond prior to treatment showed a 94% reduction in intake rate with an application of 0.75 gal yd⁻². Emulsion at this rate was added to the reservoir, and the water loss declined from a pretreatment rate of 2.53 ft day⁻¹ to 1.78 ft day⁻¹ in a week's time (30% reduction). The cylinder tests were apparently not representative of the entire reservoir, so more emulsion, 0.25 gal yd⁻², was added to the reservoir water. The water loss declined to 0.39 ft day⁻¹ (85% reduction) one week after this addition and three months later to 0.03 ft day⁻¹ (99% reduction).

The continual reduction in water loss with time for both ponds is not due to the asphalt per se. The asphalt drastically reduced water loss initially, and subsequent reduction is thought to be due to biological sealing. This latter effect was enhanced by fish and fish food put into the pond by the farmer.

Waterborne sealants have been shown to be successful in reducing seepage losses for 11 months under conditions we encountered. The longevity of this type of treatment is still under investigation.

PERSONNEL: Robert J. Reginato and Lloyd E. Myers.

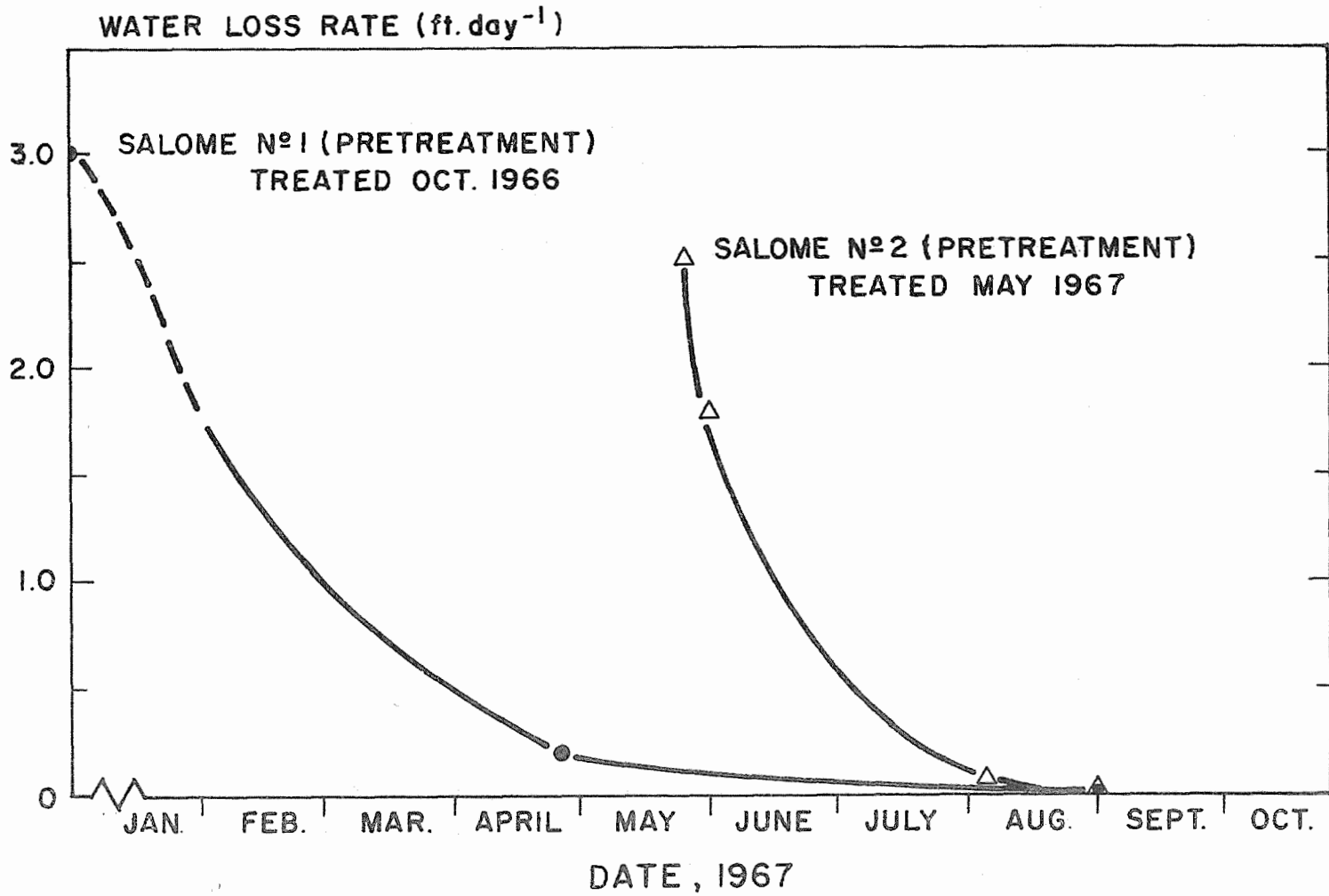


Figure 1. Rate of water loss versus time for Salome Ponds 1 and 2.

TITLE: DISPERSION AND FLOCCULATION OF SOIL AND CLAY MINERALS
AS RELATED TO THE Na AND Ca STATUS OF THE AMBIENT
SOLUTION.

LINE PROJECT: SWC W7 gG-5 CODE NO.: Ariz.-WCL-40

INTRODUCTION:

The fundamentals of Ca activity measurements were discussed in the Annual Report of 1966. In essence, the reliable measurement of the Ca and Na status of the soil solution requires precise knowledge of the activities of the two kinds of cations. However, in the case of Ca salts such as CaCO_3 , complexes and undissociated species are present which detract from the "true" Ca^{+2} activity. To overcome this shortcoming, Ca activities were measured with the newly developed Ca membrane electrode and used in conjunction with a theory developed for estimating the quantity of other forms of Ca in the CaCO_3 -water system.

THEORY:

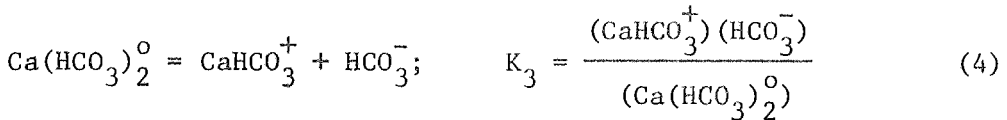
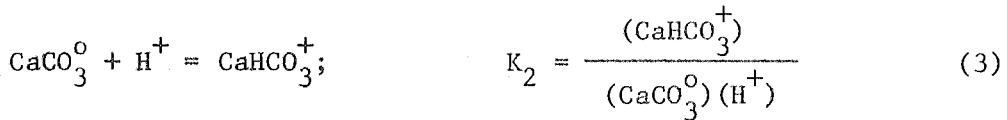
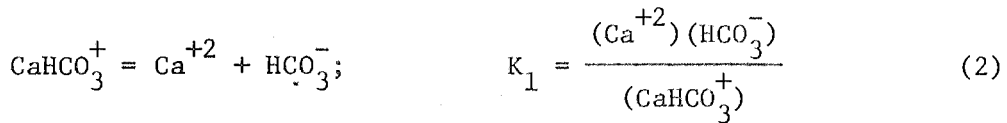
The development of a theory for the determination of the Ca complex CaHCO_3^+ and the ion-pair CaCO_3^0 or $\text{Ca}(\text{HCO}_3)_2^0$ required the imposition of mass balance to the equilibrium solution of saturated CaCO_3 , namely:

$$\text{Ca}_T = \text{Ca}^{+2} + \text{CaHCO}_3^+ + \text{CaCO}_3^0 \quad (1a)$$

$$\text{Ca}_T = \text{Ca}^{+2} + \text{CaHCO}_3^+ + \text{Ca}(\text{HCO}_3)_2^0 \quad (1b)$$

Ca_T represents the total Ca concentration. It was assumed in this case that either undissociated CaCO_3^0 or $\text{Ca}(\text{HCO}_3)_2^0$ was present as signified by equation (1a) and (1b), respectively.

The chemical equations and equilibrium constants for the various species are:



with () representing the activity of the solute. The ion activity is related to the ion concentration by the relation $(\text{Ca}^{+2}) = \gamma_{\text{Ca}^{+2}} [\text{Ca}^{+2}]$, where the bracket [] is the concentration and γ is the activity coefficient which can be estimated by the extended Debye-Hückel theory for dilute solutions. Solving equations (2), (3), and (4) for (CaHCO_3^+) , (CaCO_3^0) , and $\text{Ca}(\text{HCO}_3)_2^0$, respectively, and substituting them into (1a) or (1b) with additional algebraic treatment and rearrangement, the following are obtained:

$$\frac{\frac{[\text{Ca}_T]}{[\text{Ca}^{+2}] - 1}}{[\text{HCO}_3^-] \frac{\gamma_{\text{HCO}_3^-} \gamma_{\text{Ca}^{+2}}}{\gamma_{\text{CaHCO}_3^+}}} = \frac{1}{K_1} + \frac{1}{K_1 K_2} \cdot \frac{\gamma_{\text{CaHCO}_3^+}}{(\text{H}^+)} \quad (5)$$

$$\frac{\frac{[\text{Ca}_T]}{[\text{Ca}^{+2}] - 1}}{[\text{HCO}_3^-] \frac{\gamma_{\text{HCO}_3^-} \gamma_{\text{Ca}^{+2}}}{\gamma_{\text{CaHCO}_3^+}}} = \frac{1}{K_1} + \frac{[\text{HCO}_3^-] \gamma_{\text{HCO}_3^-} \gamma_{\text{CaHCO}_3^+}}{K_1 K_3} \quad (6)$$

Equations (5) and (6) relate to the condition where CaCO_3^0 and $\text{Ca}(\text{HCO}_3)_2^0$ are present, respectively.

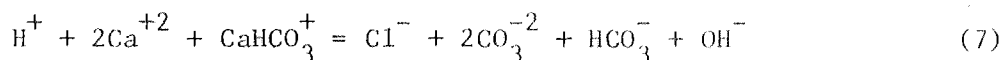
A plot of the ratio

$$\frac{\frac{[\text{Ca}_T]}{[\text{Ca}^{+2}] - 1}}{[\text{HCO}_3^-] \frac{\gamma_{\text{HCO}_3^-} \gamma_{\text{Ca}^{+2}}}{\gamma_{\text{CaHCO}_3^+}}} \text{ vs } \frac{\gamma_{\text{CaHCO}_3^+}}{(\text{H}^+)} \text{ or } [\text{HCO}_3^-] \gamma_{\text{HCO}_3^-} \gamma_{\text{CaHCO}_3^+} \text{ should}$$

yield a straight line with $K_1 = 1/\text{intercept}$ and $K_1 K_2$ or $K_1 K_3 = 1/\text{slope}$.

Both CaCO_3^0 and $\text{Ca}(\text{HCO}_3)_2^0$ could conceivably be present at the same time, and in this case equations similar to (1a) or (1b), and (5) or (6) can be developed. However, the solution involves the estimation of the equilibrium constants K_1 , K_2 , and K_3 , simultaneously, and since only two factors can be determined, namely, the slope and intercept, the three unknown parameters cannot be calculated. Results to be presented later will show that only one ion-pair form is present so that the preceding need not be considered experimentally, although the situation was considered as a possibility.

Another method which does not require the use of the Ca membrane electrode can be used as an independent check of K_1 obtained from the pH-pCa measurement. In this case, only pH measurements of $\text{CaCl}_2\text{-H}_2\text{CO}_3$ solutions are made. In addition to equation (1a) or (1b), we must utilize the charge balance equation



When the experiment is run at low pH's, the forms CaCO_3^0 or $\text{Ca}(\text{HCO}_3)_2^0$, CO_3^{-2} and OH^- can be neglected. Combining equation (7) with (1) and introducing the appropriate equilibrium constants, we have

$$K_1 = \frac{\left\{ [Ca_T] - ([H^+] - [HCO_3^-]) \right\} [HCO_3^-] \gamma_{Ca^{+2}} \gamma_{HCO_3^-}}{([H^+] - [HCO_3^-]) \gamma_{CaHCO_3^+}} \quad (8)$$

As noted, this measurement is made at low pH. Unfortunately, the Ca membrane electrode cannot be used because the Ca activity measurement is affected significantly in the presence of high concentration of H^+ ions. Also, unlike the pH-pCa method, only K_1 can be determined.

PROCEDURE:

Saturated $CaCO_3$ solutions were prepared from analytical reagent-grade, powdered $CaCO_3$. The solutions were allowed to stand with occasional shaking for at least one month prior to use. The saturated solutions were agitated in a closed system by bubbling CO_2 - N_2 gas mixtures which ranged in composition from 0.54 to 99.98% CO_2 . After bubbling the gas until the pH remained constant, Ca activity measurements were made. Atmospheric CO_2 condition was simulated by using a 350 ppm CO_2 gas mixture. The gases were pre-wetted by passing them through bubbling towers. pH and Ca^{+2} activity were measured simultaneously with the glass and membrane electrodes, respectively, using two expanded-scale pH-millivolt meters with accuracy of ± 0.1 mv. Ceramic-plug type saturated KCl calomel reference electrode was utilized. The glass electrode was calibrated in appropriate reference solutions which had been checked against NBS standard buffers. The Ca electrode was calibrated with standard $CaCl_2$ solutions. For increased accuracy, standard solutions were used which bracketed closely the EMF output of the unknown Ca solution. Total Ca in solution was determined by the versenate titration method.

$CaCl_2$ solutions were prepared from reagent-grade $CaCl_2$. pH measurements of the CO_2 -saturated $CaCl_2$ solutions were made in a similar manner as the saturated $CaCO_3$ system. Only the 99.98% gas mixture was used. All measurements were made in a constant temperature room at 25 ± 0.5 C.

Bicarbonate concentration, $[\text{HCO}_3^-]$, was estimated from the first dissociation constant (K_{1A}) of carbonic acid. Suitable ionic strength (μ) corrections were made for K_{1A} (8) and for k , the solubility constant of CO_2 , (4) such that $\text{p}K'_{1A} = 6.363 - 0.522 \sqrt{\mu}$ and $k' = 0.0344 - 0.0084 \mu$. The second dissociation constant of carbonic acid (K_{2A}) for estimating CO_3^{2-} concentration was taken as $\text{p}K'_{2A} = 10.329 + 0.0348 \mu$ calculated from the data of Harned and Sholes (5). The partial pressure of CO_2 was obtained from the barometric pressure and gas composition with suitable correction for the vapor pressure of water. Activity coefficients were derived from the Debye-Hückel theory

$$-\log \gamma = A \sqrt{\mu} / (1 + B a \sqrt{\mu}) \quad (9)$$

using the appropriate values for the constants A, a, and B tabulated by Kielland (6).

RESULTS AND DISCUSSION:

CaCO_3 - CO_2 System. The basic data necessary for estimating the different equilibrium constants which includes the CO_2 gas composition, pH, total Ca, Ca activity and the pressure of CO_2 - N_2 mixture are listed in Table 1.

The various parameters were calculated by an iteration technique. Since the concentrations of the different ionic species were unavailable at the start for determining the ionic strength and likewise the activity coefficients, the initial ionic strength was taken as $3[\text{Ca}_T]$. The components making up equations (5) and (6) were calculated based on this initial μ and the original data. The comparison fitted equation (5), but not equation (6) indicating that the species Ca^{+2} , CaHCO_3^+ , and CaCO_3^0 were present in solution and that $\text{Ca}(\text{HCO}_3)_2^0$ was absent. From the slope and intercept, K_1 and K_2 were calculated. Using the K_1 and K_2 constants, $[\text{CaHCO}_3^+]$ and $[\text{CaCO}_3^0]$ were estimated and a better

ionic strength function was derived based on the relation $\mu = (4[\text{Ca}^{+2}] + [\text{HCO}_3^-] + [\text{CaHCO}_3^+])/2$. New γ values were then determined and, successively, K_1 and K_2 . The iteration process was continued until the various factors remained constant. The activity coefficient of CaHCO_3^+ was assumed to be the same as HCO_3^- .

The $\left(\frac{[\text{Ca}_T]}{[\text{Ca}^{+2}]} - 1\right)/[\text{HCO}_3^-] \gamma_{\text{Ca}^{+2}}$ vs $\gamma_{\text{CaHCO}_3^+}/(\text{H}^+)$ values from the

final iteration step are plotted in Figure 1. K_1 and K_2 are 0.0564 ± 0.0025 and $(1.245 \pm 0.056) \times 10^7$, respectively, as determined from the intercept and slope. The linear correlation coefficient is 0.911. These compare with a K_1 of 0.0574 ± 0.0036 and K_2 of 5.886×10^7 at 22 C obtained by correcting for the activity coefficients of the various ionic species from the measurements reported at an ionic strength of 0.15 at 22 C by Greenwald (3). The K_1 values of the two methods are similar, whereas the K_2 's are not. In Greenwald's method (3), a value for K_2 had to be selected which will give K_1 's that are consistent with the experimental data. However, in the treatment reported here, K_2 is obtained directly from the experimental data without any assumption as to its value. The $\text{Ca}(\text{HCO}_3)_2^0$ form was absent in our experiments. Thus, the indiscriminate use of the formula $\text{Ca}(\text{HCO}_3)_2$ for Ca carbonate solutions is subject to error.

The concentrations of the three forms of Ca in saturated CaCO_3 solutions in equilibrium with different CO_2 composition are presented in Table 2. The relation among Ca^{+2} , CaHCO_3^+ , and CaCO_3^0 varies with the CO_2 partial pressure. The percent CaHCO_3^+ in solution decreases from 14.4 to 3.2 as the CO_2 concentration decreases from 100 to 0.54%, whereas for CaCO_3^0 the concentration increases from 1 to 7.7%; at the same time the amount of Ca^{+2} changes from 84 to 89% of the total Ca in solution. The significance of this type of relation at atmospheric CO_2 partial pressure will be discussed later.

Using the experimental data available, the solubility product of CaCO_3 , K_S , was also calculated. The K_S values listed in Table 2

are comparable with those reported by Akin and Lagerwerff (1) and Frear and Johnston (2) of 5.0×10^{-9} and 4.82×10^{-9} , respectively. The close agreement between the present and prior data gives confidence in the pH and total Ca measurements and the associated parameters used to calculate K_S .

An additional equilibrium constant (K_4) can be derived for the relation $\text{CaCO}_3^0 = \text{Ca}^{+2} + \text{CO}_3^{-2}$. In this case $K_4 = K_1 K_2 K_{2A}$ or 0.329×10^{-4} .

CaCl₂ - CO₂ System. K_1 values based on only pH measurements of CaCl₂ solutions (see equation 8) in equilibrium with 100% CO₂ are presented in Table 3 for a series of CaCl₂ concentrations. Over the concentration range of 0.008 to 0.2 M CaCl₂, the pH change was only 0.10 unit. The need for sensitive pH measurement under these conditions is apparent. The pH values of 3.80 to 3.90 preclude the presence of significant amounts of CO₃⁻² in solution. A test of the data using equation (5) showed no value for K_2 , indicating the absence of CaCO₃⁰ at these pH's.

The parameters $\text{p}K_{1A}$, k , and γ are all functionally dependent upon the ionic strength of the solution and, if the proper relation is used to estimate K_1 , then K_1 should be the same for all ionic strengths. However, column 4 of Table 3, shows that K_1 varies with μ , but a thermodynamic K_1 can be estimated by the extrapolation of the data to $\mu = 0$. The linear regression equation fitting the results is $K_1' = 0.0539 + 0.0779 \mu$; the K_1 at $\mu = 0$ is 0.0539 ± 0.0034 and compares favorably with the K_1 of 0.0564 ± 0.0025 determined by the combination pH-pCa measurement for the CaCO₃-CO₂ system. Comparison of equations (5) and (8) show that there is less error sources due to ion activity measurements in equation (5) than (8), noting that $[\text{HCO}_3^-]$ must be estimated from the pH. Thus, the pH-pCa method should theoretically give a more reliable estimate of K_1 . Also a wider pH range was covered in the CaCO₃-CO₂ than the CaCl₂-CO₂ system.

Saturated CaCO_3 under atmospheric CO_2 condition of 350 ppm CO_2 had a pH of 8.331, $[\text{Ca}_T]$ of 5.84×10^{-4} M, and (Ca^{+2}) of 3.80×10^{-4} M. Using the equilibrium constants developed previously, the concentration of CaHCO_3^+ , CaCO_3^0 , and Ca^{+2} was 0.07×10^{-4} , 1.22×10^{-4} and 4.55×10^{-4} M, respectively. Thus, we see that only 78% of the total Ca is in the ionic Ca^{+2} form, whereas the remaining 22% is made up primarily of the CaCO_3^0 ion-pair. Further study of the data and equations indicates that raising the pH, which reduces the $[\text{Ca}_T]$, will also increase the CaCO_3^0 species. The CO_3^{-2} concentration was 1.56×10^{-5} compared to the CaCO_3^0 of 1.22×10^{-4} M showing that a large proportion of the total CO_3^{-2} is tied up as the ion-pair, and part of the buffering action is due to this type of association. In the case of the $\text{CaHCO}_3^+ - \text{HCO}_3^-$ relation, there is 0.07×10^{-4} M CaHCO_3^+ and 1.09×10^{-3} M HCO_3^- indicating that only a small part of the bicarbonate is tied up as the Ca complex.

It was reported earlier in the saturated CaSO_4 system (7) that 76% of the total Ca in solution was Ca^{+2} and the remaining 24% was in the form of the ion-pair CaSO_4^0 . As was noted in the literature review section, workers have taken this limited dissociation for CaSO_4 into account, but not for the CaCO_3 system. It is apparent, therefore, that exchange studies in the presence of CaCO_3 should take into account the fact that not all of the Ca in solution is in the Ca^{+2} form.

The use of the Ca-electrode directly in calcareous soil-water system presents certain difficulties since the electrode is also responsive to other divalent and monovalent cations and unless the electrolyte condition is known and the proper correction made for it, the Ca activity measured may be erroneous. Nevertheless, the equilibrium constants determined on the better defined CaCO_3 system as presented above should be applicable to the more complex soil solution.

SUMMARY AND CONCLUSIONS:

Simultaneous H- and Ca-ion activity measurements were made to determine the forms of Ca and their associated equilibrium constants

in saturated CaCO_3 solution. The constants related to each of the species are $K_1 = 0.0564 \pm 0.0025$ for the relation $\text{CaHCO}_3^+ = \text{Ca}^{+2} + \text{HCO}_3^-$, $K_2 = (1.245 \pm 0.056) \times 10^7$ for $\text{CaCO}_3^0 + \text{H}^+ = \text{CaHCO}_3^+$, and $K_4 = 0.329 \times 10^{-4}$ for $\text{CaCO}_3^0 = \text{Ca}^{+2} + \text{CO}_3^{-2}$.

In saturated CaCO_3 solution under partial pressure condition resembling that of atmospheric CO_2 of 350 ppm CO_2 , the Ca^{+2} form makes up about 80% of the total Ca in solution; the remaining 20% is made up of the CaCO_3^0 and CaHCO_3^+ species, with the CaCO_3^0 predominating over the CaHCO_3^+ form. Under these conditions suitable correction must be employed to get the actual Ca^{+2} concentration when the Ca activity cannot be measured directly.

REFERENCES:

1. Akin, G. W., and Lagerwerff, J. V. Calcium carbonate equilibria in aqueous solutions open to the air. I. The solubility of calcite in relation to ionic strength. *Geochim. et Cosmochim. Acta* 29: 343-352. 1965.
2. Frear, G. L., and Johnston, J. The solubility of calcium carbonate (calcite) in certain aqueous solutions at 25°. *Jour. Amer. Chem. Soc.* 51:2083-2093. 1929.
3. Greenwald, I. The dissociation of calcium and magnesium carbonates and bicarbonates. *Jour. Biol. Chem.* 141:789-796. 1941.
4. Harned, H. S., and Davis, R., Jr. The ionization constant of carbonic acid in water and the solubility of carbon dioxide in water and aqueous salt solutions from 0 to 50°. *Jour. Amer. Chem. Soc.* 65:2030-2037. 1943.
5. Harned, H. S., and Sholes, S. R. The ionization constant of HCO_3^- from 0 to 50°. *Jour. Amer. Chem. Soc.* 63:1706-1709. 1941.
6. Kielland, J. Individual activity coefficients of ions in aqueous solutions. *Jour. Amer. Chem. Soc.* 59:1675-1678. 1937.
7. Nakayama, F. S., and Rasnick, B. A. Calcium electrode method for measuring dissociation and solubility of calcium sulfate dihydrate. *Anal. Chem.* 39:1022-1023. 1967.

8. Shedlovsky, T., and MacInnes, D. A. The first ionization constant of carbonic acid, 0 to 38°, from conductance measurements. Jour. Amer. Chem. Soc. 57:1705-1710. 1935.

PERSONNEL: F. S. Nakayama

Table 1. pH, total Ca, and Ca activity for saturated CaCO_3 solution in equilibrium with various CO_2 gas compositions.

CO_2 comp.	pH	$[\text{Ca}_T], \text{M}$	$(\text{Ca}^{+2}), \text{M}$	$\text{CO}_2\text{-N}_2$ pressure
%		$\times 10^3$	$\times 10^3$	atm
100	6.005 ± 0.007	8.72 ± 0.13	4.24 ± 0.20	0.9266 ± 0.0044
75.9	6.110 ± 0.001	7.65 ± 0.01	3.81 ± 0.06	0.9299 ± 0.0031
52.7	6.212 ± 0.002	6.70 ± 0.02	3.48 ± 0.01	0.9301 ± 0.0004
20.3	6.474 ± 0.009	4.66 ± 0.08	2.69 ± 0.05	0.9280 ± 0.0018
5.1	6.867 ± 0.001	2.90 ± 0.01	1.82 ± 0.02	0.9285 ± 0.0022
2.1	7.130 ± 0.001	2.06 ± 0.01	1.38 ± 0.01	0.9289 ± 0.0005
0.54	7.521 ± 0.001	1.37 ± 0.01	0.94 ± 0.01	0.9283 ± 0.0005

40-11

Table 2. Concentration of the different forms of Ca in saturated CaCO_3 at various CO_2 gas compositions.

CO_2	$[\text{Ca}^{+2}]$, M	$[\text{CaHCO}_3^+]$, M	$[\text{CaCO}_3^0]$, M	K_S
%	$\times 10^3$	$\times 10^3$	$\times 10^3$	$\times 10^9$
100	7.37	1.26	0.088	4.61
75.9	6.50	1.05	0.095	5.09
52.7	5.78	0.83	0.094	5.03
20.3	4.18	0.40	0.084	4.69
5.1	2.60	0.20	0.105	4.75
2.1	1.84	0.11	0.110	4.78
0.54	1.22	0.044	0.106	5.08

Mean 4.86 ± 0.18

Table 3. K_1 and pH values for CaCl_2 solutions in equilibrium with approximately 100% CO_2 gas composition.

CaCl_2 , M	pH	$\text{CO}_2\text{-N}_2$ press. atm	K_1
0.008	3.903 \pm 0.007	0.9249 \pm 0.0045	0.0538 \pm 0.0098
0.0085	3.900 \pm 0.005	0.9238 \pm 0.0032	0.0464 \pm 0.0045
0.00875	3.903 \pm 0.005	0.9224 \pm 0.0032	0.0571 \pm 0.0135
0.009	3.900 \pm 0.008	0.9256 \pm 0.0055	0.0498 \pm 0.0064
0.010	3.897 \pm 0.004	0.9236 \pm 0.0017	0.0500 \pm 0.0084
0.020	3.886 \pm 0.003	0.9226 \pm 0.0010	0.0608 \pm 0.0032
0.030	3.877 \pm 0.002	0.9216 \pm 0.0001	0.0680 \pm 0.0018
0.040	3.867 \pm 0.001	0.9253 \pm 0.0008	0.0684 \pm 0.0011
0.050	3.862 \pm 0.004	0.9261 \pm 0.0035	0.0739 \pm 0.0044
0.060	3.859 \pm 0.002	0.9241 \pm 0.0010	0.0802 \pm 0.0018
0.070	3.847 \pm 0.001	0.9216 \pm 0.0002	0.0703 \pm 0.0005
0.080	3.838 \pm 0.001	0.9253 \pm 0.0001	0.0689 \pm 0.0001
0.090	3.835 \pm 0.002	0.9263 \pm 0.0001	0.0716 \pm 0.0006
0.100	3.832 \pm 0.001	0.9276 \pm 0.0001	0.0743 \pm 0.0011
0.200	3.804 \pm 0.001	0.9254 \pm 0.0020	0.0793 \pm 0.0007

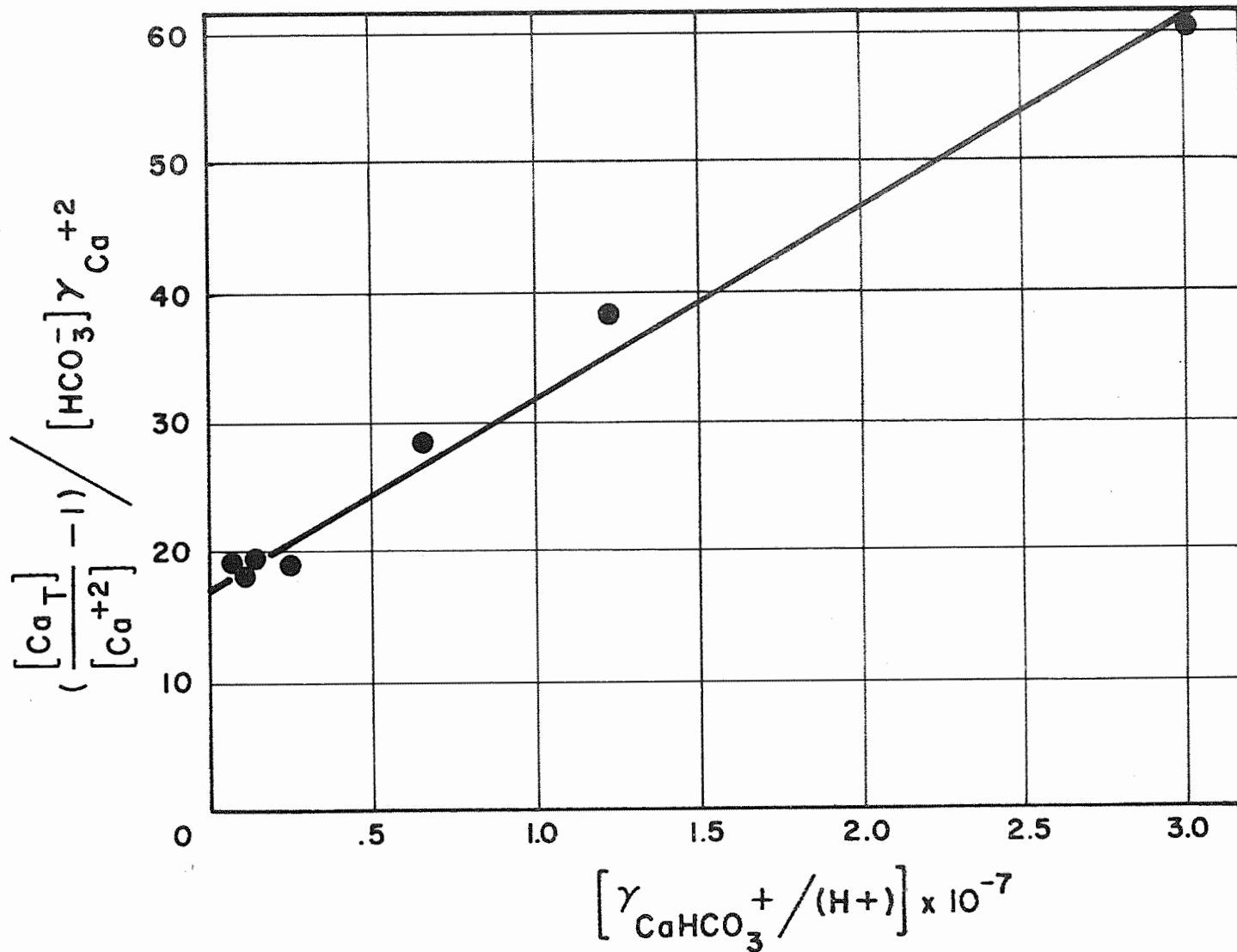


Figure 1. Plot of experimental data testing equation (5) for estimating K_1 and K_2 (see text).
Annual Report of the U.S. Water Conservation Laboratory

TITLE: MATERIALS AND METHODS FOR WATER HARVESTING AND
WATER STORAGE IN THE STATE OF HAWAII

LINE PROJECT: SWC W7 gG-4 CODE NO.: Ariz.-WCL-42

INTRODUCTION:

A description of the installations is given in previous annual reports. The data collected at the two sites by cooperators was forwarded monthly to the U. S. Water Conservation Laboratory for analysis. In March 1967 both sites were visited by Laboratory personnel. The Maui installation was visited again in December 1967.

PROCEDURE:

See Annual Report for 1966.

RESULTS AND DISCUSSION:

Kukaiiau Catchment. The storage reservoir at this catchment was completely filled with water by the end of 1966. In January 1967, after heavy rains, seepage water from the area around the pond collected under the lining causing the sheeting to balloon upwards. After the water under the lining subsided the sheeting settled back into place and appeared to be intact. Water from the reservoir was used throughout the year for livestock and was also piped several miles downslope to other pastures. With relatively heavy use the reservoir remained essentially full the entire year. From the period 1 January 1967 through 31 December 1967, 2879.6 mm of rainfall was recorded. A total of 914.4 mm fell in November 1967 with over 292.1 mm in one day. The water collected by the catchment and reservoir by months is presented in Table 1. A total of over 7 million liters of water was collected from the combined catchment and reservoir during the year. There has been no report of any damage to the sheeting on the catchment.

Maui Catchments. In February 1967 a report was received of lap joint failures on Plot No. 1, which is covered with the Hypalon

sheetings. The seams were repaired with a solvent-hypalon cement and when inspected in March 1967, appeared to be holding satisfactorily.

On Plot No. 2 covered with butyl, some of the seams were beginning to fold back when inspected in March 1967. A butyl tape had been used to patch wrinkled areas in the seams at time of installation. This tape had pulled apart and some grass had rooted through. These areas were subsequently repaired with surface patches.

The asphalt on Plot No. 3 was spongy when inspected in March 1967. There was no serious cracking but several rough spots were detected. There was a heavy cover of grass on the plot at the edges. Some grass was rooting through from above and some may have been coming up from below. Some of the grass appeared to have grown from seed deposited on the plot surface. The grass on the plot was removed and the rough spots hand treated with asphalt. The plots were all considered in excellent condition when inspected in December 1967.

Runoff data collected from the plots was not complete for the year. The clocks on the recorders would not always start when water started flowing through the flumes. Correspondence with the manufacturer of the clocks indicated it was not possible to insure starting of the clocks. The problem appears to be solved with the construction of special clocks at the Laboratory. Calibration of the clocks indicate a time scale error of less than $\pm 2\%$ for a 24 hour time period. These units have not had a start failure in 5000 stop-start cycles in the Laboratory. These new clocks will be installed early in 1968.

Preliminary analysis of the runoff data collected has been started. Some typical runoff data are presented in Table 2. For the week of 24 January 1967 a total of 32.9 mm of rain was collected with 28.1 mm in one storm. For the week the butyl collected 81.5%,

the asphalt 77.2% and the grass 17.0% of the rainfall. The butyl did collect over 100% of the rainfall for one storm of 1.5 mm. The reason for the relatively poor runoff efficiency of the butyl for the weekly total is not completely known, but it is suspected that recorder malfunctions caused erroneous runoff measurement. The runoff measured from the grass plot is considerably higher than was expected. During the week of 20 March 1967, with a total of 268.5 mm of rain, the grass plot yielded 143.3 mm for a 53% runoff efficiency. The recorders for the butyl and asphalt plots failed to operate for this period.

SUMMARY AND CONCLUSIONS:

The two experimental water harvesting structures installed in Hawaii in June 1966 were in excellent condition as of December 1967. The operational catchment and storage reservoir combination on the Island of Hawaii has been in full use the entire year. The rainfall at the site has been sufficient to keep the reservoir essentially full even with relatively high water use. Water collection for the year totalled over 7 million liters.

Preliminary analysis of the runoff data from the four plot test units on the Island of Maui has been started. The data from the plots is incomplete because of frequent failure of the waterstage recorder clocks to start when water began flowing through the flumes. New improved clocks have been built and tested and will be installed early in 1968. Preliminary calculations show that for one week with 32.9 mm of rain the butyl collected 81.5%, the asphalt 77.2% and the grass 17.0% of the rainfall. These figures are believed to be low because of measurement errors caused by recorder malfunctions. The runoff from the grass plot is considerably higher than expected. For one weekly period in March 1967 with a total of 268.5 mm of rain, the grass plot yielded 143.3 mm of runoff.

PERSONNEL: Lloyd E. Myers and Gary W. Frasier

Table 1. Quantity of water collected by catchment and reservoir at Kukaiau catchment.

Month	Rainfall (mm)	Quantity of Water Collected		
		Catchment (liters)	Reservoir (liters)	Total (liters)
Jan 67	401.1	347,740	636,910	984,650
Feb 67	156.2	135,460	245,030	380,490
Mar 67	208.5	180,770	331,080	511,850
Apr 67	301.0	260,960	477,960	738,920
May 67	98.0	84,960	155,610	240,570
Jun 67	71.9	62,340	114,170	176,510
Jul 67	143.5	124,410	227,860	352,270
Aug 67	306.6	265,820	486,850	752,670
Sep 67	29.7	25,750	47,160	72,910
Oct 67	56.4	48,900	89,560	138,460
Nov 67	916.7	794,760	1,455,640	2,250,400
Dec 67	190.0	164,730	301,700	466,430
	<u>2879.6</u>	<u>2,496,600</u>	<u>4,569,530</u>	<u>7,066,130</u>

Table 2. Runoff results from rainfall at Maui, Hawaii plots.

Starting Date	Rainfall (mm)	Runoff					
		Butyl Plot		Asphalt Plot		Grass Plot	
		(mm)	(%)	(mm)	(%)	(mm)	(%)
24 Jan 67	28.1	22.9	81.5	23.9	85.1	5.6	19.9
"	1.5	1.6	106.7	0.7	46.7	0	0
"	2.4	1.8	75.0	0.8	33.3	0	0
"	<u>0.9</u>	<u>0.5</u>	<u>55.6</u>	<u>0</u>	<u>0</u>	<u>0</u>	<u>0</u>
Total	32.9	26.8	81.5	25.4	77.2	5.6	17.0
20 Mar 67	268.5	-	-	-	-	143.3	53.4

TITLE: INTEGRATING VELOCITY PROFILE METERS

LINE PROJECT: SWC W10 gG-7

CODE NO.: Ariz.-WCL-43

INTRODUCTION:

See Annual Report for 1966.

Three styles of meters have been constructed. These are shown in Figure 1. Meters Number 1 and 2 have been tested and the results previously reported.

PROCEDURE:

The desire to have a direct discharge-rate indicating device in a channel rather than a velocity indicating mechanism inspired the design of Meter Number 3. This meter was designed to easily accept a number of shaped elements for indication of discharge as well as indication of velocity. It consisted of a vertical shaft mounted in ball bearings and a crossbar to which an element could be attached. The readout was accomplished with a dial that was attached to a torsion mechanism made from a clock spring which in turn maintained the shaft, bar, and element in the correct position. A certain amount of flexibility in magnitude of the readout was achieved by the position of the element on the crossbar. Moment arms from about 2 inches to 5 inches could easily be achieved by moving the element along the bar. The counterweight, built into all the meters was necessary to prevent the weight of the elements from influencing the readout in the event that the device was positioned slightly out of plumb. This is especially important if the device is to be hand held in field applications.

Two laboratory channels were available for studying the characteristics of the target meters designed for open channel flows. One channel was 1 foot wide, with about 20 feet between the inflow stilling baffles and the test section used for the target meters. The other was 2 feet wide with 12 feet between the baffles and the test section. Both channels were too short to produce the highly stable velocity profiles that were desired for the study.

The tests consisted of measuring the velocity profile with the pitot tube and manometer system already described in an earlier publication (2). The target meter was then inserted into the flow at approximately the same location and the force on the blade measured, Figure 2. The pitot traverse data was used to evaluate the drag coefficient. Knowledge of the value of the momentum correction factor is avoided in determining the drag coefficient by the method since its inclusion is accomplished by evaluating the theoretical relation directly (see Annual Report for 1966).

RESULTS AND DISCUSSION:

Once an element has been designed for a given channel using the concepts advanced in the Annual Report for 1966, the discharge equation becomes

$$Q = \sqrt{\frac{2gF}{C\gamma\beta k}} \quad (1)$$

where:

g = gravitational constant

F = the total drag force

C = a drag coefficient

γ = unit weight of fluid

β = momentum correction factor

k = a constant representing the ratio between A_e/A_c^2

A_e = area of element or blade exposed to the flow

A_c = cross-sectional area of the channel

Note that the depth, y , does not appear in this equation. Thus, Q is independent of flow depth.

Effects of Nonuniform Velocity Distributions. If either the velocity or discharge type of target-meter element is placed in a uniform velocity distribution, then the previously derived equations should predict the correct velocity or discharge, respectively, with

$\beta = 1$. However, real sheet flows produce nonuniform velocity distributions in at least two dimensions, and in the base of most channels, three dimensions.

For the rectangular blade, used as a velocity indicator, an accurate prediction can be obtained for the average velocity in the vertical section sampled by applying the momentum correction factor defined previously, see Annual Report, 1966. However, a modification is required to this definition for the shaped blades used as discharge indicators. Take, for example, the triangular blade used for discharge indication in rectangular channels and sheet flows. Since the theoretical relation for discharge is based on the average velocity in the stream, or in the case of sheet flows, in a vertical section, the momentum correction factor used with the triangular blade sampling a turbulent velocity profile should be based on the average velocity in the vertical section and not on the average velocity over the surface of the triangular blade. This would modify the definition of the momentum correction coefficient to

$$\beta' = \frac{1}{A_e \bar{v}_v^2} \int_0^{A_e} u^2 dA_e \quad (2)$$

where \bar{v}_v is the average velocity in the vertical section sampled, not the average velocity over the area of the blade, and u is the local velocity in the direction of main flow. The value β' will be approximately 10 to 15% higher than the generally recognized values for β because the triangular blade undersamples the low-velocity region near the bottom and exaggerates the effects of the high-velocity near the surface. Thus the theoretical equation would be more correctly written as

$$Q = \sqrt{\frac{2gF}{C\gamma\beta'k}} \quad (3)$$

A further adjustment is seen to be necessary for channels to account for the three-dimensional effect of the velocity profile. Calculations based on the Bazen data (1) indicate that the average velocity in the centerline profile of rectangular channels is approximately 8% higher than the channel average for wood plank or smooth channels and about 17% higher for rough channels lined with pea gravel and with wooden strips at intervals. The aspect ratios, width to depth, of the rectangular channels; the type of roughness elements; and the comparison of the average velocity in the channel centerline profile, v_v , with the average velocity in the channel, \bar{v} , are shown in Table 1.

Unlike the correction made to obtain β' , this correction is not due to blade geometry, but is a function of the channel and should be treated as a calibration coefficient C_c . Thus, equation (3) becomes

$$Q = C_c \sqrt{\frac{2gF}{C\gamma\beta'k}} \quad (4)$$

The value of C_c for rectangular channels that are wide compared to the inserted element appears to be about 0.85, based on Table 1. However, if the element is wide compared to the width of the channel, the centerline velocity may be significantly decreased and C_c may be greater than 1. Further studies are necessary to establish what constitutes a narrow element.

A summary of results for the three meters are tabulated in Table 2, where the tests are identified by meter number and element shape (R = rectangular, V = triangular). For example, 3V-1 means Meter Number 3, triangular blade, test 1.

The computed values for β ranged from about 1.009 to 1.042, with an average value of 1.017. This compares with 1.02 for the lined channel cross sections reported by Watts (4). A much larger variation, as would be expected, occurred with the drag coefficient. The blades designed for Meters Number 1 and 2 had average drag coefficients, C , of 1.89 and 1.85, respectively, with a total range of 1.80 to 1.96 for Meter Number 1 and 1.75 to 1.95 for Meter Number 2. The range for the rectangular element on Meter Number 3 was 1.65 to 1.75, and the average was 1.72. The triangular element on Meter Number 3 averaged 1.68 with a range from 1.64 to 1.71.

The lower drag coefficient determined for Meter Number 3 may be due to its thickness. All the rectangular elements were 1 inch wide, but Numbers 1 and 2 were only 1/8 inch thick, whereas Number 3 was 1/4 inch thick. Numbers 1 and 3 had the edges beveled at 45° from the front edge of the plate to the rear, but Number 2 was left nearly square-edged with about 3° bevel to the rear. Because meter elements Number 1 and 2 had similar drag coefficients despite differences in edge treatment and Number 1 and 3 had different drag coefficients with similar edge treatment, the thickness of the element is suspected to be the cause of the variations in the values.

Elements Number 1 and Number 3 were placed in a channel flow and their wakes observed. The wake behind Number 3 was narrower than that behind Number 1 and would account for the lower drag coefficient of element Number 3. The cause of the narrower wake appeared to be a lack of true separation at the edges of the element.

The ability of the triangular blade to function as a discharge-rate meter depends strongly on its ability to maintain a constant drag coefficient at all flow depths. In the limited tests reported here, the standard deviation on the drag coefficient was $\pm 1.2\%$. Thus, it appears that, considering twice the standard deviation as acceptable tolerance for a meter, the accuracy can be expected to

be $\pm 2.4\%$. Comparable values were obtained for the rectangular elements.

Laboratory facilities are being completed that will permit more decisive tests of the discharge-indicating meters, including an element designed for flow in circular pipes. Definite information is needed on the drag characteristics of the elements, especially the effects of element shape and thickness.

A report incorporating much of the preceding work was prepared and presented before the American Society of Agricultural Engineers (3).

SUMMARY AND CONCLUSIONS:

The objectives of this study are to develop and examine comprehensive design criteria for the sensing elements of force-deflection, or target, meters that can be used to: (a) give an integrated, or average, velocity in a sheet flow, and (b) indicate discharge rate in a wide range of channel geometries, independent of flow depth.

The first of these objectives is not too difficult to achieve. A sensing element that will reach from the flow surface to the channel floor can be used to indicate an average velocity in the vertical section sampled. Two models of a force-deflection-type meter have been constructed and tested for velocity indication. The total force exerted by the velocity profile on a 1-inch wide blade registers as a torque about a hinged edge of the blade.

A third device has been designed to accept blades of various shapes which are necessary to indicate discharge independent of flow depth in any open channel.

It is concluded that target meters can be designed for use in open channel flows and sheet flows. They can be expected to have an accuracy of about $\pm 3\%$. Also, elements can be shaped to indicate discharge directly for a wide range of channel shapes, independent

of flow depth, limited primarily by the ability to predict the general type of velocity profile existing in the flow.

REFERENCES:

1. Bazen, Henri. Researches Expérimentales sur l'Écoulement de l'Eau dans les Canaux Découverts. Mémoires Présentés par Divers Savants à l'Académie de Sciences, Paris, Vol. 19, 152 pp (with separate atlas containing 33 plates). 1865.
2. Replogle, John A. Low pressure--differential measurements in liquid flows. Amer. Soc. Agr. Engin. Trans. 10:84-86. 1967.
3. Replogle, John A. Target meters for velocity and discharge measurements in sheet flows. Paper No. 67-736 presented at the 1967 Winter Meeting, Amer. Soc. Agr. Engin., Detroit, Michigan, Dec. 12-15, 1967.
4. Watts, Fredrick J., Simons, Daryl B., and Richardson, Everett V. Variation of α and β values in a lined open channel. Amer. Soc. Civ. Engin. Proc. 93 No. HY6:217-234. 1967.

PERSONNEL: J. A. Replogle

Table 1. Comparison of the effects of channel roughness and shape on determining the discharge of a channel from the center-line velocity profile.

Data source	$\frac{\text{width}}{\text{depth}}$	$\frac{v}{\bar{v}}$	Type roughness elements
Bazin ^a Series 67, No. 3	1.64	1.083	Smooth, wooden plank
Bazin Series 64, No. 2	3.01	1.172	Wood plank with wood strips, 0.05 m on center
Bazin Series 61, No. 4	4.02	1.156	Wood plank with wood strips, 0.01 m on center
Bazin Series 56, No. 1	4.65	1.210	Pea gravel

^a Bazin, reference (1)

Table 2. Data used to compute coefficient, C.

Test No.	\bar{v} ft/sec	y ft	F lbs	β	β'	C
1R-1	1.160	0.552	0.112	1.009	-	1.852
1R-2	1.203	0.552	0.120	1.008	-	1.849
1R-3	1.222	0.552	0.124	1.007	-	1.849
1R-4	1.124	0.552	0.108	1.014	-	1.896
1R-5	1.154	0.552	0.110	1.028	-	1.804
1R-6	1.222	0.552	0.123	1.008	-	1.836
1R-7	1.504	0.751	0.270	1.0105	-	1.950
1R-8	1.452	0.775	0.252	1.0142	-	1.885
1R-9	1.444	0.751	0.252	1.0183	-	1.959
1R-10	1.480	0.751	0.252	1.0130	-	1.877
1R-11	1.497	0.751	0.264	1.0106	-	1.925
1R-12	1.499	0.751	0.270	1.0107	-	1.963
2R-1	1.642	0.745	0.292	1.016	-	1.812
2R-2	1.638	0.740	0.285	1.017	-	1.785
2R-3	1.200	0.894	0.190	1.010	-	1.932
2R-4	1.168	0.894	0.190	1.013	-	1.948
2R-5	1.587	0.629	0.241	1.018	-	1.890
2R-6	1.238	0.925	0.219	1.013	-	1.927
2R-7	1.625	1.090	0.407	1.017	-	1.752
2R-8	1.604	1.090	0.397	1.011	-	1.766
3R-1	2.184	0.466	0.323	1.027	-	1.741
3R-2	1.826	0.667	0.1842	1.019	-	1.653
3R-3	1.089	0.862	0.1469	1.012	-	1.756
3R-4	1.030	1.040	0.1572	1.022	-	1.726
3V-1	2.166	0.462	0.1011	1.023	1.133	1.654
3V-2	1.498	0.667	0.1024	1.016	1.112	1.715
3V-3	1.197	0.917	0.1258	1.019	1.133	1.714
3V-4	0.897	1.208	0.1295	1.042	1.252	1.637

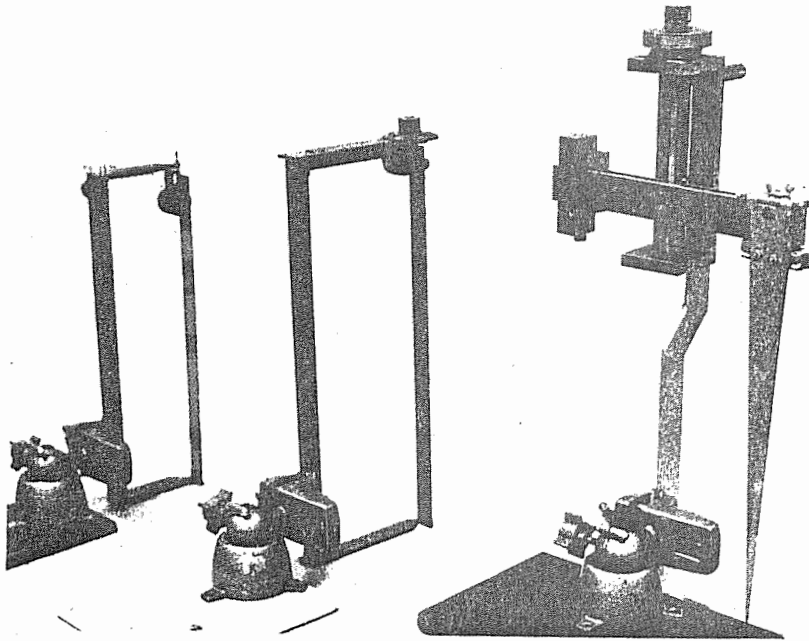


Figure 1. Meters Number 1, 2, and 3 left to right. Meter Number 3 has a discharge indicating element attached.

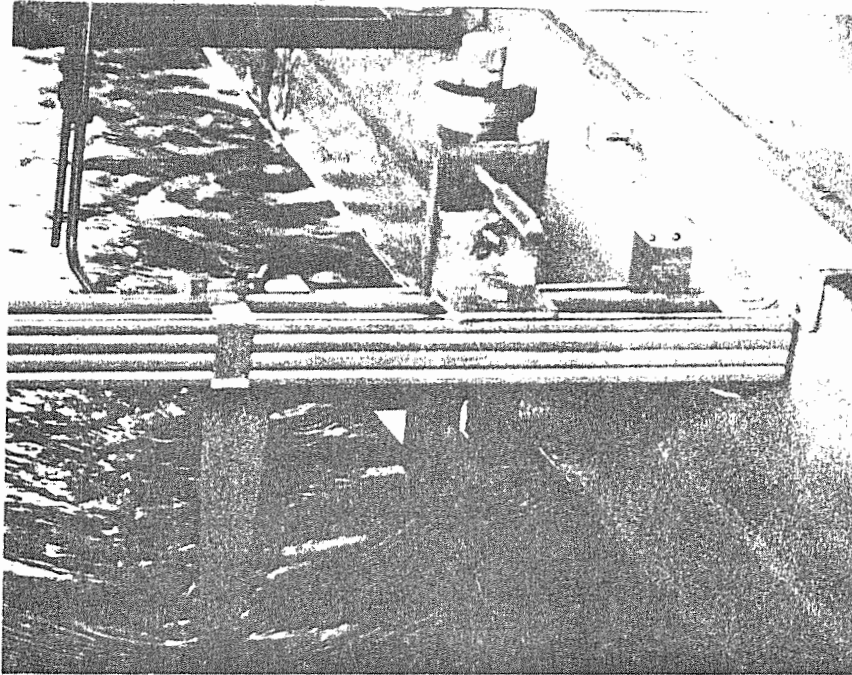


Figure 2. Meter Number 3 in 2-ft wide channel. Pitot tube is out of flow in left background.

(See description of the box used in Annual Report, 1966.) In general, operational failures were the result of low shoulders, shoulders not parallel with the box lip, separation of apron construction from box because of Bermuda grass pressure, and the old nemesis of tile outlet being higher than the field elevation.

The success of old structures still in operation, where the step-down design was not used, is credited to the use of excessively large aprons, small streams of water, Bermuda grass protection, or the outlet tile being installed well below the field elevation.

Two new erosion-preventive structures were designed to dissipate and distribute the water from a 3-ft-wide jack gate on the Woodhouse ranch that carries approximately 7000 gal. per min.

SUMMARY AND CONCLUSIONS:

An apparently successful irrigation outlet structure is designed as a square concrete box, whose upper lip is attached to the upper half of an outlet tile, which dissipates and directs the stream of water in such a way that, with other concrete attachments, the erosive effects are nearly exhausted. This conclusion is based on the performance of presently installed structures at several locations under varying conditions of use.

Certain other specifications are suggested, in addition to the proper installation of the box dissipator. Concrete shoulders should be extended at least to the foremost part of the box and at least to a height of 8 in. (higher if the field elevation of water is greater). All aprons should be below field elevation, at least 5 in., especially if it is necessary to protect them from farm equipment damage. In most cases, a 2-ft-long apron is adequate. Some of our successful structures which carry over 4000 gal. per min. are less than 5 ft wide across the shoulders. All boxes should be constructed with a steel reinforcement so that concrete work attached to the box will be stable enough to prevent leakage or movement by Bermuda grass.

Thickness of concrete should be determined by the extent and type of machinery damage to which it will be exposed.

PERSONNEL: Leonard J. Erie and John A. Replogle.

TITLE: STUDY OF UNSATURATED TWO-DIMENSIONAL SOIL WATER FLOW
 USING AN ANALOG COMPUTER.

LINE PROJECT: SWC W7 gG-5

CODE NO.: Ariz.-WCL-46

INTRODUCTION:

The objectives of this study on the two-dimensional flow of water in sloping land are:

1. To solve the steady-state flow problem on the resistance network analog.
2. To compare the results for saturated flow with those of published results.
3. To apply the analog technique to unsaturated cases for different rainfall rates, slopes, lengths of slope and soil materials.

The electrical resistance network analog is particularly well suited for steady-state measurements because: (a) the conductivity or its analog, the resistance, does not change with time, and (b) any one problem may be set up quickly and the potentials measured directly.

PROCEDURE:

The flow system to be considered is shown in Figure 1. The bottom and two ends of the soil slab are assumed to be impermeable. The slab is inclined by some angle ω measured in radians. The vertical height or depth (z) of the slab is L cm and its length or distance (y) is aL cm, where "a" is a convenient dimensionless multiplier. The hydraulic head (H) reference line passes through $z = L$, $y = 0$. It will be assumed that rain (R) or sprinkler irrigation has been falling on top of the slab long enough for steady-state flow to have been achieved in the slab. The water table thus established will intersect the surface at $z = -L$, $y = y_0$.

The resistance network imposed on the system was 10 intervals high and 20 intervals long, which gives a system of square meshes for $a = 2$, but rectangular meshes for $a = 10$. The value of L was chosen

as 100 cm and "a" was chosen as 2 and 10. In the region below the water table, the resistances were calculated according to equation (1) of Bouwer (3). This gave a basic resistance of 200 ohms for $a = 2$ for a saturated conductivity, K_s , of 1 cm/day. For $a = 10$ the basic vertical and horizontal resistances were 400 and 10,000 ohms respectively for the same K_s .

Bouwer (1) has introduced the concept of a critical pressure head, P_{cr} . The application of this idea has been shown to give good agreement with other, more complicated $K(h)$ relationships (h is the pressure head) when applied to canal seepage problems and to lateral flow above mildly sloping water tables (1). When applied to the present problem, a further simplifying assumption had to be made. In the region in which the pressure head was more negative than P_{cr} , all of the flow was in the vertical direction; thus the conductivities in this region are numerically equal to the rainfall rate.

In order to test the P_{cr} concept against another $K(h)$ relationship, the formula given by Gardner (4) for a soil like Pachappa sandy loam was used. This formula, which is of the form

$$K = \frac{a}{(-h)^n + b} \quad (1)$$

was applied where h was less than -10 cm, using values of $a = 2.7 \times 10^4$ cm⁴/day, $b = 2.6 \times 10^4$ cm³ and $n = 3$. These values were chosen so that K_s would also be equal to 1 cm/day as was the case for the systems where P_{cr} was used. In this case, no further simplifying assumptions have to be made about the region of unsaturated flow.

RESULTS AND DISCUSSION:

A convenient comparison between this method and the analytic method used by Klute, et al. (5) can be made for saturated flow. One means of comparison is by the flux of water across the soil

surface. If one forms the dimensionless ratio of the normal component of this soil surface flux with the saturated conductivity of the soil and then divides this ratio by $\sin \omega$ the results are as shown in Figure 2. This reduced flux is plotted for the full length of the slab against a reduced length y/aL . The results are for both $a = 2$ and $a = 10$. The analog results agree quite well with the analytic solution. Where the results are negative, the flow is into the slab; where they are positive, the flow is out of the slab. The fact that the values for $a = 10$ lie closer to 0 than for $a = 2$ is somewhat misleading due to the abscissa, y/aL . This figure illustrates the fact that on short slopes with saturated flow there is only a small region at the middle of the slope where there is no flow in or out of the slab, but on the longer slopes this region of near zero flux is longer.

As the rainfall rate is decreased below that necessary to maintain the water table at field surface for the entire slope, part of the slab will have negative pressure heads. The effect of this decreased rainfall rate on the position of the isobars is shown in Figure 3. In this figure the solid lines are the positions of the particular isobars for saturated conditions and the dashed lines are for $R = 0.075$ cm/day or about 12.5% of that necessary to saturate this slab. It was assumed that in this case the negative pressure heads (about -10 cm or less) were not sufficient to pull air into the soil and the conductivity was equal to K_s everywhere in the slab. The position of the water table or 0 cm isobar decreases at the upper r.h.s. with decreased rainfall rate. All of the isobars tend to merge, however, at the l.h.s. and with depth at the r.h.s. There is only a small region in the upper r.h. corner where the pressure head is less than -10 cm. The soil surface flux is plotted against position in Figure 4. For the smaller rainfall rate there is a zone of constant flux into the soil at the r.h. corner, then the flux starts to increase (become less negative)

until it becomes positive, and at the lower l.h. corner it is essentially equal to the saturated flux. The point at which the flux starts to increase from its constant rate is the point Y_0 or the point where the water table intersects the soil surface in Figure 3. It can also be seen from comparing the areas under the positive portions of the two curves (this area is equal to the total flow through the slab) that the area under the lower rainfall rate curve is less and therefore the total flow through the lower rainfall slab is less than for the saturated case. This would be expected. This figure also shows that even with rainfall rates less than enough to saturate a soil mass, the "interflow" can still contribute much to runoff.

The effect of increasing the angle of slope on the positions of the isobars is shown in Figure 5. For the results shown in this figure, both the angle of slope and the rainfall rate were increased over the values shown in Figures 3 and 4, but the rainfall was still only 12.5% of that necessary to saturate the slab. The solid lines in Figure 5 are the positions of the specified isobars where no air was assumed to have entered the slab. As can be seen, values of the pressure head of less than -50 cm were measured in the upper r.h. corner. If it was assumed that air entered the slab and the soil material had the same K_s but different P_{cr} 's, the results are the dashed lines in the figure. If P_{cr} was -50 cm then only a little part of the slab was desaturated. If P_{cr} was -10 cm then about a quarter of the slab was desaturated. In the drained area the positions of the isobars varied depending upon the P_{cr} of the material, and in fact no value of the pressure head less than -50 cm was measured in the slab with a P_{cr} of -10 cm or -30 cm; at or below the water table, however, all of the isobars were coincident regardless of the P_{cr} of the material.

The curved isobar of -30 cm for a P_{cr} of -10 cm on the r.h.s. of Figure 5 illustrates an interesting phenomenon of flow in this

region. If the equipotentials and streamlines for this figure were plotted, it would be observed that the streamlines diverge quite rapidly in the upper r.h. corner of the slab. This is due to the high angle of tilt of the slab and the fact that the r.h. boundary is a streamline. The divergence of flow can create negative pressure heads even under saturated conditions. Bouwer (2) observed this phenomenon below channel bottoms. While this situation existed for all slope angles, it was detected only in the steeper ones.

As mentioned earlier, it was possible to test the P_{cr} concept against other $K(h)$ relationships. Bouwer (1) found that for the Gardner-type function, equation (1), P_{cr} should be about -35 cm. The equipotentials, lines of constant H , for the system shown in Figure 5 are shown in Figure 6. The solid lines are for the P_{cr} value of -30 cm and -35 cm, and the dashed lines are for the function given in equation (1). The agreement is quite good and the P_{cr} of -35 cm gives a slightly better fit than -30 cm.

The effect of applying the same rainfall rates to different slopes of the same soil material is shown in Figure 7 in terms of the isobars. For $\omega = 0.8$ radian it was assumed the material had a P_{cr} of -30 cm, since as shown previously, a great deal of the slab had very negative pressure heads. At this rainfall rate very little of the slab at $\omega = 0.05$ radian was under negative pressure head. The nonreduced flux is plotted against position in Figure 8. As the angle of slope is increased, the length of slab with a constant infiltration rate is increased, as well as the rate of flow out of the upper l.h. corner. This points out that as the angle of slope increases, the increased rate of outflow due to "interflow" could contribute greatly to downhill erosion due to the seepage force of the interflow.

The results of applying the same rainfall rate, 0.1 cm/min, to a longer slope are shown in Figure 9 in terms of the isobars. Only in the r.h.s. are these results (dotted lines) different from

the saturated case (solid lines). It appears that for systems where the depth-to-length ratio becomes 10 or greater, the system acts like a long pipe with soil at each end. This agrees with the findings of Klute et al. (5). In this case, interflow can be rapidly approximated if the K-profile is known. Negative pressure heads were found only in the upper r.h. corner.

SUMMARY AND CONCLUSIONS:

Studies were performed with a resistance network analog to determine flow systems in sloping fields due to steady rainfall. The results indicate that: (a) as the rainfall rate decreases below that necessary to saturate the soil, the symmetry of the soil surface fluxes is lost; (b) as the angle of tilt increases, the rainfall rate necessary to saturate the soil increases; (c) under a fixed rainfall rate, as the angle of tilt of a soil slab increases, the rate of outflow at the lower corner of the system increases and the zone of constant infiltration increases; (d) long thin soil "slabs" act much like long pipes with soil at each end with respect to equipotentials and soil surface fluxes, especially near saturated conditions; (e) the concept of P_{cr} and a step conductivity function seem to be as good as more complicated functions in analyzing such flow systems; (f) the agreement at saturated flow between the resistance network solution and analytic solutions is quite good. The results indicate that for shallow slopes, even under low rainfall rates, the soil can store considerable water, but for steeper slopes there is less storage and a higher rate of outflow at the lower end with greater erosion losses. These findings should have application in terrace design, runoff prediction, erosion control, and drainage design.

REFERENCES:

1. Bower, H. Unsaturated flow in ground-water hydraulics. J. of Hydraulics Div., ASCE 90:121-144. 1964.
2. Bower, H. Theoretical aspects of seepage from open channels. J. of Hydraulics Div., ASCE 91:37-59. 1965.

3. Bower, H. Analyzing subsurface flow systems with electric analogs. Water Resources Res. 3:897-907. 1967.
4. Gardner, W. R. and M. Fireman. Laboratory studies of evaporation from soil columns in the presence of a water table. Soil Sci. 85:244-249. 1958.
5. Klute, A., E. J. Scott, and F. D. Whisler. Steady state water flow in a saturated inclined soil slab. Water Resources Res. 1:287-294. 1965.

PERSONNEL: F. D. Whisler and H. Bower

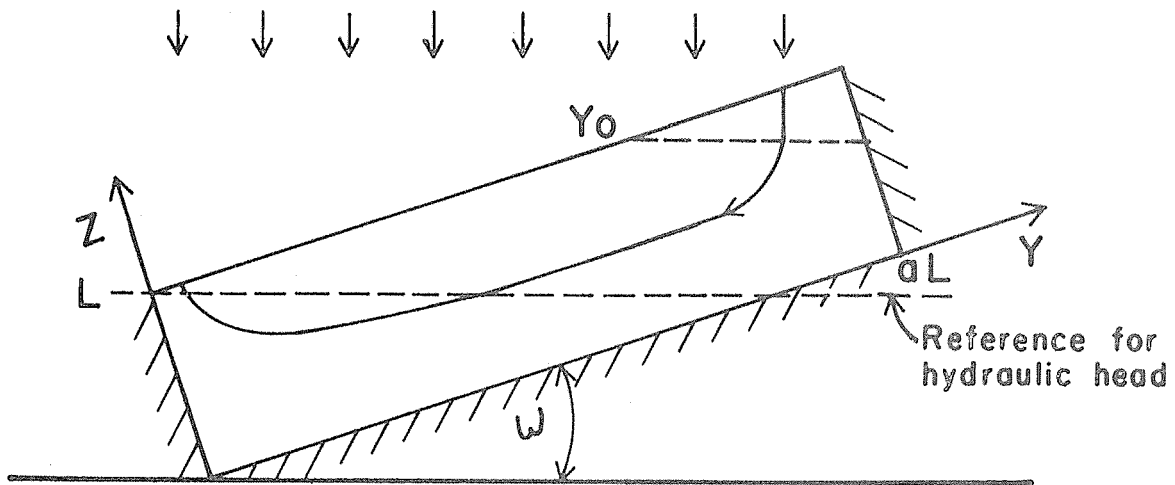


Figure 1. Schematic diagram of the flow system.

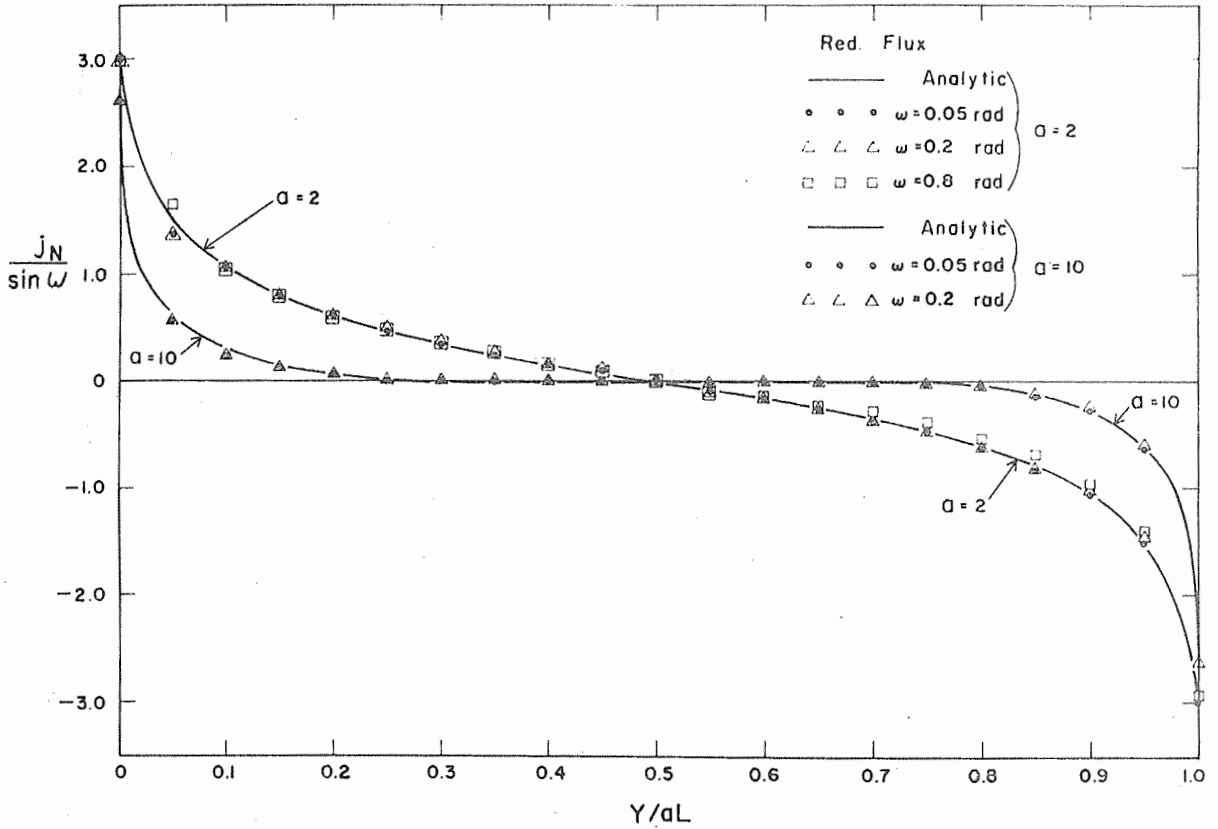


Figure 2. Reduced, dimensionless, vertical component of the soil surface flux, $\frac{j_N}{\sin \omega}$, versus reduced distance, $\frac{Y}{aL}$ for two values of a .

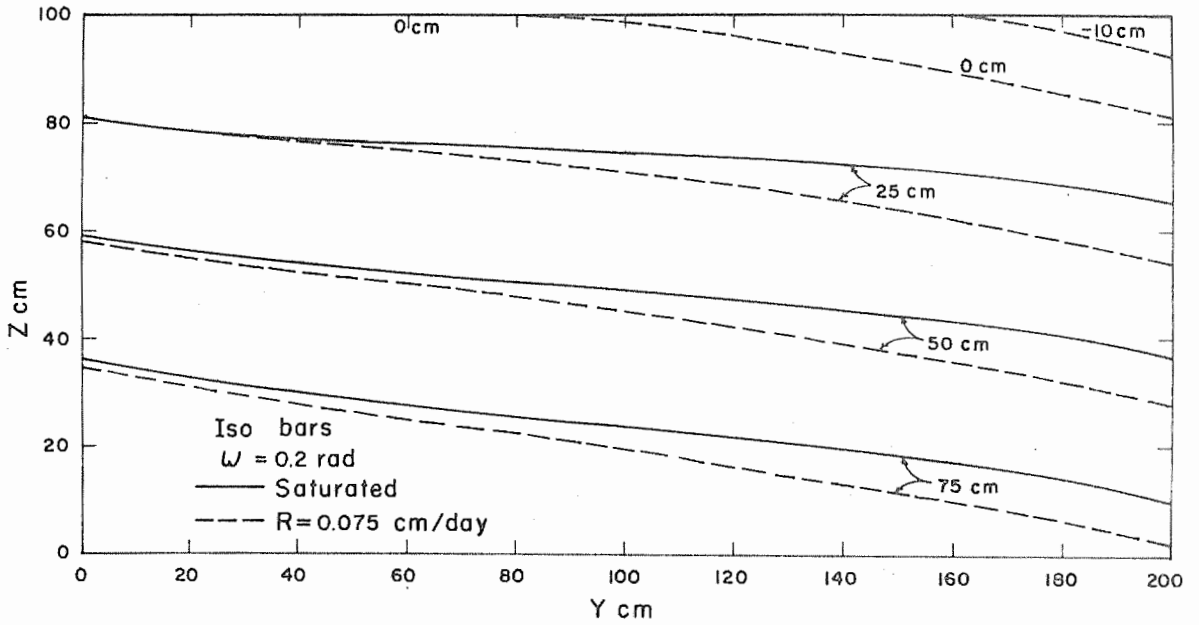


Figure 3. Isobar, h , positions as a function of depth and distance. The numbers with the curves are the values of the isobar.

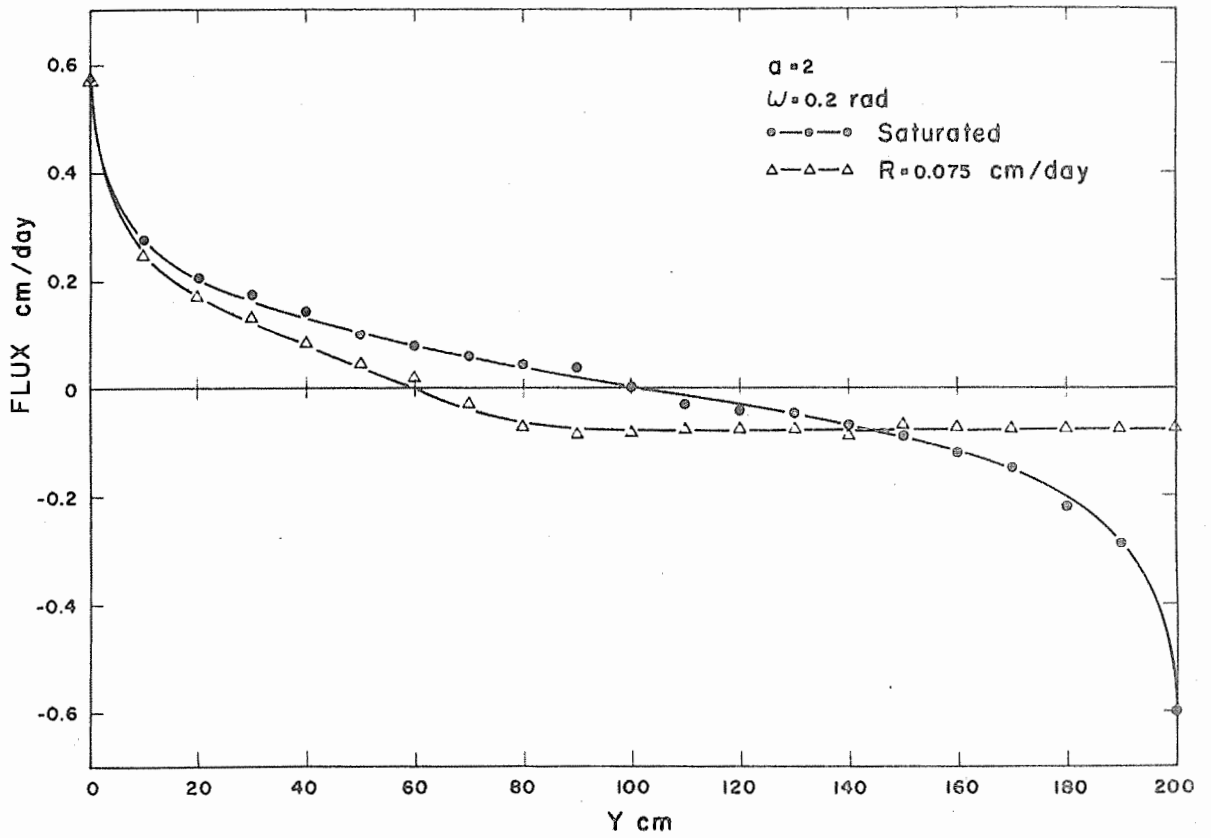


Figure 4. The total soil surface flux versus distance.

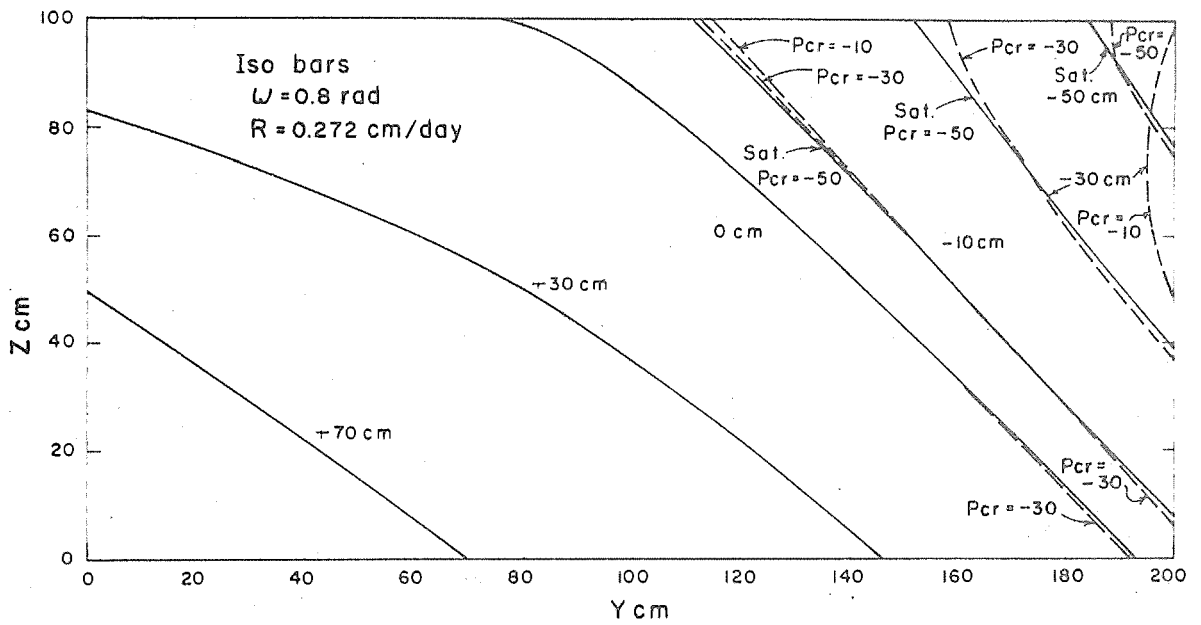


Figure 5. Isobar positions as a function of depth and distance. P_{cr} values are indicated where the curves are different from the saturated value. The other numbers with the curves are the values of the isobars.

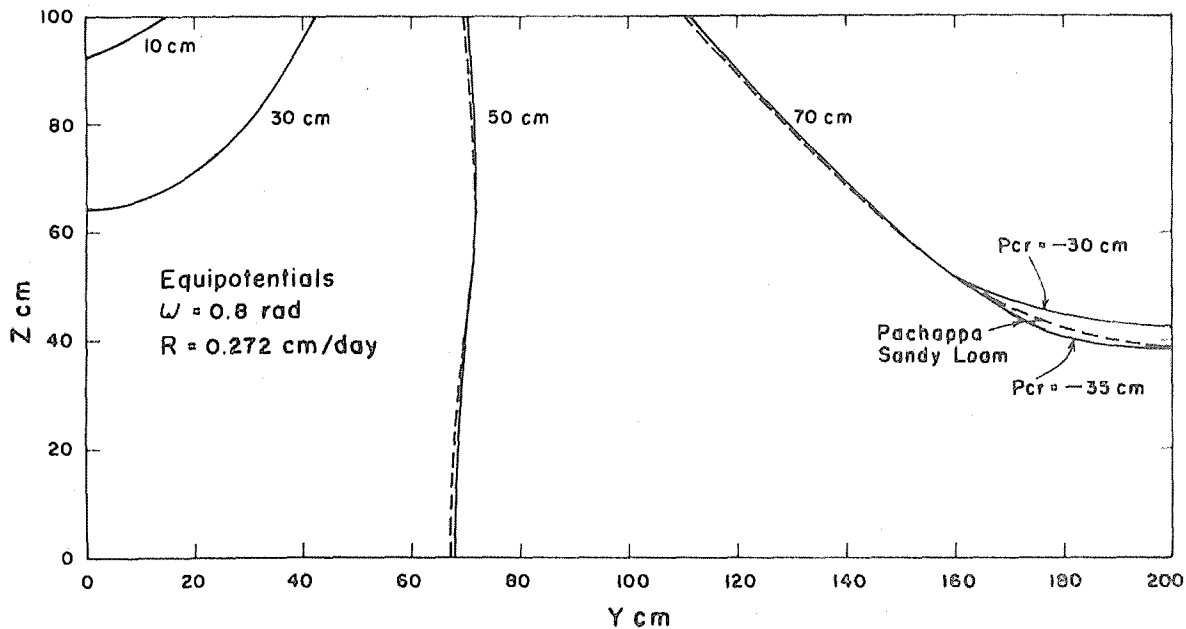


Figure 6. Equipotential positions as a function of depth and distance. The solid lines are for the indicated P_{cr} values and the dashed lines are for a Gardner type conductivity function for Pachappa sandy loam. The other numbers with the curves are the values of the equipotentials.

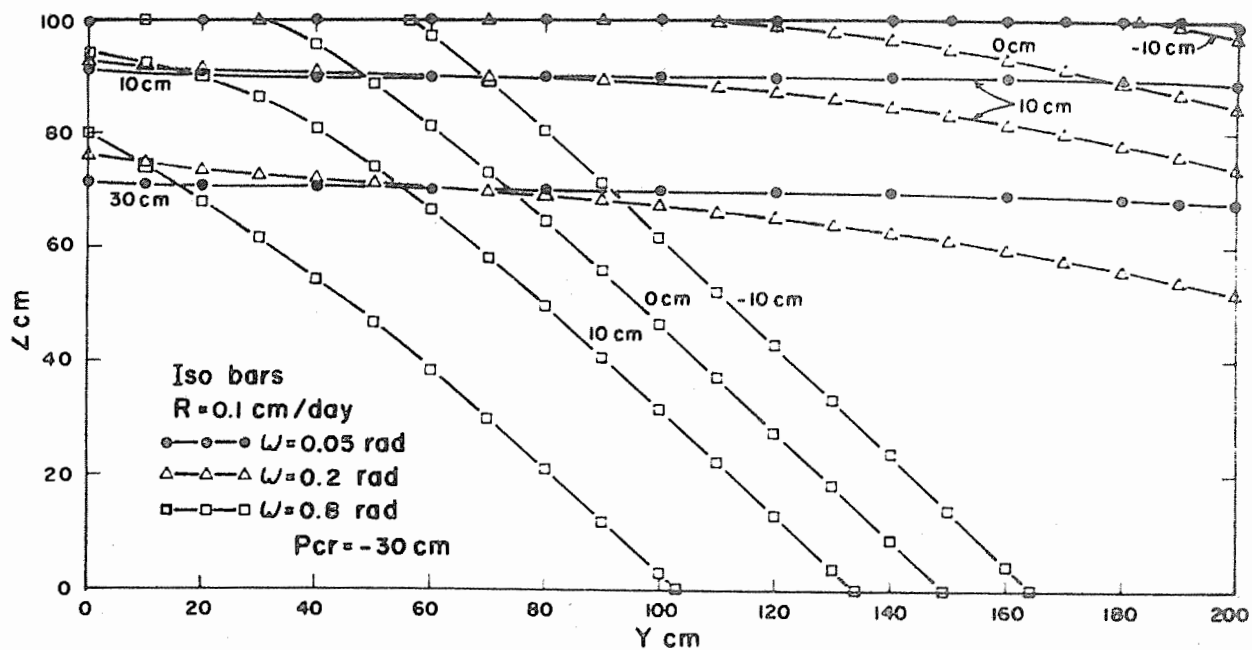


Figure 7. Isobar positions as a function of depth and distance.
 The numbers on the curves are the values of the isobars.

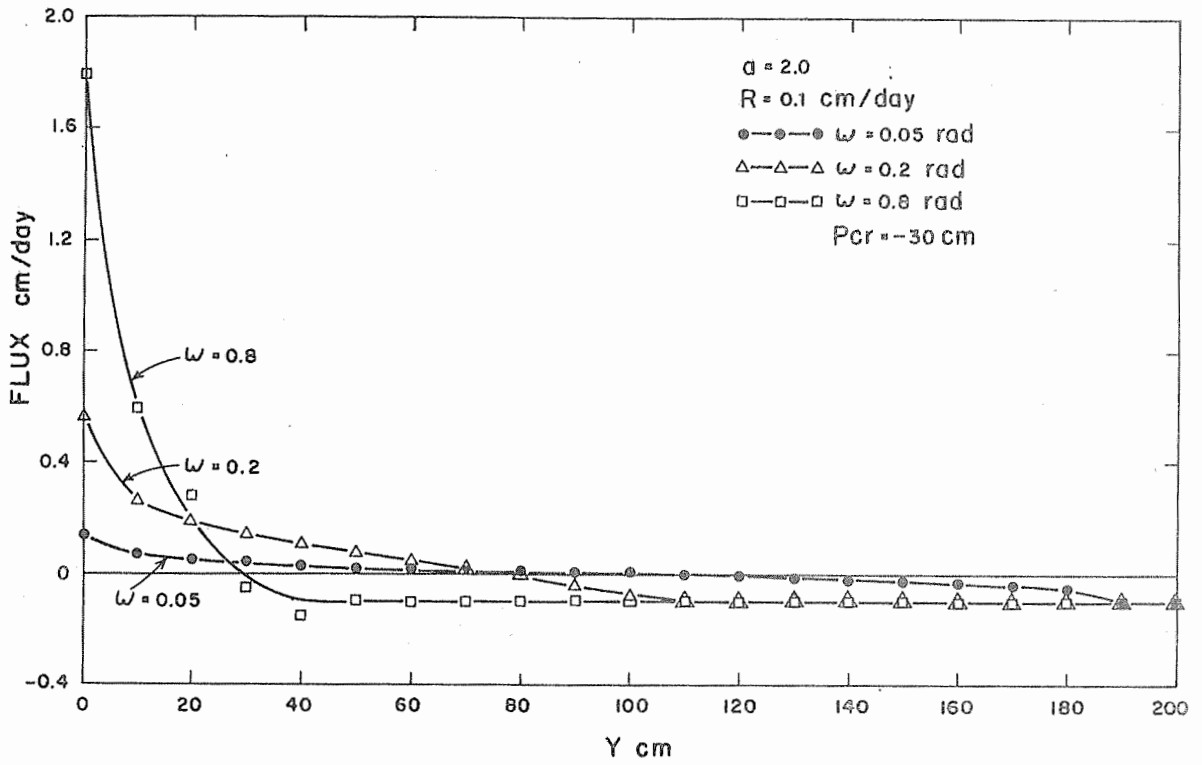


Figure 8. Total soil surface flux versus distance for three degrees of slope.

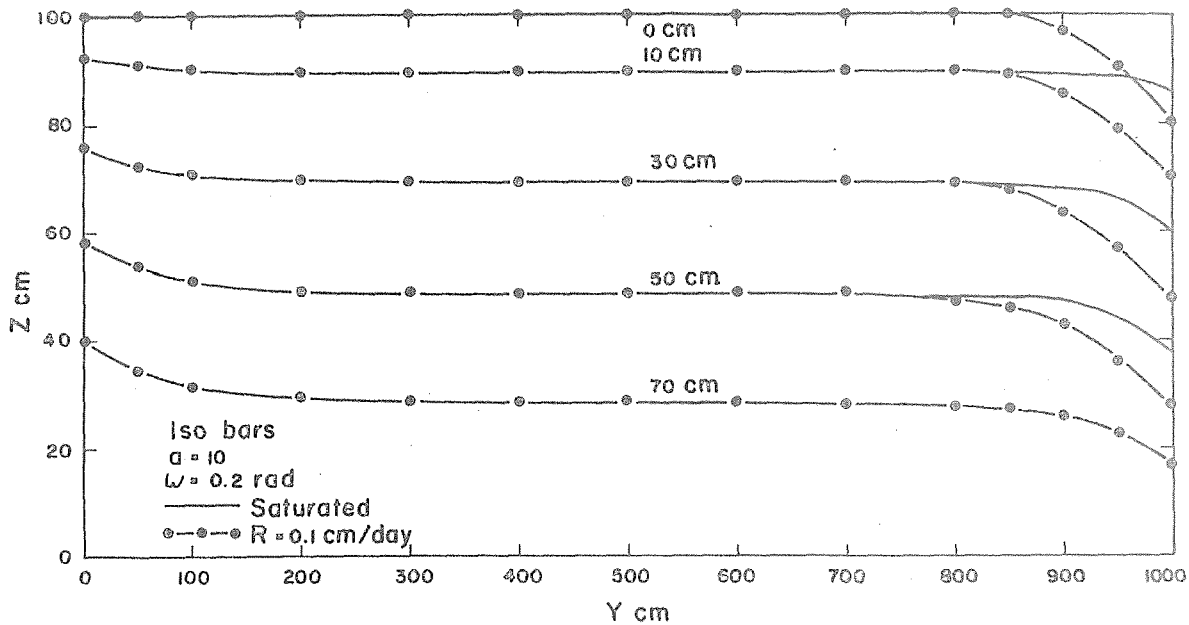


Figure 9. Isobar positions as a function of depth and distance for a of 10. The numbers on the curves are the values of the isobars.

TITLE: FLOW MEASUREMENT IN OPEN CHANNELS WITH CRITICAL DEPTH
FLUMES

LINE PROJECT: SWC W10 gG-7

CODE NO.: Ariz.-WCL-48

INTRODUCTION:

See Annual Report for 1966.

PROCEDURE:

Several flumes were designed and built for specific application on associated projects. Most of these have been in the range of 0-10 cfs, with triangular throats near 60° . These flumes have been calibrated in the laboratory and the results compared with theoretical equations. Based on the theoretical agreement for the existing flumes, a large triangular flume with a 90° -throat opening and one with a 50° -throat opening were constructed and installed on field locations but were not calibrated. Some field-evaluation data were gathered. This primarily concerned readout methods and siltation problems.

RESULTS AND DISCUSSION:

Several 60° flumes made of fiberglass have been calibrated. The results were as expected, agreeing well with the theoretical calculations. The observed friction factors ranged between 0.002 ft and 0.010 ft, averaging about 0.005 ft for the tested flow range of 0.11 ft to 1.35 ft (0.004 cfs to 3 cfs). The friction factor as measured and as calculated are discussed in a later section. In general, the flumes will be accurate to within 1%, except at low flow depths of less than 0.2 ft (approximately 0.02 cfs) the error may approach $\pm 4\%$.

The small 60° -throated flumes similar to those of Robinson (see Annual Report, 1966) were calibrated. They also behaved according to theoretical calculations until the depth of flow in the approach section reached a depth of about one-half the throat length, at which time the rating deviated significantly from

theoretical predictions. This emphasizes the importance of proper throat length.

Based on the relative success of predicting the rating curves for the 60° flumes, other flumes were designed but not calibrated. These included large aluminum flumes with 90°-throat openings capable of 80 cfs and a concrete flume with a 50°-throat opening capable of 7 cfs. Both these flumes have been in operation in the field for several months. Both are in high sediment producing areas and a problem has occurred with siltation in the approach sections that tends to plug the depth measuring taps.

Recently, the Bureau of Reclamation (2) has published the results of a measuring flume that they calibrated. It had 45° side-walls with a 4-inch-wide bottom in the throat section and a 10-inch-wide bottom in the approach section. Since trapezoidal flumes theoretically cannot produce linear calibration curves on log-log plots, their choice of a power function for the results is subject to question. Because the results from trapezoidal flumes produced by Robinson (see Annual Report, 1966) were in agreement with calculated results, a duplicate of the Bureau flume was constructed for study. Calibration has not been completed.

Head Measurement. An interesting method of measuring head has been successfully used. The flumes should, of course, be level throughout. However, if a discrepancy occurs, results will be most accurate if referred to the invert elevation of the outlet. This is easily accomplished by ponding water throughout the flume with the aid of a clay dam and measuring the water depth at the outlet. This value is then set on the readout device in the stilling wells. However, in a portable flume that may be dropped into a ditch under flowing conditions, this procedure cannot be used. Instead, the flume is approximately leveled, a point gage is mounted above the outlet that can be zeroed on the bottom through the flowing water, and then raised above the flow level in the throat. A cup device

with a tube communicating to the stilling well is then suspended below the raised point gage. Thus, the surface elevation of the stilling well above the flume outlet can be obtained from the water level in the cup without having to transfer readings to a point gage in the stilling well. This has proven to be an accurate and convenient method to use on portable flumes.

Friction Loss Calculations. The friction losses were measured by determining the difference in the head reading required to satisfy the theoretical equation and that observed for a given discharge rate. This required precision measurements of both head and discharge. Since the discharge measurements could be obtained gravimetrically with an accuracy on the order of 0.1 to 0.2%, this proved to be no problem. The accuracy of readout on the depth was limited to ± 0.001 ft. At low flow depths of 0.1 ft this error could be on the order of 1%.

Theoretical predictions of the friction losses were attempted using the methods of Ackers and Harrison (1). These values were usually 1 1/2 to 2 times the measured losses.

Design Procedures. Because the flume characteristics can be described theoretically, the size can be selected to fit a wide variety of situations. The general design procedure would follow these steps:

1. Ascertain the maximum flow rate to be measured.
2. At the site selected for installing the flume, locate the maximum water line on the ditch bank. This may be calculated by backwater-curve techniques or field observation of flow in the existing ditch. If a triangular flume is to be used, then the submergence will be governed by the maximum water level, provided the ditch is trapezoidal or rectangular, that is, if the flow characteristics of the channel are approximated by a power function with the exponent on the depth, y , less than the exponent on the flume depth. In the case of a triangular flume this value would need to be less

than 5/2. Rectangular ditches have values on the order of 3/2 and trapezoidal ditches have values between 5/2 and 3/2.

If, on the other hand, a rectangular flume is placed in a trapezoidal ditch, the submergence level must be determined for low flow stages since the higher rates are conservative and approach less submergence with increasing flow rate.

4. Select a flume geometry that provides at least 80% free flow at the high flow rate. For example, if a trapezoidal ditch discharges 7 cfs at a depth of 20 inches, select a triangular flume that will pass 7 cfs at a stage of 25 inches thus providing for 80% or less submergence. The lower flow depths will have even less submergence. The flow of the flume may be coincident with the channel floor or placed above as the location and situation demands. The selection of flume size can be accomplished by using the equations reported in Annual Report, 1966.

5. The throat section should be at least two times the maximum depth of flow expected in the approach channel. The convergence section should converge at a rate of not more than 3:1. The approach section should be long enough to assure nearly parallel flow at the pressure tap location. When the flow enters abruptly into the entrance section, this may require a length exceeding 2 times the maximum depth.

Model Study. The small flumes and the large aluminum flumes with 60° throats are geometrically proportioned to a scale ratio of 4. This afforded an opportunity to check the calibration of the larger flume by modeling techniques. This can be done as follows:

The scale, or length ratio is $L_r = 4$.

The Froude ratio is $F_r = \frac{V_r}{\sqrt{g_r L_r}} = 1$.

Since the gravitational ratio, $g_r = 1$,

the velocity ratio, $V_r = \sqrt{g_r L_r} = 2$,

and the velocity in the prototype, $V_p = 2 V_m$

where V is the velocity and the subscripts p and m refer to the prototype and model respectively.

Since $Q = AV$, the discharge ratio Q_r , is

$$Q_r = A_r V_r = 32$$

or

$$Q_p = 32 Q_m$$

Thus, since the laboratory calibration for the small flume, or model, produced the following calibration equation

$$Q_m = 1.61 Y_m^{2.62}$$

the prototype equation for the large aluminum flume becomes

$$Q_p = Q_r 1.61 \left(\frac{Y_m}{L_r} \right)^{2.62} = 1.37 Y_p^{2.62}$$

Direct calibration of the large aluminum flume gave

$$Q_p = 1.38 Y_p^{2.59}$$

Thus, the modeling laws, as expected, can be satisfactorily applied.

SUMMARY AND CONCLUSIONS:

Much of the basic theory concerning the flow characteristics of critical depth flumes has long been known. Despite this, the stage-discharge relations are still generally determined empirically because the application of the theoretical knowledge is tedious and requires detailed computations. With the aid of computers, the theoretical knowledge can be applied routinely.

Several flumes have been designed, constructed, and tested in the laboratory. In general, a computation of the friction loss in the flume permits a prediction of the flume calibration in terms of ordinary energy concepts. This prediction compares within $\pm 2\%$ for a flow range that frequently exceeds 100:1, depending on the flume size.

The narrowest section of the flume, the throat, is the most critical. It must be constructed accurately and braced against possible deflection at high flows. Its length should be at least twice the maximum expected flow depth in the approach section. The flumes should be installed level when possible, however negative or adverse slope is less detrimental than positive flume slope.

Modeling techniques, as expected, predicted a satisfactory calibration equation, based on the laboratory rating of the smaller of a pair of similar flumes with a scale ratio of 4:1, even though the flume throats were too short to conform to the theoretical equation.

REFERENCES:

1. Ackers, P., and Harrison A. J. M. Critical-depth flumes for measurements in open channels. Hydraulics Res. Sta., Dept. of Sci. and Indus. Res., Wallingsford, Berkshire, England. Hydraulics Res. Paper No. 5, 1963, 49 pp.
2. United States Department of Interior. Bureau of Reclamation Water Measurement Manual. Ed. 2, p. 87. 1967.

PERSONNEL: J. A. Replogle

TITLE: WATERPROOFING OF SOILS - AN EVALUATION OF TREATMENTS
AND INFLUENCING FACTORS

LINE PROJECT: SWC W7 gG-5

CODE NO.: Ariz.-WCL-49

INTRODUCTION:

Work continued on the development of experimental techniques for quantitatively evaluating the degree of water repellency of soils treated with thin films of low surface energy organic compounds. The technique for measuring the breakthrough pressure needed to force water through the porous but water repellent soils was refined and adapted to an automatic data recording system. Also, a method was developed for measuring the characteristic contact angle of water on treated soil surfaces. These techniques were used to establish the degree of soil surface coverage by the organic and to show the relation between water repellency and effective pore radius of a number of treated soils.

PROCEDURE:

The apparatus used for the determination of breakthrough pressure was pictured in the 1966 Annual Report, 49-7. The procedure in current use is the same as previously outlined except that now 100 grams of treated soil is packed into the lucite containers. The system has been adapted to automatic data recording by teeing a pressure transducer into the water line between the immersion tube and the standpipe. Since the electrical output of the pressure transducer (Statham PM 131) is linear, an x,t strip chart recorder tied to the transducer during a typical breakthrough pressure determination gives a continuous trace that is nearly identical in appearance to those obtained by manual data point taking (Figure 2, 1966, Annual Report 49-8).

Contact angles of water on the water repellent soils were determined using an adaptation of the sessile drop method proposed by Poynting and Thomson (1905). The method requires a rather large, flat,

level surface of the solid being tested. Water is added to this water repellent surface until such a large drop is formed that the height of the drop reaches a maximum value, i.e. the diameter of the drop is large relative to the height, and further additions of water will increase the diameter of the drop, but not the height. The contact angle is related to this maximum drop height by the relation

$$\cos \theta = 1 - \frac{\rho g h^2}{2 \gamma}$$

where θ is the contact angle, ρ is density of the water, g is gravity, h is drop height, and γ is the surface tension of the water.

A soil sample holder was designed to provide the rather large, flat soil surface needed for the contact angle measurements. A 2 inch long, 3 inch diameter steel piston was machined flat on both ends to pass with about 0.005 inch clearance inside a 2 inch long, 3 inch diameter brass cylinder. A 1/16 inch cross section O-ring was fitted into a groove cut near the upper lip of the piston - this to slightly restrain the movement of the cylinder past the piston.

In practice the cylinder was pushed over the piston until a 1/2 inch well was formed inside the cylinder. The loose, water repellent soil was poured into the well, leveled with a spatula and packed with a hydraulic press whose two compression faces were of polished steel, flat and parallel relative to each other. The resultant soil surface was essentially flat and parallel relative to the faces of the piston of the sample holder. The entire assembly was then placed on a small leveling table, and the relative height of the soil surface determined with a cathetometer. Deionized, deaerated water was added atop the soil until a drop about 1 1/2 inches in diameter was formed. The relative height of the drop was determined with the cathetometer; more water was added and the measurement repeated - this process

repeated several times to reduce the variability of measurement. The difference between the average relative heights of the soil and water (h) was then used to calculate θ .

The soils and sands used in this study were selected mainly to provide a fairly large range of particle size distributions and surface areas. All samples were sieved to less than 2 mm. Particle size analyses were determined using the hydrometer method as modified by Bouyoucos (1962). Results appear in Table 1. The value for the "crystal silica" sand is that listed by the Ottawa Silica Company.

Surface areas were determined by using a modification of the ethylene glycol method proposed by Dyal and Hendricks (1950). Monolayer end points were determined from continuous desorption plots of weight versus time, which were obtained using a Cahn RG electrobalance. The soil samples were dried over P_2O_5 , weighed and equilibrated over a saturated atmosphere of ethylene glycol, returned to the balance, which was housed in a vacuum bottle, and the system evacuated continuously with a roughing pump rated at better than 10^{-3} torr. The monolayer end point was chosen as that point where the differential of weight loss versus time became constant. The area per ethylene glycol molecule used in the calculations was that selected by Dyal and Hendricks. External areas of the soils were determined similarly on samples heated to 500 C for 5 hours. Results appear in Table 1.

The soils were made water repellent by treating them with the sodium methyl silanolate, Union Carbide R-20. Various rates of aqueous R-20 solutions were added to air dry soil samples and gently mixed in a large cake mixer until the soil surfaces seemed uniformly wetted. The soils were then air dried several days to permit the R-20 to properly bond to the soil surface.

RESULTS AND DISCUSSION:

Penetration Pressure. The pressure needed to force water into the capillary pores of the soils treated with the R-20 silicone was

found to be a positive function of the proportion of the soil surface covered with the R-20, and to be inversely related to the effective pore radius of the packed soils. Figures 1 and 2 show that the breakthrough pressure, h_w , increases as the application rate of R-20/g of soil or per unit area of soil, respectively, increases. At low surface coverage the breakthrough pressure, h_w , increases markedly for rather small increment increases in surface coverage - this undoubtedly being due to corresponding marked increases in the contact angle of the water phase in contact with the partially coated soil surfaces.

As coverage continues to increase, a distinct inflection occurs in the rate of change of h_w . Beyond the inflection point h_w quickly levels off, either immediately obtaining or quickly approaching a maximum value. Figure 2 shows that these points of inflection occur at about the same degree of surface coverage for all the soils tested, i.e. roughly 1.5×10^{-4} grams of R-20 per m^2 of soil surface area. This value is thought to correspond to monolayer surface coverage.

The coverages of R-20 per unit area shown in Figure 2 are based on the total surface area of the soils. Similar plots based on the external area of the soils were not successful in establishing a corresponding monolayer region which was similar for all soils. This either suggests that the R-20 penetrated the internal surfaces of the clay minerals present or that the method used for determination of external area was in error. Table 1 shows that all the soils tested seemed to have a high proportion of internal area. This may be reasonable for the finer textured Granite Reef and Pachappa soils, but is not for the coarse textured soils. Thus, the Dyal and Hendricks method for the determination of external soil surface areas is suspect. The method also could not be used for determining the surface area of the Ottawa sand; strangely, the method invariably yielded negative surface areas.

The breakthrough pressure equation states that the breakthrough pressure, h_w , is inversely related to the effective soil pore radius, r , thus, by inference, should also be related to soil texture. Figures 1 and 2 readily support this relationship between breakthrough pressure and soil texture, but also show that it is little more than a rough generalization, e.g. Granite Reef and Pachappa, which have a very similar particle size distribution (Table 1), have markedly different breakthrough pressures at similar organic coverages.

Increasing the bulk density of a soil by packing should decrease the effective pore radius and consequently increase the breakthrough pressure. Figure 3 shows the results of such an experiment conducted on three soils treated with monolayer or greater surface coverages of R-20. Loose soils, placed in the breakthrough pressure sample holder, were subjected to relative increases in packing by varying the number of times the hammer was dropped on the soil surface. All three soils showed an increase in breakthrough pressure, h_w , with increased packing; as would be expected the increase in h_w for the coarse, textured Salt River Bed Sand was very slight, but was quite significant for the fine textured Granite Reef soil.

Thin films of low surface energy organics adsorbed on high surface energy solids are known to effectively mask the surface properties of the covered phase. The surface energy of the system is then entirely dependent on the type and arrangement of exposed functional groups of the organic film. Thus, at monolayer coverage, the per unit area surface energy of all these soils should be the same - that of the R-20 film.

The contact angle of the water on this organic film is thermodynamically related to the surface energy of that film, but the actual effective contact angle in these porous soil systems is also affected by a composite roughness contribution, which consists of both a plainer roughness and a porosity contribution. The thermodynamic contribution to the contact angle should be the same for

all the soils at and beyond monolayer coverage; if the roughness contribution for each of the soils also is the same, then the actual contact angle of the water should be the same and the breakthrough pressure at monolayer coverage for the soils coated with the same organic film should be independent of contact angle, and should be only a function of the effective pore radius.

This hypothesis was tested by plotting the breakthrough pressure at monolayer coverage h_w^* of several of the coarse textured sands versus the inverse of the effective pore radius of the soils. The effective pore radii were obtained by determining the maximum height of rise of benzene in soil columns whose bulk densities had been adjusted to equal those of the soil packed in the breakthrough pressure apparatus. This was considered legitimate since the effective pore radii functioning in both capillary and breakthrough pressures should be the same. Benzene was used to be assured of a zero contact angle when calculating the pore radius using the common capillary rise equation.

Figure 4 shows that: (1) h_w^* is indeed linearly related to $1/r$, and (2) the factors which control the slope of the line are as predicted constants for any one particular organic coating. This technique of plotting the maximum breakthrough pressure h_w^* versus the inverse of the pore radii should serve as another useful means for evaluating the water repellency characteristics of the organic materials when adsorbed on soils. The theoretical absolute maximum of h_w^* as a function of $1/r$ is also shown in Figure 4 - this occurring when the constant terms which describe the slope of the line obtain their theoretical maximum values.

Contact Angle. The contact angle measurements also show that the surface energy of the soil is reduced as the degree of thin film coverage is increase, i.e. the contact angle increases as the degree of surface coverage increases (Table 2). Contact angles less than 90° cannot be measured by this technique since as with

the breakthrough pressure method the drops of water are drawn into the soil capillaries. Such soils are not water repellents so are of little interest anyway in this study. For θ larger than 90° , the initial increases in θ per increment increases in surface coverage are large. As monolayer coverage is approached and exceeded, the rate of increase in θ rapidly decreases, eventually attaining a nearly constant maximum value. This maximum value for R-20 treated soils is about 150 ± 5 degrees, and, as expected, seems to be relatively independent of soil type.

Roughness of the soil surface is undoubtedly partially responsible for this large angle. Shafrin and Zisman (1964) report that the contact angle for water on an adsorbed, smooth, condensed monolayer of a polydimethylsiloxane was only 101° . Since the type and density of exposed functional groups for the polydimethylsiloxane and the R-20 should be nearly the same, films of the two compounds might be expected to have similar surface energies, thus, similar contact angles. The difference between 100° and 150° , therefore, is probably largely due to the roughness of the exposed soil surfaces.

The contribution of roughness to the observed contact angle is described by the relation

$$\cos \theta'' = f_1 \cos \theta - f_2$$

where θ'' is the observed contact angle, θ is the true contact angle based on the surface energy of the smooth, solid surface, and f_1 is the ratio of actual area of solid surface covered by the liquid compared to the plainer surface area covered. Since f_1 is greater than or equal to 1, any roughness in the surface increases θ'' for $\theta > 90^\circ$, but reduces θ'' for $\theta < 90^\circ$. The factor f_2 represents the proportion of air space or air-liquid interface under the drop compared to the plainer surface covered. If air spaces are present, the factor f_2 always reduces $\cos \theta''$, i.e. increases the contact angle of the liquid on the solid surface.

Since these R-20 treated soils are both rough and porous, and since $\theta > 90^\circ$ at monolayer coverage, both f_1 and f_2 contributed to increasing the contact angle.

It would be advantageous to know if the contact angle as measured with this technique is the same as that encountered in the penetration pressure work. It may be possible to check this using the apparent linear relationship between h_w^* and $1/r$ as pictured in Figure 4. Using the slope of the line shown and 72.8 dynes per cm for the surface tension of water, the calculated value of θ is only 116° . These silicones, however, act as wetting agents when in aqueous solution, therefore, any dissolution of the R-20 off the soil into the aqueous phase would lower the surface tension of the water. Again, using the linear relationship between h_w^* and $1/r$ as pictured in Figure 4, and letting $\theta = 150^\circ$, the calculated value of γ is only 35 dynes per cm. It may be possible to determine γ to resolve the problem.

SUMMARY AND CONCLUSIONS:

The method for measuring breakthrough pressures of water repellent soils was refined and adapted to an automatic data recording system using a sensitive pressure transducer coupled to a strip chart recorder. A method was also developed for measuring the contact angle of water on these water repellent soils. The pressure needed to force water into the capillary pores of soils treated with a silicone water repellent was found to be correlated to the proportion of the soil surface covered with the organic coating and to be inversely related to the effective pore radius of the packed soil. Both of these two phenomena are predicted by the equation which describes this breakthrough pressure

$$h_w = 2\gamma \cos \theta / \rho g r$$

where h_w is the breakthrough pressure expressed here as the head

of water needed to force water into the pore structure of these water repellent soils, γ is the surface tension of the aqueous phase, ρ is its density, g is gravity, θ is the contact angle of the water, and r is the effective pore radius of the packed soil.

The breakthrough pressure method was found to be effective for establishing the application rates of organic compound necessary to obtain surface monolayer coverage. For the silicone used in these studies, Union Carbide R-20, all soils obtained monolayer coverage at about 1.5×10^{-4} g of silicone per m^2 of total soil surface area.

Preliminary work suggests that the effective contact angle of water on these organic coated soils attains a constant maximum value at the monolayer coverage point; also, this maximum contact angle apparently is relatively independent of the type of soil present. Thus, a plot of the breakthrough pressure of several soils treated with a monolayer coating of the silicone water repellent versus the inverse of the respective effective pore radii, which were determined independently using capillary rise techniques, yielded a linear relationship.

A more direct method for measuring the contact angle of organic coated soils was also developed. Preliminary work suggests this also will be useful in establishing optimum application rates and may be useful for comparing various soil treatments.

REFERENCES:

1. Bouyoucos, G. J. Hydrometer method improved for making particle size analysis of soils. *Agron. Jour.* 54:464-465. 1962.
2. Dyal, R. S. and S. B. Hendricks. Total surface of clays in polar liquids as a characteristic index. *Soil Sci.* 69:421-432. 1950.
3. Poynting and Thomson, *Properties of Matter, Textbook of Physics*, p. 156, London, 1905.

4. Shafrin, E. G. and W. A. Zisman. Upper limit of the contact angles of liquids on solids. Adv. in Chem. Series 43:145-157. 1964.

PERSONNEL: D. H. Fink

Table 1. Soils and physical constants.

Soil	Surface Area		Particle Size		
	Total	External	Sand	Silt	Clay
	m ² /g		%		
Play Sand	8.0	3.3	95.4	2.8	1.8
Salt River Bed Sand	23.4	8.7	87.3	10.7	2.0
Control Sand	32.2	14.6	39.8	60.2	6.9
Pachappa	22.2	7.0	50.3	41.9	7.8
Granite Reef	71.5	21.2	51.9	41.3	6.8
Ottawa Sand	*	*	100		

* Could not be determined by method used.

Table 2. Contact angle of water on soils treated with R-20 silicone water repellent.

Soil	Surface Coverage	Contact Angle
	g R-20/m ² of soil ($\times 10^4$)	Degrees θ
S.R.B.S.	0.13	< 90
	0.26	< 90
	0.52	137.5 \pm 5.4
	1.30	149.0 \pm 1.7
	2.61	151.8 \pm 3.3
	5.21	156.6 \pm 9.3
Granite Reef	0.17	< 90
	0.43	119.8 \pm 16.9
	0.85	154.2 \pm 2.0
	1.71	152.0 \pm 4.8

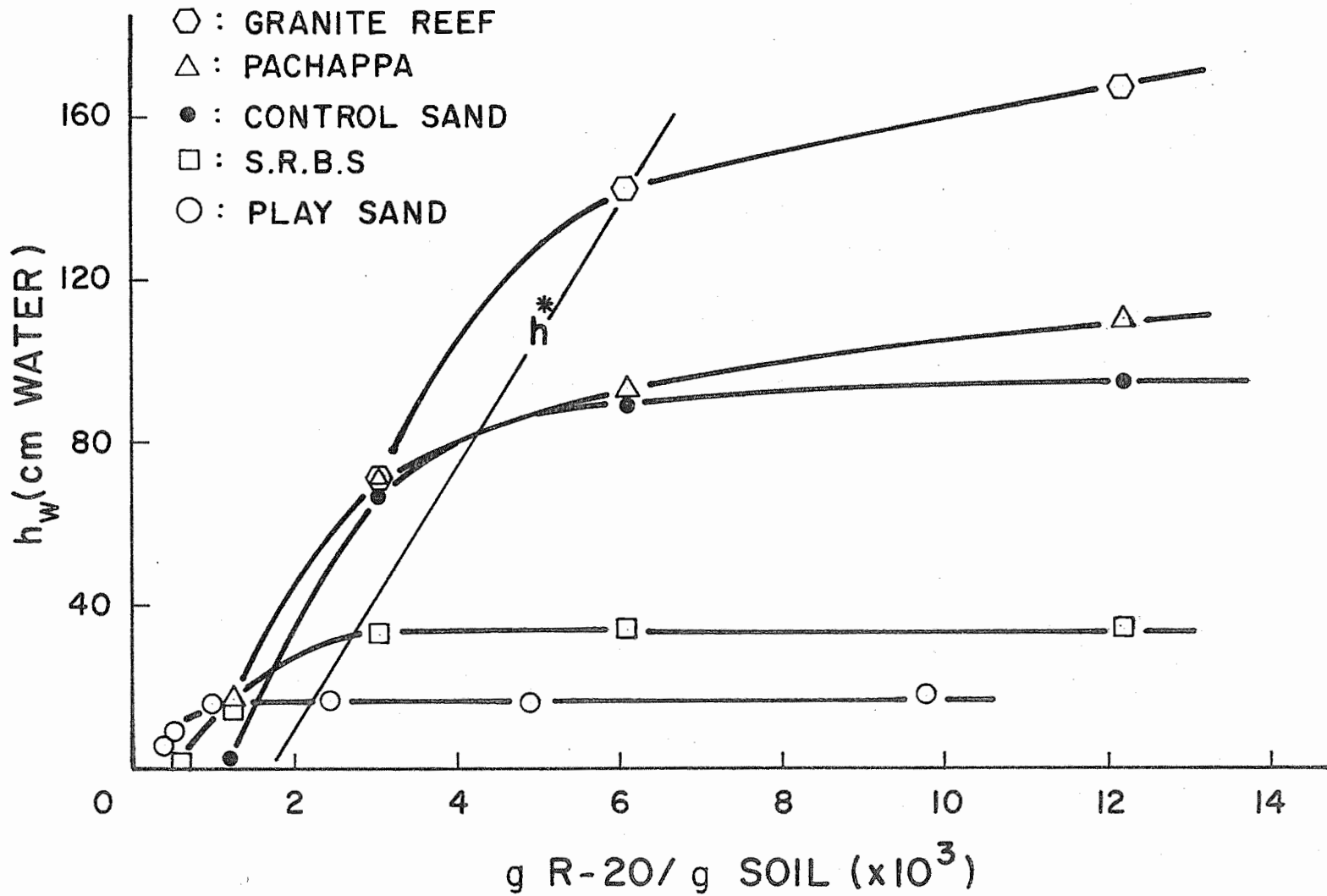


Figure 1. Breakthrough pressure of silicone treated soils versus application rate of silicone per gram of soil. Annual Report of the U.S. Water Conservation Laboratory

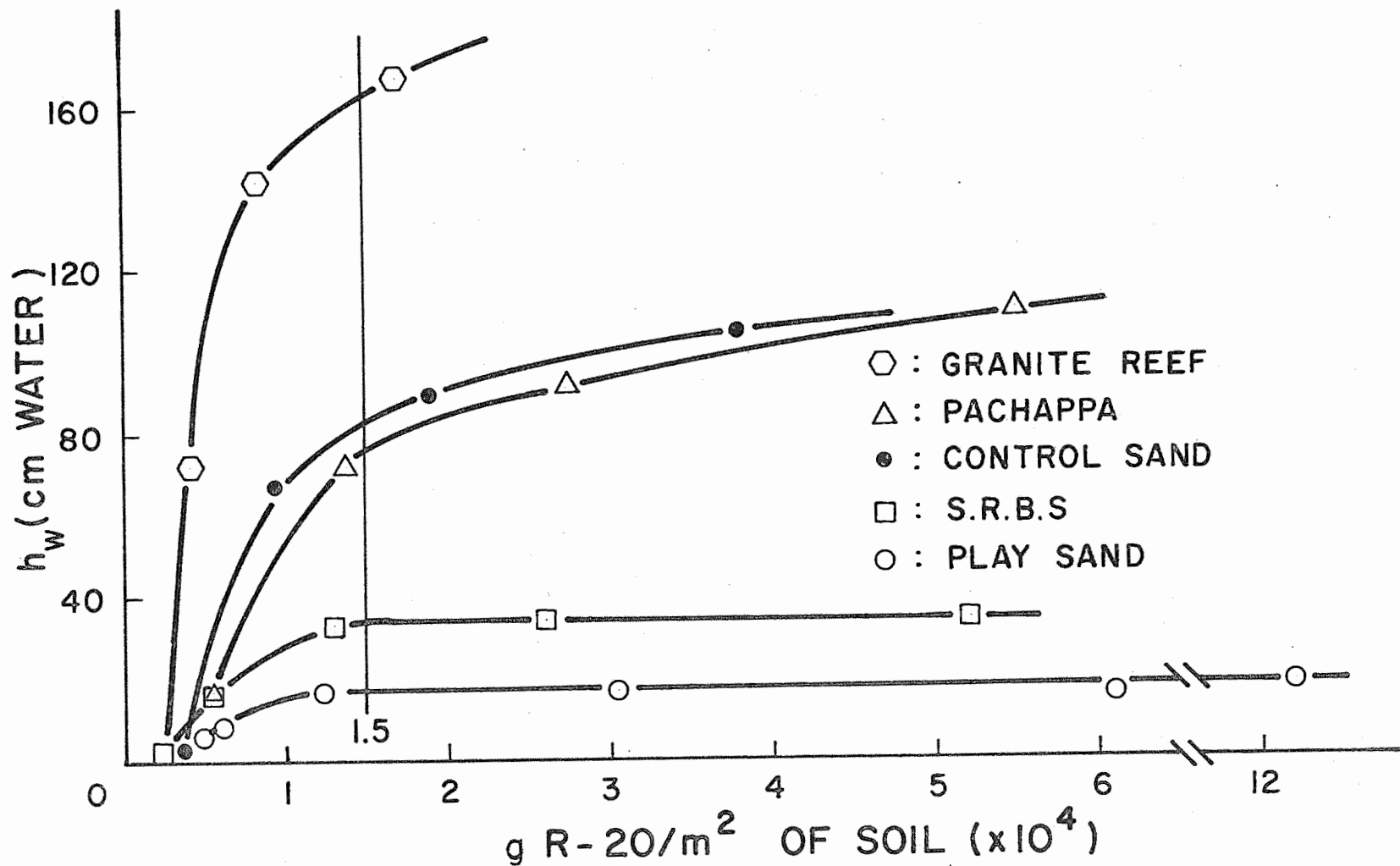


Figure 2. Breakthrough pressure of silicone treated soils versus application rate of silicone per unit area of soil.

49-15

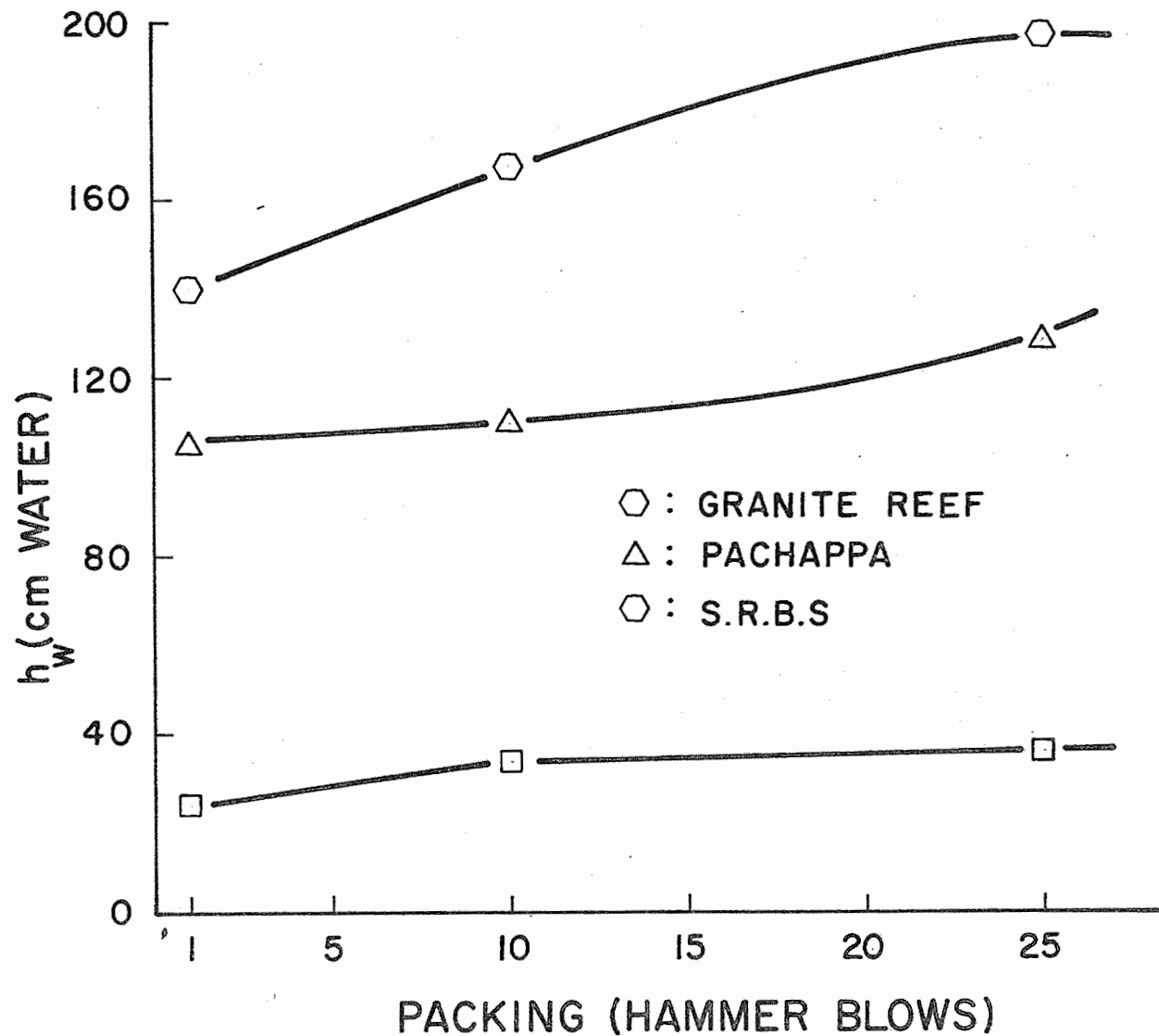


Figure 3. Breakthrough pressure of water-repellent soils versus degree of soil packing. Annual Report of the U.S. Water Conservation Laboratory

9I-67

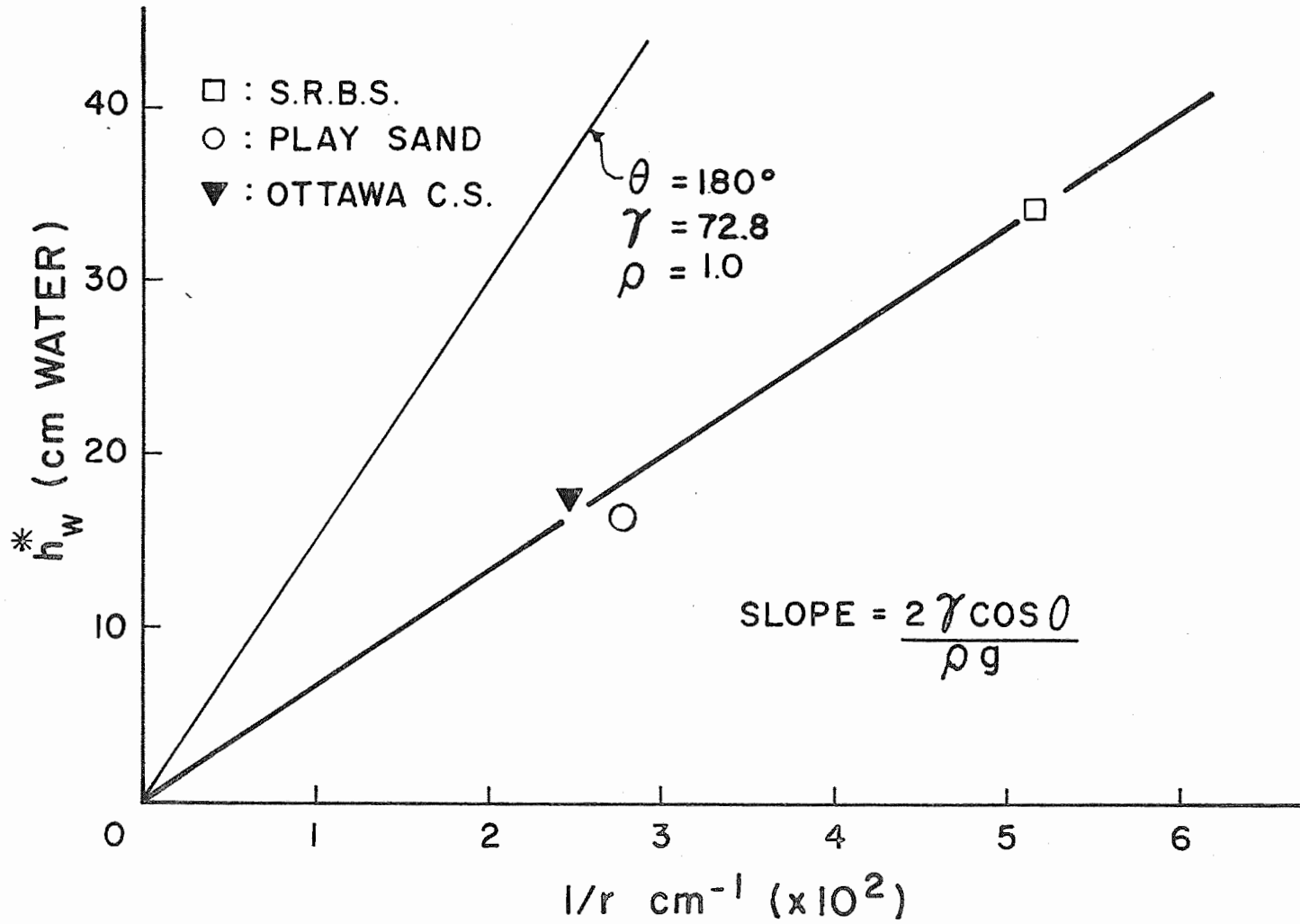


Figure 4. Breakthrough pressures at monolayer coverage of silicone coated soils versus the inverse of the effective soil pore radius. Annual Report of the U.S. Water Conservation Laboratory

TITLE: USE OF FLOATING SOLID AND GRANULAR MATERIALS TO REDUCE
EVAPORATION FROM WATER SURFACES

LINE PROJECT: SWC VII gG-3

CODE NO.: Ariz.-WCL-50

INTRODUCTION:

Previous studies on 2.7 m diameter tanks have shown it is economically possible to reduce evaporation with floating covers (see 1965 Annual Report WCL-9). The ever expanding list of possible materials to use, necessitates continued research in this area, as well as field application of the more promising products.

Ten 6.1 m square foamed polyethylene covers were tested under field conditions on a stock pond near Flagstaff, Arizona during the summer of 1967.

Several varieties of floating concrete blocks were tested to determine the best combinations of ingredients, as well as the value of protective coatings. These blocks, along with a foamed wax material, a butyl sheet and a styrofoam cover were studied on 2.1 m diameter tanks.

The 2.7 m diameter tanks, on which previous studies were conducted, were modified to simplify heat balance calculations. A tank 2.1 m in diameter and 0.6 m depth was placed inside the 2.7 m diameter tank, thus leaving a 0.3 m space between the two tanks on the bottom and around the sides. This 0.3 m space was filled with perlite ore, thus insulating the inner tank and minimizing heat exchange with the surroundings.

PROCEDURE:

Foamed Polyethylene. Ten foamed polyethylene covers approximately 6.1 m square were constructed for the purpose of evaluating their performance under field conditions. Previous studies indicated that the foamed polyethylene did not stand exposure to the sunlight for more than about one evaporation season; therefore, protective coatings were applied to the top surface. Eight of the covers were coated with a mixture of aluminum powder and Butyl latex

emulsion, and the remaining two were coated with a white acrylic emulsion. These covers were placed on a stock pond about 1/3 acre in size located near Flagstaff, Arizona in late May 1967.

Floating Concrete Blocks. Floatability tests were conducted on several different batches of concrete blocks in which the proportions of the ingredients were varied. Since a moisture barrier was needed to reduce losses thru the blocks and increase their efficiency for reducing evaporation, three approaches were investigated. These were; (1) regular blocks completely coated with a cutback asphalt, (2) regular blocks coated on the top only with a white acrylic emulsion, and (3) adding an anionic asphalt emulsion to the batch during mixing.

Sufficient blocks were placed on the 2.1 m diameter tanks to cover approximately 80% of the surface, and the evaporation as compared to an open tank was recorded.

Other Floating Covers. Three other materials were tested for efficiency in reducing evaporation on the 2.1 m diameter tanks.

The first was a foamed wax material, white in color, made into blocks about 12.1 cm in diameter and 4 cm thick. Sufficient blocks were placed on the tank to cover about 80% of the surface, and evaporation was noted. A test was also conducted in which perlite ore was placed in the voids between the wax blocks, the combination therefore covering almost the entire surface area.

The second material was a 15 mil butyl sheet floated by means of a sealed 2.5 cm diameter plastic pipe fastened around the circumference. This material, made to cover about the same area (78%) as the wax blocks, was coated on top with white latex paint, and the evaporation recorded.

The third material used was a styrofoam cover of 5.1 cm thickness, and the same area as the butyl cover (78%). The styrofoam was coated on top with a white latex paint for protection, and the evaporation recorded.

RESULTS AND DISCUSSION:

Foamed Polyethylene. The ten 6.1 m square foamed polyethylene covers were observed about once every two weeks after installation, and were found to perform satisfactorily until mid-July. During the later part of July and August, with the increased thunderstorm activity and weathering of the materials, six of the covers received severe damage. They were blown from the pond and torn beyond repair on the nearby rocks and shrubbery. One of the remaining four covers was torn slightly and the plastic pipe frame was bent; however, it was repaired and was still in fair condition, as were the other three, at the last inspection in October. All four covers did show signs of deterioration, thus indicating that the protective coatings did not extend the life of the cover significantly. This, and previous studies, indicate that although the foamed polyethylene is a very efficient material for reducing evaporation, it is still doubtful that it would be an economical method of saving water under most field conditions, due to its short life and susceptibility to wind damage.

Floating Concrete Blocks. A light-weight concrete block has been developed, using expanded 0.3 mm average diameter perlite ore as the main aggregate, that will float for a considerable length of time. Some of the blocks were on the 2.1 m diameter tanks for over six months, and no change in floatability or deterioration was noted.

Results of evaporation reduction efficiency studies are presented in Table 1, and summarized below. The asphalt coated light-weight concrete blocks initially reduced evaporation by 40%, with 80% of the surface covered, but soon dropped to 27% as the asphalt oxidized, thus saving only 32% on the average, as shown in Table 1, for the period between March 24 and May 3.

The blocks coated on the top with a white acrylic emulsion were more efficient in reducing evaporation than the asphalt coated blocks. They initially reduced evaporation by 53%, with 80% of the surface covered, but gradually dropped to 49% by the end of the

study period. The acrylic emulsion coating was turning brownish from collecting dust, and some spalling had occurred at this stage.

The concrete blocks containing asphalt within the mix initially reduced evaporation by only 39%, with 80% of the area covered, but with aging gradually increased to 60% reduction, with 78% coverage. These blocks, besides being the most efficient in the long run, would be the most economical of the floating concrete blocks tested, because they did not require additional treatment or handling after initial setting.

Other Floating Covers. The results of evaporation reduction studies using foamed wax, butyl rubber, and styrofoam are presented in Table 2, and are summarized below.

The foamed wax blocks initially reduced evaporation by 68%, with 78% coverage. After adding 0.3 mm average diameter expanded perlite ore to the voids between wax blocks, the evaporation reduction decreased to 63 percent, and as the blocks collected dust, thus changing their color, the efficiency decreased to 59%. On June 20, 1967 the perlite was removed and the blocks turned over, thus exposing a clean white surface, similar to the initial conditions of February 27. Under these conditions the evaporation reduction was 67%, or essentially the same as at the beginning of the studies. However, during the period from July 31 to September 11, the intense summer heat melted the exposed surface of the blocks. The molten wax, along with the captured dust, changed the reflective characteristics of the blocks and evaporation reduction dropped to 54%.

On September 11 new blocks were placed on the tanks and evaporation reduction remained 75% or more thru the end of the study period. Lower air temperatures during this later period were not sufficient to melt the blocks, and several rains kept the dust washed from the blocks, leaving a white surface.

The white coated butyl rubber cover reduced evaporation by 73%, with 78% of the surface covered during the hot part of the study, and

efficiency increased to over 81% as the air temperatures decreased.

The styrofoam cover was only tested during the last period, and it reduced evaporation by 78%, with 78% coverage. The results of this last period would indicate that the thin butyl cover is more efficient than the thicker styrofoam cover, probably due to heat escape thru the cover in the first case, but only thru the uncovered area in the case of styrofoam, because of its good insulating properties. In any event, further studies will be conducted during the hot season on these two materials.

SUMMARY AND CONCLUSIONS:

This, and previous studies on floating covers constructed of 6.4 mm thick white polyethylene, have shown that although the material is very efficient in reducing evaporation, the short usable life due to rapid weathering, and the potential for wind damage make it uneconomical for most field situations.

Light-weight concrete blocks have been developed that will float for a considerable time and reduce evaporation significantly. Blocks with asphalt in the mixture of ingredients were more efficient and economical than regular blocks with protective coatings. The coatings tended to deteriorate after exposure, while the blocks with asphalt in the mix became more efficient with age.

Foamed wax blocks were found to be slightly more efficient than the light-weight concrete blocks; however, due to their low melting point they did not stand up under the high air temperatures of late July and August. During the cooler part of the year the wax blocks reduced evaporation almost 100% for the amount of area covered. Adding light-weight perlite ore to the voids between wax blocks did not increase efficiency; in fact, it seemed to reduce it slightly. However, dust collecting on the blocks may have been the cause of the decrease.

Butyl rubber, floated by means of a sealed plastic pipe attached around the perimeter and painted white on top, has been the

most efficient cover studied. The butyl cover has not been damaged by wind on the rather small study tanks, but from experience with the foamed polyethylene it would appear that any membrane or sheet material would be potentially subject to wind damage. Another problem would be sinking of the cover if the plastic pipe was damaged.

The styrofoam cover was only studied for one period, and the efficiency was 100% for the area covered. Further studies, during the hot season, will be conducted on this cover to determine if changes in efficiency occur. The potential for wind damage is also present for the styrofoam cover.

PERSONNEL: Keith R. Cooley

Table 1. Evaporation reduction using lightweight concrete blocks.

Period	Open Tank	<u>Asphalt Coated</u>			<u>Acrylic Coated</u>			<u>Asphalt in Mix</u>		
	Evaporation (cm)	Evap. (cm)	Red. (%)	Area (%)	Evap. (cm)	Red. (%)	Area (%)	Evap. (cm)	Red. (%)	Area (%)
24 Mar - 3 May	16.39	11.15	32	80	-	-	-	10.02	39	80
3 May - 16 Jun	30.67	-	-	-	14.44	53	77	15.14	51	80
20 June - 31 Jul	35.24	-	-	-	17.87	49	77	16.29	54	80
31 Jul - 11 Sep	30.63	-	-	-	-	-	-	14.81	52	78
11 Sep - 2 Oct	11.36	-	-	-	-	-	-	4.50	60	78

50-7

Table 2. Evaporation reduction using other floating materials.

Period	Open Tank	Foamed Wax		Wax & Perlite			Butyl Rubber			Styrofoam			
	Evap. (cm)	Evap. (cm)	Red. Area (%)	Red. Area (%)									
27 Feb - 12 Mar	3.33	1.02	68	78	-	-	-	-	-	-	-	-	-
24 Mar - 3 May	16.39	-	-	-	6.07	63	98	-	-	-	-	-	-
3 May - 16 June	30.67	-	-	-	12.48	59	98	-	-	-	-	-	-
20 Jun - 31 Jul	35.24	11.47	67	78	-	-	-	-	-	-	-	-	-
31 Jul - 11 Sep	30.63	13.96	54	78	-	-	-	8.14	73	78	-	-	-
11 Sep - 2 Oct	11.36	2.84	75	78	-	-	-	2.21	81	78	-	-	-
4 Oct - 7 Nov	15.45	3.56	77	78	-	-	-	2.74	82	78	3.45	78	78

50-8

TITLE: WASTE WATER RENOVATION BY SPREADING TREATED SEWAGE
FOR GROUND-WATER RECHARGE

LINE PROJECT: SWC W4 gG-1 CODE NO.: Ariz.-WCL-51

INTRODUCTION:

Construction of the project on waste water renovation by ground-water recharge through surface spreading, code name project Flushing Meadows, started in January and was completed in August. The construction was done by the Salt River Project, following approval of a demonstration grant from the Federal Water Pollution Control Administration. The grant was in the amount of \$69,500 and covers mainly the construction costs and the salaries of two laboratory technicians for a 3-year period. The project is located on State land in the Salt River bed about 1 1/2 miles west of 91st Avenue. A commercial lease from the State Land Department, and an agreement with the City of Phoenix to divert sewage effluent for experimental ground-water recharge have been obtained. An effluent recharge committee, consisting of representatives of the Salt River Project, City of Phoenix, County and State Health Departments, Bureau of Reclamation, the University of Arizona, and the U. S. Water Conservation Laboratory has been formed. The committee meets periodically to discuss plans and results of the Flushing Meadows project.

For a description of the objectives of the Flushing Meadows project, reference is made to Research Outline WCL-51.

PROCEDURE:

Description of Project. The field system consists of six horizontal recharge basins, 20 x 700 ft, arranged in two groups of three stepped-down basins (Figure 1). Secondary sewage effluent from the City of Phoenix is pumped from the channel through a constant-head structure into an underground concrete pipe. The effluent then flows through risers with alfalfa valves into concrete boxes from where it discharges into the recharge basins through fiberglass, triangular critical-depth flumes. At the other end of the basins are

overflow structures to control the water depth in the basins, and again triangular flumes to measure the flow. The outflow is collected in a concrete drainage line which returns the effluent to the channel. Each flume is equipped with a water stage recorder and the infiltration rate for each basin is calculated as the difference between the inflow and outflow rate. The discharge-depth relationship for the flumes is shown in Table 1.

Three 6-inch observation wells with nonperforated casing down to the bottom were installed (Figure 1). The two wells in the center of the project area are 30 and 100 ft deep and they are equipped with submersible pumps. The well at the east side of the plot area is 200 ft deep. The well logs (Figure 2) show an irregular succession of sand and gravel layers. From information obtained by the U. S. Geological Survey, extensive deposits of clay can be expected at a depth of about 230 ft. The static water table is 12-14 ft below the basins, depending on the elevation of the basin bottom.

The soil profile in the basins consists of a layer of fine sand 1.3 to 5 ft thick with an average thickness of 3 ft. Ten percent of the particles in this sand have a diameter less than 0.06 mm and 50% less than 0.18 mm. Based on double-tube and air-entry permeameter tests, the hydraulic conductivity, K, of the fine sand is 1 to 1.5 m/day and the air-entry value is about -30 cm. The fine-sand layer is underlain by 2- to 6-inch gravel and boulders in almost continuous matrix with the space between the gravel occupied by coarse sand.

Infiltration Studies. Maintaining a water depth of about 18 cm in the basins and an inflow rate of about 0.8 cfs per basin, infiltration rates were determined for different inundation periods and schedules. Following a 1-day inundation on 30 August (period A), which had to be discontinued because of excessive settlement of the supply structures, the following inundation periods were held:

22-27 September	Period B
3-6 October	Period C
12-24 October	Period D
6 November - 18 December	Period E

For all inundation periods, the bottom of the recharge basins was bare soil. The beds were harrowed on 12 October with the exception of basin 5. This was done to determine the effectiveness of harrowing in breaking up a surface crust that was formed by rain on 3 October. On 3 November, all basins were harrowed again. For periods B, C, and D, all six basins were inundated in the same manner. For period E, each basin was inundated according to a different schedule as follows (1-2 means 1 day inundation and 2 days dryup):

Basin	Inundation schedule
1	1-3 1-2, repeat
2	2-1 2-2, repeat
3	3-4, repeat
4	1-1 1-1 1-2, repeat
5	5-9, repeat
6	5-2, repeat

The schedules for period E were set up on a weekly basis, stopping the pump with a timer on Saturday and having no pumping until the following Monday. The different schedules were selected to determine the effect of different inundation and dry-up periods on the intake behavior of the basins.

In basins 2, 5, and 6, periodic measurements were made of the water content in the fine-sand layer using the neutron method. Also, measurements of the tensions in the fine sand layer were obtained in these basins at different depths to determine the degree and extent of soil clogging.

Aquifer and Analog Studies. On 18 September, K below the two center observation wells was determined using the tube-method technique of Kirkham and Frevert.

Water levels in the two observation wells were measured daily, during recharge periods B, C and D and on several days preceding and following these periods. In conformance with the theory, the water levels during the recharge periods rose to pseudo-equilibrium values. To simulate the equilibrium levels in the shallow and in the deep center observation wells on the electrical resistance network analog, it was necessary to introduce anisotropy of the aquifer. By trial and error, the ratio of $K_{\text{horizontal}}$ to K_{vertical} was increased on the analog until the "water level rises" on the analog in the shallow and deep well matched the ones in the field. From the infiltration rate measured in the field and the electrical "intake" current measured on the analog, the actual values of $K_{\text{horizontal}}$ and K_{vertical} could be computed.

Based on previous work with the analog on ground-water mounds (1), the value of K for an assumed isotropic aquifer was also determined. This technique requires knowledge of the intake rate and of the pseudo-equilibrium height of the mound. The value of K is then calculated using a dimensionless parameter.

Water Quality Studies. Daily samples of ground water from the two center observation wells and periodic grab and 24-hr continuous samples from the influent were analyzed for pH, EC, NO_3 , NH_4 , and COD. Occasionally, ground water samples were sent to a commercial laboratory for determining the MPN of coliform bacteria. Nitrates were determined with the brucine method. The nitrate electrode and perchloric acid techniques are under study and may supplant the brucine method. Ammonium is determined with the Nessler technique.

RESULTS AND DISCUSSION:

Infiltration Studies. The infiltration rates for the first 5-day inundation period (period B) remained fairly constant with the following values observed:

Basin	Infiltration rate (ft/day)
1	3.2
2	4.0
3	3.3
4	3.6
5	3.9
6	3.1

The infiltration rates for these periods were about equal to the K-value of the fine sand. This could be expected, since the hydraulic gradient in the fine sand layer should be about one, and clogging should not yet have occurred.

The second 5-day inundation period (period C) was preceded by a 0.5-inch rainfall in the early morning hours of 3 October, the day inundation was to commence. The impact of the raindrops and the splashing effect caused some surface sealing and possibly deflocculation of the clay fraction. This is evidenced by the fact that the infiltration rates for this period started out at about one-half the final values of period B. Also, the infiltration rates during period C showed a slightly decreasing trend. The following average rates for period C were observed

Basin	Infiltration rate (ft/day)
1	1.8
2	2.0
3	1.4
4	1.9
5	1.7
6	1.7

Prior to the next recharge period (period D), the basins were harrowed with the exception of basin 5 to determine how effective harrowing would be in breaking the seal caused by the rainfall and in restoring infiltration rates. During the ensuing 12-day inundation period D, the infiltration rates exhibited a general, rather linear decline. The intake rates at the beginning and at the end of period D were as follows:

Basin	Infiltration rate (ft/day)	
	first day	last day
1	2.6	1.1
2	3.2	0.9
3	2.6	0.4
4	3.3	1.4
5	3.0	0.9
6	2.9	0.8

The lower intake rates for basin 5, as compared to previous periods, indicate that the rain of 3 October had indeed caused some seal and that harrowing was effective in restoring the infiltration rate. Thus, at the end of the drying period following period D, all basins were harrowed again to obtain a uniform surface condition.

Although growth of algae occurred during the recharge periods B, C, and D, a significant part of the algae film on the bottom broke loose again and floated to the runoff end of the basins where it collected on a screen. The remainder of the algae disintegrated during the dryup period so that each inundation period started with a relatively "clean" bottom.

The infiltration rates for the different inundation schedules of period E are shown in Figure 3. The striking feature is that the intake rates showed a general decline, with the values at the beginning of a new inundation period less than those at the end of the preceding inundation period. The only exception to this is basin 5,

where the dryup times were the longest, i.e., 9 days, and where some restoration of the infiltration rate took place during the dryups. However, the infiltration rates were never restored to the high values at the beginning of the previous intake inundation period.

The profile drainage due to gravity was relatively rapid. For example, Figure 4 shows that most of the drainage took place within 48 hours after the basin became dry. Similar observations were made for the other basins. The lack of recovery in the infiltration rates was, therefore, probably caused by growth of algae and other organisms on the bottom of the basins. During the cool, winter weather, dryup times from 1 to 4 days were not sufficient to yield a "dry" surface. Thus, the algae remained viable and intake rates continued to decline. Lack of drying was especially severe during the last few days of period E, when a total of 4.7 inches of rain fell in about a week. Because of the algae accumulation on the bottom of the basins and because of sediment that had entered the basins from the effluent channel and the banks of the basins due to the severe rainfall, period E was terminated on 19 December. At this time, the intake rates were between 0.5 and 1 ft/day, whereas they ranged between 2 and 3 ft/day at the beginning of period E.

The data in Figure 3 indicate that the actual schedule of the inundations did not affect the infiltration rates very much. An exception is the 5-9 schedule for basin 5, which yielded somewhat higher intake rates at the beginning of the inundation periods. However, the intake rates decreased rather severely during the inundation, so that the intake rates at the end of an inundation period for basin 5 were about the same as for the other basins. Thus, a wet schedule such as that of basin 6 can be expected to yield higher quantities of recharge water over a certain period of time than dryer schedules such as those of basins 1 and 5.

Figures 5, 6, and 7 show that the pressures in the fine-sand layer exhibit a decreasing trend. For basins 2 and 6, this decrease

occurred gradually from one inundation to the next with little decrease during the inundation period. For basin 5, however, there was a pronounced pressure decrease during each inundation period. Comparison of Figures 5, 6 and 7 with Figure 3 shows that the behavior in pressure paralleled that in the intake rates, which points to the conclusion that the reduction in intake rate is mainly caused by a permeability decrease of the surface soil (a pressure increase accompanying an intake-rate decrease would point to a permeability decrease of soil layers below the tensiometer depths). Further evidence that this is so is presented in Figure 8, which shows how the intake rate and the K-values for the different soil layers decrease with time for basin 2. The K-values were obtained from the pressure measurements at different depths as shown in Figure 5 and the average intake rates for the basin as shown in Figure 3, using Darcy's equation. The curves in Figure 8 show that K of the 20- to 100-cm layer is almost equal to the intake rate. Thus, the hydraulic gradient in this layer was about unity for the entire period. Discarding the points for the last day (19 December) because of possible errors in the intake rate due to the heavy rainfall, the relative K-reduction for the 0- to 10-cm layer was about twice that for the 20- to 100-cm layer. The relative K-reduction in the 10- to 20-cm layer was about three times less than that in the 0- to 10-cm layer. Thus, Figure 8 shows conclusively that the soil profile was clogging at the top. This reduced the infiltration rate and yielded unsaturated flow at unit gradient below the clogged surface layer. Similar results were obtained for basins 5 and 6.

The infiltration rate for basin 2 for period B was 4 ft/day. Because unit gradient and absence of clogging could be expected for the fine-sand layer during period B, the K-value at zero or positive pressures can be taken as the same value, or 4 ft/day. Selecting the K-values for the 20- to 100-cm layer from Figure 8 and the corresponding negative pressures from Figure 5, the relationship between K and

negative pressure could be determined. The resulting curve is shown in Figure 9.

Combining the tensiometer and water content readings yielded Figure 10, which shows the water content-pressure head relationship at three depths in basin 5.

Aquifer and Analog Studies. The results of the tube-method tests on the two center wells were as follows:

East center well (30 ft deep) $K = 8.9$ ft/day

West center well (100 ft deep) $K = 158$ ft/day

The low value for K of the east center well is probably due to an accumulation of several feet of "fines" that has been at the bottom of this well ever since it was installed. The K -value for the west center well compares favorably with the K -values evaluated from the mound behavior as shown in the following paragraphs.

For period B, the average intake rate for the basins was 3.5 ft/day. Thus, for the gross area, including the dikes between the basins, the average intake rate was $\frac{120}{220} \times 3.5 = 1.9$ ft/day.

The water level rise to the pseudo-equilibrium level for this period was 2.7 ft in the (shallow) east center well and 0.7 ft in the (deep) west center well. To simulate these rises on the resistance network analog, anisotropy with $K_{\text{horizontal}} > K_{\text{vertical}}$ had to be introduced.

The ratio of K_{hor} to K_{vert} was increased on the analog until the water level rises in the shallow and deep well were correctly simulated. This was the case when K_{hor} was equal to $16 K_{\text{vert}}$. Comparing the electrical "recharge" rate with the observed intake rate of 1.9 ft/day yielded a value of 388 ft/day for K_{hor} and 24 ft/day for K_{vert} . The equivalent isotropic hydraulic conductivity, \bar{K} , for the aquifer is $\sqrt{24 \times 388} = 97$ ft/day. The flow system for the recharge system is shown in Figure 11, where the streamlines were constructed as equipotentials after reversal of the boundary conditions.

The analog showed that the water pressure rise at the center of the base of the ground water mound was 3.5 ft above the static water table. Assuming vertical flow in the center region of the ground water mound above the static water table, the rise h_c of the center of the ground water mound is calculated according to Darcy's equation as

$$1.9 = 24 \frac{h_c - 3.5}{h_c}$$

or

$$h_c = 3.8 \text{ ft}$$

According to previous work (1), the \bar{K} -value of the aquifer can also be calculated from the value of h_c and the average intake rate. This procedure utilizes a dimensionless parameter evaluated by analog (1). The value of this parameter for the Flushing Meadows project geometry is 1.17 (as evaluated from Figure 7 in (1)). The resulting equation is

$$\frac{3.8}{220} = \frac{1}{1.17 \left(\frac{\bar{K}}{1.9} - 1 \right)}$$

from which \bar{K} is calculated as 96 ft/day. The agreement between this value of \bar{K} and the 97 ft/day calculated from K_{hor} and K_{vert} serves as a computational check on the validity of the two independent procedures.

The high degree of anisotropy is undoubtedly caused by the succession of sand and gravel layers in the aquifer. The very high value of the horizontal hydraulic conductivity is extremely advantageous for ground-water recharge in that it assures rapid lateral disposal of the recharge water while only giving relatively small

rises of the ground-water mound. The vertical hydraulic conductivity, although considerably smaller than the horizontal hydraulic conductivity, is still sufficiently large in relation to the infiltration rates to avoid significant mound buildups. Thus, high recharge rates and relatively closely spaced recharge basins can be employed without causing waterlogging of the soil beneath the basins.

Water Quality Studies. The results of the analysis of the water samples are summarized in Table 2. Presented in this table are the lowest and highest values observed and the averages up to 31 December. The TDS content of the native ground water is about 1600 ppm for the east center well and about 2200 ppm for the west center well. This compares with about 850 ppm for the sewage effluent or the Flushing Meadows "influent." Thus, TDS can be used as a tracer to determine when the native ground water is displaced by renovated water. For the (shallow) east center well, this took place during the month of September. On the 30th of August, the TDS content in the east center well water was 1800 ppm. On 20 September, it was 1400 ppm and on 1 October it was 900 ppm. From this date on, the TDS content stayed around 900 ppm. For the deep well, the salt content remained above 2000 ppm and by the end of January, native ground water was not yet replaced by renovated water. The delay in arrival of renovated water at the bottom of the west center well is due to the very slow flow velocities in the vicinity of the bottom of the deep well, as shown by the flow system of Figure 11. It is of interest to note that the ammonium and nitrate contents for the east center well are lower for the renovated water than for the native ground water. The COD-values remained about the same after the arrival of renovated water.

For the east center well, two distinct waves in the nitrate content could be observed. One wave, with values in excess of 10 ppm N occurred from 12-20 October. The second, with values in excess of 10 ppm and reaching between 20 and 25 ppm for several days, was from 12 to 20 October. In both cases, these nitrate waves occurred shortly

after the start of an inundation period following a rather prolonged dryup. Apparently, during the dryup the fluid retained in the soil profile after gravity drainage underwent a relatively complete aerobic digestion, which could lead to nitrate contents of 30 ppm N or more. When recharge was started again, this nitrified fluid was "pushed down" by the new infiltrating water to reach the ground water and the shallow observation well. After passage of the nitrate wave the decrease in the nitrate content was not accompanied by an increase in the ammonium content. It is of interest to determine whether this is due to denitrification or to incomplete mineralization and an increase in the organic nitrogen content. For this reason, determination of organic nitrogen with the Kjeldahl apparatus will be included in the routine analysis in the near future.

Presumptive coliform tests on samples from the east center well and the west center well were performed periodically by a private laboratory in Phoenix. Apparently, when the wells were installed, the well driller used effluent from the channel in the drilling operation. Thus, despite numerous flushings of the wells, initially, MPN values of 5.1 and 9.2 per 100 ml were obtained in addition to samples that were negative. During the month of September, the east center well yielded MPN values of 2.2 and less than 2.2 per 100 ml. The west center well yielded MPN values of 2.2 or less in October. On 3 October, the east center well yielded a MPN of 9.2 per 100 ml. On 11 October, it was 16 per 100 ml, and on three other dates in October it was reported as infinity. This was due to the fact that the private laboratory did not use sufficient dilutions, so that all tubes were positive, yielding an MPN of infinity. To get more accurate MPN values, the coliform tests are now being done in our own laboratory. The presumptive test will be followed by the Eijkman elevated temperature test to determine whether the coliform bacteria are of fecal or of soil origin. Tests performed on samples taken in the week of 15-19 January, 1968 yielded MPN-values of 13 to 79 per

100 ml for the east center well and 2 per 100 ml for the west center well. The Eijkman tests were all negative, indicating that the bacteria were of soil and not of fecal origin. In contrast to this, the MPN of the secondary sewage effluent was 700,000 per 100 ml and the Eijkman test was positive.

SUMMARY AND CONCLUSIONS:

Construction of the Flushing Meadows project, which is an experimental project to determine feasibility and management for optimum performance of a ground-water recharge system for renovation and reuse of secondary sewage effluent, was completed in August 1967. The project consists basically of six parallel, horizontal recharge basins, 20 x 700 ft each and spaced 20 ft apart. Constant depth (7 inches, so far) is maintained in the basins and infiltration rates are determined from the inflow and outflow rates as measured with fiberglass, triangular critical-depth flumes. The static ground-water table is about 13 ft below the bottom of the basins. Two wells, one of 30 ft and one of 100 ft depth and both cased to the bottom, were installed in the center of the project area to measure water level rises and to obtain samples of the ground water for chemical and bacteriological analysis. The soil beneath the basins consists of about 3 ft of fine, loamy sand, underlain by a succession of gravel and sand layers to a depth of 230 ft where a clay deposit begins.

Different inundation periods and schedules of inundation and dryups were employed to determine the infiltration and clogging behavior of the basins under conditions of bare soil. During these periods, the infiltration decreased from a range of 3 to 4 ft/day in September to a range of 0.5 to 1 ft/day in December. Rainfall during dryups had a definite decreasing effect on the infiltration rate and harrowing to break up the surface crust was effective in restoring the intake rates. Tensiometer readings obtained at different depths in the fine-sand layer showed conclusively that the overall

decline in the infiltration rate was due to clogging of the surface layer of the soil. Two reasons for this clogging can be brought forward, (1) growth of algae and other organisms on the bottom during inundation, and (2) settling of suspended material in the effluent. Although the dryup periods were adequate to obtain essentially complete gravity drainage of the soil profile, they were not sufficiently long to produce a "dry" surface condition, particularly in cooler weather. Thus, the algae and other organisms remained viable and restoration of intake rates to original levels was not accomplished. The settling of suspended material from the effluent was particularly severe in December 1967 and January 1968, when the effluent in the channel was black and of poor quality, probably due to turnover in the 1 1/2 mile of effluent channel between the sewage treatment plant and the project area.

Several weeks of dryup were necessary in the wintry season to dry the bottom. The sludge layer dried up in curled flakes 1 to 6 inches in size. It is planned to remove these flakes by hand raking and to install gravel filter "dams" across each basin about 50 ft from the inflow side. It is anticipated that the settling basin created in this manner between the inflow side and the gravel dam, and the filtering action of the dam itself will keep "macro" suspended material out of the recharge basins.

From the infiltration rates, the tensiometer readings, and the water content determinations with the neutron method, hydraulic conductivity and water content characteristics of the fine-sand layer could be evaluated. These characteristics will be of value in future theoretical and laboratory work regarding fundamental aspects of the problem of intermittent inundation with low quality water.

Hydraulic conductivity of the aquifer was evaluated by tube-method tests on the shallow and deep well, which yielded hydraulic conductivity values of 8.9 and 158 ft/day respectively. The low value for the east center well is probably due to an accumulation

of several feet of fines at the bottom. Hydraulic conductivity of the aquifer was also evaluated from the rise of the water levels in the shallow and deep wells in relation to the average infiltration rate for the six basins. Because rises in the piezometric head were known at two different depths below the ground water, the anisotropy of the aquifer could be evaluated with the electrical resistance network analog using a trial-and-error procedure. The resulting values were 388 ft/day for the horizontal hydraulic conductivity and 24 ft/day for the vertical hydraulic conductivity. From these values, the equivalent hydraulic conductivity as if the aquifer were isotropic is calculated as 97 ft/day. This is in excellent agreement with the value of 96 ft/day obtained with a different procedure using dimensionless parameters evaluated previously with the analog to determine hydraulic conductivity of aquifers from the semi-equilibrium position of the ground-water mound and the corresponding recharge rate.

The very high horizontal hydraulic conductivity and a vertical conductivity that is a multiple of the recharge rates render the aquifer extremely suitable for ground-water recharge. High recharge rates and relatively closely spaced basins can be employed without danger of waterlogging the soil beneath the basins and loss of the aerobic percolation zone. For the geometry of the Flushing Meadows project, the pseudo-equilibrium position of the ground-water mound was 3.8 ft above the static water table for a recharge rate of 3.5 ft/day from the basins.

Because the salt content of the effluent is only about one-half (900 ppm) of that of the native ground water at the project area (1800-2200 ppm), the salt content of the water samples from the wells was used as an indicator to determine when native ground water was replaced by renovated water. For the shallow well, this occurred a few weeks after recharge was started. For the deep well, native ground water still had not been replaced by renovated water at the

time of this report (31 January 1968). The slow response in the deep well is due to the anisotropy of the aquifer, which causes very low intensity of the flow in the deeper regions of the aquifer below the basin area. For the shallow well, the renovated water has a lower nitrate content than the native water (8 versus 13 ppm N), a lower ammonium content (0.5 versus 3 ppm N), a lower salt concentration (900 versus 1800 ppm), about the same chemical oxygen demand (15 ppm), about the same pH (8.1), and a higher coliform count (MPN of about 20 versus less than 2 per 100 ml). The Eijkman test indicated, however, that the coliform bacteria were of soil rather than of fecal origin. Thus, the analysis of water in the shallow well showed that the objectives of the project, i.e., removal of biodegradable material and pathogenic organisms (absence of *E. coli*), were accomplished.

Waves in the nitrate content, with one peak as high as 27 ppm N were observed on two occasions at the beginning of a recharge period following an extended dryup. This was probably due to complete nitrification of the "water" retained in the soil profile during the dryup period. To determine whether subsequent decreases in the nitrate content without parallel increases in the ammonium content are due to denitrification or to presence of organic nitrogen, Kjeldahl tests will be included in the routine analyses.

PERSONNEL: Herman Bouwer and Robert C. Rice

Table 1. Depth (feet) versus discharge (cfs) for Flushing Meadows flumes.

Depth	0	1	2	3	4	5	6	7	8	9
0.1	0.00420	0.00533	0.00662	0.00809	0.00974	0.0116	0.0136	0.0158	0.0183	0.0209
0.2	0.0238	0.0269	0.0302	0.0338	0.0376	0.0417	0.0460	0.0506	0.0554	0.0605
0.3	0.0659	0.0716	0.0775	0.0838	0.0903	0.0971	0.1043	0.1117	0.1195	0.1276
0.4	0.1360	0.1448	0.1538	0.1632	0.1729	0.1830	0.1935	0.2043	0.2154	0.2270
0.5	0.239	0.251	0.264	0.277	0.290	0.304	0.318	0.333	0.348	0.363
0.6	0.379	0.395	0.412	0.429	0.446	0.464	0.483	0.501	0.521	0.540
0.7	0.560	0.581	0.602	0.623	0.645	0.668	0.691	0.714	0.738	0.762
0.8	0.787	0.812	0.838	0.864	0.891	0.918	0.946	0.975	1.003	1.033
0.9	1.063	1.093	1.124	1.155	1.187	1.220	1.253	1.286	1.321	1.355
1.0	1.391	1.426	1.463	1.500	1.537	1.575	1.614	1.653	1.693	1.734
1.1	1.775	1.816	1.858	1.901	1.945	1.989	2.033	2.079	2.124	2.171
1.2	2.218	2.266	2.314	2.363	2.413	2.463	2.514	2.565	2.618	2.670
1.3	2.724	2.778	2.833	2.888	2.944	3.001	3.059	3.117	3.176	3.235
1.4	3.295	3.356	3.418	3.480	3.543	3.607	3.671	3.736	3.802	3.869
1.5	3.936	4.004	4.072	4.142	4.212	4.283				

SI-17

Table 2. Chemical parameters of influent and ground water.

	pH		TDS*		N _{NO₃} *		N _{NH₄} *		COD*	
	range	ave	range	ave	range	ave	range	ave	range	ave
Influent	7.60-8.12	7.85	723-992	857	0.02-0.22	0.10	13.0-36.7	27.1	34-59	46
East center well (native water)	8.11-8.19	8.15	1792	1792	12.20-14.05	13.13	1.8- 4.0	2.9	9-22	15
East center well (renovated water)	7.45-8.80	8.12	768-1024	900	0.02-27.50	9.54	0.1- 2.2	0.8	1-21	14
West center well (native water)	7.42-8.58	8.04	1978-2419	2162	0.01-10.80	3.62	0.3-4.0	1.2	2-24	15

51-18

* ppm

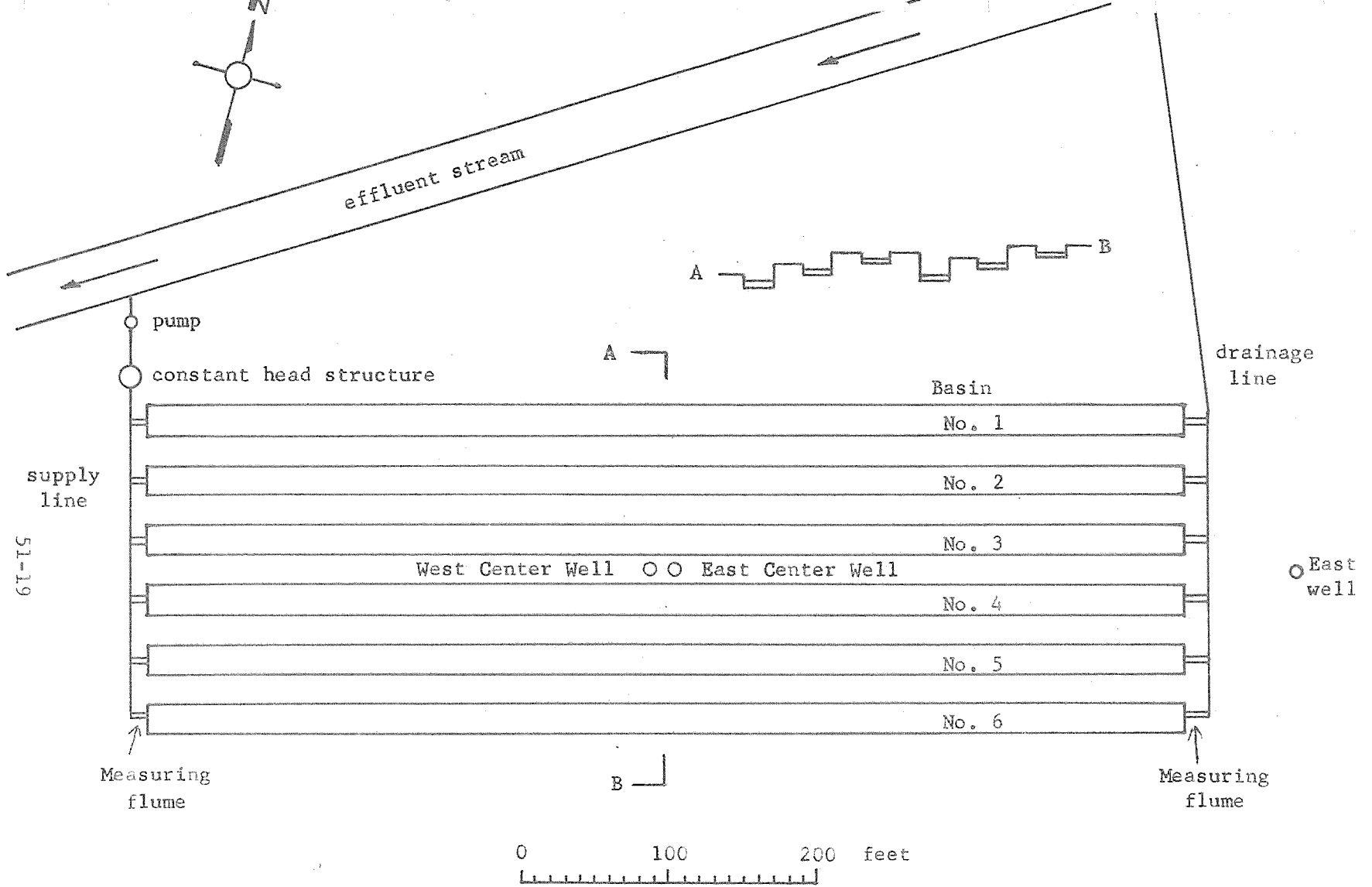


Figure 1. Schematic of Flushing Meadows Project. Annual Report of the U.S. Water Conservation Laboratory

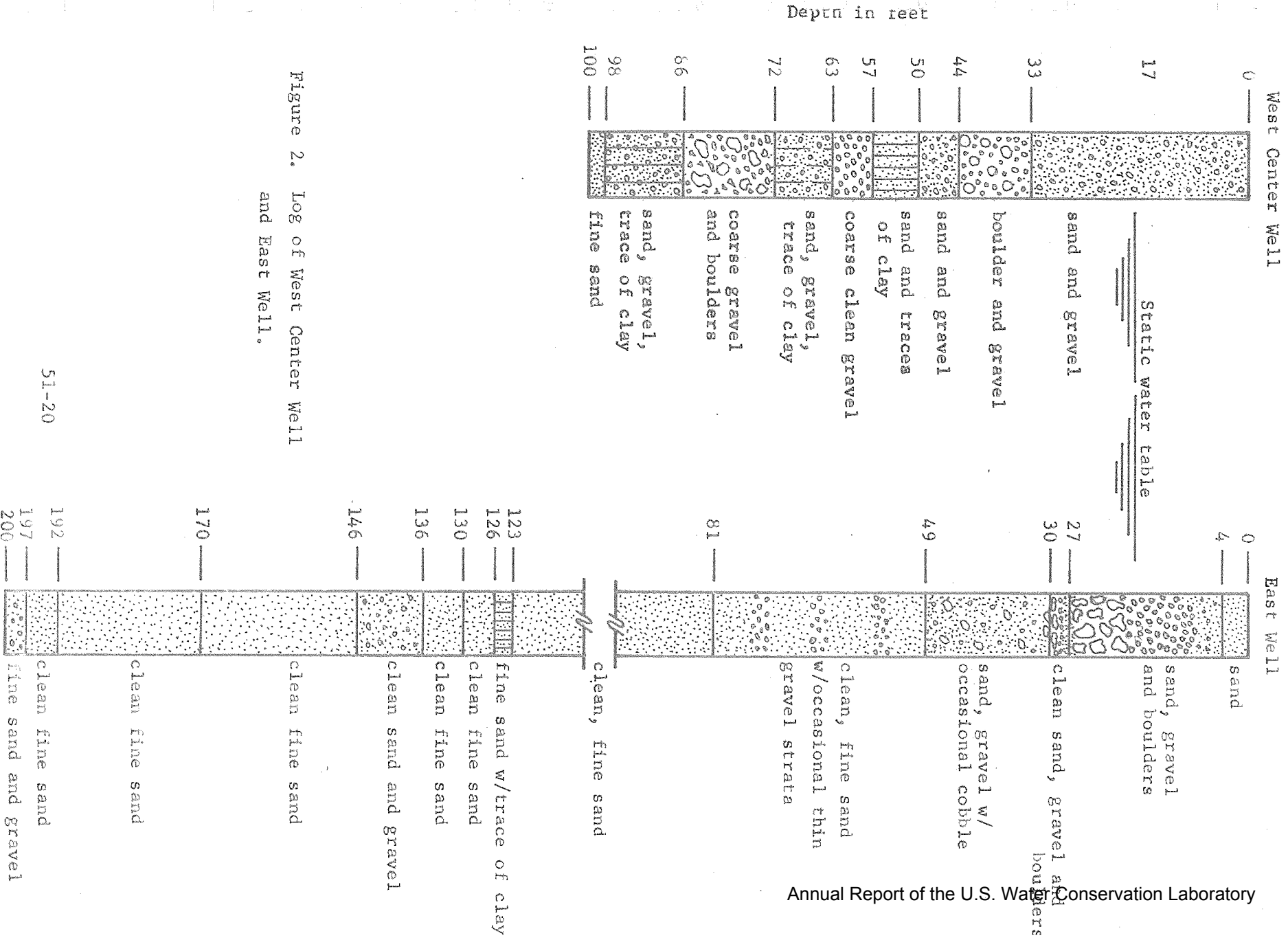


Figure 2. Log of West Center Well and East Well.

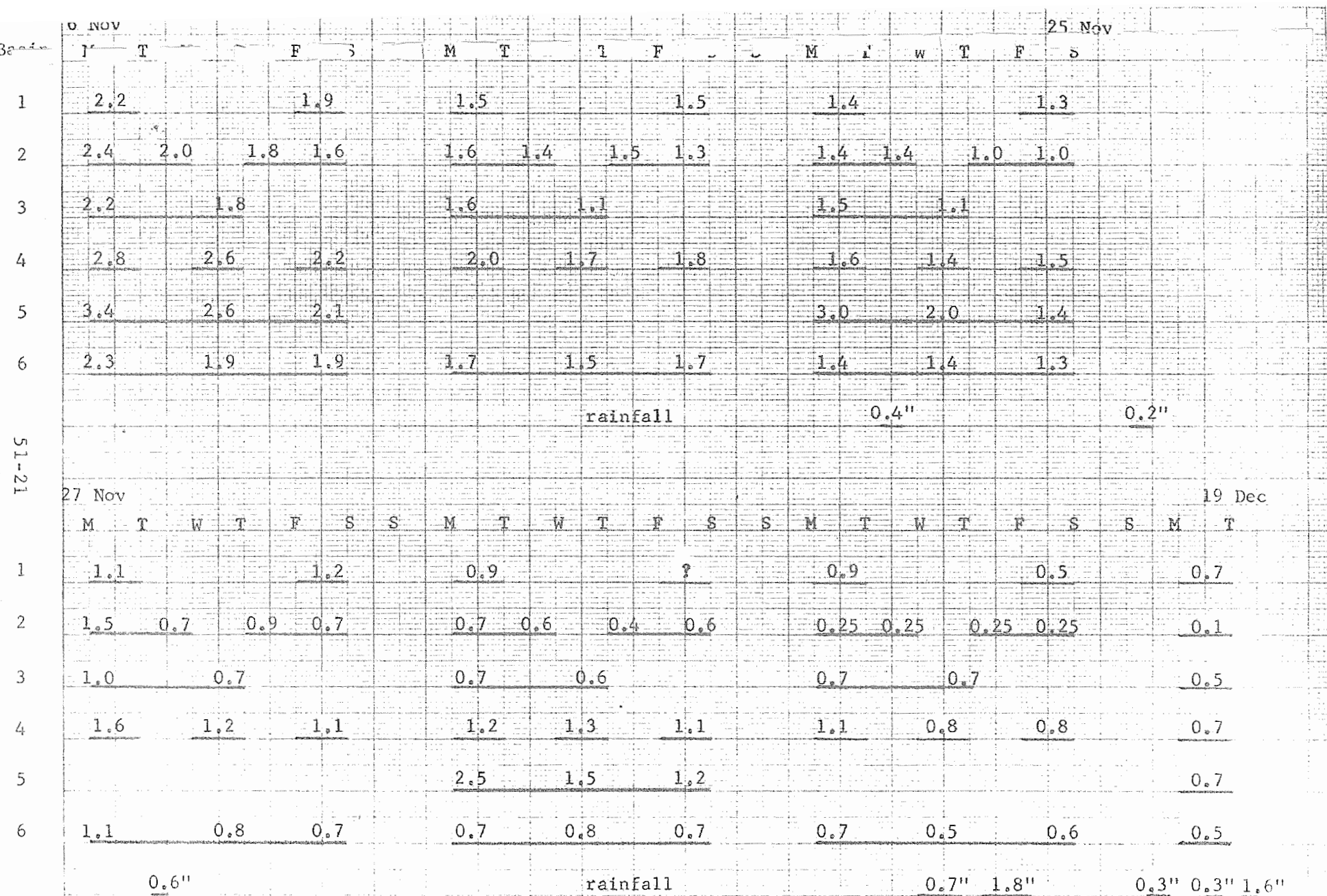


Figure 3. Intake rates in ft/day (numbers above lines) for different inundation periods (horizontal lines) during period E. Amounts of rain are also shown.

51-22

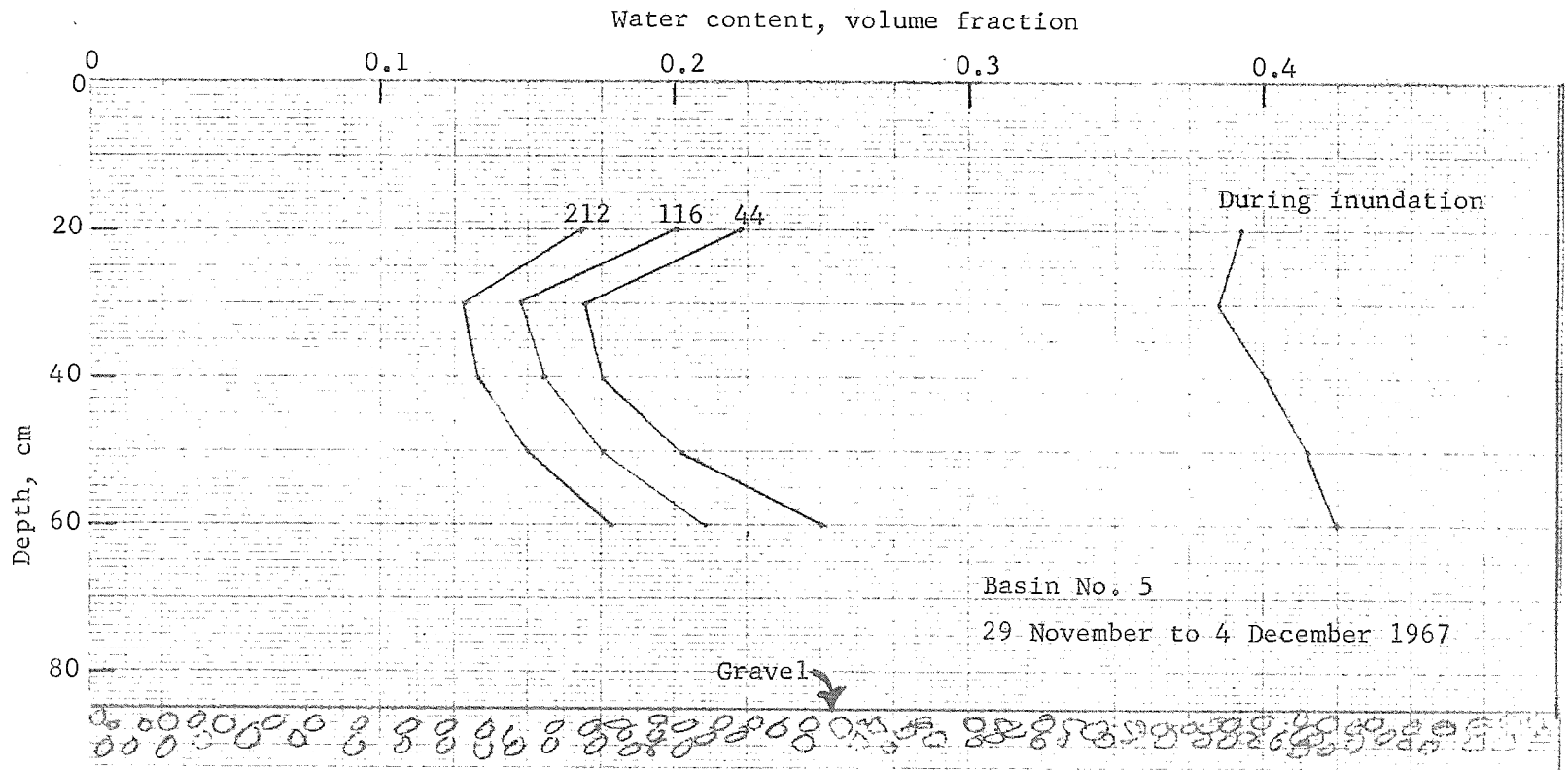


Figure 4. Water content profile of the fine-sand layer at the east end of basin 5. The numbers on the curves refer to the hours elapsed after the basin became dry.

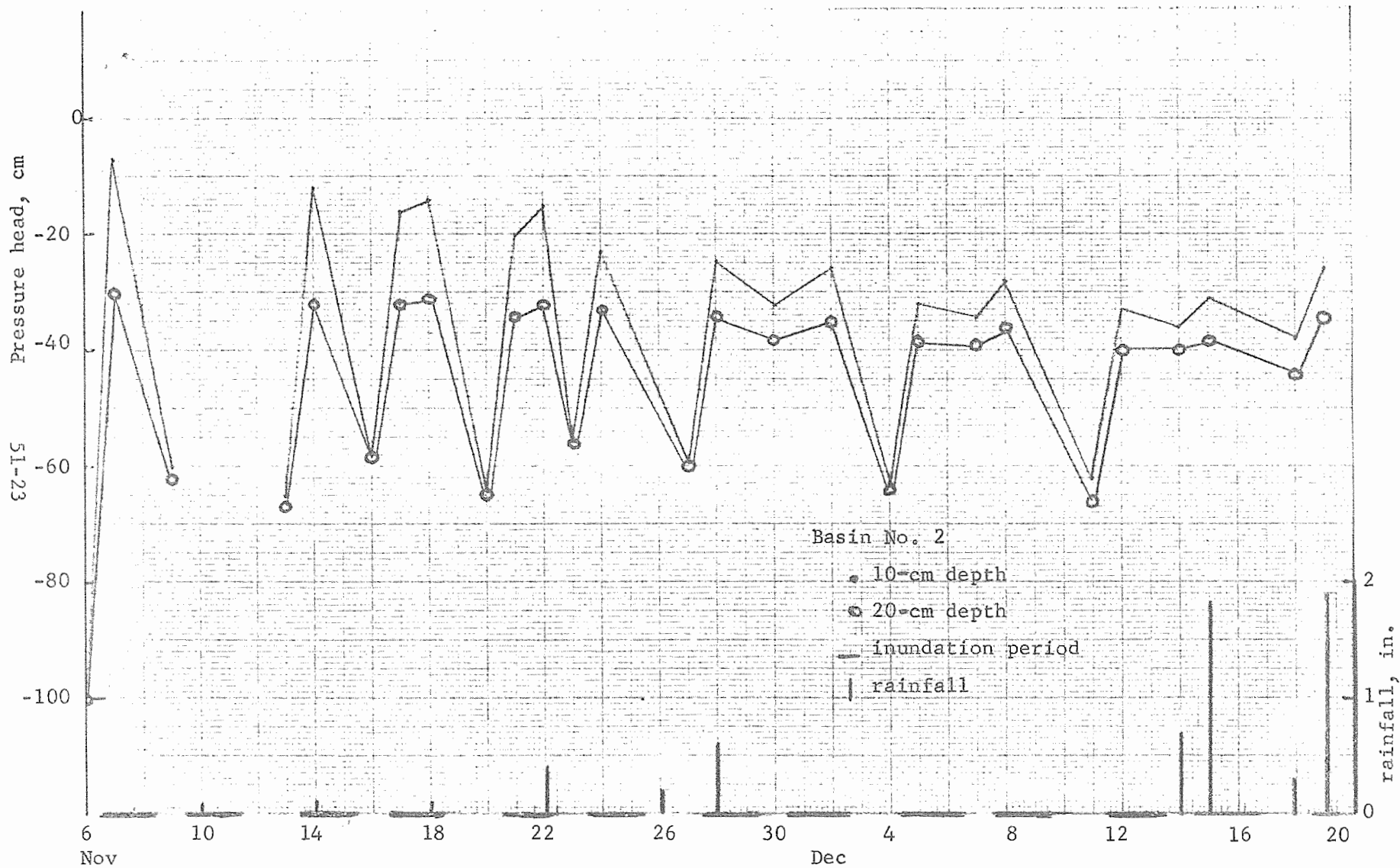


Figure 5A. Pressure head in cm water at 10- and 20-cm depth in basin 2.

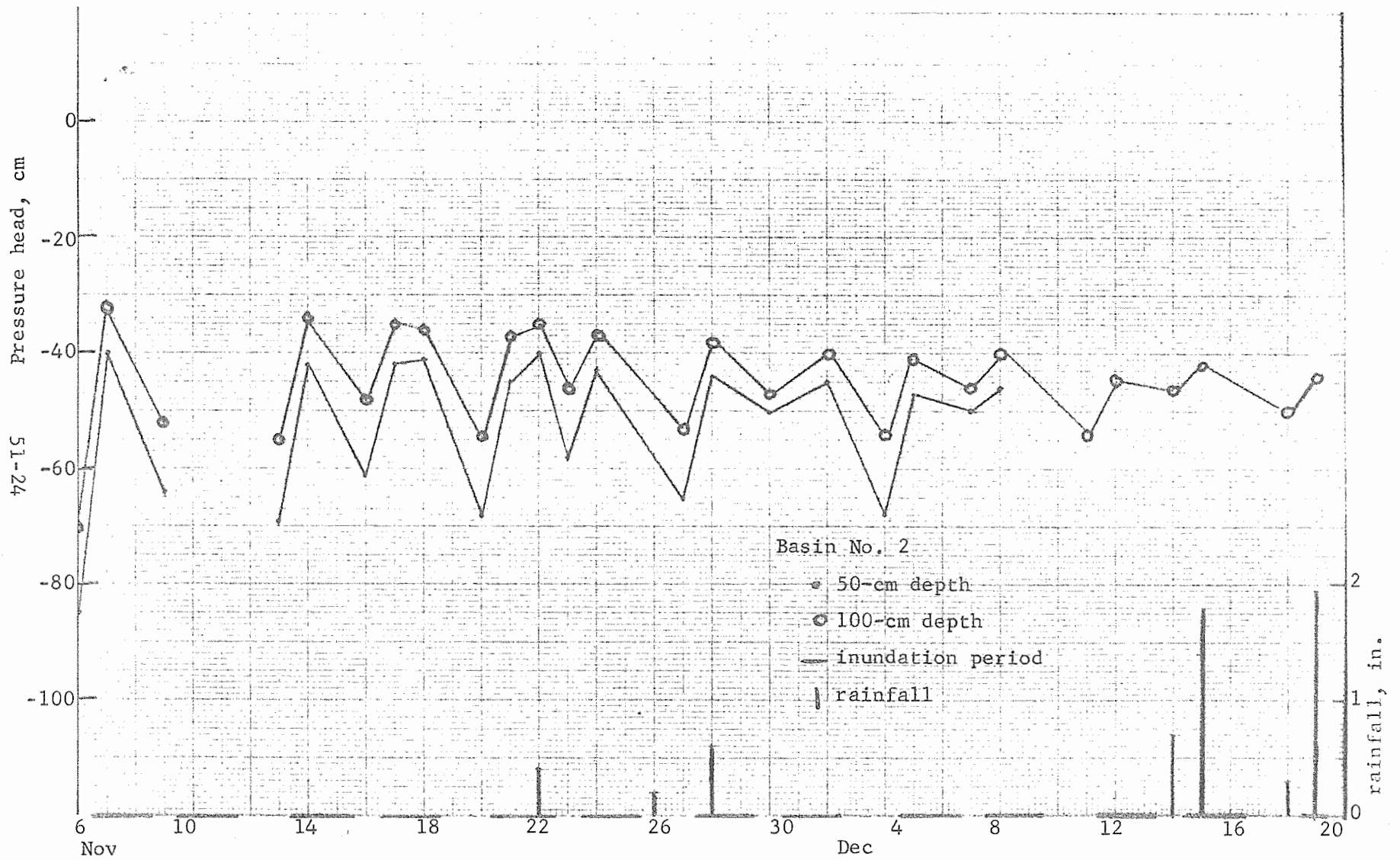


Figure 5B. Pressure head in cm water at 50- and 100-cm depth in basin 2.

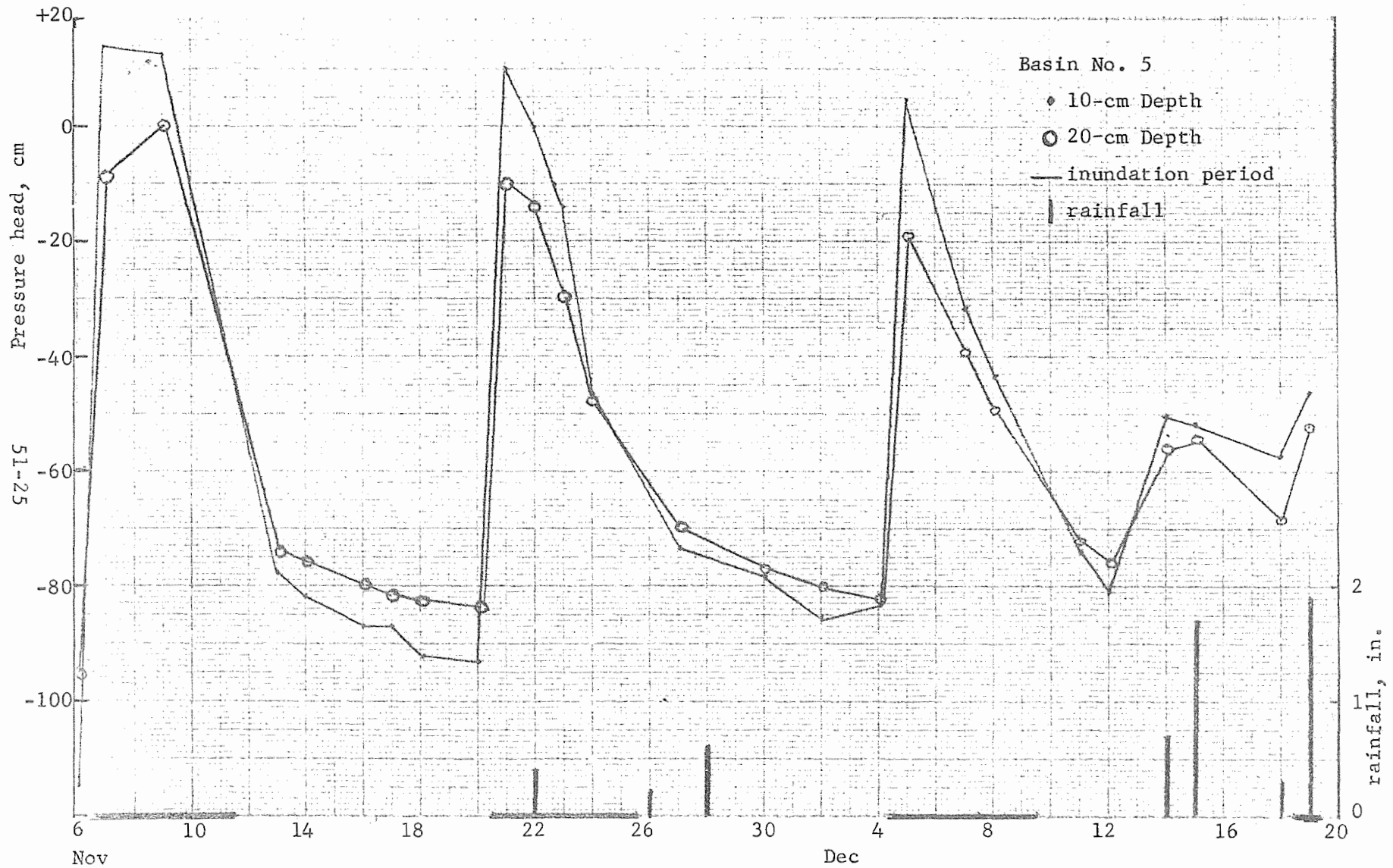


Figure 6A. Pressure head in cm water at 10- and 20-cm depth in basin 5.

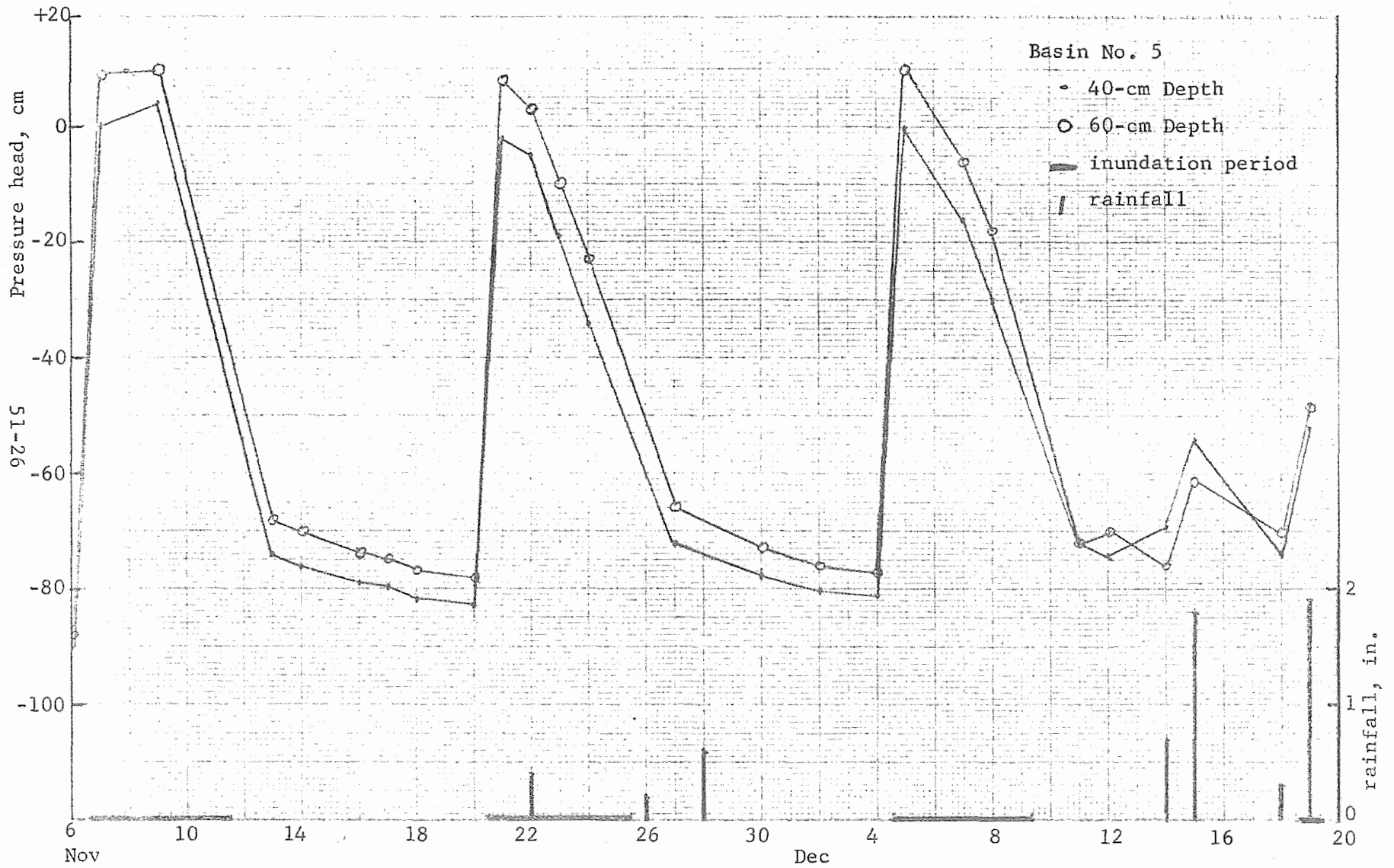


Figure 6B. Pressure head in cm water at 40- and 60-cm depth in basin 5.

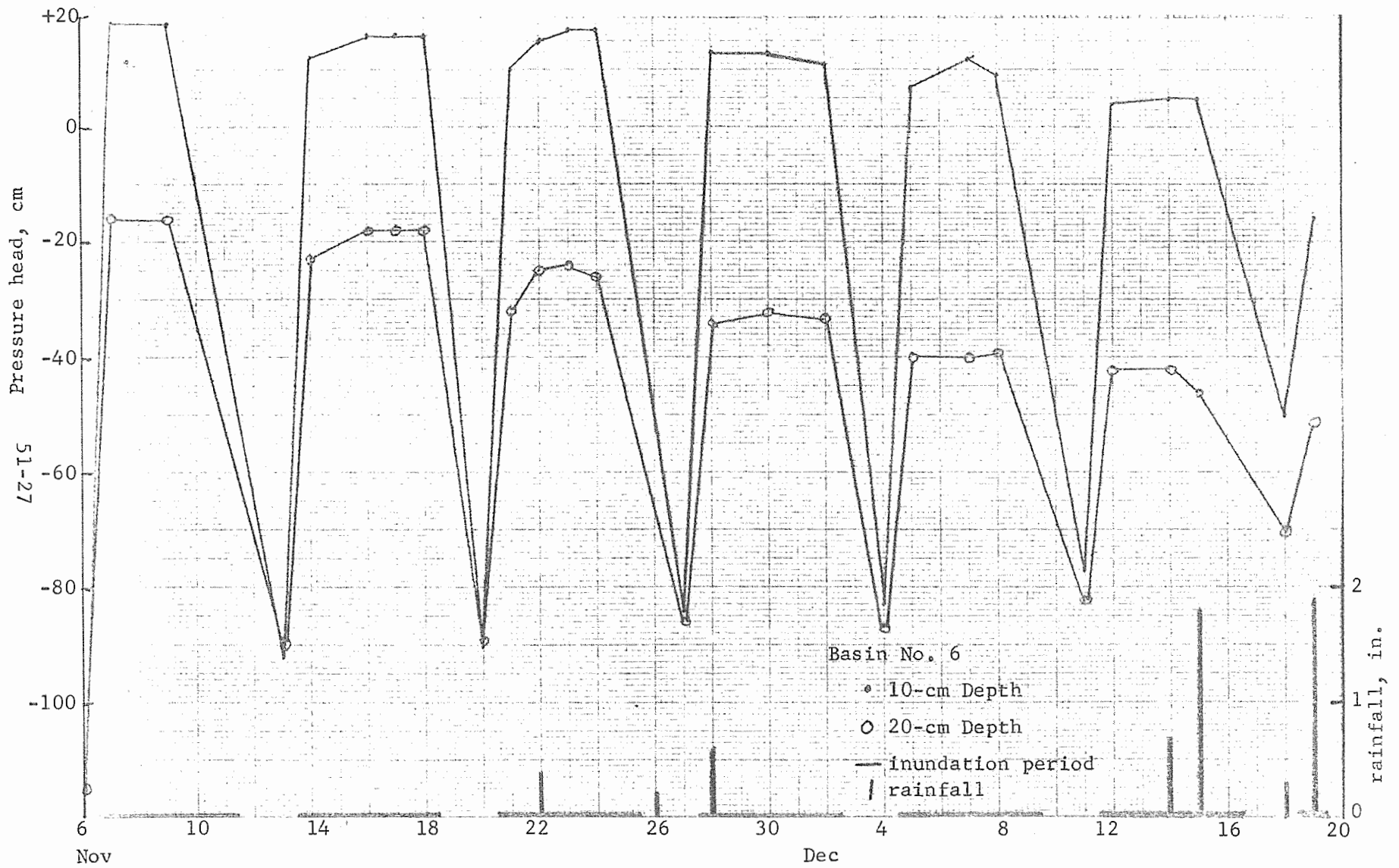


Figure 7A. Pressure head in cm water at 10- and 20-cm depth in basin 6.

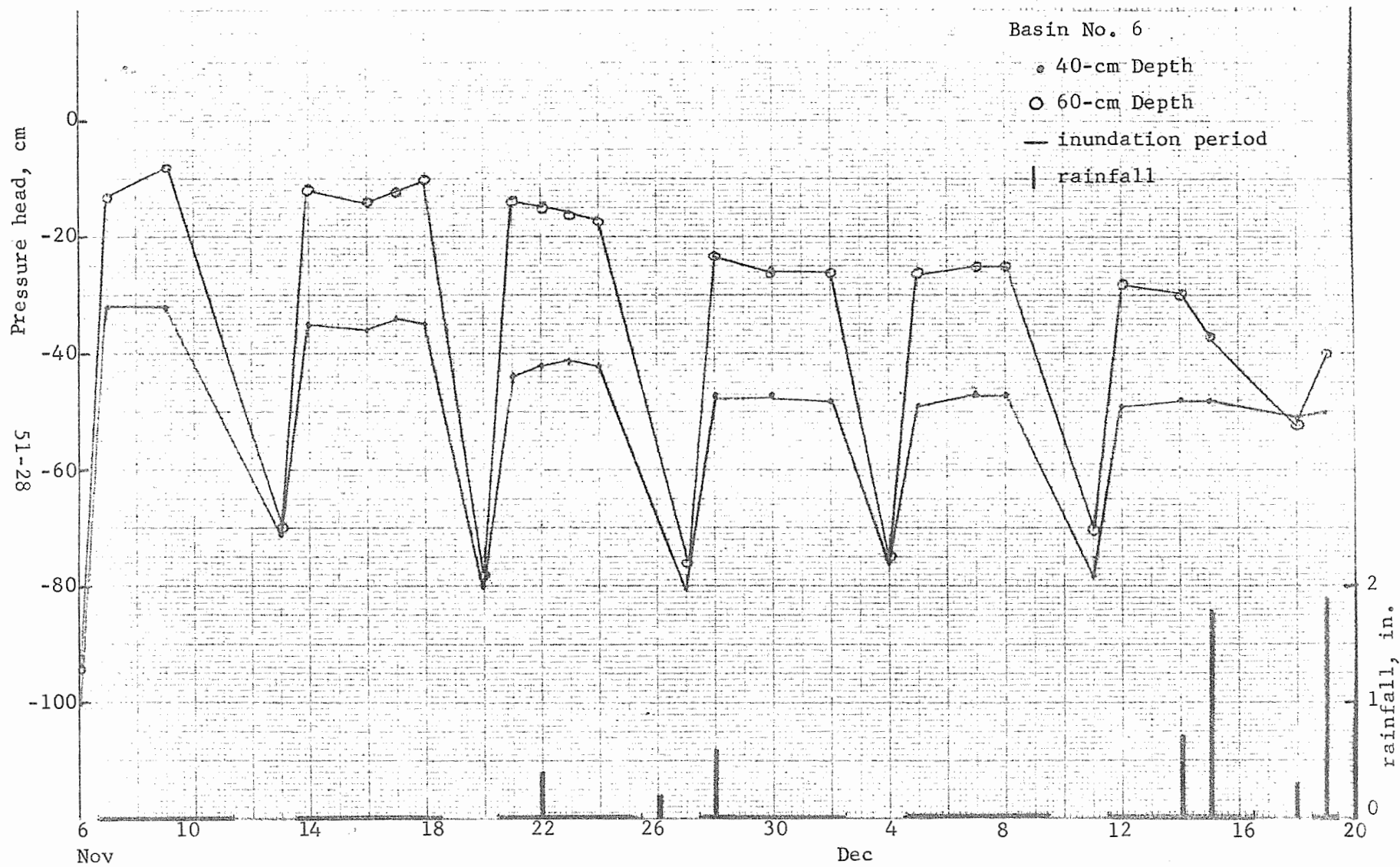


Figure 7B. Pressure head in cm water at 40- and 60-cm depth in basin 6.

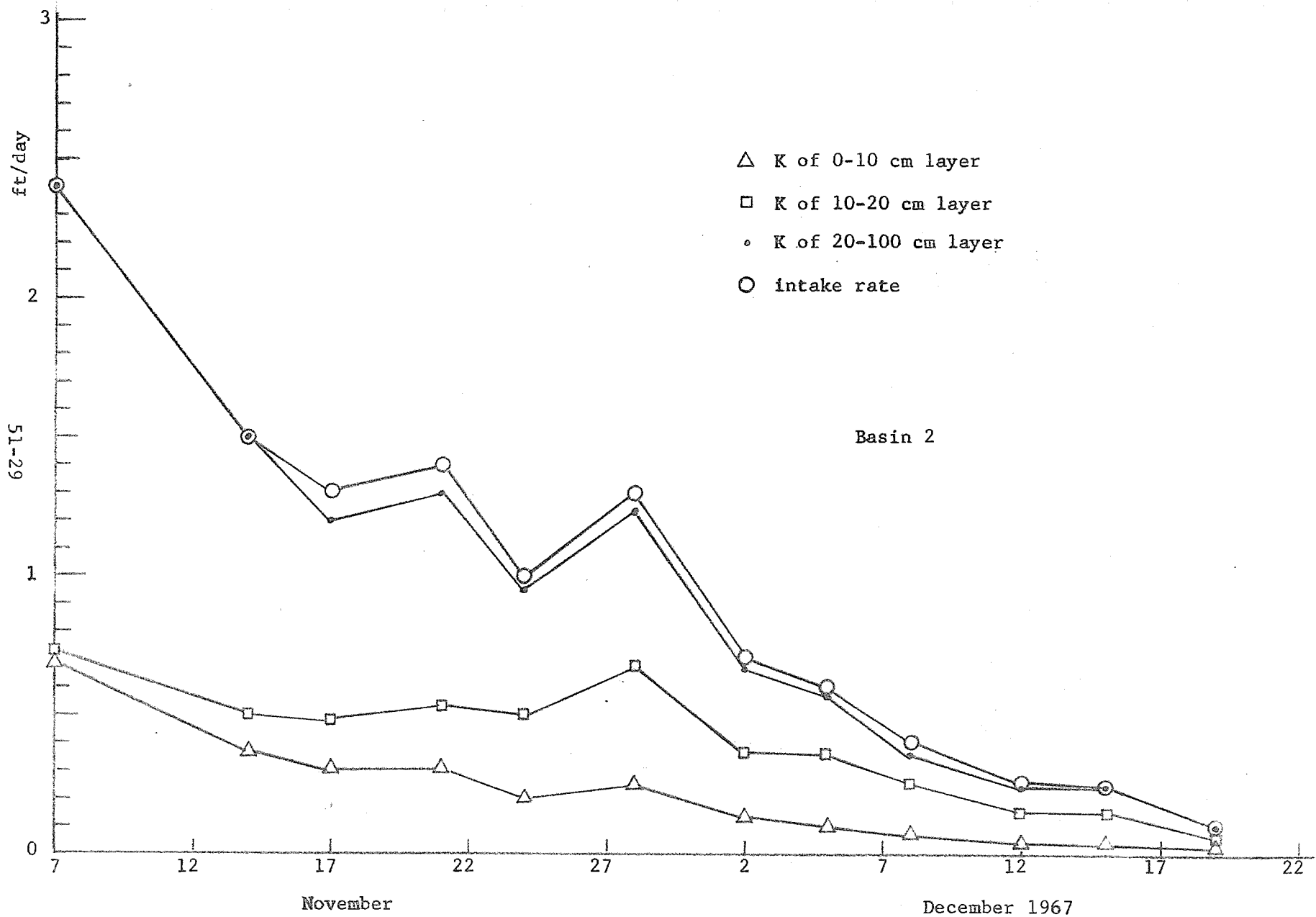


Figure 8. Values of K at different depths and of the intake rate in relation to time for Basin 2.

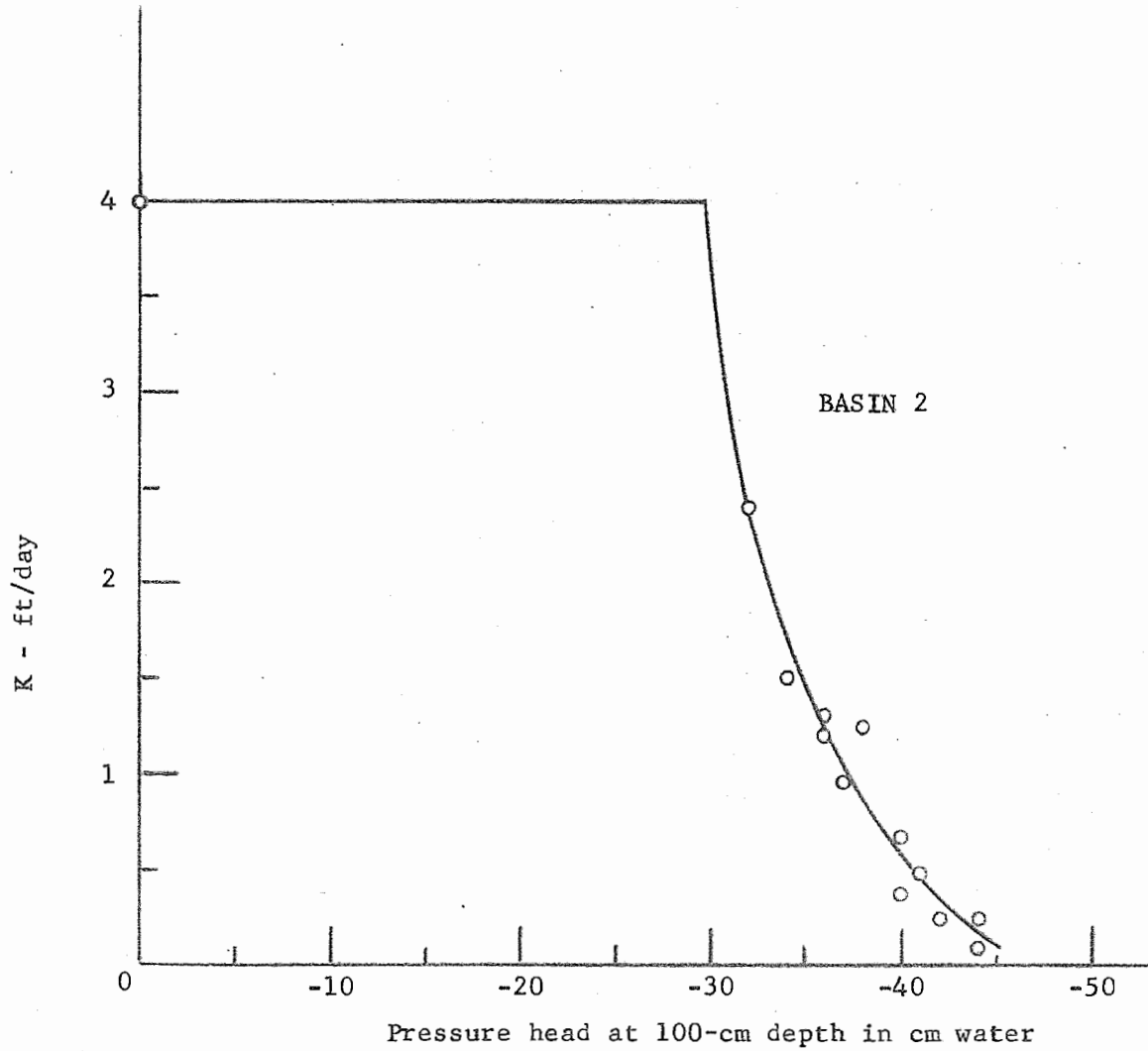


Figure 9. Relation between K and pressure head for the 20- to 100-cm soil layer of basin 2.

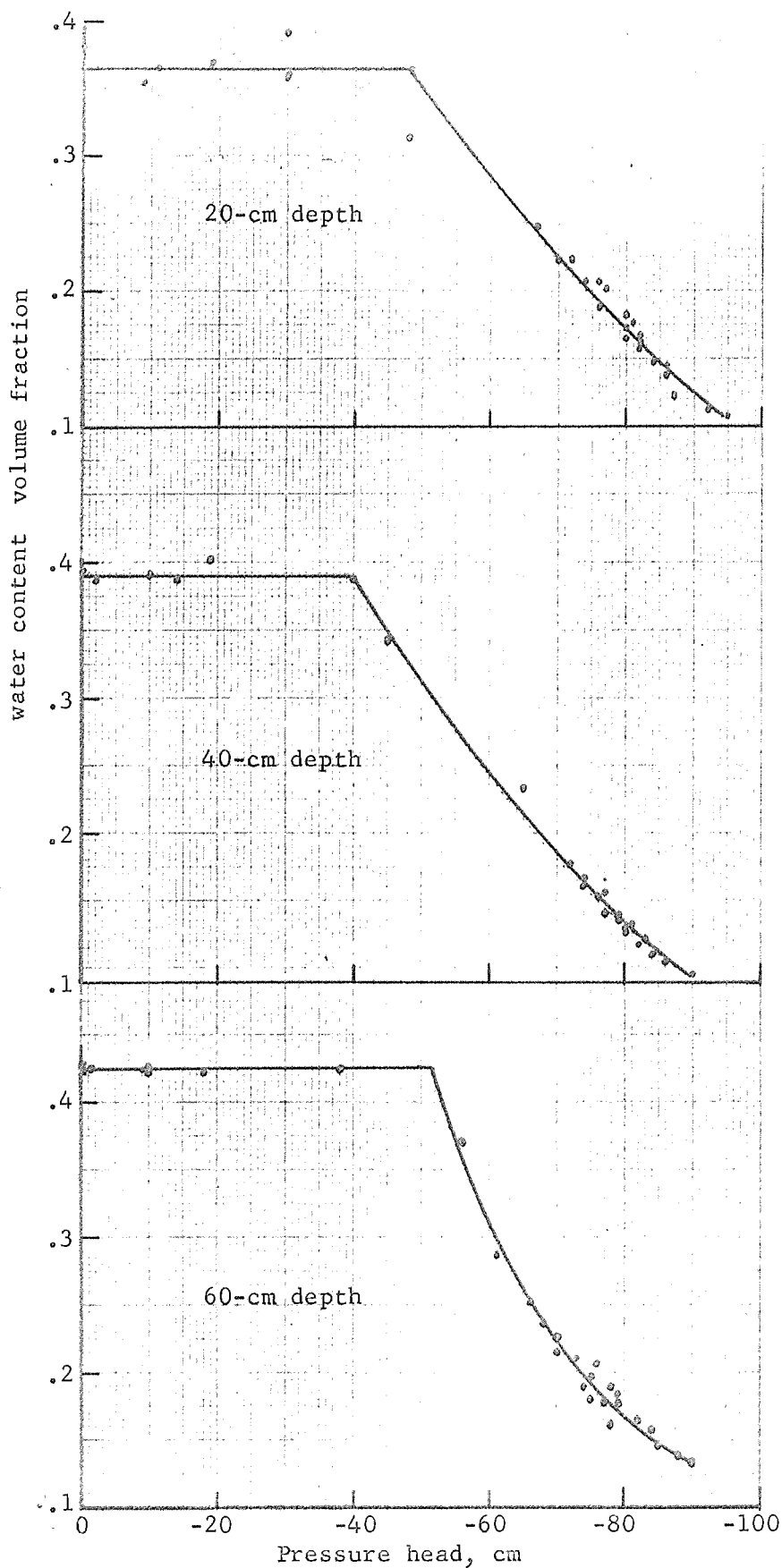


Figure 10. Water content-pressure head relationship at three different depths for basin 5.

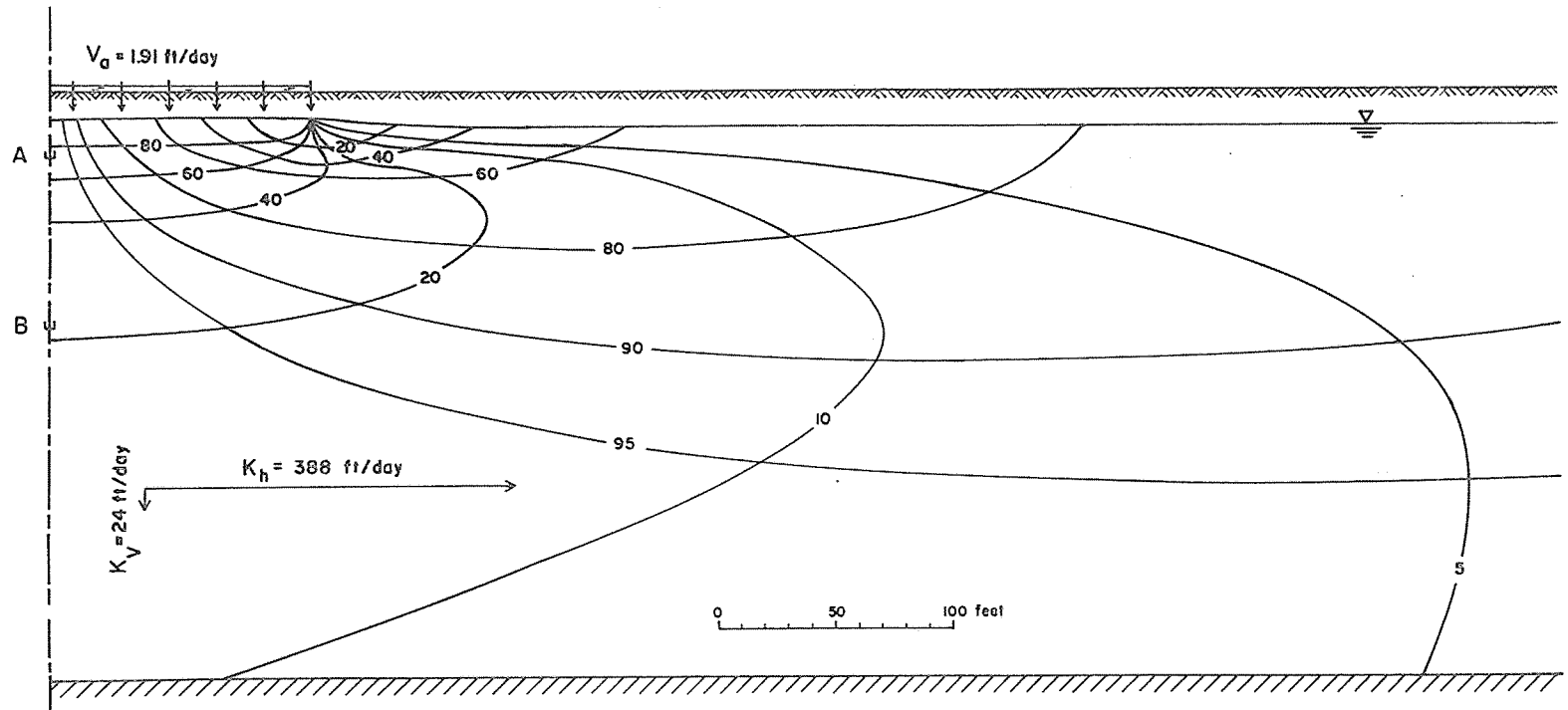


Figure 11. Flow system below water table obtained by analog for period B. The bottom of the shallow and the deep well in the center of the plot area are indicated by A and B, respectively.

APPENDIX I

LIST OF PUBLICATIONS PREPARED IN 1967

	<u>MS No.</u>
SWC W4-gG-1 Methods for water quality improvement and its storage underground.	
<u>Watson, Keith K., and Whisler, F. D.</u> System dependence of the water content-- pressure head relationship. Soil Sci. Soc. Amer. Proc. (Note) (In press)	202
<u>Watson, Keith K.</u> The measurement of the hydraulic conductivity of unsaturated porous materials utilizing a zone of entrapped air. Soil Sci. Soc. Amer. Proc. (In press)	214
<u>Whisler, F. D., and Watson, Keith K.</u> One-dimensional gravity drainage of uniform columns of porous materials. Jour. of Hydrol. (In press)	213
SWC W7-gG-2 Theory and practice for conservation of massed water supplies for agricultural use.	
<u>Bouwer, Herman.</u> Theory of seepage from open channels. Chapter in 'Advances in Hydroscience' Vol. V. (In press)	197
<u>Bouwer, Herman, and Rice, Robert C.</u> A salt penetration technique for seepage measurement. Jour. Irrig. & Drain. Div., Amer. Soc. Civil Engin. Proc. (Submitted for publication)	205
<u>Bouwer, Herman.</u> Planning and interpreting soil permeability measurements. Jour. Irrig. & Drain. Div., Amer. Soc. Civil Engin. Proc. (Submitted for publication)	219
<u>Reginato, Robert J., Myers, Lloyd E., and Nakayama, F. S.</u> Sodium carbonate for reducing seepage from ponds.	WCL Rpt. 7
<u>Rice, Robert C.</u> A fast response field tensiometer system. Trans., Amer. Soc. Agric. Engin. (Submitted for publication)	234

Conaway, A. W., and Van Bavel, C. H. M.
Remote measurement of surface temperature and
its application to energy balance and evapo-
ration studies of bare soil surfaces.
Prepared for U. S. Army Electronics Command,
Atmospheric Sciences Lab., Res. Div.,
Ft. Huachuca, Ariz. Tech. Rpt. ECOM 2-67P-1

Conaway, A. W., and Van Bavel, C. H. M.
Evaporation from a wet soil surface calculated
from radiometrically determined surface
temperatures. Jour. of Appl. Met. 6(4):650-655.
Aug. 1967. 194

Fink, Dwayne H., Rich, C. I., and Thomas, G. W.
Determination of internal surface area, external
water, and amount of montmorillonite in clay-
water systems. Soil Sci. (In press) 193

Fink, Dwayne H., Thomas, G. W., and Meyer, W. J.
Adsorption of anionic detergents by soils.
Jour. of Water Pollution Control Federation.
(Submitted for publication) 223

Franzini, J. B., Luthin, J. N., Remson, I.,
Stallman, R. W., Swartzendruber, D., and
Van Bavel, C. H. M. Quadrennial Report 1963-67,
Committee on the Physics of Soil Moisture.
Trans., Amer. Geophys. Union 48(2):744-751.
June 1967. 206

Jackson, Ray D. Osmotic effects on water flow
through a ceramic filter. Soil Sci. Soc. Amer.
Proc. (In press) 199

Lagerwerff, J. V., Nakayama, F. S., and
Frere, M. H. Hydraulic conductivity and
swelling of soils. Soil Sci. Soc. Amer. Proc.
(Submitted for publication) 216

- Nakayama, F. S., and Rasnick, B. A. Calcium electrode method for measuring the dissociation and solubility of calcium sulfate dihydrate. Anal. Chem. 39(8):1022-1023 (Note). July 1967. 200
- Nakayama, F. S. Review of "Water in the Service of Man" by H. R. Vallentine. Quart. Rev. Biol. (In press) 218
- Nakayama, F. S. Review of "Water: The Vital Essence" by Peter Briggs. Quart. Rev. Biol. (Submitted for publication) 220
- Nakayama, F. S. Calcium activity, complex and ion-pair in saturated CaCO₃ solutions. Soil Sci. (Submitted for approval) 239
- Nakayama, F. S. Review of "The Problem of Water: A World Study" by Raymond Furon. Quart. Rev. Biol. (Submitted for approval) 243
- Van Bavel, C. H. M. Surface energy balance of bare soil as influenced by wetting and drying. Prepared for U. S. Army Electronics Command, Atmospheric Sciences Lab., Res. Div., Ft. Huachuca, Ariz. Tech. Rpt. ECOM 2-67P-2
- Van Bavel, C. H. M. Comment on "Soil Moisture Estimation by the Neutron Scattering Method in Britain" by J. P. Bell and J. S. G. McCulloch. Jour. Hydrol. V(4):360. Oct. 1967. 198
- Van Bavel, C. H. M., Brust, K. J., and Stirk, G. B. Hydraulic properties of a clay loam soil and the field measurement of water uptake by roots: I. Interpretation of water content and pressure profiles. Soil Sci. Soc. Amer. Proc. (Submitted for publication) 208
- Van Bavel, C. H. M., Brust, K. J., and Stirk, G. B. Hydraulic properties of a clay loam soil and the field measurement of water uptake by roots: II. The water balance of the root zone. Soil Sci. Soc. Amer. Proc. (Submitted for publication) 209

	<u>Whisler, Frank.</u> Analyzing steady-state flow in an inclined soil slab with an electric analog. (Abst.) Agron. Absts., Amer. Soc. Agron. (Submitted for approval)	217
SWC W9-gG-6	Factors governing evapotranspiration of water from cropped fields.	
	<u>Ehrler, W. L., and Van Bavel, C. H. M.</u> Leaf diffusion resistance, illuminance and transpiration. Plant Physiol. (Submitted for publication)	212
	<u>Ehrler, W. L.</u> Daytime stomatal closure in <u>Agave Americana</u> as related to enhanced water-use efficiency. Proc., Seminar on Physiological Systems in Semi-arid Environments, Albuquerque, New Mex., Nov. 1967. (Submitted for publication)	235
	<u>Erie, Leonard J., and French, Orrin F.</u> Irrigating present-day cotton varieties with techniques determined from past research studies. Univ. of Ariz. Agric. Ext. Serv. Bul. P-5, "COTTON", Pp. 18-19. Feb. 1967.	196
	<u>Erie, Leonard J.</u> Management: A key to irrigation efficiency. Jour. Irrig. & Drain. Div., Amer. Soc. Civil Engin. Proc. (Submitted for publication)	222
	<u>Erie, Leonard J., and French, Orrin F.</u> Growth, yield and yield components of safflower as affected by irrigation regimes. Agron. Jour. (Submitted for approval)	237
	<u>Erie, Leonard J., and French, Orrin F.</u> Irrigate to satisfy cotton plant moisture needs. Univ. of Ariz., College of Agric. Report, Series P. (Submitted for publication)	238
	<u>Idso, Sherwood B.</u> Heating coefficient as a surface property. Jour. of Appl. Met. (Submitted for publication)	224

	<u>MS No.</u>
<u>Idso, Sherwood B.</u> A holocoenotic analysis of environment-plant relationships. Univ. of Minn. Agric. Exp. Sta. Tech. Bul. (In press)	230
<u>Idso, Sherwood B.</u> Comments on "The Hydrologic Importance of Transpiration Control by Stomata" by Richard Lee. Water Resources Res. (Submitted for publication)	231
<u>Idso, Sherwood B., Baker, D. G., and Blad, B.L.</u> Relations of energy balance components over natural surfaces. Quart. Jour. Royal Met. Soc. (Submitted for publication)	232
<u>Idso, Sherwood B.</u> Atmospheric and soil induced water stresses in plants and their effects upon transpiration and photosynthesis. Jour. Theoret. Biol. (Submitted for publication)	233
<u>Idso, Sherwood B., and Jackson, Ray D.</u> The significance of fluctuations in sky radiant emittance for infrared thermometry. Agron. Jour. (Submitted for publication)	240
<u>Idso, Sherwood B., and Jackson, Ray D.</u> A note on the role of sky radiance in infrared thermometry. Jour. of Appl. Met. (Submitted for publication)	241
<u>Idso, Sherwood B., and Baker, Donald G.</u> The naturally varying energy environment and its effects upon net photosynthesis. Ecology. (Submitted for publication)	242
<u>Longenecker, D. E., and Erie, Leonard J.</u> Irrigation water management - Cotton. Chapter <u>in</u> "COTTON", pub. by Ortho Div., Chevron Chem. Co., at Iowa State Univ. (In press)	201
<u>Van Bavel, C. H. M.</u> Publishing without review. Letter to Editor, SCIENCE 155(3758):34. Jan 1967.	195
<u>Van Bavel, C. H. M., and Ehrlert, W. L.</u> Water loss from a sorghum field and stomatal control. Agron. Jour. (In press)	204

- Van Bavel, C. H. M. Combination (Penman type) methods. Proc., Conf. on Evapotranspiration and Its Role in Water Resources Management, Chicago, Ill., Dec. 1966. P. 48. 226
- SWC W10-gG-7 Irrigation systems for efficient water use.
- Replogle, John A., and Birth, Gerald S. Flow. Ch. 6 in "Instrumentation Handbook" Amer. Soc. Agric. Engin. (Submitted for publication) 207
- Replogle, John A., Myers, Lloyd E., and Brust, K. J. Digest: Flow measurements with fluorescent tracers. Trans., Amer. Soc. Civil Engin. (Submitted for publication) 225
- Replogle, John A., Myers, Lloyd E., and Brust, K. J. Closure: Flow measurements with fluorescent tracers. Jour. Hydraul. Div., Amer. Soc. Civil Engin. Proc. (Submitted for publication) 228
- Replogle, John A. Target meters for velocity and discharge measurements in sheet flows. Trans., Amer. Soc. Agric. Engin. (Submitted for publication) 236
- Replogle, John A., Myers, Lloyd E., and Brust, K. J. Closure: Evaluation of pipe elbows as flow meters. Jour. Irrig. & Drain. Div., Amer. Soc. Civil Engin. Proc. (Submitted for approval) 244

APPENDIX II

SUMMATION OF IMPORTANT FINDINGS

SWC W4 gG-1 Methods for water quality improvement and its storage underground.

A computational technique has been developed for evaluating horizontal and vertical hydraulic conductivity of aquifers below ground water recharge installations. Field measurements required involve only the infiltration rate and piezometric pressure changes at two different depths in the aquifer. The method was confirmed with electrical analog studies. Horizontal and vertical conductivity at an experimental field site were found to be 388 and 24 ft/day, respectively, showing that the aquifer will permit high intake rates over large areas without excessive water table rise. This finding was confirmed with other field measurements. The method will be of considerable value in evaluating proposed ground water recharge sites. (WCL-51).

SWC W7 gG-2 Evaluation and control of seepage from water storage and conveyance structures.

Asphalt emulsions have been shown to be useful as waterborne sealants for reducing seepage losses from small reservoirs. Seepage reduction of 99% has been obtained in operational reservoirs by adding 1 gallon of emulsion per square yard of surface area to water in the reservoirs. Successful treatments should be obtained if the following requirements are met: (1) the emulsion must be highly stable and infinitely dilutable in water, (2) soils to be treated must be non-expansive, (3) pretreatment seepage rates are greater than 1 foot per day, (4) weed growth in the pond is prevented, (5) mechanical damage to the seal is prevented, and (6) water is maintained in the pond continuously. The longevity of the asphalt seal is currently under investigation. (WCL-38)

A rapid recording, multiple tensiometer system has been developed that will be extremely useful in studying the flow of water through unsaturated soil. The system, consisting of a small volume displacement transducer connected to a number of tensiometers through a hydraulic scanning valve has performed satisfactorily for over 10 months under field conditions. A diurnal variation in the pressure head, associated with the higher rate of water uptake by the roots during the day than during the night, should enable the evaluation of water uptake by roots on an hourly basis. (WCL-25)

SWC W7 gG-3 Suppression of evaporation from water surfaces.

Evaporation reduction by long-chain alkanol dispersions developed at the U. S. Water Conservation Laboratory was markedly superior to that obtained with powdered alkanol. This is contrary to opinions expressed by previous investigators who used inferior dispersions. Application of 1.1 g m^{-2} dispersed alkanol per month to outdoor tanks reduced evaporation 28%. The same application rate of powdered alkanol did not reduce evaporation. Increasing application of powder by 5 times reduced evaporation by only 15%. (WCL-9)

A formulation has been developed for floating concrete blocks that will reduce evaporation from water surfaces. Durable blocks with a specific gravity of 0.5 were obtained with a mixture of Portland cement, perlite and asphalt emulsion. There was no sign of water-logging after 6 months of floating. Average evaporation reduction on outdoor tanks was 50% when 75% of the water surface was covered. (WCL-50).

SWC W7 gG-4 Principles, facilities, and systems for water harvest.

Data from the Granite Reef experimental site indicate that hand clearing scattered brush can significantly increase runoff from similar low rainfall, low desert areas. Annual rainfall at Granite Reef averages about 225 mm. Brush clearing, at a cost of 1 cent per m^2 , has increased runoff by a total of 120 mm during the four years following treatment. At least 40 mm increased runoff will be obtained before reclearing is necessary. The resultant cost of the water is 6 cents per 1,000 liters, which compares very favorably with any other water harvesting treatment presently available. Low cost brush clearing, which does not interfere with the use of the land for grazing, should be seriously considered as a water harvesting procedure in low desert areas where average annual rainfall exceeds 200 mm.

Laboratory studies indicate that several resin emulsions and solutions are promising low cost stabilizers for controlling soil erosion. These resins are rated as highly resistant to weathering degradation and are compatible with water repellent chemicals for water harvesting. One material completely stopped erosion of a highly erosive loamy sand soil by simulated raindrops when applied at a rate of 14 g resin per m^2 . This represents a cost of less than 1 cent per m^2 or \$40 per acre. The relatively small quantity of material required implies that application by airspray may be feasible. (WCL-7)

SWC W7 gG-5 Soil water movement in relation to the conservation of water supplies.

Measurement devices and special equations have been developed to determine the amount of calcium in soil-water solutions that is "active" or available for reaction with the soil. It has been found that in a saturated calcium carbonate solution only 80% of the calcium is "active" while 20% is tied up in ion-pairs with carbonate and bi-carbonate ions. The amount of active calcium is even less if other salts, such as sodium carbonate, are present. Soil scientists have previously assumed that all of the calcium was active, with resulting errors and confusion in their findings. These new findings will be of great value in studies of soil aggregation and the movement of water through soil where the status of calcium in the soil-water solution is of paramount importance. (WCL-40)

Studies have shown that the optimum application rates of water-repellent chemicals on soil surfaces may be readily determined by measuring the pressure needed to initiate water flow through these porous but water-repellent systems. This optimum rate is nearly the same for all soils when expressed as amount of material applied per unit of surface area for the soils. A method for measuring the contact angle of water on these treated soils was developed, and results using this technique support the findings obtained by measuring breakthrough pressure. Water-repellent chemicals have considerable promise for water harvesting and for improving irrigation efficiency. (WCL-49)

SWC W9 gG-6 Factors governing evapotranspiration of water from
cropped surfaces.

Field experiments have demonstrated the feasibility of using leaf temperature measurements as a guide for scheduling irrigation of cotton plants. In clear weather the temperature of freely exposed leaves ranged from 3 C below air temperature shortly after irrigation to 3 C above air temperature immediately preceding an irrigation that had been delayed sufficiently to induce moderate symptoms of midday wilting. The rise in leaf temperature can be used as an indication of the level of soil water depletion and the need for irrigation.

Large fluctuations in clear sky radiance previously observed at this laboratory and reported in the literature were demonstrated to have been due to instrument malfunction. Typical real fluctuations were found to be so small as to require no corrections in the calculation of surface temperatures of soil and vegetation by means of infrared thermometry. (WCL-29)

SWC W10 gG-7 Irrigation systems for efficient water use.

Highly accurate water metering flumes can now be designed to fit a wide range of flow rates and channel conditions with no requirement for conformance to standard sizes or dependence on expensive modeling techniques to obtain calibrations. This has come about through a rigorous mathematical treatment of energy concepts that permits the successful theoretical prediction of the calibration curves for critical-depth flumes with an accuracy of $\pm 2\%$. Although the procedure is complex, it can be readily accomplished with computers.

(WCL-48)